

# **Carbonate chemistry and organic alkalinity in Irish coastal waters**

An exploration of the measurement and characterisation of organic alkalinity

**Daniel E. Kerr, B.Sc.**

Supervised by Dr Brian Kelleher



Thesis submitted in partial fulfilment of the requirements for the degree of Doctor of Philosophy


SCHOOL OF CHEMICAL SCIENCES

DUBLIN CITY UNIVERSITY

October 2022

# Declaration

I hereby certify that this material, which I now submit for assessment on the programme of study leading to the award of Doctor of Philosophy is entirely my own work, and that I have exercised reasonable care to ensure that the work is original, and does not to the best of my knowledge breach any law of copyright, and has not been taken from the work of others save and to the extent that such work has been cited and acknowledged within the text of my work.

Signed:  ID No.: 14427352 Date: 28<sup>th</sup> October 2022

# Dedication

*Dedicated to Bridie Byrne and Joy Kerr*

*"What we observe is not nature itself, but nature exposed to our method of questioning."*  
- Werner Heisenberg, 1955

# Acknowledgements

This thesis would not have been possible without the encouragement and support of my family, friends and colleagues. I would like to express my gratitude to the following:

My parents, Brigid and Donal, for the ceaseless support and inspiration you have given me.

Skye, for being a constant ray of sunshine in my life.

The School of Chemical Sciences technical staff, for keeping the show on the road.

Pete, for all your carbonate chemistry insights and for the opportunity to sail across the Atlantic.

Anthony, for your mentorship and guidance during my time in DCU.

Brian, for being a first-class supervisor and for giving me the opportunity to pursue this research.

I am eternally grateful to you all.

# Notable undertakings

## Scientific research cruise

**Research Cruise:** JC191

**Research Vessel:** RV James Cook

**Date:** 19 January - 1 March 2020

**Role:** Carbonate System Technical Analyst

**Details:** A hydrographic section across the North Atlantic Ocean at a nominal latitude of 24°N was occupied by the RRS James Cook (cruise identifier: JC191) from 19 January to 1 March, 2020. The ship departed from Port Everglades, USA, completing a total of 135 CTD stations over the Florida Straits, the western basin, Mid-Atlantic Ridge, and eastern basin, before ending the cruise in Santa Cruz de Tenerife, Spain. The main objectives of the JC191 research expedition was to collect physical-, chemical-, and biological-ocean data with the purpose of estimating heat, freshwater and carbon budgets on low frequency time scale

## Poster presentations

**Conference:** 30th Irish Environmental Researchers Colloquium (Environ 2020), online

**Title:** Challenges in Characterising Carbonate Chemistry in Coastal Waters

**Authors:** Daniel. E. Kerr, Brian Kelleher

**Conference:** Geoscience 2018 - Geoscience for Climate Action, Aviva Stadium, Dublin, Ireland

**Title:** PREDICT - Prediction of Irish Coastal Transformation

**Authors:** Daniel. E. Kerr, Brian Kelleher

## **Oral presentations**

**Conference:** 73rd Irish Chemistry Research Colloquium 2022, University College Dublin, Dublin, Ireland

**Title:** A Python Based Non-Linear Regression Model to Estimate Acid-Base Characteristics of Organic Alkalinity – Pilot Study Dublin Bay.

**Authors:** Daniel E. Kerr, Charles Turner, Anthony Grey, Brian Kelleher

**Conference:** Environmental Geosciences Projects, Science Foundation Ireland Research Centre in Applied Geosciences, 2021, online

**Title:** Carbon Cycling in Coastal Waters

**Authors:** Daniel E. Kerr, Brian Kelleher

**Conference:** iCRAG 2019: Resources for a Sustainable Future, Croke Park, Dublin, Ireland

**Title:** Coastal Carbon Cycling\*

**Authors:** Daniel E. Kerr, Brian Kelleher

*\* Winner of best Flash presentation award*

# Contents

<b>List of Tables</b>	<b>13</b>
<b>List of Figures</b>	<b>14</b>
0.1 The marine carbonate system . . . . .	19
0.2 Carbonate system parameters . . . . .	20
0.2.1 Total alkalinity . . . . .	21
0.2.2 Dissolved inorganic carbon . . . . .	21
0.2.3 pH . . . . .	23
0.2.4 Partial pressure of CO <sub>2</sub> . . . . .	25
0.3 Carbonate system measurement quality goals . . . . .	26
0.4 Ocean Acidification . . . . .	26
0.5 Organic Alkalinity . . . . .	27
0.6 Motivation and goals . . . . .	28
References . . . . .	29
<b>Introduction</b>	<b>19</b>
<b>1 Published Literature: The Influence of Organic Alkalinity on the Carbonate System in Coastal Waters</b>	<b>37</b>
<b>2 Analytical Approaches</b>	<b>50</b>
2.1 TA titration procedure . . . . .	52
2.2 Modifications to GOA-ON titration apparatus . . . . .	54
2.2.1 Sample Filtration . . . . .	55
2.3 OrgAlk analysis . . . . .	59
2.3.1 OrgAlk titration procedure . . . . .	60
2.4 <i>OrgAlkCalc</i> . . . . .	63
2.4.1 TA computational procedures . . . . .	63
2.4.2 OrgAlk computational procedures . . . . .	65
2.4.3 Titration data handling . . . . .	66
2.4.4 NaOH curve fitting . . . . .	70



2.4.5	Experimental method validation . . . . .	71
2.5	Titration solutions . . . . .	74
2.5.1	HCl titrant . . . . .	75
2.5.2	NaOH titrant . . . . .	76
2.6	Nutrient Analysis . . . . .	78
2.7	Complementary carbonate system analysis . . . . .	78
2.7.1	DIC analysis . . . . .	79
2.7.2	pH analysis . . . . .	81
2.8	Optical analysis and data processing . . . . .	85
	References . . . . .	90
<b>3</b>	<b>Inter-laboratory Comparison and Validation Studies</b>	<b>108</b>
3.1	Inter-laboratory validation . . . . .	110
3.1.1	WEPAL-QAUSIMEME . . . . .	110
3.1.2	VINDTA comparison . . . . .	113
3.2	Dublin Bay data buoy . . . . .	115
3.2.1	pCO <sub>2</sub> comparisons . . . . .	117
3.2.2	pH comparisons . . . . .	117
	References . . . . .	119
<b>4</b>	<b><i>OrgAlkCalc</i>: Estimation of Organic Alkalinity Quantities and Acid-base Properties With Proof of Concept in Dublin Bay</b>	<b>123</b>
4.1	Introduction . . . . .	125
4.2	Materials and methods . . . . .	129
4.2.1	Study Location and Sampling Procedure . . . . .	129
4.2.2	Apparatus and reagents . . . . .	130
4.2.3	<i>OrgAlkCalc</i> . . . . .	133
4.3	Results and Discussion . . . . .	136
4.3.1	<i>OrgAlkCalc</i> Performance . . . . .	136
4.3.2	Alkalinity distributions . . . . .	139
4.3.3	<i>OrgAlk</i> charge group characteristics . . . . .	141
4.4	Conclusion . . . . .	143
	References . . . . .	145
<b>5</b>	<b>Organic Alkalinity Dynamics in Irish Coastal Waters</b>	<b>156</b>
5.1	Introduction . . . . .	158
5.2	Materials and methods . . . . .	160
5.2.1	Study location . . . . .	160
5.2.2	Carbonate system analysis . . . . .	162

5.2.3	DOM analysis . . . . .	166
5.3	Results and Discussion . . . . .	168
5.3.1	OrgAlk dynamics . . . . .	168
5.3.2	Effects of OrgAlk on carbonate system calculations . . . . .	170
5.3.3	Carbonate chemistry distributions . . . . .	173
5.3.4	Optical properties of DOM . . . . .	176
5.4	Conclusion . . . . .	179
	References . . . . .	181
	<b>Conclusion and Future Work</b>	<b>191</b>
	References . . . . .	196
	<b>Appendix</b>	<b>197</b>

# Abbreviations

$A$	Absorption values
$a$	Naperian absorption coefficients ( $m^{-1}$ )
$a_{254}$	Measure of relative CDOM concentration
$a_{325}$	Indicator of aromatic substances on CDOM
$a_{350}$	Indicator of CDOM lignin phenol content
AcOH	Acetic acid
$B_T$	Total Borate
$C$	Concentration of acid ( $mol.kg^{-1}$ )
$CTNa$	Carbonate content of the NaOH titrant
CDOM	Coloured Dissolved Organic Matter
CE	Constant Error
$C_{HA}$	Concentration of weak acid HA
$C_{NaOH}$	Concentration of base
$CO_2$	Carbon Dioxide
$CO_2^{atm}$	Atmospheric Partial Pressure of Carbon Dioxide
$CO_2^{SW}$	Seawater Partial Pressure of Carbon Dioxide
$CO_3^{2-}$	Carbonate
CWB	Circulating Water Bath
DI	Deionised water
DIC	Dissolved Inorganic Carbon
DMM	Digital Multimeter
DMS	Dimethyl sulphide
DOM	Dissolved Organic Material
$E^o$	Standard electrode potential
$E$	Potential
e.m.f.	Electromotive Force
EEM	Excitation-emission matrix
$f$	Multiplicative factor in hydrogen ion concentration
$f$	Multiplicative factor in hydrogen ion concentration
$F_1$	Gran function
$F_{CO_2}$	Carbon Dioxide Flux
$fCO_2$	Fugacity of Carbon Dioxide
FDOM	Fluorescent Dissolved Organic Matter
$F_T$	Total Fluoride
GOA-ON	Global Ocean Acidification Observing Network
$H_0$	Initial estimate of hydrogen ion concentration
$H_2CO_3$	Carbonic Acid

$\text{HCO}_3^-$	Bicarbonate
HDPE	High density Polyethylene
$I_mO$	Ionic strength (M)
$I_mO_t$	Ionic strength of titrant (M)
$K$	Nernst factor
$K_a$	Acid Dissociation Constant
$K_B$	Dissociation constant of Boric acid
$K_{C1}$	First dissociation constant of Carbonic Acid
$K_{C2}$	Second dissociation constant of Carbonic Acid
$K_F$	Dissociation constant of Fluoride
$K_i$	Dissociation constant of $Xi_T$
KI	Potassium iodide
$K_P$	Dissociation constant of Phosphoric acid
$K_S$	Dissociation constant of Sulfate
$K_{Si}$	Dissociation constant of Silicic acid
$K_{sp}$	Calcite solubility constant
$l$	Cuvette pathlength
$m$	Mass of titrant
$m_0$	Mass of sample titrated
MAD	Median of Absolute Distribution
mCp	meta Cresol purple
$m_T$	Total mass of titrant added
MTF	Multiplicative factor in hydrogen ion concentration
MW	Molecular Weight
NDA	Normal Distribution Model
NDIR	Non-Dispersive Infrared detection
NLSF	Non-linear Least Squares Fitting
$\text{OH}^-$	Hydroxide ion concentration
OM	Organic Material
OrgAlk	Organic Alkalinity
$pH_{max}$	Maximum pH of NaOH titration
$p\text{CO}_2$	Partial pressure of Carbon Dioxide
$p\text{CO}_{2C}$	Calculated $p\text{CO}_2$
$p\text{CO}_{2DB}$	Dublin Bay Data Buoy recorded $p\text{CO}_2$
PE	Proportional Error
$pH_0$	pH prior to indicator dye addition
$pH_C$	Calculated pH
$pH_{DB}$	Dublin Bay Data Buoy recorded pH
$pH_F$	Free Scale pH
$pH_{NBS}$	Nation Bureau of Standards Scale pH
$pH_S$	Spectrophotometric pH
$pH_{SWS}$	Seawater Scale pH
$pH_T$	Total Scale pH
$pH_{Tris}$	pH of Tris buffer at specific temperature and salinity
$pK_a$	$-\log(K_a)$
ppm	Parts Per Million
PRT	Platinum Resistance Thermometer

$P_T$	Total Phosphate
$RMS$	Root Mean Square
RTD	Resistance Thermometer Detector
$S_{275-295}$	Spectral slope of wavelength interval 275-295 nm
$S_{350-400}$	Spectral slope of wavelength interval 350-400 nm
$Si_T$	Total Silicate
$S_R$	Slope Ratio
$S_T$	Total Sulfate
TA	Total Alkalinity
$TA_C$	Calculated Total Alkalinity
$TA_{DCU}$	TA measured in Dublin City University
$TA_M$	Measured Total Alkalinity
$TA_{NOC}$	TA measured in National Oceanography Centre, Southampton
$Tr$	Gas transfer constant
Tris	2-amino-2-hydroxymethyl-propane-1,3-diol
UP	Ultrapure
$U_x$	Uncertainty in assigned value
$V_0$	Initial sample volume
$V_a$	Volume of acid
$V_b$	Volume of base
$V_i$	Volume of titrant dispensed at titration point $i$
VINDTA	Versatile Instrument for the Determination of Total Inorganic Carbon and Titration Alkalinity for Analytical Laboratories
WEPAL	Wageningen Evaluating Programmes for Analytical Laboratories
$Xi_T$	Total concentration of organic alkalinity charge group $i$
$\alpha$	Degree of dissociation
$\lambda_{Ex}$	Excitation wavelength
$\lambda_{Em}$	Emission wavelength
$\lambda_{max}$	Wavelength of maximum absorbance
$\rho$	Titrant density ( $\text{g}\cdot\text{ml}^{-1}$ )
$\Omega$	Saturation state of calcium carbonate
$[H^+]$	Hydrogen ion concentration
$[H']$	Estimate of hydrogen ion concentration

# List of Tables

2.1	Degassing experimental results . . . . .	56
2.2	Choices of $K_{C_1}$ and $K_{C_2}$ provided in <i>OrgAlkCalc</i> . . . . .	70
2.3	<i>OrgAlkCalc</i> generated results of simulated seawater spiked with organic acid experiment . . . . .	72
2.4	Diluted CRM calibrated acid concentration with corresponding uncertainty in $\mu\text{mol.kg}^{-1}$ TA. . . . .	76
2.5	Concentrations of NaOH titrant over analysis period . . . . .	77
3.1	WEPAL inter-laboratory proficiency test results . . . . .	112
3.1	Comparison between reported TA values of identical seawater samples analysed in NOC and DCU. . . . .	114
3.2	Comparison of calculated and directly measured carbonate system variables . . . . .	116
4.1	<i>OrgAlkCalc</i> returned concentrations of OrgAlk charge group concentrations and associated apparent pK values. . . . .	154
4.2	Literature reported OrgAlk pKa values. . . . .	155
5.1	Spectrophotometric pH measurement validation measures . . . . .	163
5.2	Optical indices used to characterise DOM . . . . .	168
5.3	OrgAlk charge group pK values . . . . .	170
5.4	Carbonate system parameter values in Rogerstown Estuary over the study period	174
A1	Data used in <i>pyCO2SYS</i> . . . . .	8
A2	Observed optical properties of DOM in Rogerstown Estuary over the study period	9
A3	Recorded D.O. concentrations . . . . .	10

# List of Figures

1	Atmospheric levels of CO <sub>2</sub> . . . . .	20
2	Simplified diagram of the marine carbonate system . . . . .	22
3	Carbonate system Bjerrum plot . . . . .	24
4	Sources of OrgAlk in the coastal ocean . . . . .	28
2.1	TA and OrgAlk titration apparatus diagram . . . . .	102
2.2	Titration temperature throughout titrations . . . . .	103
2.3	Density as a function of temperature curves for titrant solutions . . . . .	103
2.4	NaOH titration curve for sodium acetate spiked synthetic seawater . . . . .	104
2.5	<i>OrgAlkCalc</i> generated results of simulated seawater spiked with organic acid experiment . . . . .	104
2.6	Diluted CRM calibrated acid concentration . . . . .	105
2.7	NaOH CO <sub>3</sub> <sup>2-</sup> content as a function of time . . . . .	106
2.8	Dye addition pH perturbation correction . . . . .	107
3.1	Comparison of reported versus assigned TA values for AQ15 inter-laboratory comparison exercise . . . . .	112
4.1	Map illustrating locations of sample acquisition in Dublin Bay and its associ- ated transitional waters. . . . .	130
4.2	Example NaOH titration curve fitting plot with associated residuals . . . . .	135
4.3	Impact of <i>CTNa</i> values on returned charge group acid-base properties . . . . .	138
4.4	TA and OrgAlk distributions within Dublin Bay classified by month. . . . .	140
5.1	Rogerstown Estuary sampling locations . . . . .	161
5.2	Charge group concentrations and associated apparent pK values . . . . .	169
5.3	OrgAlk effects on calculated carbonate chemistry parameters . . . . .	172
5.4	Carbonate system parameter distribution in Rogerstown Estuary across the study period . . . . .	175
5.5	Distribution of optical DOM signatures in Rogerstown Estuary . . . . .	178
A1	$\Delta \text{pH}_T$ as a function of X <sub>2</sub> concentration with respect to associated pK . . . . .	1

A2	$\Delta$ pCO <sub>2</sub> as a function of X <sub>2</sub> concentration with respect to associated pK . . . . .	2
A3	pCO <sub>2</sub> distributions . . . . .	3
A4	Biologically associated DOM distributions . . . . .	3
A5	X <sub>2</sub> as a function of <i>a</i> <sub>350</sub> . . . . .	4
A6	Example EEM plot . . . . .	5
A7	Predicted tidal height plots for Rogerstown Estuary . . . . .	6
A8	Predicted tidal height plots for Dublin Bay . . . . .	7



# **Carbonate chemistry and organic alkalinity in Irish coastal waters**

An investigation into the dynamics of organic alkalinity

**Daniel E. Kerr**

## **Abstract**

Total alkalinity (TA) is one of the four main carbonate system variables and is a conventionally measured parameter used to characterise marine water carbonate chemistry. It is an important indicator of a waterbody's buffering capacity and a measure of its ability to resist acidification, a matter of growing concern in the marine environment. Although TA is primarily associated with the inorganic components of seawater such as bicarbonate, there is a growing consensus that dissolved organic matter (DOM) can significantly contribute to TA in coastal waters. This organic fraction of TA (OrgAlk) is typically considered negligible and is not accounted for in conventional TA expressions. However, omission of OrgAlk can lead to the propagation of errors in subsequent carbonate system calculations and to misinterpretation of key carbonate chemistry descriptors such as calcium carbonate saturation states. This thesis provides an overview of OrgAlk contributions to TA and investigate the implications of its omission in carbonate system studies conducted in coastal waters. We examine the prevalence of OrgAlk across Irish coastal waters and the relationship between OrgAlk and key descriptors of biogeochemical processes. To achieve the aforementioned, we developed a Python based open-source software to estimate the quantity and acid-base properties of charge groups associated with OrgAlk for incorporation with established TA titration methods.

# Outline of Chapters

## Introduction

The introduction gives an overview of the marine carbonate system and details the topics discussed in this thesis. Additionally, the motivation and goals of this thesis are outlined.

## Chapter 1

This chapter contains the article "The influence of organic alkalinity on the carbonate system in coastal waters" published in the journal *Marine Chemistry* (Kerr et al., 2021). This article provides a literature review of the concept of organic alkalinity (OrgAlk), as well as an exploratory analysis of publicly available coastal and open ocean carbonate system data sets used to investigate the prevalence of OrgAlk. Additionally, analytical techniques to estimate the concentration and acid-base properties of OrgAlk charge groups are detailed.

## Chapter 2

This chapter outlines the analytical and computational procedures employed in the production of data presented in this thesis. TA measurement and analytical procedures are detailed, followed by a discussion of the modifications made to TA titration apparatus, reagents and computational procedures to facilitate OrgAlk analysis. Details of measures to adapt conventional carbonate system certified reference materials for use in the calibration and validation of TA measurements in transitional waters are given. OrgAlk titration procedures are given and the software programme *OrgAlkCalc* that allows for estimations of the concentrations and acid-base properties of OrgAlk charge groups using modified GOA-ON TA titration apparatus is detailed. Additionally, OrgAlk titration method validation is presented. Complementary carbonate system analysis involving DIC and pH measurement are discussed alongside ancillary dissolved organic matter optical property analysis techniques.

### **Chapter 3**

This chapter details participation in AQ-15, a seawater carbonate chemistry interlaboratory validation exercise ran by WEPAL-QAUSIMEME, Wageningen, the Netherlands. Additionally, details of a peer-based inter-laboratory validation exercise ran in collaboration with the Ocean BioGeosciences group at the National Oceanography Centre Southampton, European Way, Southampton SO14 3ZH, are discussed. Furthermore, results of an exercise to validate in situ  $p\text{CO}_2$  and pH measurements made by the Dublin Bay data buoy are given.

### **Chapter 4**

This chapter presents *OrgAlkalc*, an open source Python based programme that allows users of simply modified GOA-ON TA titration apparatus to measure TA as well as estimate the concentration and acid-base properties of charge groups associated with OrgAlk. The results generated through the use of *OrgAlkalc* using samples collected over an 8 month period (n=100) in Dublin Bay, Ireland are detailed, including distributions of TA over the study period, as well as details of the concentration and associated acid-base properties of OrgAlk charge groups.

### **Chapter 5**

This chapter presents an investigation of the carbonate system of a transitional water body, Rogerstown Estuary, Co. Dublin, Ireland, during low and high tides over a 5 week period. TA and OrgAlk analysis was conducted, along with spectrophotometric pH measurement. Measured TA and pH were used as input parameters in carbonate system calculations, with the impact of using OrgAlk adjusted and non-OrgAlk adjusted TA on calculated carbonate parameters investigated. Additionally, complementary optical analysis of dissolved organic matter was conducted in order to further elucidate the possible genesis and dynamics of OrgAlk in transitional waters.

### **Conclusion and Outlook**

The conclusion draws together the concepts and ideas presented in all preceding chapters, and suggests other research areas where they might also be applied. A discussion on the impact that this research could have on future developments in the implementation of OrgAlk characterisation methodologies to existing TA titration methods is also given.

**remove this page**

# Introduction

## 0.1 The marine carbonate system

Carbon is the fourth most abundant element by mass found within the known universe, yet it is arguably one of the most important and fundamental components of life on Earth. The global pools of carbon can be split into four intrinsically linked reservoirs: the hydrosphere, atmosphere, biosphere and lithosphere. The rate of interaction between each varies on scales of tens of thousands of years to rapid interactions well within the extent of human lifetimes (Holmes et al., 2006; Bianchi, 2007). The marine environment constitutes one of the largest pools of carbon, with the ocean containing 50 times as much carbon dioxide (CO<sub>2</sub>) as the present day atmosphere (Mackenzie et al., 2004). Atmospheric concentrations of CO<sub>2</sub> have been increasing over the past centuries; preindustrial atmospheric CO<sub>2</sub> concentrations are estimated to be around 270 ppm (Wigley, 1983), approximately 50% less than current levels, around 410 ppm (Dlugokencky et al., 2021). An increasing trend in atmospheric CO<sub>2</sub> has been documented since the 1960s at the Mauna Loa observatory on the Hawaiian islands, USA, and since the 1990s at Mace Head observatory, Galway, Ireland, as seen in figure 1 (Tans and Keeling, 2020). Seasonal variations in atmospheric CO<sub>2</sub> can be observed as the jagged oscillations that lie on the curve with these fluctuations attributed to seasonal changes in terrestrial ecosystems and to a lesser degree oceanic CO<sub>2</sub> uptake (Dettinger and Ghil, 1998). Although land based autotrophy exhibits measurable seasonal variability on CO<sub>2</sub> levels, the oceans play a much larger role in the long term regulation of atmospheric CO<sub>2</sub>.

It is estimated that the oceans have absorbed almost one third of all anthropogenic emitted CO<sub>2</sub> (Gruber et al., 2019), with the current fraction of stored emitted anthropogenic CO<sub>2</sub> approximated to be at one third of long term potential (Sabine et al., 2004). Ultimately, the value of atmospheric partial pressure of CO<sub>2</sub> (pCO<sub>2</sub>) is controlled by equilibration with dissolved inorganic carbon (DIC) present in the oceans (Raymond and Hamilton, 2018), highlighting the inextricably coupled nature of the atmospheric and oceanic carbon pools. Global carbonate system analysis has predominantly focused on understanding oceanic cycling of carbon and gaining an insight of where and for how long anthropogenic CO<sub>2</sub> is sequestered within the ocean (Sabine and Tanhua, 2010). However, the importance of the coastal ocean is increasingly coming to the fore in terms of regional and global carbon cycling (Kwon et al., 2021). The world's coastline covers  $26 \times 10^2 \text{ km}^2$ , or roughly 7% of the global ocean surface area (Gattuso et al., 1998), with about 40% of the world population living within 100 km of the coast (Liu et al., 2010). Other than anthropogenic influences, the coastal ocean is home to myriad of unique ecosystems that play a role in carbon cycling. Features such as coastal wetlands (Rogers et al., 2019), estuaries (Cai, 2011; Abril and Borges, 2005;

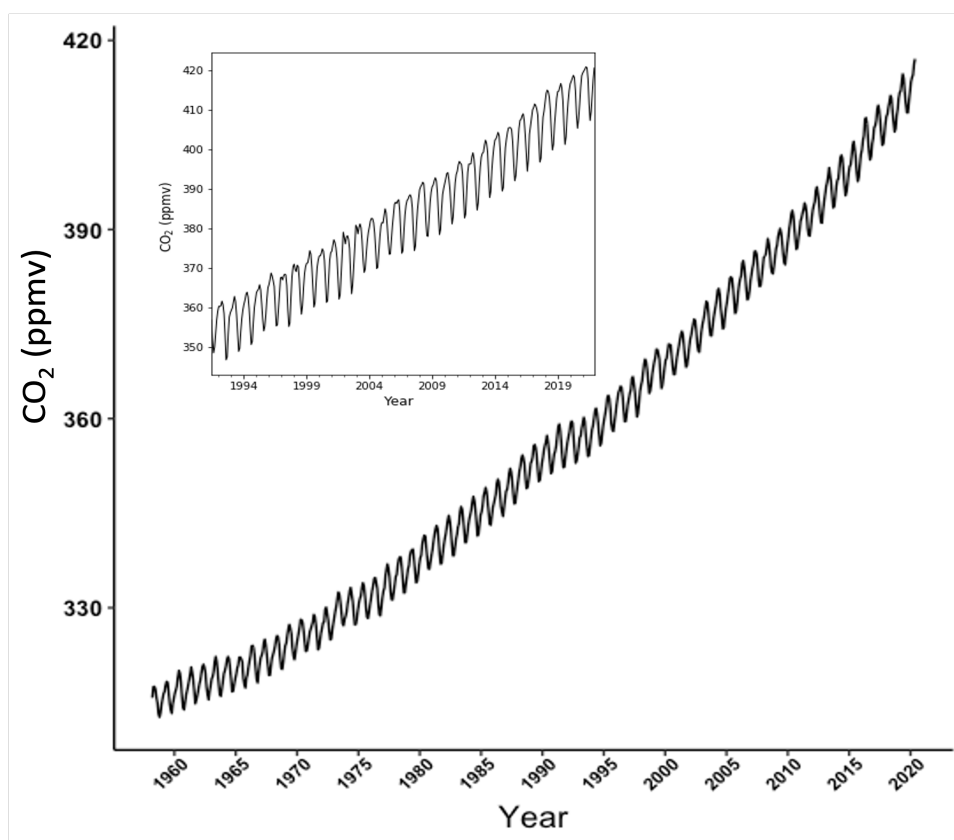


**Figure 1:** Atmospheric levels of CO<sub>2</sub> recorded at Mauna Loa Observatory, Hawaii, United States and Mace Head, Galway, Ireland (inset). Data available at <https://www.esrl.noaa.gov/gmd/ccgg/trends/data.html>

Borges, 2005) and near-shore benthic zones (Clark et al., 2017; Orekhova et al., 2019) are recognised as impacting carbonate system dynamics. It is becoming clearer that the coastal ocean plays a pivotal role in the global carbon cycle due to the dynamic nature of biogeochemical processes which take place in littoral zones, such as nutrient export to continental shelf waters (Bozec et al., 2012), the production and remineralisation of organic matter (OM) (Gattuso et al., 1998; Mackenzie et al., 2004) and the range of benthic processes which can act as sources or sinks of inorganic carbon, nutrients and OM (Abril et al., 1999). The aforementioned factors add to the complexity of the carbonate system in coastal waters and present challenges to its accurate analysis (Bauer et al., 2013).

## 0.2 Carbonate system parameters

The carbonate system in seawater can be described by four interlinked parameters: total alkalinity (TA), dissolved inorganic carbon (DIC), pH, and pCO<sub>2</sub>, see figure 2. By directly measuring two of the four parameters along with temperature, pressure and

salinity, and by utilising software *e.g.* CO2SYS (Lewis and Wallace, 1998) that links together the characterizations of relevant thermodynamic equilibria, it is therefore possible to calculate the remaining two parameters and obtain a complete picture of the system (Zeebe, 2012).

### 0.2.1 Total alkalinity

The alkaline nature of seawater has been recognised for centuries (Marsigli, 1725), although it is only within the last 40 years that the modern concept of seawater TA has been conceptualised and further refined (Dickson, 1981; Wolf-Gladrow et al., 2007). Commonly defined as the excess of proton acceptors over proton donors, a more appropriate definition of TA is the number of moles of hydrogen ion equivalent to the excess of proton acceptors over proton donors in 1 kilogram of sample (Dickson, 1981). In this case, proton acceptors are bases formed from weak acids with dissociation constants ( $K_a$ )  $\leq 10^{-4.5}$  and proton acceptors acids with  $K_a \geq 10^{-4.5}$  at zero ionic strength and at 25°C (Dickson, 1981). The conventional TA equation is given as:

$$\begin{aligned} \text{TA} = & [\text{HCO}_3^-] + 2[\text{CO}_3^{2-}] + [\text{B}(\text{OH})_4^-] + [\text{OH}^-] + [\text{HPO}_4^{2-}] \\ & + 2[\text{PO}_4^{3-}] + [\text{SiO}(\text{OH})_3^-] + [\text{NH}_3] + [\text{HS}^-] \\ & - [\text{H}^+] - [\text{HSO}_4^-] - [\text{HF}] - [\text{H}_3\text{PO}_4] + [\textit{minor bases} - \textit{minor acids}] \end{aligned} \quad (1)$$

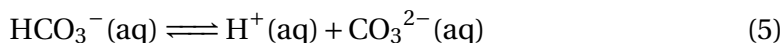
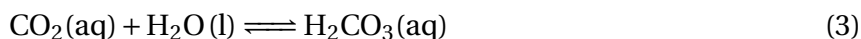
Carbonate and borate in their various stages of protonation constitute the main proton acceptors in the bulk of seawater (Dyrssen and Sillén, 1967). In the open ocean, surface TA is largely a function of salinity, with values typically ranging from approximately 2300 – 2350  $\mu\text{mol} \cdot \text{kg}^{-1}$  (Millero, 2007). In estuarine systems, TA values can differ significantly from oceanic values due to the bedrock morphology of its associated fluvial systems catchment area (McGrath et al., 2019) as well as land cover type (Raymond and Cole, 2003). Alkalinity in freshwater can originate from multiple sources: weathering of carbonate or silicate containing rocks, cation exchange reactions within soils, biological uptake and reduction of strong acids anions, precipitation of minerals and from atmospheric deposition (Mattson, 2014). The predominant input of alkalinity to inland waters is through bedrock weathering (Raymond and Hamilton, 2018).

### 0.2.2 Dissolved inorganic carbon

A substantial portion of inorganic carbon is found within the oceans, approximately 38,000 Pg C (Sundquist and Visser, 2003). Here the collective sum of all aqueous carbon dioxide ( $\text{CO}_2(\text{aq})$ ), carbonic acid ( $\text{H}_2\text{CO}_3$ ), bicarbonate ( $\text{HCO}_3^-$ ), and carbonate



( $\text{CO}_3^{2-}$ ) is termed DIC. As gaseous  $\text{CO}_2$  dissolves into solution, the following equilibrium reactions occur:



Typically, it is analytically difficult to distinguish between free  $\text{CO}_2(\text{aq})$  and  $\text{H}_2\text{CO}_3(\text{aq})$  (Dickson et al., 2007). At equilibrium with each other, the ratio of  $\text{H}_2\text{CO}_3(\text{aq})$  to  $\text{CO}_2(\text{aq})$  is roughly 1:1000 (Cole, 2013). Due to this, the sum of these species is termed  $\text{CO}_2^*(\text{aq})$ , which allows us to rewrite equations 2, 3 and 4 as:



Equation 6 refers to the solubility equilibrium of  $\text{CO}_2$  between air and seawater, while

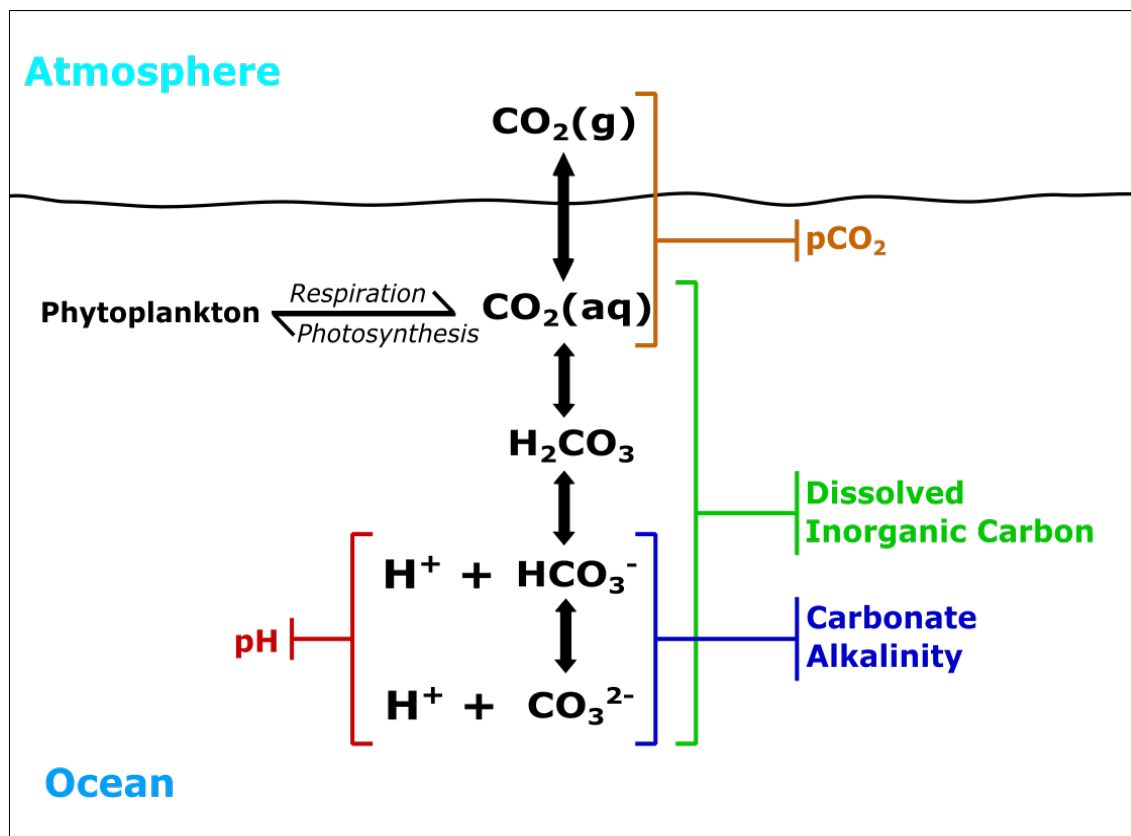


**Figure 2:** Simplified diagram illustrating the components of the marine carbonate system

equation 7 illustrates the acid dissociation reaction of  $\text{CO}_2(\text{aq})$  to yield  $\text{HCO}_3^-$  and a proton.  $\text{HCO}_3^-$  can further deprotonate to form  $\text{CO}_3^{2-}$ , as per equation 5. The concentration of  $\text{CO}_2(\text{aq})$  species is dependent on the temperature and chemical composition of seawater, primarily the concentrations of DIC and TA (Feely et al., 2007). The predominant species of inorganic carbon present is a function of pH, temperature, pressure and salinity, with the pH of seawater typically  $\approx 8.07$  (Jiang et al., 2019). At this pH and at the salinity ranges of most oceanic and coastal waters,  $\text{HCO}_3^-$  is predominant (Raymond and Hamilton, 2018), as can be seen from figure 3.

Natural pathways for DIC transport include the chemical weathering of the crustal material found within the lithosphere, which acts as both as a source and sink of carbon (Sundquist and Visser, 2003). Carbonate weathering consumes one mole of atmospheric  $\text{CO}_2$  for every two moles of  $\text{HCO}_3^-$  produced, whereas weathering of non-carbonate rocks, such as siliceous minerals, results in a one to one ratio of  $\text{CO}_2$  to  $\text{HCO}_3^-$  (Zeebe, 2012). The chemical weathering of carbonate containing minerals is a major source of  $\text{HCO}_3^-$  to coastal systems (Cole, 2013; Hieronymus and Walin, 2013). Other inputs of DIC to coastal systems also include water column or benthic respiration, groundwater inputs, photodegradation of dissolved organic matter (DOM) and inputs from intertidal marshes (Cai and Wang, 1998; Kemp et al., 1997; Neubauer and Anderson, 2003). DIC in estuarial waters typically undergoes seasonal variations (Raymond et al., 2000; McGrath et al., 2016), that are strongly linked to the temperature dependent metabolic action of both autotrophic and heterotrophic populations.

### 0.2.3 pH

pH is defined as the negative of the base 10 logarithm of the hydrogen ion concentration, or  $-\log_{10}[\text{H}^+]$ . It has been described as the master variable in many aquatic systems (Millero, 1986), influencing myriad of chemical processes: acid-base reactions, precipitation and dissolution reactions, redox reactions, as well as adsorption-desorption exchange reactions (Mattson, 2014; Riba et al., 2003). Although not a conservative parameter, the effects of temperature and pressure on pH can be estimated by measuring TA and DIC, which are both independent of temperature and pressure (Millero, 2013).

There are a number of pH scales which are used: Free ( $\text{pH}_F$ ), Total ( $\text{pH}_T$ ) and Seawater ( $\text{pH}_{\text{SWS}}$ ). The pH scale of the National Bureau of Standards ( $\text{pH}_{\text{NBS}}$ ), now called NIST, National Institute of Standards and Technology, is defined only for solutions that are traceable to buffers of low ionic strength, rendering it unsuitable for solutions of high ionic strength such as seawater. The  $\text{pH}_F$  includes only free hydrogen ion concentration (equation 8), while the  $\text{pH}_T$  includes the effect of the sulphate ion (equation 9).

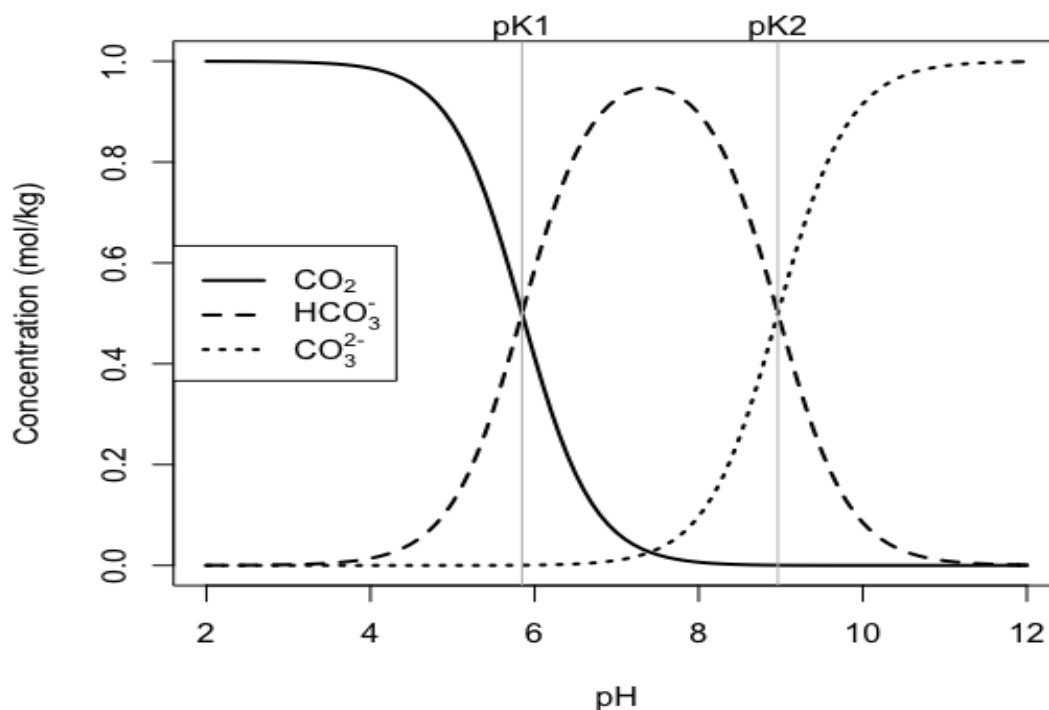


**Figure 3:** Bjerrum plot of the relative concentration of DIC species as a function of pH at 25°C. Plot constructed using *seacarb* R package (Gattuso et al., 2018).

pH<sub>SWS</sub> incorporates fluoride protonation products as well as the aforementioned ions (equation 10).

$$\text{pH}_F = -\log[\text{H}^+]_F \quad (8)$$

$$\text{pH}_T = -\log([\text{H}^+]_F + [\text{HSO}_4^-]) \quad (9)$$

$$\text{pH}_{\text{SWS}} = -\log([\text{H}^+]_F + [\text{HSO}_4^-] + [\text{HF}]) \quad (10)$$

At an absolute salinity of 35.165 and at 25°, the pH scales pH<sub>F</sub>, pH<sub>T</sub> and pH<sub>SWS</sub>, will give pH values of 8.195, 8.087, 8.078 respectively (Marion et al., 2011). As the concentrations of HSO<sub>4</sub><sup>-</sup> typically far exceeds that of HF, the discrepancy between pH<sub>T</sub> and pH<sub>SWS</sub> is small. As single ion activities cannot be measured unambiguously (Buck et al., 2010), the Total scale is recommended for use by marine chemists (Dickson et al., 2007; Marion et al., 2011). The matrix of buffers used to measure pH on the Total scale are of similar composition to seawater, therefore reducing liquid junction potential induced discrepancies (Dickson, 1984).

Compared to open ocean pH, pH values of coastal waters can vary drastically; on seasonal (Howland et al., 2000; Carstensen and Duarte, 2019), diel and tidal time scales

(Baumann and Smith, 2018; Raven et al., 2020). In regard to the coastal ocean, important factors that impact pH include biological activity (Millero, 2007; Rérolle et al., 2014) and TA discharge (McGrath et al., 2019; Raymond and Cole, 2003).

#### 0.2.4 Partial pressure of CO<sub>2</sub>

pCO<sub>2</sub> refers to the partial pressure of CO<sub>2</sub> in the gas phase that is in equilibrium with a seawater sample (Zeebe and Wolf-Gladrow, 2003). pCO<sub>2</sub> is often used in lieu of the fugacity of CO<sub>2</sub> (fCO<sub>2</sub>) as it is a directly measurable parameter. However, fCO<sub>2</sub> is the formally used parameter in carbonate system calculations as it accounts for the non-ideal behaviour of CO<sub>2</sub> gas. Fugacity can be described as a measure of the chemical potential of a constituent in the gas phase. If the fugacities of a chemical constituent in two separate masses which are in contact are unequal, then the chemical will be redistributed between the masses with net transfer of the constituent from areas of higher fugacity to lower fugacity (Murphy, 2015). For the purpose of this thesis the partial pressure of CO<sub>2</sub> will be discussed as it is a directly measurable parameter, investigated in multiple studies (Bozec et al., 2012; Cai et al., 2000; Cai and Wang, 1998; Gattuso et al., 1998; Hollibaugh and Smith, 1993; Mackenzie et al., 2004).

The difference between seawater (pCO<sub>2</sub><sup>SW</sup>) and atmospheric pCO<sub>2</sub> (pCO<sub>2</sub><sup>atm</sup>) is indicative of the direction of CO<sub>2</sub> flux (F<sub>CO<sub>2</sub></sub>):

$$F_{CO_2} = Tr * (pCO_2^{SW} - pCO_2^{atm}) \quad (11)$$

where *Tr* is a gas transfer coefficient (Wanninkhof, 2014). If pCO<sub>2</sub><sup>SW</sup> is greater than pCO<sub>2</sub><sup>atm</sup> there will be evasion of CO<sub>2</sub> and if pCO<sub>2</sub><sup>atm</sup> is greater than pCO<sub>2</sub><sup>SW</sup> there will be invasion of CO<sub>2</sub>. The importance of pCO<sub>2</sub> is evident in the fact that it gives an indication of the direction of CO<sub>2</sub> movement, as well as providing insight into the metabolic state of a waterbody. In coastal waters pCO<sub>2</sub> concentrations typically follow the salinity gradient as river waters tend to be supersaturated with respect to CO<sub>2</sub> (Raymond et al., 2000). The distribution of CO<sub>2</sub> in estuaries is a function of physical mixing between CO<sub>2</sub> supersaturated freshwaters with seawater, heterotrophy in upper estuary waters and CO<sub>2</sub> evasion to the atmosphere. Typically, if river plumes are well mixed on an inner shelf, they will act as a CO<sub>2</sub> source (Borges and Frankignoulle, 2002; Borges, 2005), with this likely due to rapid respiration of OM and mixing with CO<sub>2</sub> saturated waters. Furthermore, seasonal variation in the flux of river output can affect the status of an estuary as a sink or source of CO<sub>2</sub>. At northern latitudes, drier summer months can cause a decreased volume of river discharge resulting in increases in the residence time of river waters and hence OM, facilitating enhanced heterotrophic respiration and CO<sub>2</sub>

generation (Bozec et al., 2012). As the ionic strength of rivers is drastically different to that of oceanic waters, haline stratification can occur in estuarial zones. A consequence of this in marginally mixed systems is that the less dense, nutrient and OM rich river water can form an upper layer above more dense saline waters, providing an optimal environment for DIC consuming autotrophic organisms (Bozec et al., 2012), thus decreasing  $p\text{CO}_2$ .

### 0.3 Carbonate system measurement quality goals

Although theoretically any two carbonate system parameters can be used as input parameters in carbonate calculations, conventionally TA and DIC are used as they can be measured within a relatively low degree of uncertainty (Dickson et al., 2003; Mintrop, 2016). TA is particularly appealing as an input parameters alongside DIC or pH as it is not altered with  $\text{CO}_2$  transfer, unlike the aforementioned that can fluctuate with  $\text{CO}_2$  invasion or evasion. Acceptable levels of uncertainty associated with each parameter with respect to their use in the calculation of key descriptors of ocean acidification have been established by the Global Ocean Acidification Observing Network (GOA-ON) (Newton et al., 2014). The acceptable levels of uncertainty can be classified based on two measurement quality goals; "Climate" and "Weather". "Climate" can be defined as carbonate system parameter measurements of sufficient quality to be utilised in the computation of key descriptors of ocean acidification used to assess long term trends over multi-decadal timescales. "Weather" can be described as measurements of sufficient quality to be used in the identification of relative spatial patterns and short-term variations in acidification. The "Climate" acceptable levels of uncertainty for pH,  $p\text{CO}_2$ , TA and DIC are 0.003 pH units, 0.5% and  $2 \mu\text{mol} \cdot \text{kg}^{-1}$  for both TA and DIC, respectively. The "Weather" acceptable levels of uncertainty for pH,  $p\text{CO}_2$ , TA and DIC are 0.02 pH units, 2.5% and  $10 \mu\text{mol} \cdot \text{kg}^{-1}$  for both TA and DIC, respectively. "Climate" level precision is a challenging task and is currently only achieved by a very limited number of carbonate chemistry laboratories (Newton et al., 2014).

### 0.4 Ocean Acidification

A phenomena of growing importance inextricably linked to seawater carbonate chemistry is ocean acidification. Due to the oceans uptake of atmospheric  $\text{CO}_2$  since the industrial revolution, surface ocean  $\text{pH}_T$  has fallen by approximately 0.1 pH units (Caldeira and Wickett, 2003; Jiang et al., 2019). This decrease in pH is largely driven by the release of protons upon the reaction of  $\text{CO}_2$  with water, as per equation 7. A decrease in pH

causes a decrease in carbonate ion concentration *i.e.* a shift to the right in figure 3. As carbonate ion concentration decreases, this results in a decrease in the saturation state of calcium carbonate ( $\Omega$ ):

$$\Omega = \frac{[\text{Ca}^{2+}][\text{CO}_3^{2-}]}{K_{\text{sp}}} \quad (12)$$

where  $K_{\text{sp}}$  is the temperature and salinity dependant solubility constant of calcite or aragonite (Zeebe, 2012). Both of the aforementioned are polymorphs of calcium carbonate or different crystalline structures of the same substance.  $\Omega$  is an important parameter commonly used to track ocean acidification. Seawater is classed as being undersaturated with respect to calcium carbonate when  $\Omega < 1$ , with these conditions corrosive to calcifying organisms (Corliss and Honjo, 1981). This shift to more acidic conditions has major ramifications for carbonate chemistry and in turn calcifying organisms (Orr et al., 2005; Langer et al., 2006), with knock on effects to entire ecosystems.

## 0.5 Organic Alkalinity

As aforementioned, due to its relative ease of sampling and low degree of analytical uncertainty, TA is a predominately measured carbonate system parameter. It is measured across a diverse array of environments, from ocean wide hydrographic cruises (Lauvset et al., 2016; Wanninkhof et al., 2012) to smaller scale coastal ocean settings (Ortega et al., 2005; Rassmann et al., 2020; Rosentreter and Eyre, 2020). TA is usually assumed to be made up of both carbonate and non-carbonate inorganic seawater components, with accurate information on the total concentrations and dissociation constants of all seawater acid-base species required if carbonate system calculations involving TA are to be free of inherent uncertainty (Riebesell et al., 2010). Growing evidence suggests that organic species contained within the [*minor bases – minor acids*] term in equation 1 can contribute significantly to TA (Fong and Dickson, 2019; Kerr et al., 2021). This contribution of organic species is termed organic alkalinity (OrgAlk). OrgAlk can be thought of as titratable charge groups present on DOM with specific acid-base properties, with the molecules typically associated with OrgAlk including humic substances, carboxylic acids, amines and phenols (Cai et al., 1998; Rigobello-Masini and Masini, 2001; Muller and Bleie, 2008; Paxéus and Wedborg, 1985; Emerson and Hedges, 2008). OrgAlk has been observed to arise from an array of heterogeneous sources: terrestrially derived DOM (Hammer et al., 2017; Hunt et al., 2011; Tishchenko et al., 2006), phytoplankton (Kim and Lee, 2009), groundwater discharge (Song et al., 2020), intertidal marshes (Cai and Wang, 1998; Wang et al., 2016) and coastal sediment porewater (Lukawska-Matuszewska, 2016). In the coastal ocean DOM concen-

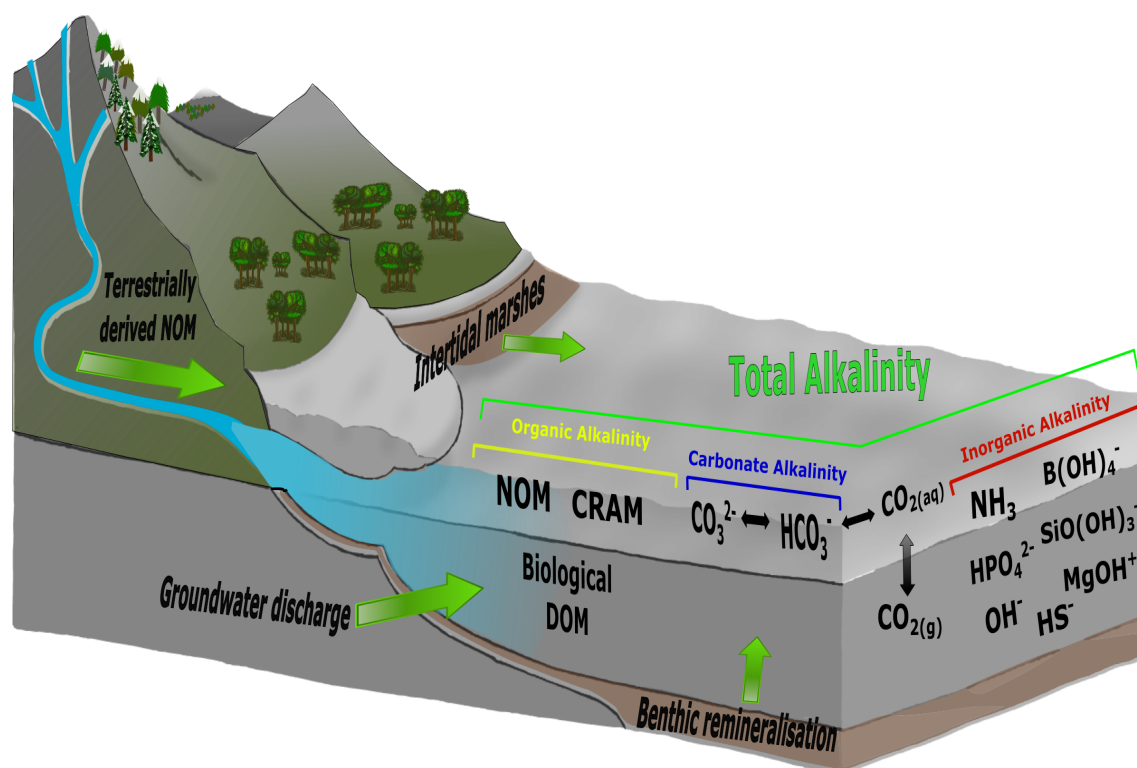


**Figure 4:** Simplified diagram illustrating the different components of TA in the coastal ocean. Green arrows indicate reported sources of OrgAlk. Taken from Kerr et al. (2021).

trations can be elevated due to terrestrial discharge and biological inputs (Lee et al., 2020; Reader et al., 2014). Consequently, the impact of OrgAlk on TA is recognised to be elevated in coastal waters (Tishchenko et al., 2006; Delaigue et al., 2020; Song et al., 2020; Lukawska-Matuszewska et al., 2018).

OrgAlk poses a challenge to the use of TA as an input parameter in carbonate system calculations of coastal seawater from two aspects: as an analytical interference in TA analysis (Sharp and Byrne, 2020) and as an unaccounted for acid-base species term in equation 1. Errors associated with using non-OrgAlk adjusted TA as an input parameter in carbonate system calculations have been recognised (Hu, 2020; Kuliński et al., 2014; Koeve and Oschlies, 2012). Evidently, OrgAlk will impact the suitability of TA as an input parameter with respect to the measurement quality goals outlined in section 0.3. This underlines the importance of ascertaining the acid-base properties of OrgAlk as to constrain possible detrimental impacts on coastal carbonate chemistry investigations.

## 0.6 Motivation and goals

Given the growing acceptance that OrgAlk plays a non-negligible role in TA measurement in coastal waters, methods to investigate the influence of OrgAlk are of significant

interest to coastal ocean carbonate system investigators. Many methods to directly quantify OrgAlk charge group concentrations and gain insight into their associated acid-base properties involve the use of high-cost apparatus and complicated computational procedures involving closed-source, proprietary software programmes. Evidently there is a need for analytical procedures that utilise low-cost, easily accessible apparatus that can be used in conjunction with open-source, freely available OrgAlk computational software programmes. Addressing these issues is the motivation of this thesis and dictated the direction of research. To explore the identified gap in OrgAlk knowledge as well as carbonate chemistry in coastal waters the following were conducted and are detailed in this thesis:

- An assessment of the current literature consensus on OrgAlk, identification of best practice analytical procedures and an investigation into the prevalence of OrgAlk through exploratory data analysis of publicly available open and coastal ocean carbonate system datasets.
- The establishment of TA and OrgAlk titration procedures based on the use of inexpensive and widely available GOA-ON listed apparatus.
- Construction of computational procedures used for TA and OrgAlk data processing using freely available open-source software with goal of open access availability.
- Validation of TA methodology through participation in independent and collaborative inter-laboratory comparison exercises, confirming the quality of produced data for inclusion in "Weather" carbonate system measurement studies.
- Validation of carbonate chemistry analytical instrumentation utilised in PREDICT, an inter-institutional multidisciplinary project focusing on coastal monitoring in Dublin Bay.
- Utilisation of established OrgAlk analytical and computational procedures to investigate the quantity and acid-base properties of OrgAlk in Irish coastal waters with a focus on the effect on carbonate system calculations.

## References

Abril, G. and Borges, A. V. (2005). Carbon Dioxide and Methane Emissions from Estuaries. In *Greenhouse Gas Emissions — Fluxes and Processes*. Tremblay A., Varfalvy L., Roehm C., Garneau M. (eds), chapter 7, pages 188–207.



- Abril, G., Etcheber, H., Le Hir, P., Bassoullet, P., Boutier, B., and Frankignoulle, M. (1999). Oxic/anoxic oscillations and organic carbon mineralization in an estuarine maximum turbidity zone (The Gironde, France). *Limnology and Oceanography*, 44(5):1304–1315.
- Bauer, J. E., Cai, W. J., Raymond, P. A., Bianchi, T. S., Hopkinson, C. S., and Regnier, P. A. (2013). The changing carbon cycle of the coastal ocean. *Nature*, 504(7478):61–70.
- Baumann, H. and Smith, E. M. (2018). Quantifying Metabolically Driven pH and Oxygen Fluctuations in US Nearshore Habitats at Diel to Interannual Time Scales. *Estuaries and Coasts*, 41(4):1102–1117.
- Bianchi, T. S. (2007). *Biogeochemistry of Estuaries*. Oxford University Press.
- Borges, A. V. (2005). Do We Have Enough Pieces of the Jigsaw to Integrate CO<sub>2</sub> Fluxes in the Coastal Ocean? *Estuaries*, 28(1):3–27.
- Borges, A. V. and Frankignoulle, M. (2002). Aspects of dissolved inorganic carbon dynamics in the upwelling system off the Galician coast. *Journal of Marine Systems*, 32(1-3):181–198.
- Bozec, Y., Cariou, T., Macé, E., Morin, P., Thuillier, D., and Vernet, M. (2012). Seasonal dynamics of air-sea CO<sub>2</sub> fluxes in the inner and outer Loire estuary (NW Europe). *Estuarine, Coastal and Shelf Science*, 100:58–71.
- Buck, R., Rondinini, S., Covington, A., Baucke, F., Brett, C., Camões, M., Milton, M., Mussini, T., Naumann, R., Pratt, K., Spitzer, P., and Wilson, G. (2010). Measurement of pH Definition, Standards, and Procedures. *Handbook of Biochemistry and Molecular Biology, Fourth Edition*, 74(11):675–692.
- Cai, W.-J. (2011). Estuarine and Coastal Ocean Carbon Paradox: CO<sub>2</sub> Sinks or Sites of Terrestrial Carbon Incineration? *Annual Review of Marine Science*, 3(1):123–145.
- Cai, W.-j. and Wang, Y. (1998). The chemistry, fluxes, and sources of carbon dioxide in the estuarine waters of the Satilla and Altamaha Rivers, Georgia. 43(4):657–668.
- Cai, W. J., Wang, Y., and Hodson, R. E. (1998). Acid-base properties of dissolved organic matter in the estuarine waters of Georgia, USA. *Geochimica et Cosmochimica Acta*, 62(3):473–483.
- Cai, W. J., Wiebe, W. J., Wang, Y., and Sheldon, J. E. (2000). Intertidal marsh as a source of dissolved inorganic carbon and a sink of nitrate in the Satilla River-estuarine complex in the southeastern U.S. *Limnology and Oceanography*, 45(8):1743–1752.
- Caldeira, K. and Wickett, M. E. (2003). Anthropogenic carbon and ocean pH. *Nature*, 425(September):2003.
- Carstensen, J. and Duarte, C. M. (2019). Drivers of pH Variability in Coastal Ecosystems. *Environmental Science and Technology*, 53(8):4020–4029.

- Clark, J. B., Long, W., and Hood, R. R. (2017). Estuarine Sediment Dissolved Organic Matter Dynamics in an Enhanced Sediment Flux Model. *Journal of Geophysical Research: Biogeosciences*, 122(10):2669–2682.
- Cole, J. J. (2013). *Chapter 6. The Carbon Cycle*. Elsevier Inc., first edit edition.
- Corliss, B. H. and Honjo, S. (1981). Dissolution of Deep-Sea Benthonic Foraminifera. *Micropaleontology*, 27(4):356.
- Delaigue, L., Thomas, H., and Mucci, A. (2020). Spatial variations in CO<sub>2</sub> fluxes in the Saguenay Fjord (Quebec, Canada) and results of a water mixing model. *Biogeosciences*, 17(2):547–566.
- Dettinger, M. D. and Ghil, M. (1998). Seasonal and interannual variations of atmospheric CO<sub>2</sub> and climate. *Tellus, Series B: Chemical and Physical Meteorology*, 50(1):1–24.
- Dickson, A. G. (1981). An exact definition of total alkalinity and a procedure for the estimation of alkalinity and total inorganic carbon from titration data. *Deep Sea Research Part A, Oceanographic Research Papers*, 28(6):609–623.
- Dickson, A. G. (1984). pH scales and proton-transfer reactions in saline media such as sea water. *Geochimica et Cosmochimica Acta*, 48(11):2299–2308.
- Dickson, A. G., Afghan, J. D., and Anderson, G. C. (2003). Reference materials for oceanic CO<sub>2</sub> analysis: A method for the certification of total alkalinity. *Marine Chemistry*, 80(2-3):185–197.
- Dickson, A. G., Sabine, C. L., and Christian, J. R. (2007). *Guide to Best Practices for Ocean CO<sub>2</sub> Measurements*. Number 8.
- Dlugokencky, E., Mund, J., Crotwell, A., Crotwell, M., and Thoning, K. (2021). Atmospheric Carbon Dioxide Dry Air Mole Fractions from the NOAA GML Carbon Cycle Cooperative Global Air Sampling Network, 1968-2020, Version: 2021-07-30.
- Dyrssen, D. and Sillén, L. G. (1967). Alkalinity and total carbonate in sea water. A plea for p-T-independent data - Dyrssen - 2010 - Tellus - Wiley Online Library. *Tellus*.
- Emerson, S. and Hedges, J. I. (2008). *Chemical Oceanography and the Marine Carbon Cycle*. Cambridge University Press.
- Feely, R. A., Sabine, C. L., and Wanninkhof, R. (2007). Uptake and Storage of Carbon Dioxide in the Ocean: The Global CO<sub>2</sub> Survey. pages 1–15.
- Fong, M. B. and Dickson, A. G. (2019). Insights from GO-SHIP hydrography data into the thermodynamic consistency of CO<sub>2</sub> system measurements in seawater. *Marine Chemistry*, 211(January):52–63.
- Gattuso, J.-P., Epitalon, J.-M., Lavigne, H., and Orr, J. (2018). Seacarb: seawater carbonate chemistry. R package version 3.2.10.

- Gattuso, J. P., Frankignoulle, M., and Wollast, R. (1998). Carbon and carbonate metabolism in coastal aquatic ecosystems. *Annual Review of Ecology and Systematics*, 29:405–434.
- Gruber, N., Clement, D., Carter, B. R., Feely, R. A., van Heuven, S., Hoppema, M., Ishii, M., Key, R. M., Kozyr, A., Lauvset, S. K., Monaco, C. L., Mathis, J. T., Murata, A., Olsen, A., Perez, F. F., Sabine, C. L., Tanhua, T., and Wanninkhof, R. (2019). The oceanic sink for anthropogenic CO<sub>2</sub> from 1994 to 2007. *Science*, 363(6432):1193–1199.
- Hammer, K., Schneider, B., Kuliński, K., and Schulz-Bull, D. E. (2017). Acid-base properties of Baltic Sea dissolved organic matter. *Journal of Marine Systems*, 173:114–121.
- Hieronymus, J. and Walin, G. (2013). Unravelling the land source: An investigation of the processes contributing to the oceanic input of DIC and alkalinity. *Tellus, Series B: Chemical and Physical Meteorology*, 65(1):1–10.
- Hollibaugh, J. T. and Smith, S. (1993). Coastal Metabolism and the Oceanic Carbon Balance. (92):75–89.
- Holmes, D. E., Chaudhuri, S. K., Nevin, K. P., Mehta, T., Methé, B. A., Liu, A., Ward, J. E., Woodard, T. L., Webster, J., and Lovley, D. R. (2006). Microarray and genetic analysis of electron transfer to electrodes in *Geobacter sulfurreducens*. *Environmental Microbiology*, 8(10):1805–1815.
- Howland, R. J., Tappin, A. D., Uncles, R. J., Plummer, D. H., and Bloomer, N. J. (2000). Distributions and seasonal variability of pH and alkalinity in the Tweed Estuary, UK. *Science of the Total Environment*, 251(252):125–138.
- Hu, X. (2020). Effect of Organic Alkalinity on Seawater Buffer Capacity: A Numerical Exploration. *Aquatic Geochemistry*, (0123456789).
- Hunt, C. W., Salisbury, J. E., and Vandemark, D. (2011). Contribution of non-carbonate anions to total alkalinity and overestimation of pCO<sub>2</sub> in New England and New Brunswick rivers. *Biogeosciences*, 8(10):3069–3076.
- Jiang, L. Q., Carter, B. R., Feely, R. A., Lauvset, S. K., and Olsen, A. (2019). Surface ocean pH and buffer capacity: past, present and future. *Scientific Reports*, 9(1):1–11.
- Kemp, W. M., Smith, E. M., Marvin-DiPasquale, M., and Boynton, W. R. (1997). Organic carbon balance and net ecosystem metabolism in Chesapeake Bay. *Marine Ecology Progress Series*, 150(1-3):229–248.
- Kerr, D. E., Brown, P. J., Grey, A., and Kelleher, B. P. (2021). The influence of organic alkalinity on the carbonate system in coastal waters. *Marine Chemistry*, 237:104050.
- Kim, H. C. and Lee, K. (2009). Significant contribution of dissolved organic matter to seawater alkalinity. *Geophysical Research Letters*, 36(20):1–5.
- Koeve, W. and Oschlies, A. (2012). Potential impact of DOM accumulation on f CO<sub>2</sub> and carbonate ion computations in ocean acidification experiments. *Biogeosciences*, 9(10):3787–3798.

- Kuliński, K., Schneider, B., Hammer, K., Machulik, U., and Schulz-Bull, D. (2014). The influence of dissolved organic matter on the acid-base system of the Baltic Sea. *Journal of Marine Systems*, 132:106–115.
- Kwon, E. Y., DeVries, T., Galbraith, E. D., Hwang, J., Kim, G., and Timmermann, A. (2021). Stable Carbon Isotopes Suggest Large Terrestrial Carbon Inputs to the Global Ocean. *Global Biogeochemical Cycles*, 35(4):1–25.
- Langer, G., Geisen, M., Baumann, K. H., Kläs, J., Riebesell, U., Thoms, S., and Young, J. R. (2006). Species-specific responses of calcifying algae to changing seawater carbonate chemistry. *Geochemistry, Geophysics, Geosystems*, 7(9).
- Lauvset, S. K., Key, R. M., Olsen, A., Van Heuven, S., Velo, A., Lin, X., Schirnick, C., Kozyr, A., Tanhua, T., Hoppema, M., Jutterström, S., Steinfeldt, R., Jeansson, E., Ishii, M., Perez, F. E., Suzuki, T., and Watelet, S. (2016). A new global interior ocean mapped climatology: The  $1^\circ \times 1^\circ$  GLODAP version 2. *Earth System Science Data*, 8(2):325–340.
- Lee, S. A., Kim, T. H., and Kim, G. (2020). Tracing terrestrial versus marine sources of dissolved organic carbon in a coastal bay using stable carbon isotopes. *Biogeosciences*, 17(1):135–144.
- Lewis, E. R. and Wallace, D. W. R. (1998). Program Developed for CO<sub>2</sub> System Calculations.
- Liu, K.-K., Atkinson, L., Quiñones, R. A., and Talaue-McManus, L. (2010). *Biogeochemistry of Continental Margins in a Global Context*.
- Lukawska-Matuszewska, K. (2016). Contribution of non-carbonate inorganic and organic alkalinity to total measured alkalinity in pore waters in marine sediments (Gulf of Gdansk, S-E Baltic Sea). *Marine Chemistry*, 186:211–220.
- Lukawska-Matuszewska, K., Grzybowski, W., Szewczun, A., and Tarasiewicz, P. (2018). Constituents of organic alkalinity in pore water of marine sediments. *Marine Chemistry*, 200:22–32.
- Mackenzie, F. T., Lerman, A., and Andersson, A. J. (2004). Past and present of sediment and carbon biogeochemical cycling models. *Biogeosciences*, 1(1):11–32.
- Marion, G. M., Millero, F. J., Camões, M. F., Spitzer, P., Feistel, R., and Chen, C. T. (2011). PH of seawater. *Marine Chemistry*, 126(1-4):89–96.
- Marsigli, L. F. (1725). *Histoire physique de la mer: Ouvrage enrichi de figures dessinées d'après le naturel*. aux dépens de la Compagnie.
- Mattson, M. (2014). *Alkalinity of Freshwater*. Number August. Elsevier Inc.
- McGrath, T., McGovern, E., Cave, R. R., and Kivimäe, C. (2016). The Inorganic Carbon Chemistry in Coastal and Shelf Waters Around Ireland. *Estuaries and Coasts*, 39(1):27–39.

- McGrath, T., McGovern, E., Gregory, C., and Cave, R. R. (2019). Local drivers of the seasonal carbonate cycle across four contrasting coastal systems. *Regional Studies in Marine Science*, 30:100733.
- Millero, F. (2013). *Chemical Oceanography, Fourth Edition*.
- Millero, F. J. (1986). The pH of estuarine waters. *Limnology and Oceanography*, 31(4):839–847.
- Millero, F. J. (2007). The marine inorganic carbon cycle. *Chemical Reviews*, 107(2):308–341.
- Mintrop, L. (2016). *VINDTA Manual for Versions 3S and 3C*. 3.5 edition.
- Muller, F. L. and Bleie, B. (2008). Estimating the organic acid contribution to coastal seawater alkalinity by potentiometric titrations in a closed cell. *Analytica Chimica Acta*, 619(2):183–191.
- Murphy, B. L. (2015). *Chemical Partitioning and Transport in the Environment*. Elsevier Ltd, third edit edition.
- Neubauer, S. C. and Anderson, I. C. (2003). Transport of dissolved inorganic carbon from a tidal freshwater marsh to the York River estuary. *Limnology and Oceanography*, 48(1 D):299–307.
- Newton, J., Feely, R. A., Jewett, E., Williamson, P., and Mathis, J. (2014). *Global Ocean Acidification Observing Network: requirements and governance Plan*. Number October.
- Orekhova, N. A., Konovalov, S. K., and Medvedev, E. V. (2019). Features of inorganic carbon regional balance in marine ecosystems under anthropogenic pressure. *Physical Oceanography*, 26(3):225–235.
- Orr, J. C., Fabry, V. J., Aumont, O., Bopp, L., Doney, S. C., Feely, R. A., Gnanadesikan, A., Gruber, N., Ishida, A., Joos, F., Key, R. M., Lindsay, K., Maier-Reimer, E., Matear, R., Monfray, P., Mouchet, A., Najjar, R. G., Plattner, G. K., Rodgers, K. B., Sabine, C. L., Sarmiento, J. L., Schlitzer, R., Slater, R. D., Totterdell, I. J., Weirig, M. F., Yamanaka, Y., and Yool, A. (2005). Anthropogenic ocean acidification over the twenty-first century and its impact on calcifying organisms. *Nature*, 437(7059):681–686.
- Ortega, T., Ponce, R., Forja, J., and Gómez-Parra, A. (2005). Fluxes of dissolved inorganic carbon in three estuarine systems of the Cantabrian Sea (north of Spain). *Journal of Marine Systems*, 53(1-4):125–142.
- Paxéus, N. and Wedborg, M. (1985). Acid-base properties of aquatic fulvic acid. *Analytica Chimica Acta*, 169(C):87–98.
- Rassmann, J., Eitel, E. M., Lansard, B., Cathalot, C., Brandily, C., Taillefert, M., and Rabouille, C. (2020). Benthic alkalinity and dissolved inorganic carbon fluxes in the Rhône River prodelta generated by decoupled aerobic and anaerobic processes. *Biogeosciences*, 17(1):13–33.

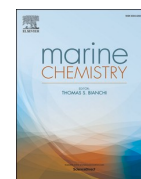
- Raven, J. A., Gobler, C. J., and Hansen, P. J. (2020). Dynamic CO<sub>2</sub> and pH levels in coastal, estuarine, and inland waters: Theoretical and observed effects on harmful algal blooms. *Harmful Algae*, 91(March):101594.
- Raymond, P. A., Bauer, J. E., and Cole, J. J. (2000). Atmospheric CO<sub>2</sub> evasion, dissolved inorganic carbon production, and net heterotrophy in the York River estuary. *Limnology and Oceanography*, 45(8):1707–1717.
- Raymond, P. A. and Cole, J. J. (2003). Increase in the export of alkalinity from North America's largest river. *Science*, 301(5629):88–91.
- Raymond, P. A. and Hamilton, S. K. (2018). Anthropogenic influences on riverine fluxes of dissolved inorganic carbon to the oceans. *Limnology and Oceanography Letters*, 3(3):143–155.
- Reader, H. E., Stedmon, C. A., and Kritzberg, E. S. (2014). Seasonal contribution of terrestrial organic matter and biological oxygen demand to the Baltic Sea from three contrasting river catchments. *Biogeosciences*, 11(12):3409–3419.
- Rérolle, V. M. C., Ribas-Ribas, M., Kitidis, V., Brown, I., Bakker, D. C. E., Lee, G. A., Shi, T., Mowlem, M. C., and Achterberg, E. P. (2014). Controls on pH in surface waters of northwestern European shelf seas. *Biogeosciences Discussions*, 11(1):943–974.
- Riba, I., García-Luquea, R. E., Blasco, J., and DelValls, T. A. (2003). Bioavailability of heavy metals bound to estuarine sediments as a function of pH and salinity values. *Chemical Speciation and Bioavailability*, 15(4):101–114.
- Riebesell, U., Fabry, V. J., and Hansson, L. (2010). *Guide to best practices for ocean acidification research and data reporting*.
- Rigobello-Masini, M. and Masini, J. C. (2001). Application of modified Gran functions and derivative methods to potentiometric acid titration studies of the distribution of inorganic carbon species in cultivation medium of marine microalgae. *Analytica Chimica Acta*, 448(1-2):239–250.
- Rogers, K., Kelleway, J. J., Saintilan, N., Megonigal, J. P., Adams, J. B., Holmquist, J. R., Lu, M., Schile-Beers, L., Zawadzki, A., Mazumder, D., and Woodroffe, C. D. (2019). Wetland carbon storage controlled by millennial-scale variation in relative sea-level rise. *Nature*, 567(7746):91–95.
- Rosentreter, J. A. and Eyre, B. D. (2020). Alkalinity and dissolved inorganic carbon exports from tropical and subtropical river catchments discharging to the Great Barrier Reef, Australia. *Hydrological Processes*, 34(7):1530–1544.
- Sabine, C. L., Feely, R. A., Gruber, N., Key, R. M., Lee, K., Bullister, J. L., Wanninkhof, R., Wong, C., Wallace, D., Tilbrook, B., Millero, F. J., Peng, T.-H., Kozyer, A., Ono, T., and Rios, A. F. (2004). The Oceanic Sink for Anthropogenic CO<sub>2</sub>. *Science*, 305(July):5–12.
- Sabine, C. L. and Tanhua, T. (2010). Estimation of anthropogenic CO<sub>2</sub> inventories in the ocean. *Annual Review of Marine Science*, 2(1):175–198.

- Sharp, J. D. and Byrne, R. H. (2020). Interpreting measurements of total alkalinity in marine and estuarine waters in the presence of proton-binding organic matter. *Deep-Sea Research Part I*.
- Song, S., Wang, Z. A., Gonnee, M. E., Kroeger, K. D., Chu, S. N., Li, D., and Liang, H. (2020). An important biogeochemical link between organic and inorganic carbon cycling: Effects of organic alkalinity on carbonate chemistry in coastal waters influenced by intertidal salt marshes. *Geochimica et Cosmochimica Acta*, 275:123–139.
- Sundquist, E. T. and Visser, K. (2003). The Geologic History of the Carbon Cycle. In *Treatise on Geochemistry*, volume 8-9, pages 425–472.
- Tans, P. and Keeling, R. (2020). Mauna Loa Observatory Atmospheric Carbon Dioxide Measurements.
- Tishchenko, P. Y., Wallmann, K., Vasilevskaya, N. A., Volkova, T. I., Zvalinskii, V. I., Khodorenko, N. D., and Shkirnikova, E. M. (2006). The contribution of organic matter to the alkaline reserve of natural waters. *Oceanology*, 46(2):192–199.
- Wang, Z. A., Kroeger, K. D., Ganju, N. K., Gonnee, M. E., and Chu, S. N. (2016). Intertidal salt marshes as an important source of inorganic carbon to the coastal ocean. *Limnology and Oceanography*, 61(5):1916–1931.
- Wanninkhof, R. (2014). Relationship between wind speed and gas exchange over the ocean revisited. *Limnology and Oceanography: Methods*, 12(JUN):351–362.
- Wanninkhof, R., Wood, M., and Barbero, L. (2012). Cruise Report: Gulf of Mexico and East Coast Carbon Cruise #2 (GOMECC-2). 2.
- Wigley, T. M. (1983). The pre-industrial carbon dioxide level. *Climatic Change*, 5(4):315–320.
- Wolf-Gladrow, D. A., Zeebe, R. E., Klaas, C., Körtzinger, A., and Dickson, A. G. (2007). Total alkalinity: The explicit conservative expression and its application to biogeochemical processes. *Marine Chemistry*, 106(1-2 SPEC. ISS.):287–300.
- Zeebe, R. E. (2012). History of Seawater Carbonate Chemistry, Atmospheric CO<sub>2</sub>, and Ocean Acidification. *Annual Review of Earth and Planetary Sciences*, 40(1):141–165.
- Zeebe, R. E. and Wolf-Gladrow, D. A. (2003). *CO<sub>2</sub> in Seawater: Equilibrium, Kinetics, Isotopes*. Number 2.

# **Chapter 1**

## **Published Literature: The Influence of Organic Alkalinity on the Carbonate System in Coastal Waters**





## The influence of organic alkalinity on the carbonate system in coastal waters

Daniel E. Kerr<sup>a</sup>, Peter J. Brown<sup>b</sup>, Anthony Grey<sup>a</sup>, Brian P. Kelleher<sup>a,\*</sup>

<sup>a</sup> Organic Geochemical Research Laboratory, Dublin City University, DCU Glasnevin Campus, Dublin 9, Ireland

<sup>b</sup> Ocean Biogeosciences Group, National Oceanography Centre, European Way, Southampton SO14 3ZH, United Kingdom

### ARTICLE INFO

#### Keywords:

Organic alkalinity  
Coastal carbonate system  
Total alkalinity  
Dissolved organic  
Matter

### ABSTRACT

Total alkalinity (TA) is one of the four main carbonate system variables and is a conventionally measured parameter used to characterise marine water carbonate chemistry. It is an important indicator of a waterbody's buffering capacity and a measure of its ability to resist acidification, a matter of growing concern in the marine environment. Although TA is primarily associated with the inorganic components of seawater such as bicarbonate, there is a growing consensus that dissolved organic matter (DOM) can significantly contribute to TA in coastal waters. This organic fraction of TA (OrgAlk) is typically deemed negligible and is not accounted for in conventional TA expressions. However, omission of OrgAlk can lead to the propagation of errors in subsequent carbonate system calculations and to misinterpretation of key carbonate chemistry descriptors such as calcium carbonate saturation states. Here we provide an overview of OrgAlk contributions to TA and investigate the implications of its omission in carbonate system studies conducted in coastal waters. We examine the prevalence of OrgAlk across both coastal and pelagic waters using publicly available carbonate system data products, such as GLODAP and GOMECC. Current measures to account for, incorporate and characterise the contribution of OrgAlk to TA are also critically examined.

### 1. Introduction: changing carbonate chemistry

The exchange of carbon dioxide (CO<sub>2</sub>) between the atmosphere and oceans has been greatly perturbed by anthropogenic carbon release since the industrial revolution. Atmospheric CO<sub>2</sub> levels prior to the industrial era are estimated to be around 270 ppm (Wigley, 1983). This is approximately 50% less than today's value, measured to be around 410 ppm (Dlugokencky et al., 2021). This marked increase in the concentration of atmospheric CO<sub>2</sub> has been mitigated by the oceans, which have absorbed approximately one third of anthropogenically produced CO<sub>2</sub> (Gruber et al., 2019; Sabine et al., 2004), keeping atmospheric levels lower by ~80 ppm (Friedlingstein et al., 2020). This has resulted in dramatic changes in seawater chemistry (Fabricius et al., 2020; Orr et al., 2005; Riebesell and Gattuso, 2015) that have led to a lowering of seawater pH, collectively referred to as ocean acidification. On average, surface ocean pH has fallen by approximately 0.1 pH units (Caldeira and Wickett, 2003; Jiang et al., 2019; Orr et al., 2005). With end-of-century partial pressure of CO<sub>2</sub> (pCO<sub>2</sub>) predicted to reach 900–1000  $\mu$ atm, ocean acidification seriously threatens the stability of ocean ecosystems, fish stocks and food security (Leis, 2018; McNeil and Sasse, 2016).

Ocean acidification is tracked by measuring changes in seawater pH as well saturation state of seawater with respect to aragonite. The latter is commonly used to track ocean acidification because it is a measure of carbonate ion concentration. pH is one of the four main parameters, the other three being dissolved inorganic carbon (DIC), fugacity of CO<sub>2</sub> (fCO<sub>2</sub>) and total alkalinity (TA) (Dickson et al., 2007). TA does not change with CO<sub>2</sub> introduction to, or removal from, a waterbody (CO<sub>2</sub> invasion or evasion) and is a conservative parameter with respect to temperature and salinity (Wolf-Gladrow et al., 2007). As TA does not change with ambient CO<sub>2</sub>, it is easier to sample for and store compared to other carbonate system parameters such as pH and DIC. As TA can be measured to a good degree of accuracy, within 1–2  $\mu$ mol.kg<sup>-1</sup>, it is a preferred tracer variable in numerical models of the oceanic carbon cycle and is the predominantly measured parameter alongside DIC to describe the carbonate system. As advances in spectrophotometric pH analysis have been made in recent years (Ma et al., 2019), more laboratories may opt to use pH and DIC for speciation calculations. However, due to the aforementioned relative ease that TA samples can be collected and stored with, it remains a predominantly measured parameter in many carbonate system studies. TA can be thought of as a measure of a

\* Corresponding author.

E-mail address: [brian.kelleher@dcu.ie](mailto:brian.kelleher@dcu.ie) (B.P. Kelleher).

<https://doi.org/10.1016/j.marchem.2021.104050>

Received 14 June 2021; Received in revised form 20 September 2021; Accepted 5 October 2021

Available online 20 October 2021

0304-4203/© 2021 The Authors. Published by Elsevier B.V. This is an open access article under the CC BY license (<http://creativecommons.org/licenses/by/4.0/>).

waterbody's buffering capacity and is inherently linked to pH (Eggleston et al., 2010). Therefore, accurate TA assessment is important in our understanding of the risks associated with the acidification of marine waters. This is especially relevant in littoral systems, as the carbonate chemistry of coastal waters is substantially more dynamic than the open ocean (Borges and Gypens, 2010). These systems exhibit vast temporal and spatial differences in carbonate chemistry due to periodic seasonal cycling (Joeseof et al., 2017; Rheuban et al., 2019) fluctuations in fluvial export and nutrient delivery (Borges and Gypens, 2010; Hydes and Hartman, 2012; Raymond and Cole, 2003), upwelling events (Borges and Frankignoulle, 2002; Millero, 2007) as well as microbial activity (Brewer and Goldman, 1976; Wolf-Gladrow et al., 2007).

The aforementioned factors add to the overall heterogeneity of carbonate system dynamics in coastal waterbodies and to the uncertainty regarding future impacts of acidification. Only by studying the variability and long-term trends of carbonate chemistry in coastal areas can the natural and anthropogenic processes that affect these systems be delineated (Sutton and Newton, 2020). Furthermore, the global and general circulation models utilised in many predicted ocean acidification scenarios (Carter et al., 2016; Ilyina et al., 2009) do not resolve the intricacies of acidification of the coastal ocean (Duarte et al., 2013). For example, areas such as the north-eastern US coastline are particularly susceptible to acidification due to low TA freshwater discharge (Gledhill et al., 2015; Rheuban et al., 2019), whereas the Baltic Sea is possibly more resistant to acidification due to observed TA increases over the past decades (Gustafsson and Gustafsson, 2020; Müller et al., 2016). These differences in fluvial TA output are typically linked to the bedrock of the river catchment area (McGrath et al., 2016), highlighting the site specificity of TA in coastal systems. Due to this, it is important to ensure that TA dynamics in coastal waters are as accurate and well characterised as possible.

Typically TA is attributed solely to the inorganic components of seawater such as bicarbonate ( $\text{HCO}_3^-$ ), carbonate ( $\text{CO}_3^{2-}$ ) and borate (Dyrssen and Sillén, 1967), with other inorganic seawater constituents also making small contributions, as outlined in Table 1. Organic molecules that are present in seawater can also contribute to TA, with this contribution termed organic alkalinity (OrgAlk). There is a growing consensus that OrgAlk can be a significant fraction of TA in coastal waters (Cai et al., 1998; Muller and Bleie, 2008; Patsavas et al., 2015; Song et al., 2020; Yang et al., 2015) and potentially impact carbonate system reference materials (Sharp and Byrne, 2021). Furthermore, questions regarding interferences in TA analysis in coastal environments due to the presence of organic molecules have also been raised (Fong and Dickson, 2019; Hu et al., 2015; Patsavas et al., 2015; Sharp and Byrne, 2020; Song et al., 2020). These compounds, which are thought to be part of dissolved organic carbon (DOC), can possess charged functional groups that can react during TA titrations, thus altering the overall TA signal (Kim and Lee, 2009; Kuliński et al., 2014; Paxéus and Wedborg, 1985). The presence and influence of these organic species are typically omitted in the analysis of TA in the open ocean as they are thought to be present in such small amounts that they can be safely neglected (Dickson et al., 2007) although the consensus view on this is changing (Fong and Dickson, 2019). OrgAlk is not explicitly accounted

for in conventional TA calculations. This presents a two-fold issue, as organic molecules can directly and significantly affect the buffering capacity of a water sample (Hunt et al., 2011) as well as present an analytical interference in TA computation (Sharp and Byrne, 2020). Although the dissociation of organic acids associated with DOM will not affect seawater alkalinity directly, their contribution to alkalinity will proportionally decrease the contributions of other seawater constituents, such as those outlined in Table 1. Any discrepancies in TA analysis induced by OrgAlk can potentially propagate errors in subsequent calculated carbonate system parameters (Abril et al., 2015; Hunt et al., 2011; Koeve and Oschlies, 2012), such as pH and  $\text{pCO}_2$ . This is pertinent in coastal systems that can be sensitive to slight changes in carbonate chemistry (Hoppe et al., 2012), such as estuaries in colder northern regions that are particularly at risk of acidification due to higher DIC/TA ratios and increased  $\text{CO}_2$  solubility (Cai et al., 2020). Evidently, if the nature of carbonate chemistry in coastal systems is to be accurately depicted, analytical interferences and calculation errors associated with OrgAlk must be mitigated. The purpose of this review is to provide an overview of OrgAlk contributions to TA, how it is quantified, as well as discuss the implications of its omission in carbonate system studies conducted in coastal waters. The relationship between OrgAlk and DOC is investigated through the use of coastal and pelagic large scale carbonate system data sets. Furthermore, methods to evaluate, characterise and account for OrgAlk will be discussed.

## 2. Alkalinity: the oceans innate buffering ability

Although an understanding of inorganic carbon cycling in the ocean began with the development of appropriate analytical methods in the 1960's (Dyrssen and Sillén, 1967), it is only in more recent years that standardised analytical methods have been documented (Dickson et al., 2007). In order to appreciate OrgAlk, it is necessary to have an understanding of the carbonate system in seawater. The inorganic carbon system can be described by four interlinked parameters: TA, DIC, pH, and  $\text{fCO}_2$ . By directly measuring two of these four parameters, utilising equilibrium constants specific to the nature of the aquatic system of study, as well as supplying data on temperature, salinity, pressure and specific inorganic seawater constituents, it is possible to calculate the remaining two parameters and obtain accurate information of carbonate chemistry (Zeebe, 2012). Equilibrium constants for the carbonate system exist for a range of aquatic environments, from the open ocean (Lueker et al., 2000) to brackish coastal waters (Cai and Wang, 1998; Millero, 2010). A substantial portion of the inorganic carbon found on Earth is contained within marine water, estimated to be on the order of 38,000 Pg C (Sundquist and Visser, 2003). The collective sum of all aqueous  $\text{CO}_2$  ( $\text{CO}_2(\text{aq})$ ), carbonic acid ( $\text{H}_2\text{CO}_3$ ), bicarbonate and carbonate is termed total dissolved inorganic carbon, or DIC. As gaseous  $\text{CO}_2$  dissolves into solution, the following equilibrium reactions occur:



The dominant species of inorganic carbon present in seawater is a function of pH, temperature and salinity, with total scale pH (pHT) of surface seawater typically around 8.07 (Jiang et al., 2019). At this pH and within the salinity and pressure ranges of most coastal waters,  $\text{HCO}_3^-$  and  $\text{CO}_3^{2-}$  are the dominant species (Raymond and Hamilton, 2018). In a simple seawater system such as that described by Wolf-Gladrow et al. (2007),  $\text{HCO}_3^-$  and  $\text{CO}_3^{2-}$  are the dominant proton acceptors; proton acceptors being those negatively charged molecules that can assimilate free positively charged protons. As per the conventional definition of TA, proton acceptors are those bases formed from

**Table 1**  
Contribution of various seawater constituents to open ocean TA (modified from Millero (2001)).

Species	% TA
$\text{HCO}_3^-$	89.8
$\text{CO}_3^{2-}$	6.9
$\text{B}(\text{OH})_4^-$	2.9
$\text{SiO}(\text{OH})_3^-$	0.2
$\text{MgOH}^+$	0.1
$\text{OH}^-$	0.1
$\text{HPO}_4^{2-}$	0.1

weak acids with a dissociation constant  $K \leq 10^{-4.5}$ , whereas proton donors are those acids with  $K > 10^{-4.5}$  (Dickson, 1981). As TA is defined as the measure of the amount of proton acceptors per kilogram of seawater (Wolf-Gladrow et al., 2007),  $\text{HCO}_3^-$  and  $\text{CO}_3^{2-}$  make up the bulk of TA.

TA was expressed solely in terms of the strong base anions that would react with an added strong acid such as HCl (Rakestraw, 1949). The initial model of TA was further refined by the incorporation of the concepts of the proton condition and subsequently the zero level of protons (Butler, 1964). This is a defined neutral position from which the concentration of  $\text{H}^+$  can be measured relative to, and is defined by the species of unionised carbonic acid, boric acid, and water (Dickson, 1992). The TA term was further expanded to include other acid-base components of seawater, such as hydrogen sulfate and hydrogen fluoride. This TA term does not incorporate the influence of additional inorganic proton acceptors which can contribute to total TA such as those outlined in Table 1. A revised TA equation (Dickson et al., 2007) can be represented by the following:

$$[TA] = [\text{HCO}_3^-] + 2[\text{CO}_3^{2-}] + [\text{BO}(\text{OH})_4^-] + [\text{OH}^-] + [\text{HPO}_4^{2-}] + 2[\text{PO}_4^{3-}] + [\text{SiO}(\text{OH})_3^-] + [\text{NH}_3] + [\text{HS}^-] - [\text{H}^+] - [\text{HSO}_4^-] - [\text{HF}] - [\text{H}_3\text{PO}_4] + [\text{minor bases} - \text{minor acids}] \quad (5)$$

Eq. (5) is the conventional expression used to describe TA in seawater and incorporates the contributions of carbonate and non-carbonate acid-base species to TA. It is within this final term “minor bases - minor acids” in which the impact of OrgAlk arises.

### 3. Organic alkalinity

The suspected influence of organic species on the accurate analysis of carbonate system parameters was initially reported by Goldman and Brewer (1980), who observed that the presence of organic acids excreted by phytoplankton cultures had an influence on measured TA compared to control samples. As previously stated, the presence and influence of organic species is typically omitted in the analysis of TA in open ocean scenarios. The influence of OrgAlk on discrepancies between calculated and directly measured carbonate system data when using non-OrgAlk adjusted TA as an input parameter have been identified, as outlined in Table 2.

The possibility of discrepancies associated with organic alkalinity has led to a recent study of the carbonate system in estuarine waters to not use TA as an input variable (Yao et al., 2020). Several studies have identified sources of OrgAlk to the coastal ocean (Fig. 1).

As coastal waters are heavily influenced by both nutrient and carbon inputs that stimulate the production and remineralisation of organic matter, they play a significant role in the global carbon cycle (Abril et al., 1999; Bozec et al., 2012; Frankignoulle et al., 1998; Neubauer and

Anderson, 2003). Many shallow coastal ecosystems are considered to be net sources of  $\text{CO}_2$  due to the remineralisation of terrestrially sourced or autochthonous organic matter (Borges, 2005). In coastal waters, the connection between net metabolism and nutrient dynamics will change the characteristics of carbon exported to littoral zones (Raymond and Bauer, 2000). The aforementioned processes play an important role in the dynamics of the coastal carbonate system and can have a direct impact on TA. For example, the uptake of inorganic nutrient species by photoautotrophs during primary production, organic matter remineralisation and nitrification can influence TA (Wolf-Gladrow et al., 2007). The sign and magnitude of the effect on TA is governed by the charge of the nutrient species as well as the molar ratios at which marine plankton uptake said nutrient species (Redfield et al., 1963).

Most nutrient species present in seawater are negatively charged and so in order to maintain electroneutrality, photoautotrophs exchange charged non-nutrient ions in the appropriate direction to compensate for the uptake of charged nutrient species. The uptake of a negatively charged nutrient species will result in a net negative charge within the

cell, which in turn is balanced by the uptake or release of  $\text{H}^+$  or  $\text{OH}^-$  respectively. Conversely, the uptake of positively charged nutrient species is balanced by release or uptake of  $\text{H}^+$  or  $\text{OH}^-$  respectively. This loss of  $\text{H}^+$  or gain of  $\text{OH}^-$  increases TA, as per 5. The remineralisation of organic matter will release nutrient species and will have the reverse effect of assimilation during primary production. Bacterially mediated nitrification has been observed to cause TA to display non-conservative behaviour, with respect to salinity, in estuarine waters (Frankignoulle et al., 1996). This is due to the nitrification process consuming 2 mol of TA for every 1 mol of nitrate produced. The net change in TA due to the assimilation or release of nutrient species can be seen in Table 3.

### 4. Measuring organic alkalinity

Many of the existing methods to quantify OrgAlk operate through conventional methods of TA analysis and calculation, or through modified TA analysis procedures, as can be seen in Fig. 2. TA has been studied for decades (Dickson, 1992; Rakestraw, 1949) and thus throughout the years varying methods of analysis have been developed, such as direct titration (Greenberg et al., 1932), potentiometry (Dyrssen, 1965) and spectrophotometry (Brelund and Byrne, 1993; Yang et al., 2015). A significant bolster to TA analysis was the introduction of certified reference materials (CRMs) that enable the calibration and validation of instruments and analysis methods. CRMs for TA have been available since 1996 from Dr. Andrew G. Dickson of Scripps Institution of Oceanography, University of California, San Diego.

There are two best practice methods to produce directly measured TA (TAM) data, both of which are potentiometric titrations (Dickson et al., 2007). The first method involves an incremental addition of strong acid such as HCl to a precisely known volume of seawater within a closed cell. The pH of the reaction is monitored closely by the use of a pH electrode (Millero et al., 1993). TAM is calculated with titrant volume and electromotive force (emf) data through one of two methods; a non-linear least squares curve fitting (NLSF) technique (Dickson, 1981) or a difference derivative method (Hernández-Ayón et al., 1999). These non-purged, closed cell TA titrations allow for the simultaneous determination of DIC. As DIC can be more accurately determined through coulometric methods (Johnson et al., 1985), coulometry is typically the more routine procedure. The second method involves an open cell purged

**Table 2**

Errors associated with calculated carbonate parameters when using non-OrgAlk adjusted TA as an input parameter.

Input parameters	$p\text{CO}_2$	pH	DIC
TA - DIC	Underestimated <sup>a,b,c</sup>	Overestimated <sup>c,d</sup>	N/A
TA - pH	Overestimated <sup>c</sup>	N/A	Overestimated <sup>d</sup>

<sup>a</sup> Hu (2020).

<sup>b</sup> Koeve and Oschlies (2012).

<sup>c</sup> Kulinski et al. (2014).

<sup>d</sup> Yang et al. (2015).

<sup>e</sup> Hunt et al. (2011).

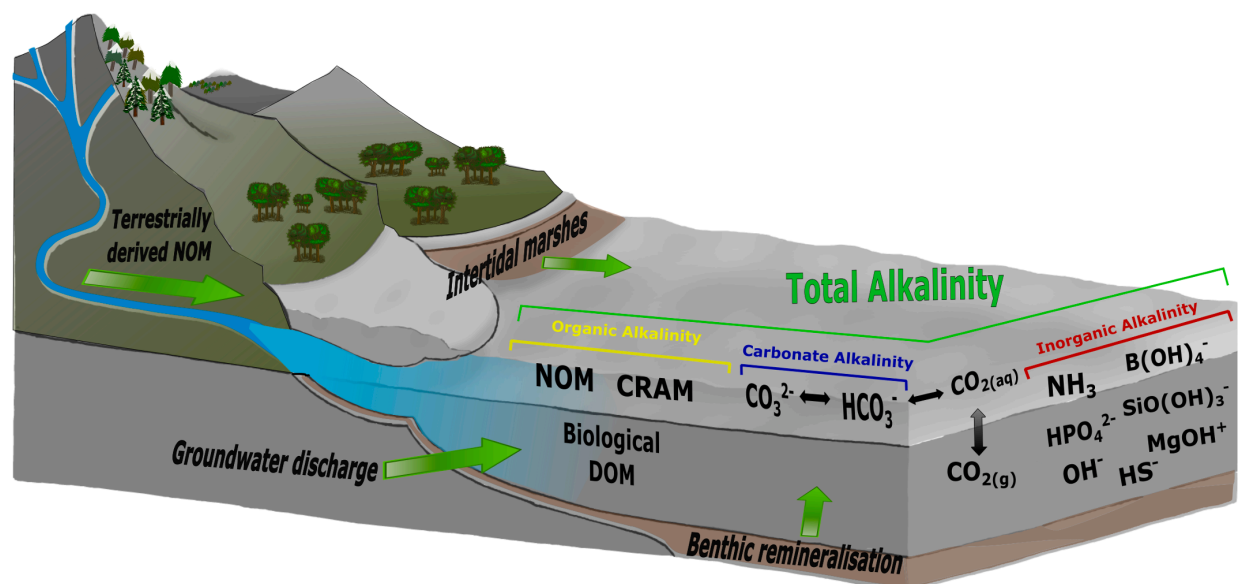


**Fig. 1.** Simplified diagram illustrating the different components of TA in the coastal ocean; carbonate, inorganic and organic. Green arrows indicate reported sources of OrgAlk, such as intertidal marshes (Cai et al., 1998; Wang et al., 2016), groundwater discharge (Song et al., 2020), terrestrially derived humics (Hunter et al., 2011; Tishchenko et al., 2006) and sediment (Lukawska-Matuszewska, 2016; Lukawska-Matuszewska et al., 2018). NOM - natural organic matter, CRAM - carboxyl rich aliphatic matter. (For interpretation of the references to colour in this figure legend, the reader is referred to the web version of this article.)

**Table 3**

Net change in moles of TA per mole of nutrient assimilated or released (adapted from Wolf-Gladrow et al., 2007).

Nutrient	Assimilation	Release
Sulphate	+2	-2
Phosphate	+1	-1
Nitrate	+1	-1
Nitrite	+1	-1
Ammonia	-1	+1

titration. A single-step addition of strong acid brings the sample to a predetermined pH dependent on suspected alkalinity. Subsequently, CO<sub>2</sub> present in the sample is purged either through sparging with a CO<sub>2</sub> free gas or by stirring. Further incremental acid addition brings sample pH to approximately 3 while pH is continuously measured. Sample pH can be determined by potentiometric or spectrophotometric means (Li et al., 2013). Titration data in the 3.0–3.5 pH range are then used in a NLSF approach to subsequently calculate TAM (Dickson et al., 2003).

In recent years however, concerns over the suitability of potentiometric methods for waters of high dissolved organic material (DOM) concentrations have been raised (Hu et al., 2015; Sharp and Byrne, 2020). The ambiguity which surrounds OrgAlk as a factor impacting the use of TA as an accurate input parameter in carbonate system calculations has been found to vary with the specific method of TA analysis used. In recent work (Sharp and Byrne, 2020), the differences in OrgAlk arising between five different TA analysis methods was investigated. It was found that in a modelled system, the presence of titratable organic molecules elicit responses of differing magnitudes between the different measurement approaches. A notable finding of the study was the apparent unsuitability of open cell multi-step and direct titrations which utilise modified Gran function (MGF) or NLSF techniques when compared to other TA measurement methods in the presence of organic molecules with pK < 6. This is significant as numerous studies have linked this pK range with carboxyl functional groups of DOM present in marine and fluvial waters (Hertkorn et al., 2006; Masini et al., 1998; Muller and Bleie, 2008; Paxéus and Wedborg, 1985; Perdue et al., 1980).

As open cell titrations allow for the incorporation of a back titration procedure to measure OrgAlk, open cell methods may prove beneficial in future investigations.

## 5. Calculated OrgAlk

TAM is non-discriminatory and incorporates all proton acceptors formed from weak acids, regardless of inorganic or organic nature. Organic molecules that have titratable functional groups with pK values within the titration pH range of the specific analysis method will exert an influence on TA. Using two other carbonate parameter data and software programs that contain accurate carbonate system thermodynamic constants, such as the multi-platform CO<sub>2</sub>SYS software program (Lewis and Wallace, 1998), it is possible to calculate alkalinity (TAC). Contributions from organic proton acceptors are not included in TAC and it is assumed that TAC accounts only for the protolytes present in Eq. (5). OrgAlk values are calculated as the difference between TAM and TAC, such that:

$$[OrgAlk_c] = [TAM] - [TAC] \quad (6)$$

This method for calculating OrgAlk has been used by numerous investigators (Delaigue et al., 2020; Hammer et al., 2017; Hernández-Ayon et al., 2007; Kim and Lee, 2009; Kuliński et al., 2014; Patsavas et al., 2015; Song et al., 2020). It is important to note that OrgAlk values obtained through this method are inherently inclusive of any residual errors associated with TAC, possibly leading to errors in the sign and magnitude of OrgAlk. These residual errors are likely responsible for the negative OrgAlk values displayed in Figs. 3–5, which were constructed utilising multiple coastal and oceanic carbonate system data products to illustrate relationships between OrgAlk, salinity, DOC and TA, see details below. The residual errors associated with TAM minus TAC are generally attributed to errors in input parameters or with the thermodynamic models which relate them (Fong and Dickson, 2019). TAC errors may be more pronounced in low salinity coastal waters where carbonate system thermodynamic constants have not been as rigorously evaluated (Woosley, 2021). This could translate to large errors in OrgAlk values observed in lower salinity waters compared to

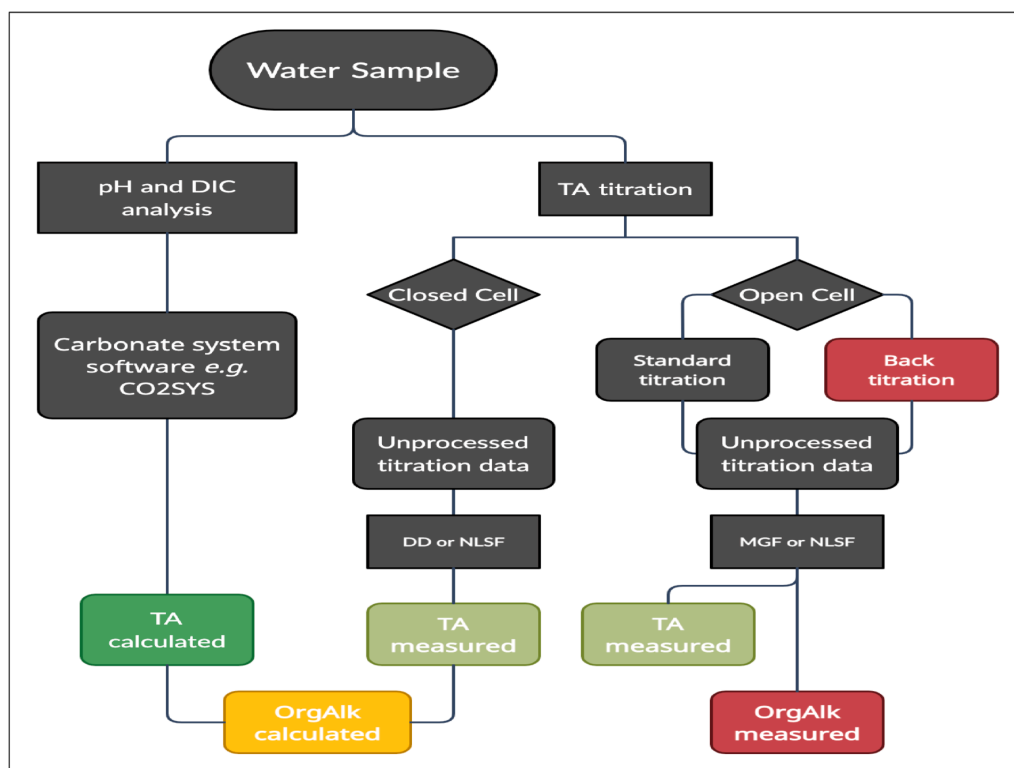


**Fig. 2.** Flowchart illustrating possible routes for OrgAlk determination. OrgAlk calculated is defined as TA measured minus TA calculated. Calculated OrgAlk values obtained through this method are inherently inclusive of any residual errors associated with calculated TA as well as discrepancies with the carbonate system thermodynamic equilibrium constants used. Note, DD - direct derivative, MGF - modified Gran function, NLSF - non-linear least squares function.

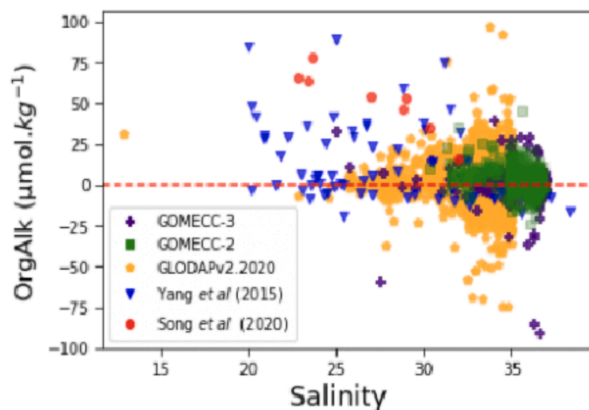


**Fig. 3.** OrgAlk expressed as a function of salinity for each dataset utilised. OrgAlk<sub>C</sub> is reported for all datasets except Song et al. (2020) where OrgAlk<sub>M</sub> was reported as OrgAlk directly measured through back titration methods.

those in more saline waters. The carbonate system thermodynamic constants that describe the solubility of CO<sub>2</sub> and dissociation of carbonate species in seawater as a function of temperature and salinity have been determined in a number of studies (Lueker et al., 2000; Millero, 2010; Prieto and Millero, 2002; Woosley, 2021). Each set of constants have their own uncertainties, therefore the specific choice of constants used in carbonate system calculations can introduce bias. Similarly, the choice of constants associated with carbonate system calculations such as the dissociation constants for boric, hydrofluoric, phosphoric and to a minor degree sulfuric acid (Woosley, 2021) can also introduce bias. The

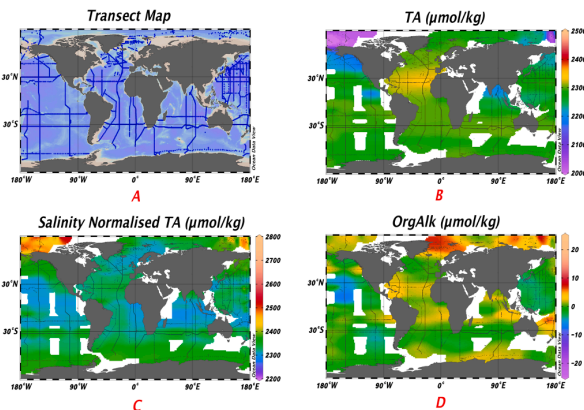


**Fig. 4.** Surface plots of the GLODAPv2.2020 data product illustrating (a) hydrographic cruises data were taken from (b) TA concentrations, (c) TA normalised to a salinity of 35 and (d) OrgAlk calculated using Eq. (6).

presence of OrgAlk in seawater has been hypothesised as a potential factor in the disparity between directly measured and calculated carbonate system parameters in studies investigating carbonate thermodynamic inconsistency issues (Fong and Dickson, 2019; Millero et al., 2002; Patsavas et al., 2015).

## 6. Measured OrgAlk

OrgAlk can also be directly measured (OrgAlk<sub>M</sub>) by means of back titration (Cai et al., 1998), with this method used and modified in a number of studies (Hunt et al., 2011; Ko et al., 2016; Muller and Bleie,

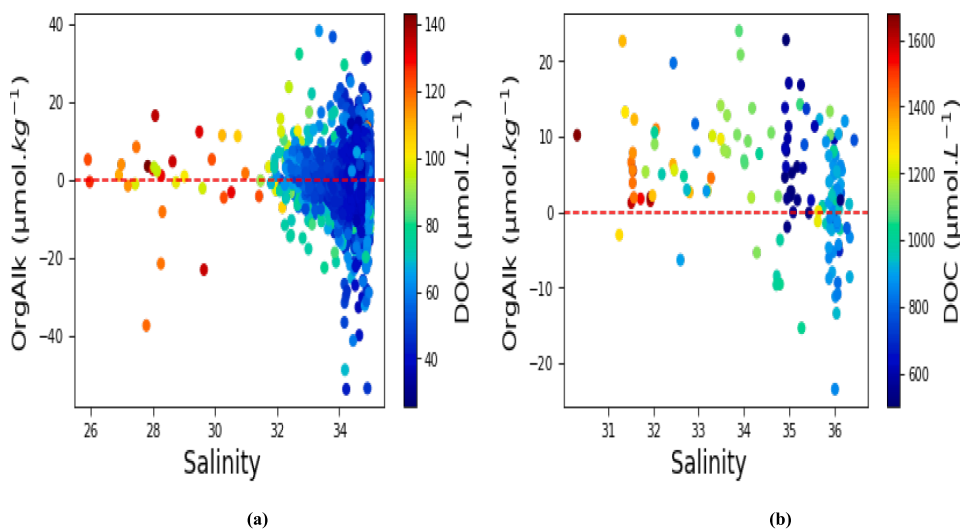


**Fig. 5.** Calculated OrgAlk values as a function of salinity for (a) GLODAPv2.2020 and (b) GOMECC-2. A positive skew in OrgAlk distributions is observed in less saline waters which coincides with increased DOC concentrations, whereas distributions are largely normal in more saline waters.

2008; Yang et al., 2015). Back titrations are carried out after TA titrations have taken place, thus all carbonate associated TA has been removed. The sample is kept under a N<sub>2</sub> atmosphere to prevent CO<sub>2</sub> invasion and returned to its original pH using a CO<sub>2</sub> free NaOH solution. Re-titration with HCl ensues, with the resultant alkalinity value attributed to OrgAlk<sub>M</sub>, minus the contributions of non-carbonate species present. Importantly, as OrgAlk<sub>M</sub> is a directly obtained value it should be free from the aforementioned residual errors associated with OrgAlk<sub>C</sub>. Good agreement has been found between OrgAlk<sub>M</sub> by back titration methods and OrgAlk<sub>C</sub> in phytoplankton cultures, although for field samples the agreement was not as pronounced (Ko et al., 2016). Other studies report no strong statistical relationship between OrgAlk<sub>M</sub> and OrgAlk<sub>C</sub> observed in field samples (Song et al., 2020). Disparity between OrgAlk<sub>M</sub> by back titration methods and OrgAlk<sub>C</sub> calculated from pH and DIC can potentially be attributed to the bias in chosen carbonate system thermodynamic constants and associated acid-base system constants. Furthermore, in the case of Song et al. (2020), interference to spectrophotometric pH measurement associated with the potential impact of coloured and fine particulate materials could cause errors in pH as an input parameter to TAC and thus OrgAlk<sub>C</sub>. More similarity between OrgAlk<sub>M</sub> and OrgAlk<sub>C</sub> was observed in samples with noticeably less coloured and fine particulate materials (Song et al., 2020). Back titration methods have recently been recommended for implementation on future hydrographic research cruises in order to characterise OrgAlk in spatially heterogeneous oceanic waters (Sharp and Byrne, 2020). The utilisation of back titration methods in studies which overdetermine the carbonate system would glean insights into the magnitude of effect of OrgAlk on the internal consistency of marine carbonate system measurements.

## 7. Evidence of OrgAlk

Publicly available data sources, such as the Global Ocean Data Analysis Project (GLODAP) (Lauvset et al., 2016; Olsen et al., 2016), and the various Gulf of Mexico and East Coast Carbon Cruises (GOMECC-2, GOMECC-3) (Barbero et al., 2019; Wanninkhof et al., 2012) provide quality controlled information on core oceanic biogeochemical variables and present the opportunity for exploratory investigations of OrgAlk. Any data for which TA along with two other carbonate system parameters have been measured simultaneously allow for the calculation of OrgAlk as per Eq. (6). Based on this, the GLODAPv2.2020, GOMECC-2 and GOMECC-3 data products were filtered to include data for which

DIC, TA, pHT, phosphate and silicate, along with key physiochemical variables were simultaneously and directly measured. TA was then calculated using DIC and pHT as the input parameters through pyCO<sub>2</sub>-SYS version 1.6.0 (Humphreys et al., 2020). The carbonate equilibrium constants of Lueker et al. (2000), bisulfate dissociation constant of Dickson (1990) and borate to salinity ratio of Lee et al. (2010) were used throughout all carbonate system calculations. Additionally, the reported calculated OrgAlk and directly measured OrgAlk values were included from the works of Yang et al. (2015) and Song et al. (2020) respectively. The generated and reported OrgAlk<sub>C</sub> values were used to illustrate the distributions of OrgAlk in coastal and pelagic zones, as well as investigate the relationship between OrgAlk and organic carbon as shown in Figs. 3–5.

In Fig. 3 OrgAlk values appear normally distributed around 0  $\mu\text{mol. kg}^{-1}$  in more saline waters. In less saline freshwater influenced waters OrgAlk appears skewed toward positive values. This could be attributed to fluvially discharged organics contributing to OrgAlk in coastal waters with mixing then occurring, subsequently diminishing the OrgAlk signal. Conservative mixing of OrgAlk was indicated in laboratory experiments involving the dilution of organic rich Baltic seawater (Ulfsbo et al., 2015). Furthermore, simulated models have shown that as mixing occurs OrgAlk becomes relatively conservative with respect to salinity (Cai et al., 1998; Hu, 2020).

As OrgAlk is associated with the presence of DOM, oceanic areas that receive inputs of terrestrially derived or autochthonously produced DOM may exhibit significant organic contributions to TA. This is evident in the upper Arctic and tropical ocean zones, as can be seen in Fig. 4. The Arctic Ocean is subject to high DOM loadings arising from fluvial inputs (Cooper et al., 2005; Stedmon et al., 2011), and displays elevated OrgAlk<sub>C</sub> values as seen in Fig. 4. It is important to note that the CO<sub>2</sub> system constants and coefficients used for calculation can have spatial biases that can result in larger differences between measured and calculated TA values, and thus OrgAlk<sub>C</sub>. It is possible that the higher OrgAlk<sub>C</sub> values observed in Arctic waters are due to high DOM inputs. Furthermore, distinct changes in Arctic DOC export have been linked to seasonal cycles (Kaiser et al., 2017), suggesting that OrgAlk may play a more pronounced role in Arctic waters at times of elevated discharge. Here DOC refers to the fraction of DOM that specifically relates to the mass of carbon in the dissolved material. Similarly, the tropics are areas of intense riverine DOC discharge, accounting for 55–62% of the global riverine DOC export (Dai et al., 2012; Li et al., 2017). Although there is not as noticeable an OrgAlk signal associated with the large freshwater

discharge of the Amazon River this could be due to the characteristics of DOM transferred, as the impacts of OrgAlk attributed to DOM have been found to vary spatially across transitional waterbodies (Song et al., 2020).

## 8. DOM as a contributor to OrgAlk

The magnitude of OrgAlk appears greater in littoral zones due to massive riverine and groundwater discharges of allochthonous organics (Gattuso et al., 1998; Romankevich, 1984). The predominant source of DOM to the coastal ocean arises from riverine inputs that contribute an estimated 0.25 Gt DOC  $y^{-1}$  (Cauwet, 2002; Hedges et al., 1997). Although rivers represent a main source of DOM, intertidal salt marshes (Pakulski, 1986; Sousa et al., 2017), autochthonous production by phytoplankton (Hernández-Ayon et al., 2007; Kim and Lee, 2009; Ko et al., 2016) as well as exchanges with adjacent coastal waters (Bianchi, 2007) are all potential sources. As  $TA_M$  in coastal waters has been observed to be consistently higher than  $TA_C$  (Patsavas et al., 2015), the presence of organic bases in lower salinity coastal waters may present an additional fraction of TA unaccounted for by  $TA_C$ . Furthermore, OrgAlk values of up to 45  $\mu\text{mol}\cdot\text{kg}^{-1}$  have been attributed to terrigenous organic matter (Tishchenko et al., 2006), indicating evidence of the influence of terrestrial inputs of organics on TA in coastal waters. Although many studies indicate positive OrgAlk values across a range of aquatic environments (Table 4) negative OrgAlk values, ranging from  $-49$  to  $-18$   $\mu\text{mol}\cdot\text{kg}^{-1}$ , likely associated with humic acids originating from groundwater discharge have been reported (Delaigue et al., 2020). As can be seen in Fig. 5b, higher DOC concentrations are observed in less saline waters, with this coinciding with positively skewed OrgAlk values. This is also observable but to a smaller degree in Fig. 5a.

DOM in transitional waters is a complex amalgam of both aromatic and aliphatic hydrocarbons that can possess charged functional groups (Leenheer and Croué, 2003). It is well established that terrestrially derived DOM is more aromatic (including lignin) and contains more carboxyl and hydroxyl functional groups than marine DOM (Lam et al., 2007; McCaul et al., 2011; Sleighter and Hatcher, 2008). Carboxyl and phenolic hydroxyl functional groups are thought to be the largest contributors to the acidity of humic substances (Perdue et al., 1980), and display a continuum of pK values within the pH range of TA titrations (Lodeiro et al., 2020; Ritchie and Perdue, 2003). The largest fraction of DOM in the riverine environment is humic in nature (Cauwet, 2002) with the OrgAlk associated with humic-like structures an important fraction of river water buffering capacity, representing 13–66% of TA in some river systems (Hunt et al., 2011). Furthermore, the identification through nuclear magnetic resonance spectroscopy of carboxylic acid groups in carboxyl rich aliphatic matter (CRAM) (Hertkorn et al., 2006; Woods et al., 2010), which comprises a major fraction of refractory

DOC, presents a possible candidate for oceanic OrgAlk (Fong and Dickson, 2019). Functional groups of CRAM with  $pK_a$  values ranging from 4.5–6 can contribute significantly to OrgAlk as their basic forms comprise <95% of their total concentration at seawater pH (Fong and Dickson, 2019).

Several studies have observed that OrgAlk increases can be attributed to increases in DOM concentration: in phytoplankton incubation investigations (Kim and Lee, 2009), in natural samples spiked with DOM (Kuliński et al., 2014), in modelled scenarios (Sharp and Byrne, 2020), in coastal seawater (Song et al., 2020) and in sediment pore waters (Lukawska-Matuszewska et al., 2018). Delineation of the relationship between OrgAlk and DOM concentration can only be achieved for organic molecules that have titratable functional groups with pK values within the titration pH range of the specific analysis method. Consistently higher concentrations of DOC in the inner estuaries of several European river systems compared to the marine water they enter have been observed, with DOC concentrations ranging from 55 to 600  $\mu\text{M}$  (Middelburg and Herman, 2007). Consequently, the magnitude of OrgAlk associated with DOM may be accentuated in transitional waterbodies as these systems serve as points of transference between the terrestrial and marine environments (Canuel et al., 2012). It has been found that the magnitude of the impact of OrgAlk attributed to DOM can vary spatially across transitional waterbodies (Song et al., 2020). Mixing of different waterbodies in estuaries appear to be the main factor governing observed DOM characteristics along estuarine gradients (Asmala et al., 2016). Processes such as photochemical and microbial degradation may also impact the organic molecules associated with OrgAlk (Fichot and Benner, 2014). The chemical diversity of DOM has been observed to increase as an aqueous matrix becomes more marine in nature, possibly due to the array of DOM degradation products and influence of autochthonously produced cellular materials (Sleighter and Hatcher, 2008; Zark and Dittmar, 2018).

## 9. Microbiological associated OrgAlk

In addition with the impact of terrestrially derived organics, as coastal areas are typically sites of intense biological activity, autochthonous organic material can also factor into OrgAlk (Muller and Bleie, 2008). It has been reported that microbiologically produced DOM can have significant contributions to TA (Hernández-Ayon et al., 2007; Kim et al., 2006; Ko et al., 2016). Phytoplankton are known to produce DOM by extracellular excretion (Biddanda and Benner, 1997; Jiao et al., 2010), typically constituting 5 to 30% of their total primary production (Karl et al., 1998), some of which may possess charged functional groups and thus factor in to TA. Incubation studies conducted on three different phytoplankton species (*P. minimum*, *S. costatum* and *C. curvisetus*) indicated that measured OrgAlk was directly related to phytoplankton DOM

**Table 4**

Contributions of OrgAlk to TA as well as analysis method employed in studies of the carbonate system across various aquatic systems.

Contribution to TA ( $\mu\text{mol}\cdot\text{kg}^{-1}$ )	OrgAlk source	OrgAlk method	Sample matrix	Reference
1–6	Bacteria	Filtration	Coastal seawater	Kim et al. (2006)
0–4	Plankton			
~ 40	Phytoplankton	Calculated	Coastal seawater	Kim and Lee (2009)
< 45	Terrigenous organic matter	Calculated	Coastal seawater	Tishchenko et al. (2006)
160–220	Organic acids	Calculated	River water	Hunt et al. (2011)
~ 56	Organic acids	Calculated	Coastal seawater	Hammer et al. (2017)
14–109				
100–190	Phytoplankton DOM	Calculated	Coastal seawater	Hernández-Ayon et al. (2007)
20–75				
8–73	Organic acids	Calculated	Coastal bottom waters	Lukawska-Matuszewska (2016)
2–2953	Organic acids	Calculated	Coastal sediment pore waters	
104–1505	Organic acids	Calculated	Coastal sediment pore waters	Lukawska-Matuszewska et al. (2018)
22–58	Organic acids	Calculated	Coastal seawater	Kuliński et al. (2014)
≤ 50	Organic acids	Back titration	Estuarine water	Cai et al. (1998)
34 ± 7		Back titration		
32 ± 8	Organic acids	Calculated	Coastal water	Song et al. (2020)
–49 to –18	Humic acids	Calculated	Fjord water	Delaigue et al. (2020)

production, with an organism dependent effect observed (Kim and Lee, 2009). DOM associated OrgAlk produced by phytoplankton has been observed in similar incubation studies (Hernández-Ayon et al., 2007; Kim et al., 2006; Ko et al., 2016; Muller and Bleie, 2008). OrgAlk has displayed a seasonality in surface waters of the Baltic Sea corresponding to Spring bloom events (Hammer et al., 2017), further alluding to the relationship between OrgAlk and phytoplankton produced DOM.

Negatively charged functional groups present on bacterial and phytoplankton cell walls have also been observed to contribute to TA (Kim et al., 2006). These charged functional groups acquire a charge through dissociation and protonation reactions (González-Dávila, 1995). Subsequently, the presence of both positively and negatively

(Fassbender et al., 2018). Direct means of assessing OrgAlk are beneficial in ensuring quantification is as accurate as possible, and free from the errors inherent to OrgAlk<sub>C</sub>. Furthermore, direct methods can allow investigators to better ascertain the acid-base characteristics of DOM associated with OrgAlk. Characterisations of the DOM charge groups in a water sample and their associated dissociation constants can be carried out by performing titrations with NaOH. This method of OrgAlk acid-base characterisation can readily be implemented with the same experimental set up as the aforementioned back titration methods to quantify OrgAlk. Using the model of Cai et al. (1998) as adapted by Yang et al. (2015), the dissociation constants of weak organic acids can be ascertained as follows:

$$V_0 \sum_i \frac{X_{iT}}{1 + \frac{[H^+]_T}{K_i}} + V_0 \frac{B_T}{1 + \frac{[H^+]_T}{K_B}} + V_0 \frac{P_T}{1 + \frac{[H^+]_T}{K_P}} + V_0 \frac{Si_T}{1 + \frac{[H^+]_T}{K_{Si}}} - (V_0 + v) \left( [H^+]_T - \frac{K'_w}{[H^+]_T} \right) - v C_{HCl} + V_0 \frac{K'_w}{C_H^0} \quad (7)$$

charged functional groups implies a changing net charge, depending on matrix pH (Van Der Wal et al., 1997). The consensus that negatively charged functional groups are predominant over positively charged groups in microbial cell walls is widely accepted (Corpe, 1970; Terayama, 1954). The proton binding capabilities of these functional groups in acidic conditions has been attributed to carboxyl groups (Carstensen and Marquis, 1968). Although recognised as a potential source of OrgAlk, the contributions to TA from bacterial and phytoplankton cell walls are typically small, reported values being between of 1–6 and 0–4  $\mu\text{mol.kg}^{-1}$  respectively (Kim et al., 2006; Ko et al., 2016).

## 10. Characterising and accounting for OrgAlk

### 10.1. OrgAlk correction factors

Methods to directly account for OrgAlk in TA calculations have been investigated. Millero et al. (2002) observed that when accounting for a constant amount of organic acids (8  $\mu\text{mol.kg}^{-1}$ ) and including a single term for an organic acid with a  $pK_a$  of 4, discrepancies between calculated and directly determined  $f\text{CO}_2$  were lower compared to computed values that omitted the inclusion of the organic acid term. The chosen  $pK_a$  of 4 falls within the broad distribution of  $pK_a$  values reported for carboxylic acid functional groups on humic and fulvic substances (Masini, 1994; Paxéus and Wedborg, 1985). When accounting for this organic acid, the range was consistent with the uncertainty in computed values resulting from stated uncertainties in the measurements of DIC and TA. Similar bulk corrections to bring directly measured values for carbonate parameters in line with calculated values have been undertaken in related studies (Fong and Dickson, 2019; Patsavas et al., 2015). Comparisons of suggested OrgAlk correction values of 2.4–7.3  $\mu\text{mol.kg}^{-1}$  (Fong and Dickson, 2019) are in agreement with the estimated concentration of carboxylic acids present in CRAM ( $\sim$  3–5  $\mu\text{mol.kg}^{-1}$ ) (Hertkorn et al., 2013). These methods are applicable only in the post processing correction of large scale data sets and do not offer direct information on OrgAlk. As coastal DOM is a spatially and temporally heterogeneous mixture of terrestrial, autochthonous and marine derived organic materials, the quantity of and acid-base characteristics of OrgAlk may prove too varied to accurately apply post processing corrections.

### 10.2. Acid-base characteristics of OrgAlk

Discrepancies between OrgAlk<sub>C</sub> and OrgAlk<sub>M</sub> have been reported to be as large as 8  $\mu\text{mol.kg}^{-1}$  (Yang et al., 2015), and in some cases OrgAlk<sub>C</sub> concentrations are not statistically distinguishable from zero

where  $K_i$ ,  $K_B$ ,  $K_P$  and  $K_{Si}$  are the dissociation constants of a weak organic acid  $X_i$ , boric acid, phosphate, and silicic acid and  $X_{iT}$ ,  $B_T$ ,  $P_T$  and  $Si_T$  are the total concentrations of organic acid, borate, phosphate and silicate.  $K'_w$  is the ion product of seawater,  $v$  is the volume of HCl titrant, and  $V_0$  is the volume of sample titrated with NaOH.  $C_{HCl}$  and  $C_H^0$  are the concentrations of HCl titrant and hydrogen ion concentration after titration with NaOH, respectively. The values of  $K_i$  and  $C_H^0$  are obtained through non-linear least squares fitting techniques. This method allows for the identification of the  $pK_a$  values of functional groups on DOM which exert an influence during TA titration.

Another approach to incorporate the contribution of OrgAlk and to minimise subsequent errors in carbonate system calculations was developed by Kuliński et al. (2014) who included a bulk  $pK$  value for the acid-base species in DOM ( $pK_{DOM}$ ). This procedure requires DOC concentrations to be known along with OrgAlk values. By assuming that organic acids (HOrg) present in DOM behave like a weak monoprotic acid, the dissociation constant of said acid can be determined by:

$$K_a = \frac{[H^+][Org^-]}{[HOrg]} \quad (8)$$

Previous work have indicated that the titratable groups associated with DOM can occur in concentrations exceeding that of OrgAlk itself, and that the contribution of DOM to OrgAlk is not quantitative (Muller and Bleie, 2008). This is acknowledged as the fraction of DOM,  $f$ , which acts as an acid-base species. Subsequently, Eq. (8) is modified to:

$$K_{DOM} = \frac{[H^+][OrgAlk]}{(f \cdot DOC) - [OrgAlk]} \quad (9)$$

OrgAlk is then defined by:

$$OrgAlk = \frac{K_{DOM} \cdot f \cdot DOC}{[H^+] + K_{DOM}} \quad (10)$$

This method was developed and implemented by Kuliński et al. (2014) and returned a  $pK_{DOM}$  of 7.53 and an  $f$  value of 0.14 for Baltic seawater. The deviation reported between OrgAlk<sub>C</sub> and OrgAlk calculated using Eq. (10) was  $\leq$  2  $\mu\text{mol.kg}^{-1}$ . Similar methodology has been applied to further studies of OrgAlk in the Baltic Sea (Hammer et al., 2017), where similar  $pK_{DOM}$  and  $f$  values were reported,  $7.27 \pm 0.11$  and  $0.17 \pm 0.02$  respectively.

The data produced by Kuliński et al. (2014) was further explored through the use of humic ion-binding model (Tipping et al., 2011) coupled to a specific ion interaction model (Pitzer, 1991) to investigate the contribution of OrgAlk (Ulfsbo et al., 2015). Returned  $f$  values of 0.125 show good agreement with the revised  $f$  value of 0.12 obtained by



Kuliński et al. (2014), indicating that proton-binding models may be another possible method to characterise OrgAlk.

The aforementioned bulk  $pK_{DOM}$  methods are spatiotemporally specific, as the fixed fraction of DOM which exhibits acid-base characteristics during alkalinity titrations has recently been indicated to vary substantially with location and time in coastal waters (Song et al., 2020). DOM characteristics can be drastically modified along estuarine gradients (Asmala et al., 2016; Zhou et al., 2020) and can change with temporal cycles as frequent as tidal (Santos et al., 2009; Tzortziou et al., 2008). Furthermore, coastal systems are subject to loadings of DOM that are specific to the nature of their hydrological and geographic setting. Thus as the acid-base characteristics of DOM will change, the appropriate  $pK_{DOM}$  and  $f$  values will likely vary accordingly. However, it is worth noting that as the components of deep-sea DOM are more universal in nature compared to more site specific DOM of individual biomes (Zark and Dittmar, 2018), a bulk  $pK_{DOM}$  term may be applicable to waters with DOM of more uniform characteristics and constant concentration.

## 11. Recommendations

### 11.1. Filtration as an inherent step in OrgAlk analysis

Best practice methods for the analysis of carbonate chemistry in the open ocean typically assume filtration is not required (Dickson et al., 2007). Filtration of samples taken from coastal waters is necessary to mitigate interference from high biomass and heavy particulate loads that may interfere with carbonate chemistry analysis. Published methods detail acceptable methods of filtration for TA, pH and DIC analysis (Bockmon and Dickson, 2014), and employ 0.45  $\mu\text{m}$  pore size filters. Such filtration methods should be implemented in studies of OrgAlk as interferences in DIC or pH analysis arising from the presence of particulates can cause inaccuracies in OrgAlk<sub>C</sub> (Song et al., 2020). Furthermore, if back titrations or similar are to be pursued, samples for OrgAlk<sub>M</sub> determination should be filtered to remove particulates, as particulate organic matter has been shown to contribute non-negligible amounts to TA (Kim et al., 2006). As some studies characterise OrgAlk as a function of DOC (Hammer et al., 2017; Kuliński et al., 2014) yet do not filter samples for TA analysis, the contribution from particulates may be erroneously attributed to DOC and thus lead to overestimations of true OrgAlk values. The incorporation of a filtration step would allow for the characterisation of DOM associated OrgAlk and for direct comparisons with DOC qualitative and quantitative analysis methods. Filter pore size used would depend on the nature of the study, with smaller pore sizes of 0.2  $\mu\text{m}$  used in the characterisation of marine and coastal DOM (Benner et al., 1992; Shimotori et al., 2016).

### 11.2. Complementary spectroscopic DOM analysis

A possible route by which OrgAlk can be characterised is by linking it to the spectral characteristics of DOC. DOC is routinely measured through wet or high temperature oxidation with subsequent non-dispersive infra-red detection of liberated  $\text{CO}_2$ . Spectroscopic methods have also been utilised to estimate and characterise DOC in both terrestrial and coastal waters (Carter et al., 2013; Fichot and Benner, 2011). Although susceptible to errors which can be minimised with re-parameterization using locally generated data, an advantage inherent to spectroscopic estimations of DOC concentration is that it also offers insights into DOC characteristics (Chin et al., 1994; Helms et al., 2009; Weishaar et al., 2003). Thus, qualitative data on DOM composition derived from such procedures coupled with directly obtained information on the acid-base characteristics of OrgAlk can potentially establish approximate associations between spectral DOM characteristics and  $pK_{DOM}$  values. Performed in numerous coastal ecosystems that have similar hydrographic and climatic features, this could allow for the use of ecosystem specific spectral linked bulk  $pK_{DOM}$  values. As the content

and characteristics of carboxylic groups in humic substances from a diverse range of systems exhibit only small variations (Huizenga and Kester, 1979; Oliver et al., 1983), coastal areas in which terrestrial organics account for the major share of OrgAlk may be particularly suited to bulk  $pK_{DOM}$  utilisation. Furthermore, the acid-base properties of humic substances are not thought to undergo significant alterations arising from changes in matrix ionic strength (Masini, 1994), indicating that bulk humic  $pK$  values may be applicable across the ionic strength range in estuarine environments. However, as coastal systems are also subject to autochthonous loadings of DOM through microbiological production, humic like DOM constitutes only a portion of the potential organic contributors to TA. Given the vast array of TA and OrgAlk methodologies available as well as the heterogeneity of coastal DOM, characterising the acid-base properties of OrgAlk is a challenging task.

## 12. Conclusion

It appears that the remarks of Bradshaw et al. (1981) regarding the presence of unknown protolytes are still reiterated in contemporary research. The recent reevaluation of inconsistencies in carbonate system data from several hydrographic research cruises and subsequent attribution of these discrepancies to the likely influence of OrgAlk reinforces the significance of this alkalinity fraction. The share of TA which is constituted by OrgAlk appears to be larger in littoral zones that are subject to increased loadings of terrestrially discharged DOM. Evidence of a small yet tangible influence of OrgAlk on pelagic TA continues to grow. As the contributions to TA from minor acid-base species in pelagic waters are oftentimes deemed negligible, these findings further reinforce the importance of accounting for OrgAlk. As discussed, there is a growing consensus that neglecting to account for the contribution of OrgAlk when using TA as an input parameter can lead to miscalculation of the remaining carbonate system parameters, as well as important descriptors of the carbonate system such as calcite and aragonite saturation states. Miscalculations of these descriptors can lead to gross misrepresentations of the characteristics of the carbonate system in littoral areas sensitive to slight perturbations in carbonate chemistry. In order to fully account for the impact of OrgAlk, the concentrations, characterisations and associated  $pK$  values of the proton accepting portion of DOM must be accurately known. As seasonal events as well as tides can affect DOM characteristics and quantity, the acid-base characteristics attributed to OrgAlk associated molecules may vary accordingly with these cycles. If approaches such as the inclusion of OrgAlk terms in carbonate chemistry calculations are to be pursued, this would require the systematic description of general DOM concentrations and acid-base characteristics in coastal waters with respect to salinity, seasonal and trophic state of a system. Given the heterogeneity in concentration and equilibrium behaviour of OrgAlk components, the inclusion of OrgAlk terms in carbonate system calculations remains a demanding challenge. Given this, the suitability of TA as an appropriate parameter in the derivation of remaining carbonate system parameters in waters subject to enhanced OrgAlk loadings remains questionable, unless matters to incorporate its influence are carried out.

## Declaration of Competing Interest

None.

## Acknowledgements

The authors would like to thank Science Foundation Ireland, the geological survey of Ireland and the Marine Institute (Investigator Programme, grant number 16/IA/45209).





- measurements. *Deep. Res. Part I Oceanogr. Res. Pap.* 49, 1705–1723. [https://doi.org/10.1016/S0967-0637\(02\)00093-6](https://doi.org/10.1016/S0967-0637(02)00093-6).
- Muller, F.L.L., Bleie, B., 2008. Estimating the organic acid contribution to coastal seawater alkalinity by potentiometric titrations in a closed cell. *Anal. Chim. Acta* 619, 183–191. <https://doi.org/10.1016/j.aca.2008.05.018>.
- Müller, J.D., Schneider, B., Rehder, G., 2016. Long-term alkalinity trends in the Baltic Sea and their implications for CO<sub>2</sub>-induced acidification. *Limnol. Oceanogr.* 61, 1984–2002. <https://doi.org/10.1002/lno.10349>.
- Neubauer, S.C., Anderson, I.C., 2003. Transport of dissolved inorganic carbon from a tidal freshwater marsh to the York River estuary. *Limnol. Oceanogr.* 48, 299–307. <https://doi.org/10.4319/lno.2003.48.1.0299>.
- Oliver, B.G., Thurman, E.M., Malcolm, R.L., 1983. The contribution of humic substances to the acidity of colored natural waters. *Geochim. Cosmochim. Acta* 47, 2031–2035. [https://doi.org/10.1016/0016-7037\(83\)90218-1](https://doi.org/10.1016/0016-7037(83)90218-1).
- Olsen, A., Key, R.M., Van Heuven, S., Lauvset, S.K., Velo, A., Lin, X., Schirnick, C., Kozyr, A., Tanhua, T., Hoppema, M., Jutterström, S., Steinfeldt, R., Jeansson, E., Ishii, M., Pérez, F.F., Suzuki, T., 2016. The global ocean data analysis project version 2 (GLODAPv2) - an internally consistent data product for the world ocean. *Earth Syst. Sci. Data* 8, 297–323. <https://doi.org/10.5194/essd-8-297-2016>.
- Orr, J.C., Fabry, V.J., Aumont, O., Bopp, L., Doney, S.C., Feely, R.A., Gnanadesikan, A., Gruber, N., Ishida, A., Joos, F., Key, R.M., Lindsay, K., Maier-Reimer, E., Matear, R., Monfray, P., Mouchet, A., Najjar, R.G., Plattner, G.K., Rodgers, K.B., Sabine, C.L., Sarmiento, J.L., Schlitzer, R., Slater, R.D., Totterdell, L.J., Weirig, M.F., Yamanaka, Y., Yool, A., 2005. Anthropogenic Ocean acidification over the twenty-first century and its impact on calcifying organisms. *Nature* 437, 681–686. <https://doi.org/10.1038/nature04095>.
- Pakulski, J.D., 1986. The release of reducing sugars and dissolved organic carbon from *Spartina alterniflora* Loisel in a Georgia salt marsh. *Estuar. Coast. Shelf Sci.* 22, 385–394. [https://doi.org/10.1016/0272-7714\(86\)90063-6](https://doi.org/10.1016/0272-7714(86)90063-6).
- Patsavas, M.C., Byrne, R.H., Wanninkhof, R., Feely, R.A., Cai, W.J., 2015. Internal consistency of marine carbonate system measurements and assessments of aragonite saturation state: insights from two U.S. coastal cruises. *Mar. Chem.* 176, 9–20. <https://doi.org/10.1016/j.marchem.2015.06.022>.
- Paxéus, N., Wedborg, M., 1985. Acid-base properties of aquatic fulvic acid. *Anal. Chim. Acta* 169, 87–98. [https://doi.org/10.1016/S0003-2670\(00\)86210-8](https://doi.org/10.1016/S0003-2670(00)86210-8).
- Perdue, E.M., Reuter, J.H., Ghosal, M., 1980. The operational nature of acidic functional group analyses and its impact on mathematical descriptions of acid-base equilibria in humic substances. *Geochim. Cosmochim. Acta* 44, 1841–1851. [https://doi.org/10.1016/0016-7037\(80\)90233-1](https://doi.org/10.1016/0016-7037(80)90233-1).
- Pitzer, K.S., 1991. Ion interaction approach: theory and data correlation. In: *Activity Coefficients in Electrolyte Solutions*, pp. 75–153.
- Prieto, F.J.M., Millero, F.J., 2002. The values of pK<sub>1</sub> + pK<sub>2</sub> for the dissociation of carbonic acid in seawater. *Geochim. Cosmochim. Acta* 66, 2529–2540. [https://doi.org/10.1016/S0016-7037\(02\)00855-4](https://doi.org/10.1016/S0016-7037(02)00855-4).
- Rakestraw, N.W., 1949. The conception of alkalinity or excess base of sea water. *J. Mar. Res.* VII 15–20.
- Raymond, P.A., Bauer, J.E., 2000. Bacterial consumption of DOC during transport through a temperate estuary. *Aquat. Microb. Ecol.* 22, 1–12. <https://doi.org/10.3354/ame022001>.
- Raymond, P.A., Cole, J.J., 2003. Increase in the export of alkalinity from North America's largest river. *Science* (80) 301, 88–91. <https://doi.org/10.1126/science.1083788>.
- Raymond, P.A., Hamilton, S.K., 2018. Anthropogenic influences on riverine fluxes of dissolved inorganic carbon to the oceans. *Limnol. Oceanogr. Lett.* 3, 143–155. <https://doi.org/10.1002/lol2.10069>.
- Redfield, A.C., Ketchum, B.H., Richards, F.A., 1963. The influence of organisms on the composition of seawater. In: Hill, M.N. (Ed.), *The Sea*. Interscience, New York, pp. 1–34.
- Rheuban, J.E., Doney, S.C., McCorkle, D.C., Jakuba, R.W., 2019. Quantifying the effects of nutrient enrichment and freshwater mixing on coastal ocean acidification. *J. Geophys. Res. Ocean.* 124, 9085–9100. <https://doi.org/10.1029/2019JC015556>.
- Riebesell, U., Gattuso, J.P., 2015. Lessons learned from ocean acidification research. *Nat. Clim. Chang.* 5, 12–14. <https://doi.org/10.1038/nclimate2456>.
- Ritchie, J.D., Perdue, E.M., 2003. Proton-binding study of standard and reference fulvic acids, humic acids, and natural organic matter. *Geochim. Cosmochim. Acta* 67, 85–96. [https://doi.org/10.1016/S0016-7037\(02\)01044-X](https://doi.org/10.1016/S0016-7037(02)01044-X).
- Romankevich, E.A., 1984. Geochemistry of organic matter in the ocean. *Mar. Chem.* <https://doi.org/10.1007/978-3-642-49964-7>.
- Sabine, C.L., Feely, R.A., Gruber, N., Key, R.M., Lee, K., Bullister, J.L., Wanninkhof, R., Wong, C.S., Wallace, D., Tilbrook, B., Millero, F.J., Peng, T.-H., Kozyr, A., Ono, T., Rios, A.F., 2004. The oceanic sink for anthropogenic CO<sub>2</sub>. *Science* (80) 305, 5–12.
- Santos, I.R., Burnett, W.C., Dittmar, T., Suryaputra, I.G.N.A., Chanton, J., 2009. Tidal pumping drives nutrient and dissolved organic matter dynamics in a Gulf of Mexico subtropical estuary. *Geochim. Cosmochim. Acta* 73, 1325–1339. <https://doi.org/10.1016/j.gca.2008.11.029>.
- Sharp, J.D., Byrne, R.H., 2020. Interpreting measurements of total alkalinity in marine and estuarine waters in the presence of proton-binding organic matter. *Deep. Res. Part I*. <https://doi.org/10.1016/j.dsr.2020.103338>.
- Sharp, J.D., Byrne, R.H., 2021. Technical note: excess alkalinity in carbonate system reference materials. *Mar. Chem.* 233, 103965. <https://doi.org/10.1016/j.marchem.2021.103965>.
- Shimotori, K., Satou, T., Imai, A., Kawasaki, N., Komatsu, K., Kohzu, A., Tomioka, N., Shinohara, R., Miura, S., 2016. Quantification and characterization of coastal dissolved organic matter by high-performance size exclusion chromatography with ultraviolet absorption, fluorescence, and total organic carbon analyses. *Limnol. Oceanogr. Methods* 14, 637–648. <https://doi.org/10.1002/lom3.10118>.
- Sleigher, R.L., Hatcher, P.G., 2008. Molecular characterization of dissolved organic matter (DOM) along a river to ocean transect of the lower Chesapeake Bay by ultrahigh resolution electrospray ionization Fourier transform ion cyclotron resonance mass spectrometry. *Mar. Chem.* 110, 140–152. <https://doi.org/10.1016/j.marchem.2008.04.008>.
- Song, S., Wang, Z.A., Gonnee, M.E., Kroeger, K.D., Chu, S.N., Li, D., Liang, H., 2020. An important biogeochemical link between organic and inorganic carbon cycling: effects of organic alkalinity on carbonate chemistry in coastal waters influenced by intertidal salt marshes. *Geochim. Cosmochim. Acta* 275, 123–139. <https://doi.org/10.1016/j.gca.2020.02.013>.
- Sousa, A.I., Santos, D.B., Da Silva, E.F., Sousa, L.P., Cleary, D.F.R., Soares, A.M.V.M., Lillebo, A.I., 2017. “Blue carbon” and nutrient stocks of salt marshes at a temperate coastal lagoon (Ria de Aveiro, Portugal). *Sci. Rep.* 7, 1–11. <https://doi.org/10.1038/srep41225>.
- Stedmon, C.A., Amon, R.M.W., Rinehart, A.J., Walker, S.A., 2011. The supply and characteristics of colored dissolved organic matter (CDOM) in the Arctic Ocean: pan Arctic trends and differences. *Mar. Chem.* 124, 108–118. <https://doi.org/10.1016/j.marchem.2010.12.007>.
- Sundquist, E.T., Visser, K., 2003. The Geologic history of the carbon cycle, in: *Treatise on Geochemistry*, pp. 425–472. doi:10.1016/B0-08-043751-6/08133-0.
- Sutton, A., Newton, J., 2020. Reaching consensus on assessments of ocean acidification trends. *EOS Trans. Am. Geophys. Union* 101. <https://doi.org/10.1029/2020EO150944>.
- Terayama, H., 1954. Application of the method of colloid titration to the study of bacteria. *Arch. Biochem. Biophys.* 50, 55–63. [https://doi.org/10.1016/0003-9861\(54\)90008-9](https://doi.org/10.1016/0003-9861(54)90008-9).
- Tippling, E., Lofts, S., Sonke, J.E., 2011. Humic ion-binding model VII: a revised parameterisation of cation-binding by humic substances. *Environ. Chem.* 8, 225–235. <https://doi.org/10.1071/EN11016>.
- Tishchenko, P.Y., Wallmann, K., Vasilievskaya, N.A., Volkova, T.I., Zvalinskii, V.I., Khodorenko, N.D., Shkirkovskaya, E.M., 2006. The contribution of organic matter to the alkaline reserve of natural waters. *Oceanology* 46, 192–199. <https://doi.org/10.1134/S0001437006020068>.
- Tzortziou, M., Neale, P.J., Osburn, C.L., Megonigal, J.P., Maie, N., Jaffré, R., 2008. Tidal marshes as a source of optically and chemically distinctive colored dissolved organic matter in the Chesapeake Bay. *Limnol. Oceanogr.* 53, 148–159. <https://doi.org/10.4319/lno.2008.53.1.0148>.
- Ulfso, A., Kulinski, K., Anderson, L.G., Turner, D.R., 2015. Modelling organic alkalinity in the Baltic Sea using a humic-Pitzer approach. *Mar. Chem.* 168, 18–26. <https://doi.org/10.1016/j.marchem.2014.10.013>.
- Van Der Wal, A., Norde, W., Zehnder, A.J.B., Lyklema, J., 1997. Determination of the total charge in the cell walls of gram-positive bacteria. *Colloids Surf. B: Biointerfaces* 9, 81–100. [https://doi.org/10.1016/S0927-7765\(96\)01340-9](https://doi.org/10.1016/S0927-7765(96)01340-9).
- Wang, Z.A., Kroeger, K.D., Ganju, N.K., Gonnee, M.E., Chu, S.N., 2016. Intertidal salt marshes as an important source of inorganic carbon to the coastal ocean. *Limnol. Oceanogr.* 61, 1916–1931. <https://doi.org/10.1002/lno.10347>.
- Wanninkhof, R., Wood, M., Barbero, L., 2012. *Cruise Report: Gulf of Mexico and East Coast Carbon Cruise #2 (GOMECC-2)* 2.
- Weishaar, J.L., Aiken, G.R., Bergamaschi, B.A., Fram, M.S., Fujii, R., Mopper, K., 2003. Evaluation of specific ultraviolet absorbance as an indicator of the chemical composition and reactivity of dissolved organic carbon. *Environ. Sci. Technol.* 37, 4702–4708. <https://doi.org/10.1021/es030360x>.
- Wigley, T.M.L., 1983. The pre-industrial carbon dioxide level. *Clim. Chang.* 5, 315–320. <https://doi.org/10.1007/BF02423528>.
- Wolf-Gladrow, D.A., Zeebe, R.E., Klaas, C., Körtzinger, A., Dickson, A.G., 2007. Total alkalinity: the explicit conservative expression and its application to biogeochemical processes. *Mar. Chem.* 106, 287–300. <https://doi.org/10.1016/j.marchem.2007.01.006>.
- Woods, G.C., Simpson, M.J., Kelleher, B.P., Mccaull, M., Kingery, W.L., Simpson, A.J., 2010. Online high-performance size exclusion chromatography - nuclear magnetic resonance for the characterization of dissolved organic matter. *Environ. Sci. Technol.* 44, 624–630. <https://doi.org/10.1021/es903042e>.
- Wootley, R.J., 2021. Evaluation of the temperature dependence of dissociation constants for the marine carbon system using pH and certified reference materials. *Mar. Chem.* 229, 103914. <https://doi.org/10.1016/j.marchem.2020.103914>.
- Yang, B., Byrne, R.H., Lindemuth, M., 2015. Contributions of organic alkalinity to total alkalinity in coastal waters: a spectrophotometric approach. *Mar. Chem.* 176, 199–207. <https://doi.org/10.1016/j.marchem.2015.09.008>.
- Yao, H., McCutcheon, M.R., Staryk, C.J., Hu, X., 2020. Hydrologic controls on CO<sub>2</sub> chemistry and flux in subtropical lagoonal estuaries of the northwestern Gulf of Mexico. *Limnol. Oceanogr.* 1–19. <https://doi.org/10.1002/lno.11394>.
- Zark, M., Dittmar, T., 2018. Universal molecular structures in natural dissolved organic matter. *Nat. Commun.* 9, 1–8. <https://doi.org/10.1038/s41467-018-05665-9>.
- Zeebe, R.E., 2012. History of seawater carbonate chemistry, atmospheric CO<sub>2</sub>, and ocean acidification. *Annu. Rev. Earth Planet. Sci.* 40, 141–165. <https://doi.org/10.1146/annurev-earth-042711-105521>.
- Zhou, Y., He, D., He, C., Li, P., Fan, D., Wang, A., Zhang, K., Chen, B., Zhao, C., Wang, Y., Shi, Q., Sun, Y., 2020. Spatial changes in molecular composition of dissolved organic matter in the Yangtze River Estuary: Implications for the seaward transport of estuarine DOM. *Sci. Total Environ.* 143531. <https://doi.org/10.1016/j.scitotenv.2020.143531>.

## **Chapter 2**

# **Analytical Approaches**

## Abstract

Conventional total alkalinity (TA) titrations are non-discriminatory and measure the total excess of proton donors over proton acceptors in a water sample, regardless of inorganic or organic nature. However, measured TA ( $TA_M$ ) is typically attributed to inorganic species such as bicarbonate and carbonate, with smaller contributions from other inorganic acid-base species and negligible contribution from the organic fraction of alkalinity (OrgAlk). Additionally, the conventional definitions of TA omit OrgAlk contributions. This is problematic, as coastal waters can have elevated OrgAlk concentrations that can directly impact TA analysis and the uncertainty associated with calculated carbonate system parameters. TA calculated from DIC and pH ( $TA_C$ ) accounts only for inorganic alkalinity, whereas as aforementioned,  $TA_M$  measures all alkalinity components. This allows for estimations of OrgAlk by subtracting  $TA_C$  from  $TA_M$ , with this excess alkalinity attributed to titratable organic acid-base species. This method has limitations however, as it is inclusive of uncertainties in the input parameters used to calculate TA, as well as any uncertainties in the thermodynamic equilibrium constants used. Additionally, it does not give any insight into the potential acid-base properties of OrgAlk, which are essential if OrgAlk effects on calculated carbonate system parameters are to be minimised. Evidently, more direct methods to investigate OrgAlk are required if its contributions to TA are to be recognised. Here we present a discussion of the establishment of TA titration methodologies in DCU using Global Ocean Acidification Observing Network (GOA-ON) listed apparatus, including modifications made to enable OrgAlk titrations to estimate the concentrations and acid-base properties of OrgAlk. Additionally, *OrgAlkCalc*, an open-source Python based programme used to process generated titration files and calculate concentrations and acid-base properties of OrgAlk is detailed. Furthermore, details of additional carbonate system analysis of DIC and pH are given, along with details of complementary optical analysis of DOM.

## 2.1 TA titration procedure

In order to carry out direct quantitative and qualitative analysis of OrgAlk it is necessary to first analyse TA. TA analysis was primarily carried out using an open-cell, potentiometric titration procedure as outlined in SOP 3b of Guide to Best Practices for Ocean CO<sub>2</sub> Measurements Dickson et al. (2007). TA analysis was also carried out using a Versatile INstrument for the Determination of Total inorganic carbon and titration Alkalinity 3C (VINDTA) system as part of collaborative method validation exercises, outlined in section 3.1.2

The open-cell method is suitable for TA values encountered in coastal systems and is capable of an uncertainty of  $2 \mu\text{mol}\cdot\text{kg}^{-1}$ . Additionally, this method does not explicitly require knowledge of the concentrations of nutrient species which contribute to TA, such as phosphate and silicate, as the titration data used does not fall within the pH ranges at which these species exhibit a buffering effect. Furthermore, open-cell TA titrations are the established method used in carbonate system certified reference material (CRM) production (Dickson et al., 2003). For these reasons, open-cell methods of TA titration were pursued, using modified GOA-ON "in a Box" TA titration apparatus. Details of modifications made to GOA-ON "in a Box" kit apparatus are given in section 2.2. The TA titration apparatus can be seen in figure 2.1.

For the TA titration procedure, approximately 50 g of filtered seawater was dispensed into the titration vessel that had previously been rinsed with deionised water (DI) and thoroughly dried to remove any previous sample. While the sample was allowed to come to 25°C, the acid burette tip was rinsed with DI water and wiped with a laboratory tissue in order to remove any traces of the previously ran sample and prevent any carry-over contamination. The acid burette used was a National Institute of Standards and Technology-traceable (NIST) calibrated Gilmont GS-1200 micrometer style burette, with a 2 mL capacity and smallest dispensation volume of 0.002 mL. The manufacturer specified accuracy was  $\pm 0.5 \%$  of the reading. The acid burette was

filled by placing the tip of the burette into the acid titrant solution and retracting the micrometer plunger by twisting the screw head. Once filled, any trapped air bubbles were eliminated by placing the burette in a vertical position with the tip up, tapping gently and screwing the plunger back until all air was expelled. The burette was then refilled to account for titrant expelled during air bubble elimination until the dispenser read 0 mL. Any additional liquid on the burette tip was rinsed and wiped off prior to use. The burette was then placed into the sample solution, with care taken that solely the tip was in contact with the sample.

The electrode used to monitor the electromotive force (e.m.f.) during titration progression was a Metrohm Aquatrode plus, a combined pH electrode for pH titrations in ion-deficient aqueous media. This electrode was chosen to accommodate the analysis of low ionic strength estuarine samples. The reference electrolyte used was 3 M KCl and the bridge electrolyte used was a 0.7 M sodium chloride (NaCl) solution. This was intended to match the ionic strength of seawater (Mintrop, 2016). Although the bridge electrolyte can be adjusted to match the ionic strength of the sample being analysed, it was decided to use 0.7M NaCl for all samples, as after an exchange of electrolyte the electrode required significant time until the system was stable again (Metrohm, 2021). Prior to placing the electrode in the sample solution it was rinsed with 0.7 M NaCl to remove any traces of the previous sample and gently blot dried using a laboratory tissue to remove the residual rinse solution. The electrode was then securely placed in the sample solution ensuring the glass membrane was fully submerged.

The rinsed and dried sample temperature probe was then placed in the sample solution, with care taken not to contact it with either the electrode or burette tip. A Teflon coated stir bar was then introduced to the titration vessel that was positioned on top of a magnetic stirrer plate. The stir bar was rinsed with DI and dried with a laboratory tissue between samples. The titration vessel used was a 100 mL jacketed beaker connected to a circulating waterbath set at 25°C. The stirrer was turned on, ensuring adequate mixing without splashing the sample solution. The titration then



proceeded with an initial addition of acid to bring the sample pH to approximately 3.5. The sample was then stirred for 10 minutes to allow evolved CO<sub>2</sub> to escape, see section 2.2.1 for further details. After this time, the titration procedure proceeded with fixed incremental additions of acid until a final pH of approximately 3.0 had been reached. Increments of 0.02 mL were used, generating roughly 25 data points per titration.

## 2.2 Modifications to GOA-ON titration apparatus

The titration apparatus used in all reported TA and OrgAlk analysis was based on a modified GOA-ON "in a Box" TA titration kit (GOA-ON, 2022). The GOA-ON "in a Box" titration apparatus is a low-cost kit capable of producing weather-quality ocean acidification measurements. GOA-ON "in a Box" kits have been distributed to scientists in sixteen countries across Africa, Pacific Small Island Developing States, and Latin America, playing an important role in facilitating carbonate system measurements for researchers without access to state of the art equipment. Specific modifications were made to the apparatus and procedure outlined by GOA-ON in order to further improve the precision of the measurement technique and computational procedures. Furthermore, additional apparatus were included to facilitate OrgAlk titrations. In line with the motivations outlined in section 0.6, all additionally utilised apparatus were cost-effective and easily incorporated. The following details all modifications made to GOA-ON "in a Box" TA titration kit apparatus.

### Measurement of sample size

Although volume based sample measurement using calibrated 50 mL volumetric pipettes is outlined in the GOA-ON methodology, it was instead decided to opt for a mass based sample measurement technique. It is noted that although mass balances are typically costly analytical instruments, many laboratories have access them. Upon commencing analysis, approximately 50 mL of sample was drawn into a 60 mL syringe, with mass of the sample filled syringe recorded using a Sartorius CP224S Analytical Balance, ac-

curate to  $\pm 0.1$  mg. The syringe contents was then carefully emptied into the titration vessel. The mass of the empty syringe was then recorded and total mass of sample dispensed in grams calculated as the difference between the filled and emptied syringe. This procedure was advantageous over volume based sample measurement as it eliminated the need for sample density determination in order to convert from volume to mass units.

### 2.2.1 Sample Filtration

As particulates can pose a significant source of analytical interference to TA measurement in the coastal ocean (Chanson and Millero, 2007; Bockmon and Dickson, 2014), all samples for TA and subsequent OrgAlk analysis were filtered. For the TA and OrgAlk data presented in chapter 4, borosilicate GF/F filters were used. It is acknowledged that although borosilicate can introduce alkalinity (Huang et al., 2012; Mos et al., 2021), given the limited exposure ( $\leq 5$  minutes) between sample solution and the filter, the borosilicate associated alkalinity addition is believed to be negligible. For all other TA and OrgAlk data reported,  $0.45 \mu\text{m}$  nylon membrane filters were used.

### CO<sub>2</sub> degassing

CO<sub>2</sub> degassing is generally achieved though sparging the acidified sample solution using a suitable CO<sub>2</sub> free gas, typically ultrapure (UP) N<sub>2</sub>. Alternative methods involve stirring the acidified sample for a specific time duration to facilitate the evasion of evolved CO<sub>2</sub>. A simple experiment to assess stirring as a viable CO<sub>2</sub> evasion method was designed. TA values returned from identical 0.7 M NaCl solutions were compared when using stirring or N<sub>2</sub> sparging as the degassing method. In theory, if stirring was not a sufficient method of CO<sub>2</sub> degassing then residual amounts of bicarbonate would be present after the initial acidification step and therefore would influence the final TA value returned. Samples were either stirred vigorously without splashing or sparged with a continuous flow of UP N<sub>2</sub> for 10 minutes and further titrated as normal. T-test

of the mean value for replicate (n=3) stirred and sparged samples were performed in order to assess the statistical significance of differences, if any. As can be seen in table 2.1, no statistically significant difference in TA values recorded for each degassing methods was found, with a confidence level of 95%. It is important to note that degassing tests were performed on 0.7 M NaCl solutions with inherently limited carbonate alkalinity, and that although similar these solutions are not the same as seawater.

**Table 2.1:** Experimental analysis investigating suitability of stirring as an adequate CO<sub>2</sub> degassing method compared to ultrapure N<sub>2</sub> sparging. (a) Results from degassing experiments. (b) Two-sample equal variance t-test to compare mean degassed and non-degassed values (n=3). Results indicated no statistically significant difference ( $\alpha=0.05$ ) TA measurements between the two degassing methods.

(a)			(b)		
Date	Sample	TA ( $\mu\text{mol} \cdot \text{kg}^{-1}$ )		Degassed	Non-degassed
10/11/2021	Degassed A	152.0943688	Mean	152.65	151.63
	Degassed B	152.9865327	Variance	0.23	3.45
	Degassed C	152.8682429	Observations	3	3
10/11/2021	Non-degassed A	153.700549	Pearson Correlation	-0.92	
	Non-degassed B	151.094046	Hypothesized Mean Difference	0	
	Non-degassed C	150.1077419	df	2	
			t Stat	0.8	
			P(T<=t) one-tail	0.3	
			t Critical one-tail	2.9	
			P(T<=t) two-tail	0.53	
			t Critical two-tail	4.3	

### Sample and titrant temperature

For the GOA-ON outlined TA titration procedure, a single sample temperature is recorded once the titration has ceased with the assumption that sample temperature remained constant throughout the titration. As sample temperature can vary slightly through the titration, this can lead to possible uncertainty introduction in TA processing as many parameters involved in TA computational procedures are temperature dependent. Furthermore, titrant temperature throughout the titration is also assumed to remain constant at room temperature. This single value for titrant temperature is then

used in conjunction with a titrant density factor to determine mass dispensed at each titration point. In our case, this constant titrant temperature approach was not viable as titrant temperature was found to vary by  $\pm 0.10$  °C on average throughout the titration, see figure 2.2.

To address these issues we adapted the apparatus to include separate temperature probes to record sample and titrant temperature at each titration point. Sample temperature was recorded throughout the titration using a corrosion resistant, four wire resistance thermometer detector (RTD) (RS PRO, Stock No.: 123-5583). Titrant temperature was also recorded using a four wire RTD (RS PRO, Stock No.: 891-9141) insulated with polyethylene foam securely fastened to the titrant containing section of the burette.

The observed decrease in titrant temperature during the TA titration as per figure 2.2 can be explained through contact between the burette tip and sample solution. During the CO<sub>2</sub> degassing stage of the TA titration which commenced at titrant point  $\approx 15$ , to facilitate CO<sub>2</sub> evasion the rate of stirring is increased. This was observed to cause the burette tip to be removed from contact with the sample, due to the formation of a dip in the stirring solution. Upon cessation of contact with the sample solution, the temperature of the titrant decreased by 0.10 °C on average. When the CO<sub>2</sub> degassing stage was terminated and stirring returned to its original speed, contact between the burette tip and solution was resumed causing an observable increase in temperature.

During the NaOH titration, detailed in section 2.3.1, as the burette tip was in contact with the sample solution throughout the entire titration, a consistent increase in titrant temperature was observed. The jagged nature of the NaOH curve is possibly explained by noise in the signal caused by vibrations induced by dispersion of titrant from the burette, as typically RTD sensors are very sensitive to vibrations (Dames, 2008). Further evidence of noise introduction due to vibration is present in the TA curve, where significant noise is observed only in the region of the curve where initial titrant addition occurs (titration points 10 - 15). After the initial titration addition the

burette is stationary, no vibrations occur resulting in drastically reduced noise.

### **Titrant volume to density conversions**

Recorded titrant temperature data was used to convert volume of titrant dispensed at each titration point to mass units. This was achieved by using an experimentally derived equation that described mass dispensed as a function of volume and temperature. The equation was found by dispensing defined increments of titrant at controlled temperatures onto a mass balance. This resulted in a recorded mass for a known volume at a given temperature, allowing for the construction of a mass dispensed per volume at given temperature function, see figure 2.3. This process was carried out for all titrant solutions used. Density units of  $\text{g} \cdot \text{mL}^{-1}$  were used as volume dispensed was recorded in mL. The volume-to-mass function is described in more detail in section 2.4.3.

### **Additional base titrant burette**

As OrgAlk titrations involve the titration of an acidified seawater sample against a NaOH titrant, an additional burette was incorporated into the analytical apparatus. An additional burette was preferred rather than switching titrant solutions between a singular burette due to concerns of titrant carry over contamination and unnecessary wastage. The additional base burette was identical to the acid burette, with corresponding temperature measurement.

### **Digital multimeter switching system and instrument control software**

Due to the incorporation of multiple additional temperature sensors to the TA titration apparatus, there was a need to modify the configuration of the digital multimeter (DMM) used to record titration data. The DMM used was a Keithley model 2701. As per the GOA-ON methodology, the DMM is used in 'front' mode, allowing for only one titration variable to be recorded at any given time. In order to accommodate the

additional RTDs, a 40-channel differential multiplexer module (MM) was integrated into the DMM. The MM was well suited for use with RTDs as it allowed for 4-wire measurement configuration that can compensate for lead wire resistance issues (Dames, 2008), ensuring accurate measurement. Upon installation of the MM, the DMM could be operated in 'rear' mode, allowing for acquisition of consecutive measurements of multiple parameters. Keithley Kickstart DataLogger instrument control software was used in order to facilitate the acquisition of data from multiple parameters. At each titration point the sample potential and temperature as well as titrant temperature was recorded.

## 2.3 OrgAlk analysis

Given the growing evidence that OrgAlk can contribute significantly to TA in the coastal ocean, methods to investigate OrgAlk are of increasing importance. A widely used method to quantify OrgAlk is to calculate the difference between directly measured TA ( $TA_M$ ) and TA calculated ( $TA_C$ ) through DIC and pH measurements (Delaigue et al., 2020; Song et al., 2020; Kim and Lee, 2009; Hernández-Ayon et al., 2007). As  $TA_C$  incorporates only carbonate and non-carbonate inorganic proton acceptors, the difference between  $TA_M$  and  $TA_C$  can theoretically be attributed to the contribution from OrgAlk charge groups. Certain issues are associated with the aforementioned, specifically that OrgAlk obtained through this method is inherently inclusive of any residual uncertainties associated with  $TA_C$ . Furthermore this method provides no information on the acid-base properties of OrgAlk that are required for its explicit inclusion in TA calculations. Evidently, more in-depth methods to directly ascertain the quantity and acid-base properties of OrgAlk are preferable.

Methods to directly investigate OrgAlk were first reported by Cai et al. (1998), who defined OrgAlk as the sum of proton binding sites, or charge groups, present on DOM. The proton binding properties of charge groups present on DOM can be described by applying numerical models to curves generated through NaOH titrations of acidified

seawater (Paxéus and Wedborg, 1985; Perdue et al., 1984). This has previously been undertaken by considering OrgAlk as an aggregate of multiple distinct charge group species, each considered as a monobasic acid-base system with its own pK and total concentration (Cai et al., 1998; Muller and Bleie, 2008; Song et al., 2020). In these models it is assumed that OrgAlk can be described by 1 - 3 monoprotic weak acids, with the total concentration of each charge group being conservative. It has been established that the dissociation reactions of charge groups present on fully dissolved organic materials following a back titration, *e.g.* NaOH titration from pH  $\sim$ 3 to pH  $\sim$ 8 followed by HCl titration back to pH  $\sim$ 3, are reversible (Milne et al., 1995; Huizenga and Kester, 1979) indicating minimal impact to OrgAlk acid-base properties.

In the aforementioned numerical models, no ionic strength dependence on charge group properties is assumed; typically ionic strength plays a lesser role compared to chemical characteristics and charge group heterogeneity (Masini, 1993; Tipping and Hurley, 1992). In essence, a charge balance equation (see equation 2.10) that accounts for the concentrations and dissociation constants of acid-base species in a water sample is used to describe the shape of the titration curve. This method has been utilised and adapted by numerous researchers in recent studies of OrgAlk (Yang et al., 2015; Ko et al., 2016; Song et al., 2020). The analytical and computational procedures chosen for the investigation of OrgAlk quantity and acid-base properties were an adaptation of the method outlined in Ko et al. (2016) and Song et al. (2020).

### 2.3.1 OrgAlk titration procedure

The OrgAlk analysis procedure involved 3 distinct stages: a TA titration, a NaOH titration and an OrgAlk titration. During the TA titration all carbonate alkalinity is consumed, with the resultant acidified seawater having a pH of  $\sim$ 3. The NaOH titration then proceeds by small additions of NaOH titrant until the sample pH has been returned to its original value. At this point, the NaOH titration ceases and the OrgAlk titration begins. The OrgAlk titration proceeds identically to the TA titration procedure

with the exception that the returned alkalinity value is attributed to OrgAlk, as at this stage carbonate alkalinity has been consumed. A complete OrgAlk titration procedure resulted in the generation of 3 individual titration files for each sample analysed: a TA, NaOH and OrgAlk file.

### **Stage 1 - TA titration**

Prior to commencing the TA titration, the e.m.f. reading of the sample before any acid addition was recorded. This value served as a measure of the pH that the sample was to be returned to during the NaOH titration. The TA titration then proceeded identically to that as outlined in section 2.1. Once the TA titration has been completed, the acid burette was then removed from the sample solution, appropriately cleaned and refilled.

### **Stage 2 - NaOH titration**

Proceeding directly after the TA titration, the initial step of the NaOH titration procedure was to fill the NaOH burette. This was done under a N<sub>2</sub> atmosphere to prevent the dissolution of ambient CO<sub>2</sub> into the NaOH titrant. The burette was filled according to the procedure outlined in section 2.1. A N<sub>2</sub> gas stream was then directed onto the sample within the titration vessel as to minimise the presence of CO<sub>2</sub> during the NaOH titration and potential uptake at higher pH. The base burette was then placed into the sample solution, taking care that only the terminal section of the burette tip was in contact with the sample solution. Increments of NaOH were then added to the sample solution, with the volume dispensed at each increment such that the pH increase was approximately 0.1, allowing for adequate curve resolution. The titration ceased when e.m.f. readout has been returned to its original value, indicating that the sample had been returned to its original pH. The difference between original sample pH and sample pH at the end of the NaOH titration using e.m.f. as an indicator was on average  $-0.003 \pm 0.02$  (n=94). The base burette was then removed from the sample solution and



purged of any remaining titrant before being cleaned. Unlike the acid burette, the base burette was stored empty between titrations as to avoid uptake of CO<sub>2</sub>.

During certain NaOH titrations, the formation of a gelatinous white precipitate was observed on the burette tip. In the titrations that this precipitate was observed, agreement between replicate measurements decreased. In experimental analysis of NaOH titrations on sodium acetate spiked 0.7M NaCl solutions, no white precipitate build up was observed in any instance. This would suggest the precipitate was likely due to the presence of cations present in the seawater matrix. Furthermore, the occurrence of this precipitate was more commonly observed in higher salinity samples. A likely candidate was Mg<sup>2+</sup> as this cation is present in considerable amounts in seawater, being the most common cation after Na<sup>+</sup> (Pilson, 2013). Upon reaction of Mg<sup>2+</sup> with OH<sup>-</sup>, white gelatinous Mg(OH)<sub>2</sub> precipitates. The formation of Mg(OH)<sub>2</sub> likely hindered dispensation of titrant during the NaOH titration. It was found that by ensuring only the terminal section of the burette tip was in contact with the sample solution precipitate build up was mitigated. It is believed that the shear force generated at the surface of the mixing sample solution prevented the build up of detrimental amounts of Mg(OH)<sub>2</sub> precipitate.

### **OrgAlk titration**

The OrgAlk titration proceeded identical to the TA titration procedure outlined in section 2.1 with the exception of the CO<sub>2</sub> degassing stage. The degassing stage was not explicitly necessary as the titration vessel had been under a N<sub>2</sub> atmosphere since the initiation of the NaOH titration. A smaller initial addition of acid was needed to bring the sample solution to a pH of ~3.5, as at this point sample carbonate alkalinity had been removed. After initial acidification to pH ~3.5, the sample was then titrated with increments of 0.02 mL acid until a final pH of ~3.0 has been reached. The generated titration data was then processed using *OrgAlkCalc*, as outlined below.

## 2.4 *OrgAlkCalc*

All TA, NaOH and OrgAlk titration files were processed using *OrgAlkCalc* to calculate final TA values, as well as estimate the concentrations of OrgAlk charge groups and associated acid-base properties. *OrgAlkCalc* is a Python based, open-source programme that allows users to process TA and OrgAlk titration files generated through the use of adapted GOA-ON apparatus with minimal programming experience. *OrgAlkCalc* is available at [OrgAlkCalc](#) or in the reference section below (Kerr and Turner, 2022). TA is calculated using a simple Gran approach (Gran, 1952) coupled with a NLSF procedure (Dickson et al., 2003) as outlined below.

### 2.4.1 TA computational procedures

The generated TA titration data was used in a Gran titration (Gran, 1952, 1950) to provide an initial estimate of TA. The Gran function can be described by:

$$F_1 = (m_0 + m) \exp\left(\frac{E}{K}\right) \quad (2.1)$$

where  $m_0$  is the mass of sample titrated,  $m$  is mass of titrant dispensed,  $E$  is potential and  $K$  is the Nernst factor that can be described by:

$$K = \frac{R \cdot T}{F} \quad (2.2)$$

where  $R$  the universal gas constant,  $T$  the temperature in Kelvin and  $F$  the Faraday constant. Equation 2.1 is linear in  $m$ , therefore plotting  $F_1$  against  $m$  allows for  $m$  at the equivalence point to be calculated using a linear-least squares procedure. This initial estimate of TA was calculated using  $m$  at the equivalence point by:

$$TA = mC/m_0 \quad (2.3)$$

Where  $C$  is the concentration ( $\text{mol}\cdot\text{kg}^{-1}$ ) of acid used. Once this initial estimate of TA had been obtained, an estimate of the standard electrode potential ( $E_{estimate}^o$ ) was found by taking the average value of  $E^o$  calculated at each titration point using:

$$E_{estimate}^o = E - K \cdot \ln\left(\frac{-m_0 TA + mC}{m_0 + m}\right) \quad (2.4)$$

Using  $E_{estimate}^o$ , an initial estimate for hydrogen ion concentration ( $[H']$ ) at each titration point was obtained, such that:

$$[H'] = \exp\frac{E_{estimate}^o - E}{K} \quad (2.5)$$

$[H']$  was used to calculate Gran pH *i.e.*  $Gran_{pH} = -\log[H']$ .  $Gran_{pH}$  was then used to define the range of titration data used in a non-linear least squares curve fitting (NLSF) procedure. Only data within the pH range 3.0 - 3.5 was included as within this range the vast majority of  $\text{CO}_3^{2-}$  had been consumed, see figure 3. Further, in the circumstance that  $\text{CO}_3^{2-}$  was present, its concentration is typically less than  $0.5 \mu\text{mol}\cdot\text{kg}^{-1}$  (Dickson et al., 2003). The initial estimate of TA and  $E_{estimate}^o$  were then used in a non-linear least squares calculation procedure where the vector of residuals of equation 2.6 are minimised.

$$TA + \left(\frac{S_T}{1 + K_S Z / (f[H'])}\right) + \left(\frac{F_T}{1 + K_F / (f[H'])}\right) + \left(\frac{m_0 + m}{m_0}\right) \left(\frac{f[H']}{Z}\right) - \left(\frac{m}{m_0}\right) C = 0 \quad (2.6)$$

$E^o$  was not directly adjusted in this process but rather assigned a multiplicative factor  $f$ , where:

$$f = [H^+] / [H'] \quad (2.7)$$

In the NLSF procedure,  $f$  was given an initial value of 1 and adjusted along side the initial estimate of TA. In equation 2.6,  $F_T$  and  $S_T$  are the total fluoride and sulfate concentrations;  $K_F$  and  $K_S$  are the respective dissociation constants of each. Each was

calculated using literature reported equations:  $F_T$  (Riley, 1965),  $K_F$  (Perez and Fraga, 1987),  $S_T$  (Morris and Riley, 1966) and  $K_S$  (Dickson, 1990a). The impact of uncertainties in  $K_S$  in equation 2.6 was minimised by the inclusion of the  $Z$  term, where:

$$Z = (1 + S_T/K_S) \quad (2.8)$$

$f[H']$  represents the total hydrogen ion concentration and  $f[H']/Z$  represents the free hydrogen ion concentration. Equation 2.6 was used to define a vector of residuals to be minimised in the NLSF procedure. In this procedure, the values of TA and  $f$  were adjusted until the sum of the squared residuals is minimised. The NLSF returned value for  $f$  can be used to calculate the true value of  $E^o$  ( $E_{true}^o$ ) using:

$$E_{true}^o = E_{estimate}^o + K(f) \quad (2.9)$$

Subsequently, true  $[H^+]$  can be found by using  $E_{true}^o$  and equation 2.5. The NLSF returned TA value is then converted to units of  $\mu\text{mol} \cdot \text{kg}^{-1} \cdot \text{g}^{-1}$ .

## 2.4.2 OrgAlk computational procedures

To estimate OrgAlk concentrations and associated pK values, *OrgAlkCalc* uses an iterative NLSF procedure along with a simple model derived from charge balance equation 2.10 to fit OrgAlk charge group concentrations and apparent pK values to the NaOH titration curve (Song et al., 2020; Ko et al., 2016; Cai et al., 1998). The charge balance equation can be described by the following:

$$\begin{aligned} & V_0 \sum \frac{X_{iT}}{1 + \frac{[H^+]}{K_i}} + V_0 \frac{B_T}{1 + \frac{[H^+]}{K_B}} + V_0 \frac{P_T}{1 + \frac{[H^+]}{K_P}} + V_0 \frac{S_{iT}}{1 + \frac{[H^+]}{K_{Si}}} \\ & + V_b \frac{CTNa}{1 + \frac{[H^+]}{K_{C_1}} + \frac{K_{C_2}}{[H^+]}} + 2 \cdot V_b \frac{CTNa}{1 + \frac{[H^+]^2}{K_{C_1} \cdot K_{C_2}} + \frac{[H^+]}{K_{C_2}}} + (V_0 + V_a)(H_0) \quad (2.10) \\ & - (V_0 + V_a + V_b)([H^+] - [OH^-]) - V_b \cdot C_{NaOH} = 0 \end{aligned}$$

where  $V_0$  is the initial mass of sample,  $V_a$  is the total volume of acid added during the TA titration and  $V_b$  is the volume of base added at each titration point.  $K_i$ ,  $K_B$ ,  $K_P$  (as  $\text{H}_2\text{PO}_4^-$ ),  $K_{Si}$ ,  $K_{C_1}$  and  $K_{C_2}$  refer to the dissociation constants of charge group  $i$  of organic acids, boric acid, phosphoric acid, silicic acid and carbonic acid, respectively.  $X_{iT}$ ,  $B_T$ ,  $P_T$  and  $Si_T$  are the total concentrations of charge group  $i$  of organic acids, borate, phosphate and silicate, respectively.  $CTNa$  refers to the total concentration of  $\text{CO}_3^{2-}$  in the NaOH titrant, discussed in detail in section 2.5.2.  $[H^+]$  and  $[OH^-]$  are the concentration of protons and hydroxide ions, while  $H_0$  is the initial proton concentration of the NaOH titration.  $C_{NaOH}$  is the concentration of the NaOH titrant. By adjusting the values of  $X_i$  and  $K_i$  in a NLSF procedure to minimise the residuals in equation 2.10, *OrgAlkCalc* can produce estimations of the quantity and acid-base properties of OrgAlk.

### 2.4.3 Titration data handling

In order to convert raw titration data into a format compatible with the necessary procedures used to compute TA as well as the quantity and acid-base properties of OrgAlk, specific data handling techniques were employed. As with TA titration files, both the NaOH and OrgAlk titration files were amended to include columns containing volume of titrant dispensed data. Once amended to contain the aforementioned, metadata integral to titration processing such as sample name, salinity and mass, as well as concentration of titrants used were assigned to each sample. Rather than treat each file individually, all sample metadata was incorporated into a master titration file (MTF). The MTF was organised such that each row corresponded to all required metadata for a given sample. Each MTF row also contained the path identifying the computer directory locations and specific names of the TA, NaOH and OrgAlk titration files. Metadata integral to the NaOH curve fitting procedure was also contained in the MTF, such as the initial estimates of the dissociation constants of OrgAlk and the calculated carbonate content of the NaOH titre. Options to include concentrations of inorganic species that

impact alkalinity titrations such as phosphate and silicate are also included in the MTF, along with options for which  $K_{C_1}$  and  $K_{C_2}$  definitions to use, see below. This made it possible for *OrgAlkCalc* to access all necessary titration data and associated metadata from a single file. Likewise, when processing titration samples contained within the MTF, *OrgAlkCalc* automatically exported the results to a master results file. This feature added to the accessibility and ease of use of *OrgAlkCalc*.

Once samples has been appropriately amended and the MTF populated with the necessary information, *OrgAlkCalc* was executed. The sequence in which each titration file was processed differed slightly to the analysis procedure previously outlined. Initially the TA titration file was processed as detailed in section 2.4.1. Data essential to OrgAlk titration file processing was then extracted from the NaOH titration file. The OrgAlk titration file was then processed similarly to the TA titration file, however the updated parameters extracted from the NaOH file were used. Finally, the curve fitting procedures were applied to the NaOH titration data and estimates of the quantity and acid-base properties of OrgAlk were returned. Throughout the execution of the aforementioned computation procedures, specific functions included in *OrgAlkCalc* to minimise uncertainty were utilised.

### Volume to mass conversions

As mentioned in section 2.2.1, the volume of titrant dispensed at each titration point was converted to mass units to more accurately define titrant quantities. The total mass of titrant added ( $m_T$ ) was calculated as the cumulative sum of volume converted to mass at each titration point.

$$m_T = \sum_{i=1}^n V_i \cdot \rho \quad (2.11)$$

where  $V_i$  is the volume dispensed at titration point  $i$  and  $\rho$  is the experimentally derived density function. Initially  $m_T$  was calculated as the total volume of titrant added converted to mass using the last recorded temperature value. However, due to slight variations in titrant temperature throughout the titration (see section 2.2) this did not

give an accurate value for  $m_T$ . Calculation as per 2.11 negated uncertainties in  $m_T$  as the specific temperature at each dispensation point is utilised in volume-to-mass conversions.

### Salinity and ionic strength refactoring

Due to the differences in ionic strength between the titrant solutions and samples as discussed in section 2.5, sample ionic strength was altered upon titrant addition. As the ionic strength of the titrant solutions was accurately known, it was possible to calculate the change in ionic strength at each titration point and refactor the resultant salinity value. This was achieved by first converting sample salinity to ionic strength:

$$ImO_0 = \frac{19.924 \cdot S}{1000 - 1.005 \cdot S} \quad (2.12)$$

where  $ImO_0$  is initial ionic strength and  $S$  is sample salinity (Dickson, 1990b). The ionic strength at each titration point ( $ImO$ ) due to titrant addition is calculated as:

$$ImO = \frac{ImO_0 \cdot V_0 + m \cdot ImO_t}{V_0 + m} \quad (2.13)$$

where  $V_0$  is the initially recorded sample mass,  $m$  is mass of titrant and  $ImO_t$  is titrant ionic strength. Note that the value of  $V_0$  differs for the TA, NaOH and OrgAlk titrations, such that:

$$\begin{aligned} V_{0TA} &= V_0 \\ V_{0NaOH} &= V_0 + V_a \\ V_{0OrgAlk} &= V_0 + V_a + V_b \end{aligned} \quad (2.14)$$

$ImO$  is then refactored to salinity by:

$$S = \frac{1000 \cdot ImO}{19.924 + 1.005 \cdot ImO} \quad (2.15)$$

The above allows for recalculation of salinity dependent thermodynamic equilibrium constants for each titration point, and mitigation uncertainties inherent to TA titrations in solutions of varying ionic strength. In addition to any implications for activity coefficients and subsequently the various pK values used, changes in solution composition resulting from titrant addition can also impact the degree to which the pH electrode exhibits Nernstian behaviour. This impact is acknowledged, although it is believed to be small (Okamura et al., 2014).

### **Thermodynamic equilibria**

Salinity and temperature dependant thermodynamic equilibrium constants as well as total concentrations of specific inorganic species were calculated using sample specific data. The aforementioned were calculated at each titration point using dilution-adjusted  $S$  or  $ImO$ , as well as temperature if required. The following were calculated using literature reported functions:  $F_T$  (Riley, 1965),  $K_F$  (Perez and Fraga, 1987),  $S_T$  (Morris and Riley, 1966),  $K_S$  (Dickson, 1990a),  $B_T$  (Lee et al., 2010) and  $K_B$  (Dickson, 1990b).  $K_{C_1}$  and  $K_{C_2}$  were utilised in the processing of the NaOH titration. As multiple variations of  $K_{C_1}$  and  $K_{C_2}$  have been described in the literature (Woosley, 2021), *OrgAlkCalc* contains multiple  $K_{C_1}$  and  $K_{C_2}$  options. Typically the choice of  $K_{C_1}$  and  $K_{C_2}$  reflects the ionic strength of the coastal seawater samples being investigated and pH scale used. The choice of  $K_{C_1}$  and  $K_{C_2}$  can be specified to best suit study location and sample matrix, as outlined in 2.2. It is important to note the potential for added uncertainty on model results arising from disparities between pH scale inherent to the choice of constants and pH inherent to the NaOH titration, the latter being on the  $pH_{SWS}$  scale. However, the degree of added uncertainty is likely small as the difference between  $pH_T$  and  $pH_{SWS}$  are approximately 0.01 (Marion et al., 2011).



**Table 2.2:** Choices of  $K_{C_1}$  and  $K_{C_2}$  provided in *OrgAlkCalc*. Matrix refers to the composition of samples used to originally ascertain values  $K_{C_1}$  and  $K_{C_2}$ 

$K_{C_1}$ and $K_{C_2}$ options	Salinity range	Temperature range (°C)	Matrix
Lueker et al. (2000)	19 - 35	2 - 35	seawater
Cai et al. (1998)	0 - 40	2 - 35	estuary water
Mehrbach et al. (1973) refit by Dickson and Millero (1987)	19 - 35	2 - 35	seawater
Millero (2010)	0.10 - 50	1 - 50	seawater
Prieto and Millero (2002)	12 - 45	5 - 45	seawater

#### 2.4.4 NaOH curve fitting

NaOH curve fitting proceeded in four distinct stages: (1) NaOH titration data in the range  $\text{pH} \leq 5$  was used to constrain  $H_0$ ,  $X_1$  and  $K_1$ . This approach was taken as in this low pH range the contribution of charge groups with high pK values can be omitted (Cai et al., 1998). (2)  $H_0$  was then fixed and a NLSF curve fitting technique was performed iteratively for titration data in the range  $\text{pH} \leq \text{pH}_{\text{max}} \cdot 0.75$  in order to constrain  $X_1$  and  $K_1$ .  $\text{pH}_{\text{max}}$  refers to the highest pH of the NaOH titration. The multiplier 0.75 was chosen as it allowed for sufficient sequential curve fitting of  $X_2$ , and  $X_3$  if required. The initial estimates of  $H_0$  and  $X_i$  were taken as the concentration of  $\text{H}^+$  at the start of the NaOH titration and  $\text{OrgAlk}_M$  minus  $CTNa$ , respectively. Initial estimates of  $K_i$  were provided by the user in the master titration file. (3) Values of  $X_1$  and  $K_1$  were then fixed and values of  $X_2$  and  $K_2$  were constrained using all data. (4) Finally,  $X_2$  and  $K_2$  were fixed and values of  $X_3$  and  $K_3$  were constrained using all data. After each step, model outputs were used in a refactored equation 2.10 to solve for  $V_b$ . This calculated  $V_b$  ( $V_{bC}$ ) value was compared to the experimentally derived  $V_b$  ( $V_{bM}$ ) value in order to produce a root mean square (RMS) residual value, see figure 4.2. Residuals were defined as  $V_{bM}$  minus  $V_{bC}$  and RMS was calculated as the square root of the sum of residuals divided by  $n-1$ ,  $n$  being the number of data points in the titration curve.

For each curve fitting procedure, the initial conditions were set to iterate curve fitting until the difference between each consecutive repetitions returned RMS ( $\Delta$ RMS) was less than  $1 \times 10^{-10}$ , with this value referred to as the convergence factor. In the instance that  $\Delta$ RMS was greater than the convergence factor after 100 repetitions, the convergence factor increased by a factor of 10. This processes repeated until  $\Delta$ RMS < convergence factor. The final convergence factor value was recorded and served as an initial indication of the validity of model returned results.

### 2.4.5 Experimental method validation

In order to ascertain *OrgAlkCalc* performance, exploratory analysis using a simulated seawater solution spiked with a known concentration of a well characterised organic acid was conducted. The organic acid chosen was acetic acid (AcOH). AcOH is monoprotic, short-chain fatty acid that is the conjugate acid of acetate, an important substrate for various microbial metabolic processes in the marine environment (Zhuang et al., 2019a,b). The acid-base properties of AcOH are well characterised across a range of ionic strengths (Mizera et al., 1999; Daniele et al., 1983; Chen et al., 1996), making it an ideal candidate for use in *OrgAlkCalc* performance testing. Furthermore, as the pK of AcOH as reported is  $4.76 \pm 0.01$  (Mizera et al., 1999), it does not exhibit a strong buffering effect in the pH range utilised in TA-*OrgAlk* Gran titrations (pH 3.0 - 3.5). This minimised the possibility of deviation from linearity of the Gran function (Cai et al., 1998; Sharp and Byrne, 2020). Although it is acknowledged that real-world organic molecules can possess charge groups that exhibit pK values within the pH range 3.0 - 3.5, the purpose of this experiment was to ascertain *OrgAlkCalc* performance in estimating the quantity and acid-base properties of *OrgAlk*, therefore the use of a non-interfering analyte was required. Using a 0.7 M NaCl solution as the background media to simulate seawater ionic strength and sodium acetate (Sigma-Aldrich, item ID: 241245) as the AcOH source, 50, 150 and 250  $\mu\text{mol} \cdot \text{kg}^{-1}$  solutions AcOH were prepared. The AcOH solutions were subject to identical processes used in sample prepa-

ration and analysis. OrgAlk analysis proceeded as outlined in section 2.3.1, with all titration data processing carried out using *OrgAlkCalc*. It is important to note that the non-carbonate inorganic species present in seawater that impact TA, specifically borate, sulphate and hydrogen fluoride, were not included in the computational procedures performed on the AcOH solutions as they were 0.7 M NaCl solutions and not actual seawater. AcOH pK was calculated as a function of ionic strength at 0 and 0.7 M using the formulae of Mizera et al. (1999). The OrgAlk titration procedure was also carried out on the 0.7 M NaCl used as a background solution in order to ascertain *CTNa*. As during the TA titration carbonate alkalinity is consumed, for a NaCl solution assumed to contain negligible amounts of organics, the alkalinity value returned by the OrgAlk titration should correspond to the quantity of carbonate introduced during the NaOH titration due to innate NaOH titrant carbonate content. Titration specific *CTNa* was subtracted from OrgAlk<sub>M</sub> to correct from NaOH titrant introduced alkalinity.

**Table 2.3:** Results generated by *OrgAlkCalc* for AcOH spiked simulated seawater. Units for AcOH, TA, *CTNa*, OrgAlk<sub>M</sub> and OrgAlk<sub>C</sub> are  $\mu\text{mol} \cdot \text{kg}^{-1}$ .  $pK_C$  refers to *OrgAlkCalc* returned pK value whereas  $pK_0$  and  $pK_{0.7}$  refer to the pK of AcOH calculated per Mizera et al. (1999) for a 0 and 0.7 M ionic strength solution, respectively. The uncertainty on reported values was calculated as the standard deviation of replicate measurements (n=3).

Concentration AcOH	TA	<i>CTNa</i>	OrgAlk <sub>M</sub>	OrgAlk <sub>C</sub>	$pK_C$	$pK_0$	$pK_{0.7}$
50	82.46±1.05	15.56±0.11	37.67±2.14	48.02±0.7	4.85±0.009		
150	179.56±0.31	17.71±0.01	124.16±0.79	129.99±6.22	4.71±0.002	4.74±0.01	4.506±0.01
250	268.94±2.69	19.63±0.05	210.36±2.55	220.6±5.64	4.72±0.016		

As can be seen in table 2.3 and figure 2.5a, OrgAlk<sub>C</sub> gives a better estimation of OrgAlk quantity compared to OrgAlk<sub>M</sub>. This can possibly be attributed to slight discrepancies in the calculation of *CTNa*, as overestimation of *CTNa* with subsequent subtraction from OrgAlk<sub>M</sub> can lead to underestimation of OrgAlk. As OrgAlk<sub>C</sub> was returned from the NLSF procedure that used OrgAlk<sub>M</sub>-*CTNa* as the initial estimate to be adjusted in curve fitting, OrgAlk<sub>C</sub> is likely a more accurate reflection of true OrgAlk

quantities.

The magnitude of the difference between actual AcOH concentration and  $\text{OrgAlk}_C$  was observed to increase as AcOH concentration increased. This can possibly be related to changes in the degree of dissociation of AcOH as a function of AcOH concentration. Ostwald's Dilution law states that the degree of dissociation of a weak acid is inversely proportional to the square root of concentration and directly proportional to the square root of dilution, given by the equation:

$$\alpha \propto \frac{1}{\sqrt{C_{HA}}} \text{ or } \alpha \propto \sqrt{V} \quad (2.16)$$

As the concentration of weak acid ( $C_{HA}$ ) increases, the degree of dissociation ( $\alpha$ ) will proportionally decrease. As the concentration of AcOH was increased in each simulated seawater solution, this then would decrease  $\alpha_{AcOH}$ . If  $\alpha_{AcOH}$  decreases, this will decrease the quantity of acetate present acting as proton acceptors during the OrgAlk titration, diminishing the overall OrgAlk signal. This phenomena could lead to underestimations of  $\text{OrgAlk}_C$  returned in OrgAlk analysis of environmental samples. However, as marine DOM is a heterogeneous mixture of diverse organic molecules (Asmala et al., 2016) with the average concentration of individual DOM compounds assumed to be very low (Hansell et al., 2009), the issue of concentration related dissociation suppression may not be as significant an issue.

$pK_C$  and  $pK_0$  were observed to display greater agreement than  $pK_C$  and  $pK_{0.7}$ . This was expected as the model used to characterise the apparent acid-base properties of OrgAlk charge groups does not contain ionic strength dependencies of  $pK$ . Given that  $pK_0$  was equal to  $pK_{AcOH}$  at no ionic strength, *OrgAlkCalc* returned values were in excellent agreement, on average varying by  $\pm 0.02$ . Differences between  $pK_C$  and  $pK_{0.7}$  were considerably greater seeing a tenfold increase in  $\Delta pK$ , on average 0.25. Maximum observed uncertainties in returned  $pK$  values of humic acids across ionic strengths of 0.01 - 1.0 M calculated using NaOH titration curve fitting procedures were 0.75 (Masini et al., 1998). More recently reported errors in  $pK$  values resulting from ignoring ionic

strength were given as 0.49 (Song et al., 2020). The reported uncertainty due to non-inclusion of ionic strength dependencies of  $pK$  generated by *OrgAlkCalc* falls within this range.

## 2.5 Titrant solutions

Typically, titrants used in TA titrations are made up in a NaCl background solution that largely matches the ionic strength of the samples being titrated. In the case of open ocean TA analysis, the HCl titrant is made up in a 0.6M NaCl to give a final ionic strength of 0.7 M, matching open ocean seawater. In estuarine environments, due to freshwater inputs, ionic strength can vary considerably. In these scenarios, matching HCl titrant and sample ionic strength would only be possible through the use of multiple, individually standardised titrant solutions of varying ionic strength. Given the apparatus used in this investigation, this was not a feasible option as multiple HCl burettes were not available. Furthermore, switching the titrant of the burette to be used for each sample of differing ionic strength was not considered due to concerns of titrant carry-over contamination.

For the TA titration it is likely that changes in sample ionic strength resulting from titrant addition is more important for closed-cell titrations, where all acid-base reactions are relevant in the evaluation of the whole titration curve compared to an open-cell approach where strictly it is only  $K(\text{HSO}_4)$  and  $K(\text{HF})$  that are involved (A. Dickson, personal communication, May 24<sup>th</sup>, 2021). Given these factors, it was decided to not alter the ionic strength of the HCl titrant and make it up solely in a DI background. Similarly, the NaOH titrant was also made up in a DI background as this is in line with previously reported literature (Song et al., 2020; Ko et al., 2016; Yang et al., 2015). Measures to minimise the impact on ionic strength dependent equilibrium constants in computational procedures were implemented. This was achieved by factoring in the slight dilution of the sample upon titrant addition and refactoring ionic strength, allowing for the recalculation of ionic strength dependent variables at each titration point.

### 2.5.1 HCl titrant

The HCl titrant used in the TA titration methods outlined above was a 0.1 M HCl solution made using HCL concentrate (Honeywell Fluka) diluted to 1L with DI water. The concentration of the acid titrant used in TA titrations is typically the largest source of possible analytical uncertainty. Acid concentration is expressed in units of molality rather than molarity as volumes of acid added are often converted to mass units to minimise titrant dispensation related uncertainties, see section 2.2.1. An uncertainty of  $0.0001 \text{ mol} \cdot \text{kg}^{-1}$  in acid concentration approximately equals a TA uncertainty of  $2 \mu\text{mol} \cdot \text{kg}^{-1}$ , highlighting the importance of accurate and precise acid standardisation.

#### HCl calibration

Acid titrant calibration was carried out using a carbonate system CRM with an assigned TA value. The CRM was run as a sample using the methodology outlined in 2.1. A calibrated acid concentration value was obtained by processing the titration data as per section 2.4.1 with the exception that in equation 2.6 the value of TA was set as the CRM assigned TA. This allowed equation 2.6 to be solved for  $C$  and a value for calibrated acid concentration obtained.

#### CRM dilution experiment

As carbonate system CRM salinity is equal to that of open ocean seawater, dilution experiments were conducted to investigate the effect of salinity on returned calibrated acid concentration. Ideally the CRM used to calibrate acid concentration for TA titrations should have a TA and salinity similar to that of the samples being analysed. CRM dilution was carried out by conducting a series of gravimetric dilutions on CRMs using  $\text{N}_2$  sparged DI water. The resulting TA concentration post dilution,  $TA_{Diluted}$ , was calculated by:

$$TA_{Diluted} = TA_{CRM} \cdot \left( \frac{m_{CRM}}{m_{CRM} + m_{DI}} \right) + \left( \frac{TA_{DI}}{1000} \cdot m_{DI} \right) \quad (2.17)$$

where  $TA_{CRM}$  and  $TA_{DI}$  are the TA values of the CRM and DI used for dilution respectively.  $m_{CRM}$  and  $m_{DI}$  refer to the mass (g) of CRM and DI. Calibrated acid concentration was then calculated using  $TA_{Diluted}$  in the methods discussed in section 2.5.1.

**Table 2.4:** Diluted CRM calibrated acid concentration with corresponding uncertainty in  $\mu\text{mol.kg}^{-1}$  TA.

Salinity	$\Delta$ acid concentration ( $\text{mol.kg}^{-1}$ )	$\Delta$ TA ( $\mu\text{mol.kg}^{-1}$ )
7.52	$4.815 \times 10^{-3} \pm 4.596 \times 10^{-3}$	$-108.88 \pm 103.93$
13.80	$1.612 \times 10^{-3} \pm 1.062 \times 10^{-3}$	$-36.51 \pm 24.06$
20.11	$3.629 \times 10^{-4} \pm 6.676 \times 10^{-4}$	$-8.27 \pm 15.16$
26.31	$-5.304 \times 10^{-4} \pm 3.395 \times 10^{-4}$	$1.11 \pm 7.75$

As can be seen from figure 2.6, the deviation away from true CRM values increases substantially with degree of dilution. The uncertainty associated with each calibrated acid concentration are related to the standard deviation of replicate measurements (n=3), with error increasing with degree of dilution, indicating that at lower  $TA_{Diluted}$  uncertainty is likely introduced by the dilution process. Furthermore, changes in ionic strength of CRM solution likely played a role in the larger errors observed at lower salinities. As per table 2.4, the corresponding  $\Delta$  TA for each given  $\Delta$  acid concentration is significant even at lower dilutions. The use of diluted CRM calibrated acid concentrations would in each instance lead to a under-representation of true TA. Given this potential for significant uncertainty introduction, it was decided not to proceed with dilute CRM acid standardisation. The suitability of single point acid calibration is further discussed in section 3.1.1.

## 2.5.2 NaOH titrant

The NaOH titrant used was a 0.1 M solution made using NaOH concentrate (Reagecon) diluted to 1L with DI water sparged with ultrapure  $\text{N}_2$  to minimise dissolved  $\text{CO}_2$ .

**Table 2.5:** Concentrations of NaOH titrant over analysis period in mol · kg<sup>-1</sup>. Mean and standard deviation values relate to replicate measurements (n=3).

Date	Mean mol · kg <sup>-1</sup>	Standard deviation mol · kg <sup>-1</sup>	Relative standard deviation
24/11/2021	0.0979	0.0007	0.7588
01/12/2021	0.0967	0.0000	0.0010
01/12/2021	0.0966	0.0006	0.5975
08/12/2021	0.0978	n/a	n/a
08/12/2021	0.0972	0.0004	0.4506
10/01/2022	0.0981	0.0006	0.5920
17/01/2022	0.0981	0.0009	0.9638
17/01/2022	0.0977	0.0007	0.6916
04/02/2022	0.0977	0.0009	0.9331
04/02/2022	0.0975	0.0004	0.3881
29/03/2022	0.0981	0.0006	0.6141
13/04/2022	0.0981	0.0005	0.5421
21/04/2022	0.0983	0.0011	1.0807
09/05/2022	0.0981	1.61 × 10 <sup>-7</sup>	0.0002
22/05/2022	0.0992	0.0003	0.3066

**NaOH calibration**

The NaOH titrant was standardised against NIST traceable, dried potassium hydrogen phthalate Standard Reference Material (Certipur) (Muller and Bleie, 2008). The mean average deviation associated with triplicate NaOH standardisation was 0.0004 mol.L<sup>-1</sup>.

**NaOH carbonate content**

An important factor to consider in the OrgAlk titration was the CO<sub>3</sub><sup>2-</sup> content of the NaOH titrant (*CTNa*). The presence of CO<sub>3</sub><sup>2-</sup> in the NaOH titrant has been attributed to dissolved CO<sub>2</sub> (Song et al., 2020) as well as reagent impurities (Yang et al., 2015). As the NaOH titrant is added to the sample solution, this will inadvertently introduce carbonate alkalinity to the sample and contribute to the final OrgAlk value. To counteract this, it is important to quantify *CTNa*.

*CTNa* was measured over the analysis period by performing the aforementioned



titration procedure on a 0.7 M NaCl solution that had been purged of CO<sub>2</sub> using ultra-pure N<sub>2</sub>. During the TA titration, carbonate alkalinity was consumed. Additionally, the 0.7 M NaCl solutions was assumed to have a negligible concentration of organics, with care taken to ensure proper handling and cleaning of glassware used. Based on the aforementioned, the alkalinity value returned from the OrgAlk titration for a 0.7 M NaCl organic free solution corresponds to the alkalinity introduced due to NaOH titrant addition. This alkalinity was attributed to the CO<sub>3</sub><sup>2-</sup> content of the NaOH titrant, *CTNa*. Over the analysis period mean *CTNa* values varied between approximately 25 - 70 μmol·kg<sup>-1</sup>, see figure 2.7. The equation of the polynomial associated with the aforementioned was used to estimate *CTNa* throughout the analysis period. The addition of CO<sub>3</sub><sup>2-</sup> to samples through titration with NaOH is discussed further in section 4.3.1.

## 2.6 Nutrient Analysis

Nutrient analysis and data processing was performed by research colleagues, Andrew Donohoe and Jill Keogh. Phosphate analysis was performed using an adapted vanadate molybdate method (Donohoe et al., 2018) and ammonia analysis was carried out using methodology adapted from Grasshoff et al. (1998). Of the OrgAlk analysis conducted in this thesis, complementary nutrient analysis is only reported for the Rogerstown Estuary work.

## 2.7 Complementary carbonate system analysis

DIC and pH analysis was performed on specific samples complementary to TA and OrgAlk analysis in order to carry out carbonate chemistry calculations. DIC measurements were conducted on a limited number of Dublin Bay seawater samples in order to use DIC alongside TA as an input parameter to calculate pH and pCO<sub>2</sub> for comparison with directly measured pH and pCO<sub>2</sub>. pH measurements were conducted on a limited number of Dublin Bay seawater samples as well as transitional seawater sam-

ples collected from Rogerstown Estuary, Dublin, in order to use pH alongside TA as an input parameter in carbonate chemistry calculations.

### **2.7.1 DIC analysis**

DIC analysis generally involves the acidification of a known mass of seawater and quantification of subsequently evolved gaseous CO<sub>2</sub>. Detection of liberated CO<sub>2</sub> is performed typically one of two ways; coloumetric detection or non-dispersive infrared detection (NDIR). Although NDIR methods are utilised in ocean carbonate system research, coloumetric detection remains the standard given its low level of analytical uncertainty (Zhai, 2021; Wills and Johnson, 1994). The basis of DIC analysis by coloumetric means was developed in the 1980's and refined in the early 1990's (Johnson et al., 1985; Johnson and Sieburth, 1987; Johnson et al., 1993).

#### **DIC analysis procedure**

All DIC analysis was carried out on a VINDTA 3C supplied by the Marianda company, Kiel, Germany. CRMs provided by Prof. A. Dickson, Scripps Institute of Oceanography, USA, were used to calibrate the system and provide a DIC calibration factor. It is important to note that although filtration is advised for coastal DIC samples (Bockmon and Dickson, 2014), this was not possible in our case. Measures were initially taken to place a gas-tight inline filter in the sample drawing tube of the VINDTA to facilitate filtration upon filling of the DIC burette. Upon investigation it was found that the force generated by the peristaltic pump used for filling the DIC burette was too low to facilitate filtration. To work around this issue, particulates present were allowed ample time to settle prior to measuring DIC. Additionally, the sample was drawn from the upper regions of the sample bottle and care was taken to disturb the sample solution as little as possible. This method has been deemed satisfactory as a means to mitigate the impact of particulates on DIC measurement using a VINDTA system (A. Flohr, personal communication, July 27<sup>th</sup>, 2022).

Analysis proceeded in the following fashion: an accurately known volume of seawater was acidified with 85% phosphoric acid, with the subsequently liberated CO<sub>2</sub> stripped from the solution using a carbon free gas, typically UP N<sub>2</sub>. The carrier gas was passed through a CO<sub>2</sub> absorbent prior to entering the stripping chamber. The resultant gas stream was then passed through a condenser in order to remove water vapour, which acts as an interferent in the titration process. The gas stream then entered the coulometer cell, that consisted of a cathode and anode compartment. The cathode compartment was filled with an aqueous dimethylsulfide (DMS) solution containing monoethanolamine and a coulometric indicator, thymolphthalein. The monoethanolamine reacted with CO<sub>2</sub> to form a titratable weak acid, hydroxyethylcarbamic acid, that lowered the pH and subsequently diminished the colour of the indicator, which was blue at a pH of 10.5 and colourless at a pH of 9.3 in aqueous solutions (Johnson et al. (1985)). The cathode compartment contained a platinum electrode that was utilised in the hydrolysis of water to produce hydroxide ions. The generated hydroxide ions were used to titrate the generated weak acid. The anode compartment contained a silver anode and aqueous DMS, as well as saturated potassium iodide (KI) in water, with further reagent grade KI crystals added in order to ensure the saturation of the solution was maintained throughout analysis. The assembly was positioned between a light source and a photodetector present in the coulometer apparatus. The cathode solution, when saturated with CO<sub>2</sub>, was transparent in colour and therefore the initial percentage transmission (%T) was 100%.

Upon commencing the coulometric titration procedure, all CO<sub>2</sub> present in the cathode solution was purged by passing an electrical current between the two electrodes, producing hydroxide ions at the cathode and subsequently reducing the hydroxyethylcarbamic acid, until a %T of 30% was obtained, with this serving as the baseline transmittance. The sample gas stream was then passed through the cell, while photodetection monitored the change in the solutions colour as a %T. As the %T increased due to the pH induced colour change, the titration current was automatically activated

to stoichiometrically generate base at the cathode at a rate proportional to the % $T$ . Once enough current, measured in counts, had passed through the solution to return it to its baseline transmittance value, the titration ceased. The resulting counts value was then converted to  $\mu\text{mol}\cdot\text{kg}^{-1}$  DIC using the aforementioned DIC calibration factor. Substandards of open ocean surface seawater were analysed to identify possible instrumental drift. Precision for DIC was  $1.22 \mu\text{mol}\cdot\text{kg}^{-1}$  ( $n=3$ ) and was calculated as the standard deviation of the difference between replicate results of substandards.

### 2.7.2 pH analysis

Spectrophotometric pH determination is based on the addition of a well characterised indicator dye to a seawater sample while measuring the absorbance of the protonated ( $\text{HI}^-$ ) and deprotonated ( $\text{I}^{2-}$ ) species of the dye, each of which have a distinct wavelength of maximum absorbance ( $\lambda_{max}$ ). Commonly used indicator dyes include meta-Cresol purple (mCp), thymol blue and phenol red (Liu et al., 2011; Hudson-Heck and Byrne, 2019; Robert-Baldo et al., 1985). The value of the second dissociation constant of the aforementioned dyes is in the range of pH values typically encountered in seawater. This allows the pH of a dye-seawater solution to be calculated as a function of indicator dye dissociation constant and the ratio of absorbance values of  $\text{I}^{2-}$  and  $\text{HI}^-$  :

$$pH = pK + \log_{10} \left( \frac{[\text{I}^{2-}]}{[\text{HI}^-]} \right) \quad (2.18)$$

$[\text{I}^{2-}]/[\text{HI}^-]$  in the above equation is found by multi-wavelength spectrophotometric measurement such that:

$$\frac{[\text{I}^{2-}]}{[\text{HI}^-]} = \frac{A_1/A_2 - \epsilon_1(\text{HI}^-)/\epsilon_2(\text{HI}^-)}{\epsilon_1(\text{I}^{2-})/\epsilon_2(\text{HI}^-) - A_1/A_2 \cdot \epsilon_2(\text{I}^{2-})/\epsilon_1(\text{HI}^-)} \quad (2.19)$$

where  $A_1$  and  $A_2$  are the recorded absorbance values at  $\lambda_{max}$  for  $\text{I}^{2-}$  and  $\text{HI}^-$ , respectively; and  $\epsilon_\lambda(\text{HI}^-)$  and  $\epsilon_\lambda(\text{I}^{2-})$  are the extinction coefficients of  $\text{HI}^-$  and  $\text{I}^{2-}$  at each respective  $\lambda_{max}$ . The pK and extinction coefficients of the indicator dye are functions

of temperature and salinity, and are well characterised (DeGrandpre et al., 2014; Liu et al., 2011). Equation 2.19 can be substituted into equation 2.18 to give:

$$pH = pK + \log_{10} \left( \frac{A_1/A_2 - \varepsilon_1(HI^-)/\varepsilon_2(HI^-)}{\varepsilon_1(I^{2-})/\varepsilon_2(HI^-) - A_1/A_2 \cdot \varepsilon_2(I^{2-})/\varepsilon_1(HI^-)} \right) \quad (2.20)$$

Typically  $A_1/A_2$  is referred to as  $R$ ,  $\varepsilon_1(HI^-)/\varepsilon_2(HI^-)$  as  $e_1$ ,  $\varepsilon_1(I^{2-})/\varepsilon_2(HI^-)$  as  $e_2$  and  $\varepsilon_2(I^{2-})/\varepsilon_1(HI^-)$  as  $e_3$ . Equation 2.20 can then be rewritten as:

$$pH = pK + \log_{10} \left( \frac{R - e_1}{e_2 - R \cdot e_3} \right) \quad (2.21)$$

Spectrophotometric pH measurements have innate advantages over glass cell electrode methods. Dye based measurements are not prone to drift unlike electrodes and have a low degree of associated uncertainty, with measurement uncertainties of 0.004 pH units achievable (Müller and Rehder, 2018; DelValls and Dickson, 1998). Furthermore, if existing knowledge of dye extinction coefficients or protonation characteristics is improved upon, archived spectrophotometric pH data can be quantitatively revised (Clayton and Byrne, 1993). These factors present spectrophotometric pH measurement as an attractive alternative to traditional glass cell electrode methods. An important consideration of dye based spectrophotometric pH measurements worth acknowledging is the impact of potential impurities present in indicator dyes (Yao et al., 2007). Methods to purify indicator dyes have been developed (Liu et al., 2011; Pat-savas et al., 2013), however as purification procedures involve specific instrumentation and chemical reagents, purified dye is available only to a small number of laboratories (Douglas and Byrne, 2017a). Given the high degree of precision observed in this work using unpurified dye, the impact of dye impurities is acknowledged but not further pursued.

### **pH analysis procedure**

Spectrophotometric pH analysis was carried out using a method adapted from SOP 6b of Dickson et al. (2007) based on the work of Clayton and Byrne (1993). pH was measured using a Shimadzu UV 2600 scanning UV-Vis spectrophotometer with a TCC-100 thermoelectrically temperature controlled cell holder installed. Given the capabilities of the available spectrophotometer, the use of a 1 cm pathlength cuvette was required. Although conventional methods typically utilise a 10 cm pathlength cuvette, there are a growing number of studies that employ the use of 1 cm pathlength cuvettes (Fangue et al., 2010; Ohline et al., 2007; Perez De Vargas Sansalvador et al., 2016; Takeshita et al., 2020). In our case, the cuvette used was a 1 cm pathlength fused quartz cuvette with airtight stopper (Thorlabs, item ID: CV10Q35A). This cuvette was ideally suited as the airtight stopper minimised ambient CO<sub>2</sub> exchange.

Sample was transferred to the cuvette via a peristaltic pump and Tygon tubing. The cuvette was allowed to overflow by 1.5 times its volume before dye addition to ensure minimal CO<sub>2</sub> exchange. When the cuvette was full, the tubing was slowly removed while the pump was still running to negate the introduction of a headspace. Filtration was performed using the methodology outlined in Bockmon and Dickson (2014) using a gas-tight inline filter with 0.45 µm Durapore Membrane Filters (Millipore, item ID: HVLPO4700). A new filter was used for each sample. Care was taken to ensure all air bubbles in the filter and tubing were removed each time the filter was replaced. The cuvette was placed in the thermoelectrically temperature controlled cell holder set to 25°C. Additionally, a RTD (RS PRO, Stock No.: 891-9141) that was small enough to place in the gap present when the cuvette was placed in the cell holder was used to provide a more accurate temperature.

The indicator dye used was a 3 mM mCp solution stored in air-tight 1.5 mL amber chromatography vials with preset septum screw lids. The dye was prepared in DI water as it was to be used in the analysis of samples from a wide salinity range (Li et al., 2020). Dye was drawn from the vials and introduced to the cuvette using a gas-tight

GC syringe (Fisher, item ID: 10177754). The use of GC syringes allowed for highly accurate volume dispensation while ensuring gas-tight conditions. When drawing dye, the syringe was overfilled and purged until the required volume remained to eliminate air bubbles. 20  $\mu\text{L}$  dye was slowly added to the bottom of the cuvette with minimal turbulence. The air-tight stopper was quickly inserted ensuring that expelled sample due to stopper introduction did not contain any dye. The cuvette was then cleaned with laboratory wipe, inverted to ensure complete mixing between sample and dye solution and placed in the sample cell holder. When allowing the sample-dye solution to come to 25°C, the blank cuvette was filled, cleaned and placed in the reference cell holder.

The absorbance of the sample-dye solution was then recorded at  $\lambda_{max}$  for both  $\text{I}^{2-}$  and  $\text{HI}^-$ . The absorbance at a non-absorbing wavelength,  $\lambda_{720nm}$ , was also recorded. Measurement at  $\lambda_{720nm}$  was carried out to correct for any baseline shift due to error in repositioning cell or instrumental shifts. Additionally, if absorbance at  $\lambda_{720nm}$  was greater than  $\pm 0.001$ , the sample cell was removed and the optical window re-cleaned. Considering this,  $R$  was calculated as:

$$R = \frac{(A_{578nm} - A_{730nm})}{(A_{434nm} - A_{730nm})} \quad (2.22)$$

Once a value for  $R$  was obtained,  $e_1$ ,  $e_2$ ,  $e_3$  and dye pK were calculated using sample salinity and temperature at measurement using the summary equations for pH calculation on the  $\text{pH}_T$  scale of Douglas and Byrne (2017b).

### pH perturbation corrections

Prior to analysis the pH of the dye was adjusted to match sample pH as per Dickson et al. (2007). pH generally varied across the sampling locations, therefore dye pH was adjusted to the mean sample pH value. Methods to further minimise sample pH perturbations due to dye addition were carried out following the methodology of Lai et al. (2016) and Mosley et al. (2004). The multiple dye volume addition procedure outlined below has recently been recommended to determine dye perturbation adjustment Li

et al. (2020). Sequential equivolume dye additions were introduced to a sample with the corresponding pH for each individual dye addition calculated. This allowed for construction of a curve to extrapolate back to sample pH before dye addition ( $\text{pH}_0$ ). Error was calculated as the standard deviation of triplicate measurements. This extrapolation method was validated by performing sequential dye additions on a 2-amino-2-hydroxymethyl-1,3-propanediol (Tris) buffer solution, provided by Dr. A. Dickson, Scripps Institute of Oceanography, USA. The pH of Tris buffer ( $\text{pH}_{\text{Tris}}$ ) is well characterised across a range of temperature and salinity values and can be calculated using the expression of DeValls and Dickson (1998). Using the assigned salinity value of the tris buffer and the exact temperature of the buffer at the time of measurement  $\text{pH}_{\text{Tris}}$  was calculated in triplicate. As can be seen from figure 2.8,  $\text{pH}_{\text{Tris}}$  and  $\text{pH}_0$  differ by  $0.00091 \pm 0.00127$ , illustrating the effectiveness of this technique. If this correction was not applied and the recorded pH at 20 $\mu\text{L}$  of dye added was taken as sample pH, the uncertainty on pH would be 0.013. This value is considerably above the 0.005 pH unit perturbation typically associated with dye addition (Chierici et al., 1999). This is believed to have arisen from pH differences  $> 0.05$  between the indicator dye and Tris buffer used. The pH of the indicator was not adjusted in this instance as to simulate the possible differences between mean sample pH adjusted indicator pH and individual sample pH as aforementioned.

## 2.8 Optical analysis and data processing

Descriptive analysis of coastal DOM was conducted through the measurement of chromophoric dissolved organic matter (CDOM) alongside fluorescent dissolved organic matter (FDOM), two intrinsically linked parameters. CDOM refers to the fraction of DOM that interacts with solar radiation, whereas FDOM refers to the fraction of CDOM that exhibits fluorescence upon excitation at specific wavelengths (Nelson and Siegel, 2013). Interpretation of the absorbance and fluorescence spectra of filtered coastal seawater samples typically involves the utilisation of indices that link the optical prop-



erties of DOM to specific identifiers of DOM source or molecular signature (Gabor et al., 2014; Lee et al., 2018), see table 5.2 for more detail.

All glassware used for optical analysis of DOM was stringently cleaned to prevent organic contamination following the guidelines of Wurl (2017). Polypropylene gloves were worn at all times when handling glassware intended for use in organic analysis. The sample collection bottles used were 100 mL amber glass vials with Teflon lined screw caps. The sample storage vials were 10 mL clear glass vials with screw cap lids. All screw caps were rinsed with methanol and UP water, and allowed to dry in an oven before use. All glassware was soaked in 10% HCl and rinsed thoroughly with DI before being capped with tinfoil and allowed to dry in an oven. Glassware was then furnaceed for 6 hours at 450°C. Once furnaceed, the glassware caps were screwed on over the foil to minimise air exposure until time of sample collection. Glassware that could not be furnaceed was rinsed with methanol, followed by UP water.

Samples were collected by rinsing the sample bottle 3 times with the solution it was to contain prior to filling. Once collected, samples were stored in the dark on ice in a cool box. Filtration of sample was carried out on the same day as collection. Filtration apparatus was identical to that outlined in section 2.7.2 with the exception of the filter used. In this instance, the filters used were 0.45  $\mu\text{m}$  nylon membrane. Proper precautions were taken to minimise possibility of organic contamination. Prior to use and between samples, the filter holder, all tubing used and 0.45  $\mu\text{m}$  nylon membrane filter were rinsed with methanol and DI. The 0.45  $\mu\text{m}$  nylon membrane filter was then placed inside the filter holder and the peristaltic pump turned on, with the tubing and filter holder fully flushed with methanol 3 times, followed by DI 3 times.

The sample was then passed through the filter, allowing for a flushing volume of  $\sim 50$  mL. Approximately 7.5 mL of filtrate was then collected in a 10 mL glass vial that was subsequently wrapped in tinfoil to prevent exposure to ambient light. Samples were then stored upright, in the dark in a freezer until analysis within 1 week of collection. When thawing, samples were stored in the dark and analysed the same day as

thawed. In this thesis, both absorbance and fluorescence analysis of coastal DOM was conducted, as detailed below.

### **Absorbance analysis**

CDOM can be measured with relative ease and provides insights into the optical properties of DOM. The optical properties of DOM are routinely used as indicators of DOM source and inherent molecular composition across a wide range of environments (Coble, 2007; Fellman et al., 2010; Stedmon and Nelson, 2015). All CDOM analysis was carried out using a Shimadzu UV 2600 scanning UV-Vis spectrophotometer in spectrum mode and a 1 cm pathlength cuvette. Spectra were collected across the range 240 - 600 nm with an interval of 0.5 nm and scan speed set to slow. UP water was used as the blank. Absorption values ( $A$ ) were converted to Napierian absorption coefficients ( $a$ ) using:

$$a = 2.303 \cdot A \cdot l^{-1} \quad (2.23)$$

where  $l$  is the pathlength in meters.  $a$  values were log transformed and linear regression performed on the wavelength intervals 275 - 295 nm and 350 - 400 nm to calculate the spectral slope of each,  $S_{275-295}$  and  $S_{350-400}$ , respectively (Helms et al., 2008). Additionally, slope ratio ( $S_R$ ), an indicator of molecular weight (MW) and exposure to photochemical degradation (Helms et al., 2008; Guéguen and Cuss, 2011) was calculated as  $S_R = S_{275-295} : S_{350-400}$ . Further indices were also calculated:  $a_{350}$ , an indicator of DOM lignin phenol content (Benner and Kaiser, 2011; Hernes and Benner, 2003);  $a_{325}$ , an indicator of the presence of aromatic substances (Catalá et al., 2015; Nelson et al., 2004), and  $a_{254}$ , commonly used as a measure of relative concentration of CDOM (Li et al., 2021).

### **Fluorescence analysis**

Fluorescence spectroscopy can give indications of the molecular characteristics of the fluorescent portion of DOM, and has long been applied to the study of marine organics

(Coble et al., 1990; Coble, 1996; Parlanti et al., 2000). As *OrgAlkCalc* returned estimates of the acid-base properties of OrgAlk, data interpretation alongside three-dimensional excitation-emission-matrix (EEM) fluorescence spectra may provide further insights into the types and sources of DOM associated with OrgAlk.

All fluorescence analysis was carried out using a LS-55 Perkin-Elmer Fluorescence Spectrometer and a 1 cm pathlength quartz fluorescence cuvette (Thorlabs, item ID: CV10Q7FA). Sample was transferred to the cuvette using a furnaceed Pasteur pipette and transferred to the fluorescence spectrometer cell holder, all while exposure to light was minimised. Three dimensional excitation–emission fluorescence spectra were constructed using excitation wavelengths ( $\lambda_{Ex}$ ) 200 - 450 nm with 5 nm intervals. Emission wavelengths ( $\lambda_{Em}$ ) were scanned across the range 300 to 600 nm with 0.5 nm intervals. UP water was used as the blank and was subtracted from sample spectra. Measures were taken to account for the reabsorption of emitted light by excited fluorophores using an absorbance-based approach. Inner-filter effects (IFE) was corrected for using the following (Ohno, 2002; Parker and Barnes, 1957):

$$I_0 = \frac{I}{(10^{-l(A_{Ex} + A_{Em})})} \quad (2.24)$$

where  $I_0$  is fluorescence with no IFE,  $I$  is the fluorescence intensity,  $l$  is half the cuvette pathlength, and  $A_{Ex}$  and  $A_{Em}$  are the absorbance values at  $\lambda_{Ex}$  and  $\lambda_{Em}$ , respectively.  $A_{Ex}$  and  $A_{Em}$  were obtained by performing a spectral scan across the range of wavelengths of analysis (200 - 600 nm). Raman calibration to account for instrument specific fluorescence intensities was performed during each analysis. EEMs were normalized to the integral of the Raman peak between 390 nm and 410 nm for  $\lambda_{Ex}$  of 350 nm using a Milli-Q water blank Lawaetz and Stedmon (2009). The the integral of the Raman peak at given  $\lambda_{Ex}$  ( $A_{rp}^{\lambda_{Ex}}$ ) was found by:

$$A_{rp}^{\lambda_{Ex}} = \int_{\lambda_{Em}^1}^{\lambda_{Em}^2} I_{\lambda_{Em}} \delta \lambda_{Em} \quad (2.25)$$

where  $I_{\lambda_{Em}}$  is the measured intensity of the Ramen peak at each  $\lambda_{Em}$ .  $A_{rp}$  can easily be found by summing the intensity at every wavelength. This was then used to normalise the intensity of sample fluorescence at any given wavelength:

$$F_{\lambda_{Ex}\lambda_{Em}}(R.U.) = \frac{I_{\lambda_{Ex}\lambda_{Em}}(A.U.)}{A_{rp}} \quad (2.26)$$

where  $F_{\lambda_{Ex}\lambda_{Em}}$  is the normalised fluorescence signal in Ramen Units (R.U.) and  $I_{\lambda_{Ex}\lambda_{Em}}$  is the retuned intensity at given  $\lambda_{Ex}/\lambda_{Em}$  in arbitrary units (A.U.). Ramen and Rayleigh peaks were removed using *eemR* (Massicotte, 2017), with removed Ramen and Rayleigh scatter replaced with 0. Once processed, the DOM fluorescence peaks of (Coble, 1996) were identified and labelled. Biological index (BIX) (Huguet et al., 2009), an indicator of recent autochthonous DOM production was calculated using *eemR*.

## References

- Asmala, E., Kaartokallio, H., Carstensen, J., and Thomas, D. N. (2016). Variation in riverine inputs affect dissolved organic matter characteristics throughout the estuarine gradient. *Frontiers in Marine Science*, 2(JAN):1–15.
- Benner, R. and Kaiser, K. (2011). Biological and photochemical transformations of amino acids and lignin phenols in riverine dissolved organic matter. *Biogeochemistry*, 102(1):209–222.
- Bockmon, E. E. and Dickson, A. G. (2014). A seawater filtration method suitable for total dissolved inorganic carbon and pH analyses. *Limnology and Oceanography: Methods*, 12(APR):191–195.
- Cai, W. J., Wang, Y., and Hodson, R. E. (1998). Acid-base properties of dissolved organic matter in the estuarine waters of Georgia, USA. *Geochimica et Cosmochimica Acta*, 62(3):473–483.
- Catalá, T. S., Reche, I., Álvarez, M., Khatiwala, S., Guallart, E. F., Benítez-Barrios, V., Fuentes-Lema, A., Romera-Castillo, C., Nieto-Cid, M., Pelejero, C., Fraile-Nuez, E., Ortega-Retuerta, E., Marrasé, C., and Álvarez-Salgado, X. A. (2015). Water mass age and aging driving chromophoric dissolved organic matter in the dark global ocean T. *Global biogeochemical cycles*, (29):917–934.
- Chanson, M. and Millero, F. J. (2007). Effect of filtration on the total alkalinity of open-ocean seawater. *Limnology and Oceanography: Methods*, 5(SEP):293–295.
- Chen, J. F., Xia, Y. X., and Choppin, G. R. (1996). Derivative Analysis of Potentiometric Titration Data to Obtain Protonation Constants. *Analytical Chemistry*, 68(22):3973–3978.
- Chierici, M., Fransson, A., and Anderson, L. G. (1999). Influence of m-cresol purple in-

- indicator additions on the pH of seawater samples: Correction factors evaluated from a chemical speciation model. *Marine Chemistry*, 65(3-4):281–290.
- Clayton, T. D. and Byrne, R. H. (1993). Spectrophotometric seawater pH measurements: total hydrogen ion concentration scale calibration of m-cresol purple and at-sea results. *Deep-Sea Research Part I*, 40(10):2115–2129.
- Coble, P. G. (1996). Characterization of marine and terrestrial DOM in seawater using excitation-emission matrix spectroscopy. *Marine Chemistry*, 51(4):325–346.
- Coble, P. G. (2007). Marine optical biogeochemistry: The chemistry of ocean color. *Chemical Reviews*, 107(2):402–418.
- Coble, P. G., Green, S. A., Blough, N. V., and Gagosian, R. B. (1990). Characterization of dissolved organic matter in the Black Sea by fluorescence spectroscopy.
- Dames, C. (2008). Resistance Temperature Detectors. In *Encyclopedia of Microfluidics and Nanofluidics*, pages 1790–1790.
- Daniele, P. G., Rigano, C., and Sammartano, S. (1983). Ionic strength dependence of formation constants-I. Protonation constants of organic and inorganic acids. *Talanta*, 30(2):81–87.
- DeGrandpre, M. D., Spaulding, R. S., Newton, J. O., Jaqueth, E. J., Hamblock, S. E., Umansky, A. A., and Harris, K. E. (2014). Considerations for the measurement of spectrophotometric pH for ocean acidification and other studies. *Limnology and Oceanography: Methods*, 12(DEC):830–839.
- Delaigue, L., Thomas, H., and Mucci, A. (2020). Spatial variations in CO<sub>2</sub> fluxes in the Saguenay Fjord (Quebec, Canada) and results of a water mixing model. *Biogeochemistry*, 17(2):547–566.
- DelValls, T. A. and Dickson, A. G. (1998). The pH of buffers based on 2-amino-2-

- hydroxymethyl-1,3-propanediol ('tris') in synthetic sea water. *Deep-Sea Research Part I: Oceanographic Research Papers*, 45(9):1541–1554.
- Dickson, A. G. (1990a). Standard potential of the reaction:  $\text{AgCl(s)} + \frac{1}{2}\text{H}_2(\text{g}) = \text{Ag(s)} + \text{HCl(aq)}$ , and the standard acidity constant of the ion  $\text{HSO}_4^-$  in synthetic sea water from 273.15 to 318.15 K. *The Journal of Chemical Thermodynamics*, 22(2):113–127.
- Dickson, A. G. (1990b). Thermodynamics of the Dissociation of Boric Acid in Potassium Chloride Solutions from 273.15 to 318.15 K. *Journal of Chemical and Engineering Data*, 35(3):253–257.
- Dickson, A. G., Afghan, J. D., and Anderson, G. C. (2003). Reference materials for oceanic  $\text{CO}_2$  analysis: A method for the certification of total alkalinity. *Marine Chemistry*, 80(2-3):185–197.
- Dickson, A. G. and Millero, F. J. (1987). A comparison of the equilibrium constants for the dissociation of carbonic acid in seawater media. *Deep Sea Research Part A, Oceanographic Research Papers*, 34(10):1733–1743.
- Dickson, A. G., Sabine, C. L., and Christian, J. R. (2007). *Guide to Best Practices for Ocean  $\text{CO}_2$  Measurements*. Number 8.
- Donohoe, A., Lacour, G., McCluskey, P., Diamond, D., and McCaul, M. (2018). Development of a cost-effective sensing platform for monitoring phosphate in natural waters. *Chemosensors*, 6(4).
- Douglas, N. K. and Byrne, R. H. (2017a). Achieving accurate spectrophotometric pH measurements using unpurified meta-cresol purple. *Marine Chemistry*, 190:66–72.
- Douglas, N. K. and Byrne, R. H. (2017b). Spectrophotometric pH measurements from river to sea: Calibration of mCP for 0 S 40 and 278.15 T 308.15 K. *Marine Chemistry*, 197:64–69.

- Fangue, N. A., O'Donnell, M. J., Sewell, M. A., Matson, P. G., MacPherson, A. C., and Hofmann, G. E. (2010). A laboratory-based, experimental system for the study of ocean acidification effects on marine invertebrate larvae. *Limnology and Oceanography: Methods*, 8(AUG):441–452.
- Fellman, J. B., Hood, E., and Spencer, R. G. (2010). Fluorescence spectroscopy opens new windows into dissolved organic matter dynamics in freshwater ecosystems: A review. *Limnology and Oceanography*, 55(6):2452–2462.
- Gabor, R. S., Baker, A., McKnight, D. M., and Miller, M. P. (2014). *Fluorescence Indices and Their Interpretation*.
- GOA-ON (2022). Global Ocean Acidification Observing Network, 'in a Box' TA titration kits.
- Gran, G. (1950). Determination of the Equivalent Point in Potentiometric Titrations. *Acta Chemica Scandinavica*, pages 559–500.
- Gran, G. (1952). Determination of the equivalence point in potentiometric acid-base titrations. *Dansk tidsskrift for farmaci*, 35:236–242.
- Grasshoff, K., Kremling, K., and Ehrhardt, M. (1998). *Methods of Seawater Analysis*. Third, com edition.
- Guéguen, C. and Cuss, C. W. (2011). Characterization of aquatic dissolved organic matter by asymmetrical flow field-flow fractionation coupled to UV-Visible diode array and excitation emission matrix fluorescence. *Journal of Chromatography A*, 1218(27):4188–4198.
- Hansell, D. A., Carlson, C. A., Repeta, D. J., and Schlitzer, R. (2009). Dissolved Organic Matter in The Ocean A Controversy Stimulates New Insights. *Oceanography*, 22(SPL.ISS. 4):202–211.



- Helms, J. R., Stubbins, A., Ritchie, J. D., and Minor, E. C. (2008). Absorption spectral slopes and slope ratios as indicators of molecular weight, source, and photo-bleaching of chromophoric dissolved organic matter. *Limnology and Oceanography*, 53(3):955–969.
- Hernández-Ayon, M. J., Zirino, A., Dickson, A. G., Camiro-Vargas, T., and Valenzuela-Espinoza, E. (2007). Estimating the contribution of organic bases from microalgae to the titration alkalinity in coastal seawaters. *Limnology and Oceanography: Methods*, 5(7):225–232.
- Hernes, P. J. and Benner, R. (2003). Photochemical and microbial degradation of dissolved lignin phenols: Implications for the fate of terrigenous dissolved organic matter in marine environments. *Journal of Geophysical Research: Oceans*, 108(9).
- Huang, W. J., Wang, Y., and Cai, W. J. (2012). Assessment of sample storage techniques for total alkalinity and dissolved inorganic carbon in seawater. *Limnology and Oceanography: Methods*, 10(SEPTEMBER):711–717.
- Hudson-Heck, E. and Byrne, R. H. (2019). Purification and characterization of thymol blue for spectrophotometric pH measurements in rivers, estuaries, and oceans. *Analytica Chimica Acta*, 1090:91–99.
- Huguet, A., Vacher, L., Relexans, S., Saubusse, S., Froidefond, J. M., and Parlanti, E. (2009). Properties of fluorescent dissolved organic matter in the Gironde Estuary. *Organic Geochemistry*, 40(6):706–719.
- Huizenga, D. L. and Kester, D. R. (1979). Protonation equilibria of marine dissolved organic matter. *Limnol. Oceanogr*, 24(1):145–150.
- Johnson, K. M., King, A. E., and Sieburth, J. M. N. (1985). Coulometric TCO<sub>2</sub> analyses for marine studies; an introduction. *Marine Chemistry*, 16(1):61–82.

- Johnson, K. M. and Sieburth, J. M. N. (1987). COULOMETRIC TOTAL CARBON DIOXIDE ANALYSIS FOR MARINE STUDIES: AUTOMATION AND CALIBRATION. *Marine Chemistry*, 21(21):117–133.
- Johnson, K. M., Wills, K. D., Butler, D. B., Johnson, W. K., and Wong, C. S. (1993). Coulometric total carbon dioxide analysis for marine studies: maximizing the performance of an automated gas extraction system and coulometric detector. *Marine Chemistry*, 44(2-4):167–187.
- Kerr, D. E. and Turner, C. (2022). OrgAlkCalc: A Python Programme to Estimate the Concentrations and Acid-Base Properties of Organic Alkalinity. <https://github.com/charles-turner-1/OrgAlkCalc.git>.
- Kim, H. C. and Lee, K. (2009). Significant contribution of dissolved organic matter to seawater alkalinity. *Geophysical Research Letters*, 36(20):1–5.
- Ko, Y. H., Lee, K., Eom, K. H., and Han, I. S. (2016). Organic alkalinity produced by phytoplankton and its effect on the computation of ocean carbon parameters. *Limnology and Oceanography*, 61(4):1462–1471.
- Lai, C. Z., DeGrandpre, M. D., Wasser, B. D., Brandon, T. A., Clucas, D. S., Jaqueth, E. J., Benson, Z. D., Beatty, C. M., and Spaulding, R. S. (2016). Spectrophotometric measurement of freshwater pH with purified meta-cresol purple and phenol red. *Limnology and Oceanography: Methods*, 14(12):864–873.
- Lawaetz, A. J. and Stedmon, C. A. (2009). Fluorescence intensity calibration using the Raman scatter peak of water. *Applied Spectroscopy*, 63(8):936–940.
- Lee, K., Kim, T. W., Byrne, R. H., Millero, F. J., Feely, R. A., and Liu, Y. M. (2010). The universal ratio of boron to chlorinity for the North Pacific and North Atlantic oceans. *Geochimica et Cosmochimica Acta*, 74(6):1801–1811.
- Lee, M. H., Osburn, C. L., Shin, K. H., and Hur, J. (2018). New insight into the applicability of spectroscopic indices for dissolved organic matter (DOM) source discrim-

- ination in aquatic systems affected by biogeochemical processes. *Water Research*, 147:164–176.
- Li, D., Pan, B., Han, X., Li, J., Zhu, Q., and Li, M. (2021). Assessing the potential to use CDOM as an indicator of water quality for the sediment-laden Yellow river, China. *Environmental Pollution*, 289(April):117970.
- Li, X., García-Ibáñez, M. I., Carter, B. R., Chen, B., Li, Q., Easley, R. A., and Cai, W. J. (2020). Purified meta-Cresol Purple dye perturbation: How it influences spectrophotometric pH measurements. *Marine Chemistry*, 225:1–29.
- Liu, X., Patsavas, M. C., and Byrne, R. H. (2011). Purification and characterization of meta-cresol purple for spectrophotometric seawater pH measurements. *Environmental Science and Technology*, 45(11):4862–4868.
- Lueker, T. J., Dickson, A. G., and Keeling, C. D. (2000). Ocean pCO<sub>2</sub> calculated from dissolved inorganic carbon, alkalinity, and equations for K<sub>1</sub> and K<sub>2</sub>: Validation based on laboratory measurements of CO<sub>2</sub> in gas and seawater at equilibrium. *Marine Chemistry*, 70(1-3):105–119.
- Marion, G. M., Millero, F. J., Camões, M. F., Spitzer, P., Feistel, R., and Chen, C. T. (2011). PH of seawater. *Marine Chemistry*, 126(1-4):89–96.
- Masini, J. C. (1993). Evaluation of neglecting electrostatic interactions on the determination and characterization of the ionizable sites in humic substances. *Analytica Chimica Acta*, 283(2):803–810.
- Masini, J. C., Abate, G., Lima, E. C., Hahn, L. C., Nakamura, M. S., Lichtig, J., and Nagatomy, H. R. (1998). Comparison of methodologies for determination of carboxylic and phenolic groups in humic acids. *Analytica Chimica Acta*, 364(1-3):223–233.
- Massicotte, P. (2017). eemR: Tools for Pre-Processing Emission-Excitation-Matrix (EEM) Fluorescence Data.

- Mehrbach, C., Culberson, C. H., Hawley, J. E., and Pytkowicz, R. M. (1973). Measurement of the Apparent Dissociation Constants of Carbonic Acid in Seawater At Atmospheric Pressure. *Limnology and Oceanography*, 18(6):897–907.
- Metrohm (2021). Ion-selective electrodes (ISE) Manual.
- Millero, F. J. (2010). Carbonate constants for estuarine waters. *Marine and Freshwater Research*, 61:139–142.
- Milne, C. J., Kinniburgh, D. G., de Wit, J. C., van Riemsdijk, W. H., and Koopal, L. K. (1995). Analysis of metal-ion binding by a peat humic acid using a simple electrostatic model. *Journal of Colloid And Interface Science*, 175(2):448–460.
- Mintrop, L. (2016). *VINDTA Manual for Versions 3S and 3C*. 3.5 edition.
- Mizera, J., Bond, A. H., Choppin, G. R., and Moore, R. C. (1999). Dissociation Constants of Carboxylic Acids at High Ionic Strengths. *Actinide Speciation in High Ionic Strength Media*, pages 113–124.
- Morris, A. W. and Riley, J. P. (1966). The bromide/chlorinity and sulphate/chlorinity ratio in sea water. *Deep-Sea Research and Oceanographic Abstracts*, 13(4):699–705.
- Mos, B., Holloway, C., Kelaher, B. P., Santos, I. R., and Dworjanyn, S. A. (2021). Alkalinity of diverse water samples can be altered by mercury preservation and borosilicate vial storage. *Scientific Reports*, 11(1):1–11.
- Mosley, L. M., Husheer, S. L., and Hunter, K. A. (2004). Spectrophotometric pH measurement in estuaries using thymol blue and m-cresol purple. *Marine Chemistry*, 91(1-4):175–186.
- Muller, F. L. and Bleie, B. (2008). Estimating the organic acid contribution to coastal seawater alkalinity by potentiometric titrations in a closed cell. *Analytica Chimica Acta*, 619(2):183–191.

- Müller, J. D. and Rehder, G. (2018). Metrology of pH measurements in brackish waters- part 2: Experimental characterization of purified meta-cresol purple for spectrophotometric pHT measurements. *Frontiers in Marine Science*, 5(JUL):1–9.
- Nelson, N. B., Carlson, C. A., and Steinberg, D. K. (2004). Production of chromophoric dissolved organic matter by Sargasso Sea microbes. *Marine Chemistry*, 89(1-4):273–287.
- Nelson, N. B. and Siegel, D. A. (2013). The global distribution and dynamics of chromophoric dissolved organic matter. *Annual Review of Marine Science*, 5:447–476.
- Ohline, S. M., Reid, M. R., Husheer, S. L., Currie, K. I., and Hunter, K. A. (2007). Spectrophotometric determination of pH in seawater off Taiaroa Head, Otago, New Zealand: Full-spectrum modelling and prediction of pCO<sub>2</sub> levels. *Marine Chemistry*, 107(2):143–155.
- Ohno, T. (2002). Fluorescence inner-filtering correction for determining the humification index of dissolved organic matter. *Environmental Science and Technology*, 36(4):742–746.
- Okamura, K., Kimoto, H., Hatta, M., Noguchi, T., Nakaoka, A., Suzue, T., and Kimoto, T. (2014). Potentiometric open-cell titration for seawater alkalinity considering temperature dependence of titrant density and Nernst response of pH electrode. *Geochemical Journal*, 48(2):153–163.
- Parker, C. A. and Barnes, W. J. (1957). Some experiments with spectrofluorimeters and filter fluorimeters. *The Analyst*, 82(978):606–618.
- Parlanti, E., Wörz, K., Geoffroy, L., and Lamotte, M. (2000). Dissolved organic matter fluorescence spectroscopy as a tool to estimate biological activity in a coastal zone submitted to anthropogenic inputs. *Organic Geochemistry*, 31(12):1765–1781.
- Patsavas, M. C., Byrne, R. H., and Liu, X. (2013). Purification of meta-cresol purple and

- cresol red by flash chromatography: Procedures for ensuring accurate spectrophotometric seawater pH measurements. *Marine Chemistry*, 150:19–24.
- Paxéus, N. and Wedborg, M. (1985). Acid-base properties of aquatic fulvic acid. *Analytica Chimica Acta*, 169(C):87–98.
- Perdue, E. M., Reuter, J. H., and Parrish, R. S. (1984). A statistical model of proton binding by humus. *Geochimica et Cosmochimica Acta*, 48(6):1257–1263.
- Perez, F. F. and Fraga, F. (1987). Association constant of fluoride and hydrogen ions in seawater. *Marine Chemistry*, 21(2):161–168.
- Perez De Vargas Sansalvador, I. M., Fay, C. D., Cleary, J., Nightingale, A. M., Mowlem, M. C., and Diamond, D. (2016). Autonomous reagent-based microfluidic pH sensor platform. *Sensors and Actuators, B: Chemical*, 225:369–376.
- Pilson, M. E. (2013). *An Introduction to the Chemistry of the Sea*. Second edition.
- Prieto, F. J. M. and Millero, F. J. (2002). The values of  $pK_1 + pK_2$  for the dissociation of carbonic acid in seawater. *Geochimica et Cosmochimica Acta*, 66(14):2529–2540.
- Riley, J. P. (1965). The occurrence of anomalously high fluoride concentrations in the North Atlantic. *Deep-Sea Research and Oceanographic Abstracts*, 12(2):219–220.
- Robert-Baldo, G. L., Morris, M. J., and Byrne, R. H. (1985). Spectrophotometric Determination of Seawater pH Using Phenol Red. *Analytical Chemistry*, 57(13):2564–2567.
- Sharp, J. D. and Byrne, R. H. (2020). Interpreting measurements of total alkalinity in marine and estuarine waters in the presence of proton-binding organic matter. *Deep-Sea Research Part I*.
- Song, S., Wang, Z. A., Gonnee, M. E., Kroeger, K. D., Chu, S. N., Li, D., and Liang, H. (2020). An important biogeochemical link between organic and inorganic carbon cycling: Effects of organic alkalinity on carbonate chemistry in coastal waters influenced by intertidal salt marshes. *Geochimica et Cosmochimica Acta*, 275:123–139.

- Stedmon, C. A. and Nelson, N. B. (2015). *The Optical Properties of DOM in the Ocean*. Elsevier Inc., second edi edition.
- Takeshita, Y., Johnson, K. S., Coletti, L. J., Jannasch, H. W., Walz, P. M., and Warren, J. K. (2020). Assessment of pH dependent errors in spectrophotometric pH measurements of seawater. *Marine Chemistry*, 223(April):103801.
- Tipping, E. and Hurley, M. A. (1992). A unifying model of cation binding by humic substances. *Geochimica et Cosmochimica Acta*, 56(10):3627–3641.
- Wills, K. and Johnson, K. M. (1994). High-accuracy measurements of total dissolved inorganic carbon in the ocean: comparison of alternate detection methods - a comment. *Marine Chemistry*, 48(1):87–88.
- Wosley, R. J. (2021). Evaluation of the temperature dependence of dissociation constants for the marine carbon system using pH and certified reference materials. *Marine Chemistry*, 229:103914.
- Wurl, O. (2017). *Practical Guidelines for the Analysis of Seawater*.
- Yang, B., Byrne, R. H., and Lindemuth, M. (2015). Contributions of organic alkalinity to total alkalinity in coastal waters: A spectrophotometric approach. *Marine Chemistry*, 176:199–207.
- Yao, W., Liu, X., and Byrne, R. H. (2007). Impurities in indicators used for spectrophotometric seawater pH measurements: Assessment and remedies. *Marine Chemistry*, 107(2):167–172.
- Zhai, W. (2021). Characteristics of Marine Chemical Environment and the Measurements and Analyses of Seawater Carbonate Chemistry. *Research Methods of Environmental Physiology in Aquatic Sciences*, pages 3–16.
- Zhuang, G. C., Montgomery, A., and Joye, S. B. (2019a). Heterotrophic metabolism of C1 and C2 low molecular weight compounds in northern Gulf of Mexico sediments:

Controlling factors and implications for organic carbon degradation. *Geochimica et Cosmochimica Acta*, 247:243–260.

Zhuang, G. C., Montgomery, A., Samarkin, V. A., Song, M., Liu, J., Schubotz, F., Teske, A., Hinrichs, K. U., and Joye, S. B. (2019b). Generation and Utilization of Volatile Fatty Acids and Alcohols in Hydrothermally Altered Sediments in the Guaymas Basin, Gulf of California. *Geophysical Research Letters*, 46(5):2637–2646.



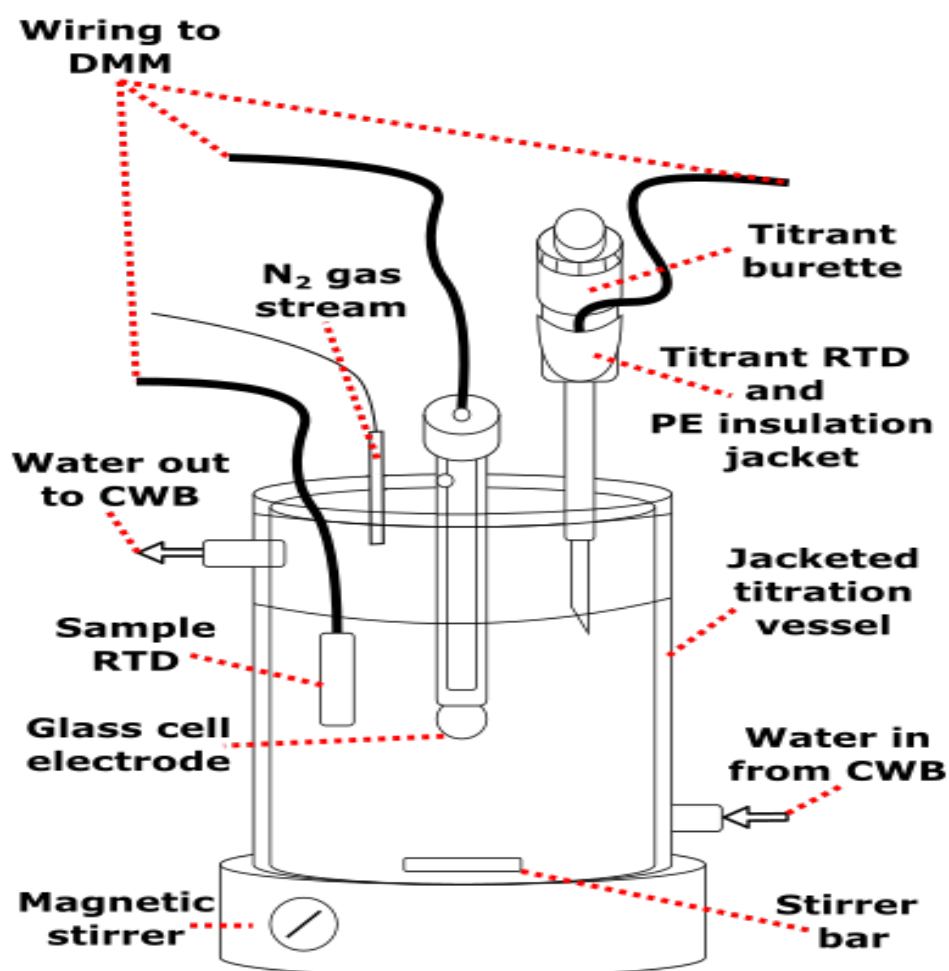


**Figure 2.1:** Diagram illustrating the apparatus used for the TA and OrgAlk titrations. Note that for OrgAlk titrations the titrant burette was changed accordingly and that for purpose of illustration vessel cap is not shown. CWB - circulating water bath, RTD - resistance thermometer detector, DMM - digital multimeter

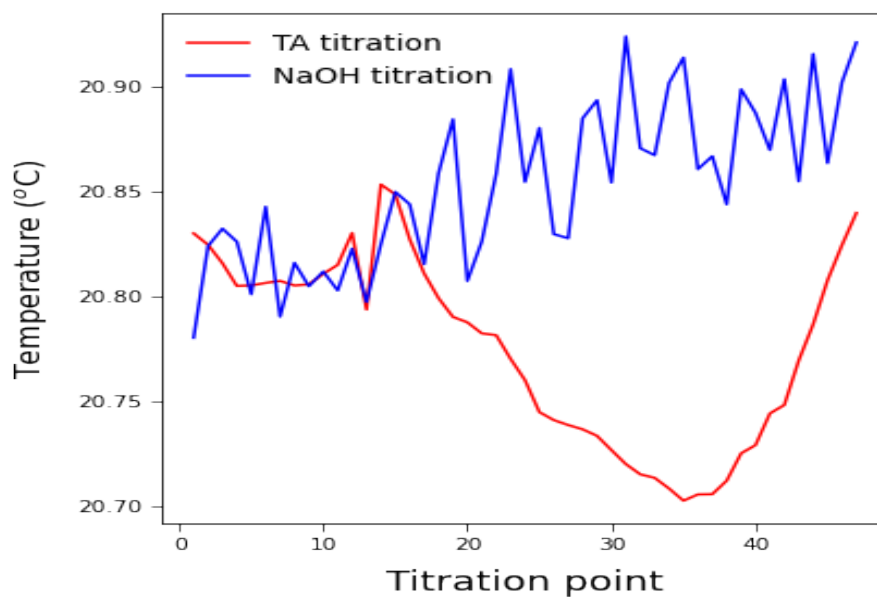


**Figure 2.2:** Average recorded titrant temperature (n=7) for both the TA and NaOH titrations.

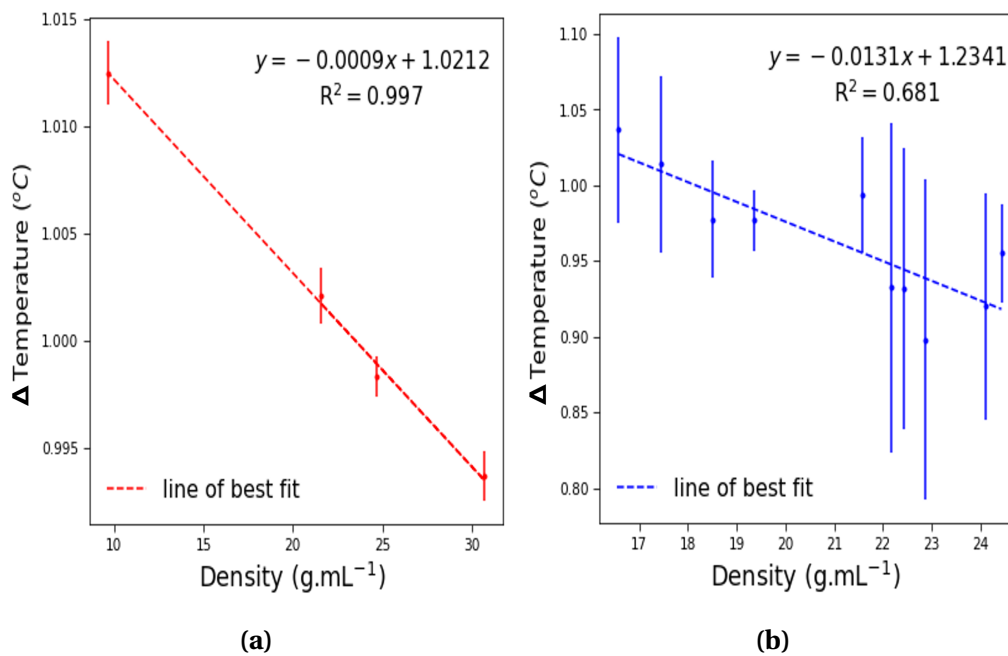


**Figure 2.3:** Graphical representations of (a) HCl density as a function of temperature and (b) NaOH density as a function of temperature .

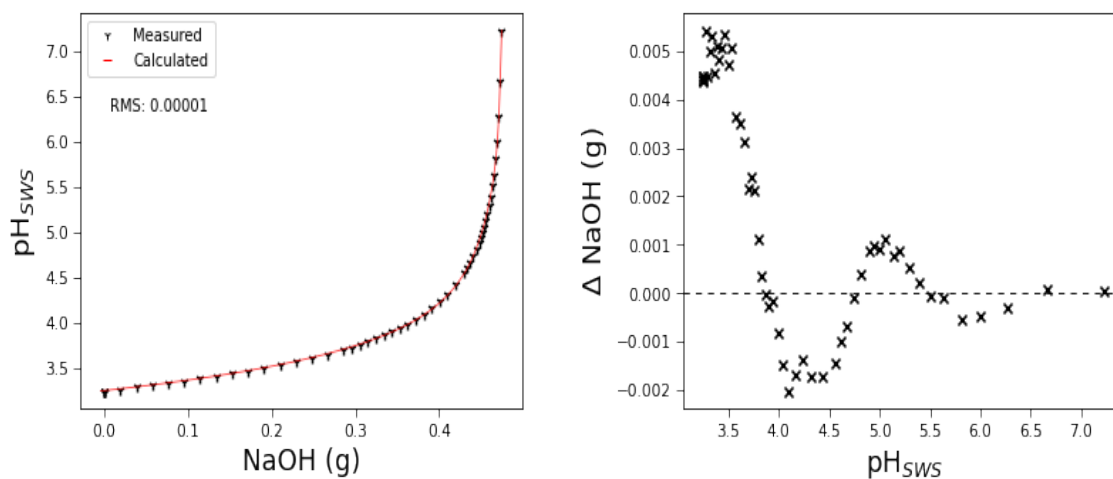


**Figure 2.4:** Plot of pH as a function of mass of NaOH added during the NaOH titration. The black markers indicate  $V_{bM}$  added while the red line indicates  $V_{bC}$ . The goodness of fit is reflected by the residual mean squared (RMS) value. Residuals can be seen as a function of pH in the right hand figure.

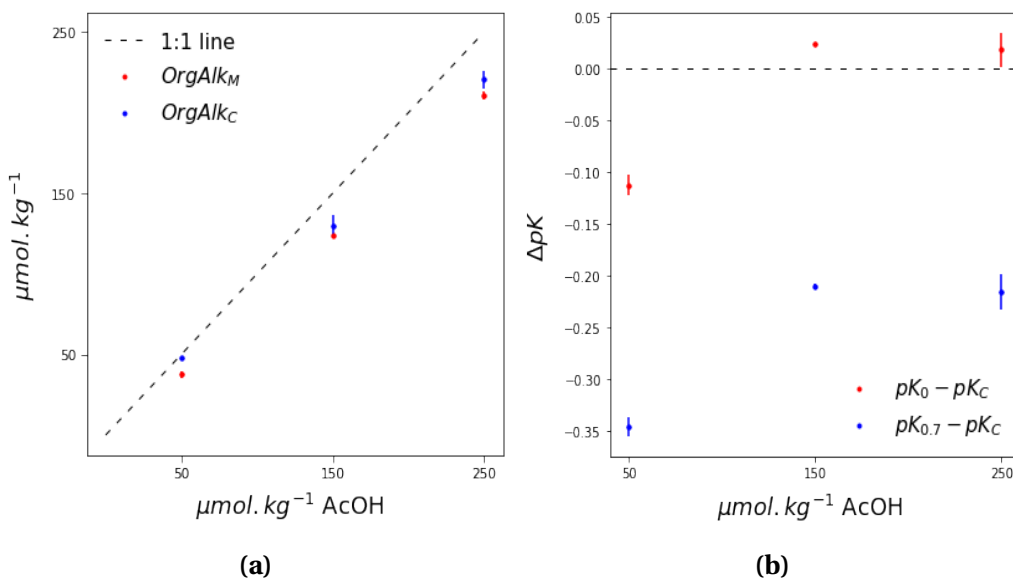


**Figure 2.5:** Graphical representations of (a) OrgAlk titration measured (OrgAlk<sub>M</sub>) and OrgAlk<sub>Calc</sub> calculated (OrgAlk<sub>C</sub>) OrgAlk concentrations compared to concentrations of simulated seawater AcOH spiked solutions. (b) Difference between literature reported values for  $pK$  of AcOH at 0 and 0.7 M ionic strength ( $pK_0$  and  $pK_{0.7}$ ) and OrgAlk<sub>Calc</sub> estimated AcOH  $pK$ .

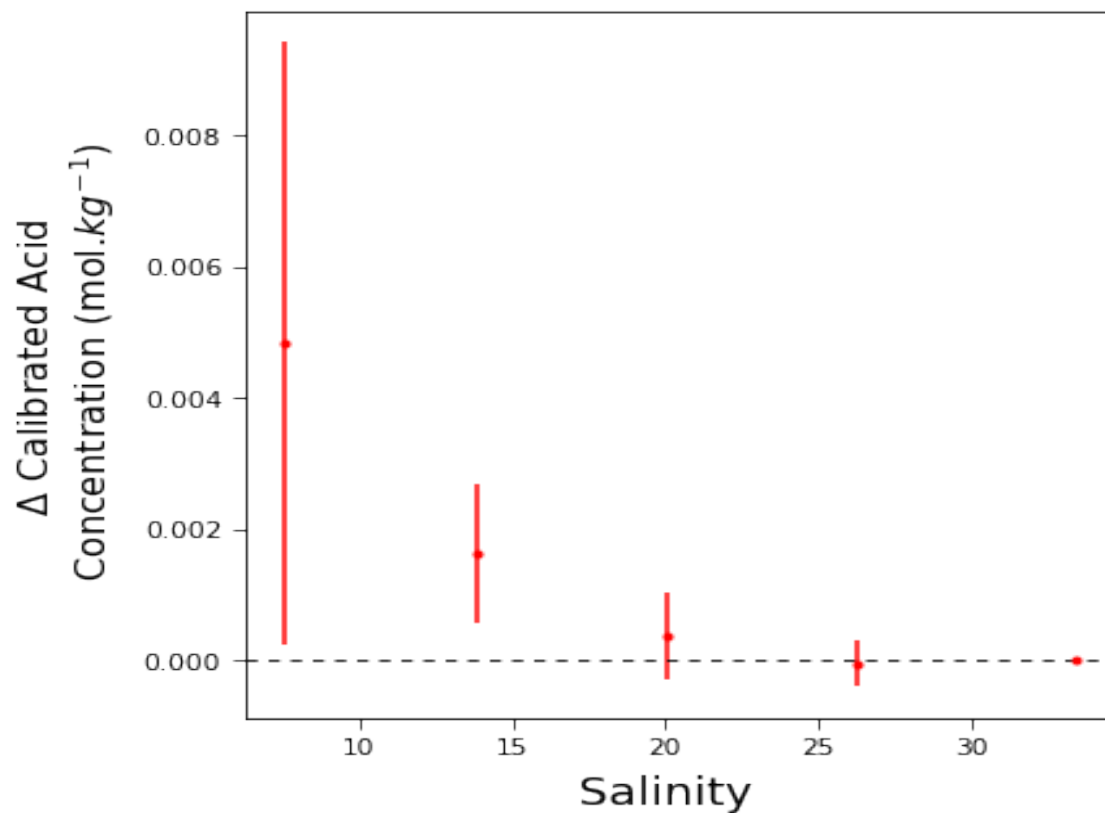


**Figure 2.6:** Calibrated acid concentrations calculated from CRM dilutions. The larger standard deviation values as dilution factor increases likely arises from issues with accuracy of dilution process and ionic strength variation. Error bars relate to the standard deviation of replicate measurements (n=3).

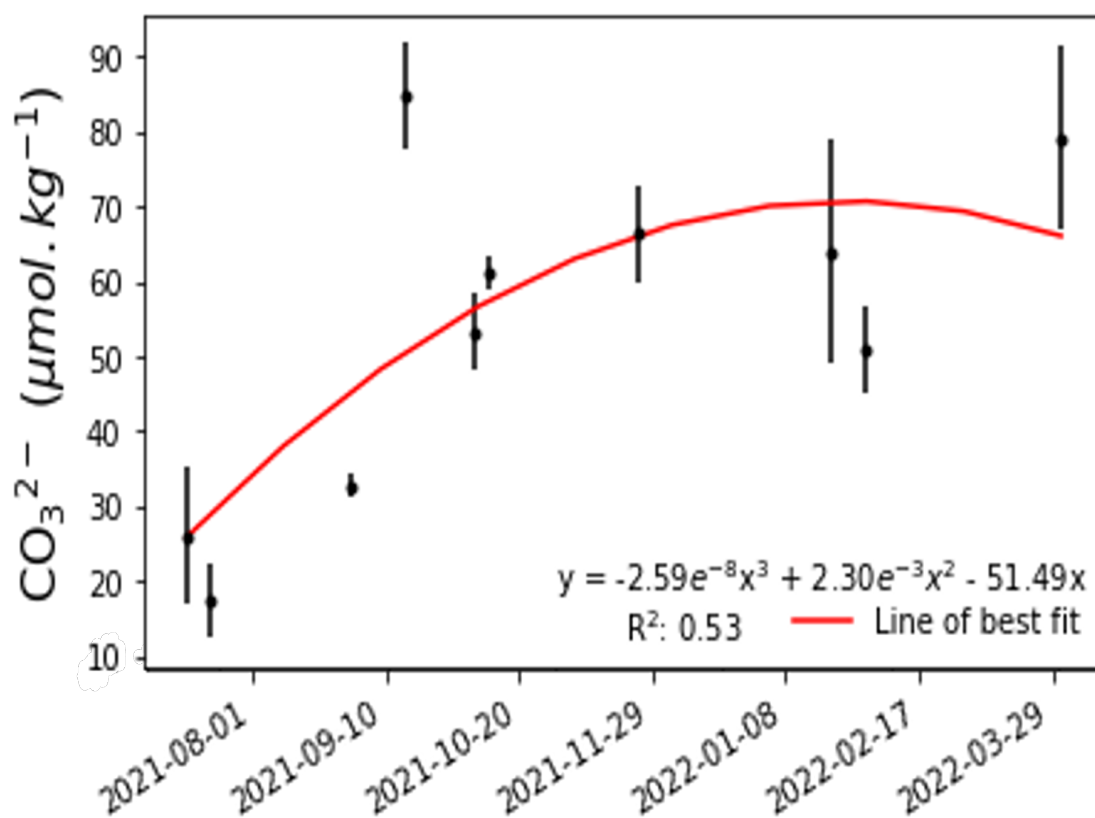


**Figure 2.7:** NaOH  $\text{CO}_3^{2-}$  content (*CTNa*) as a function of time. *CTNa* was observed to increase until 01/08/22, when the method of NaOH titrant storage was altered to minimise exposure to ambient  $\text{CO}_2$ .

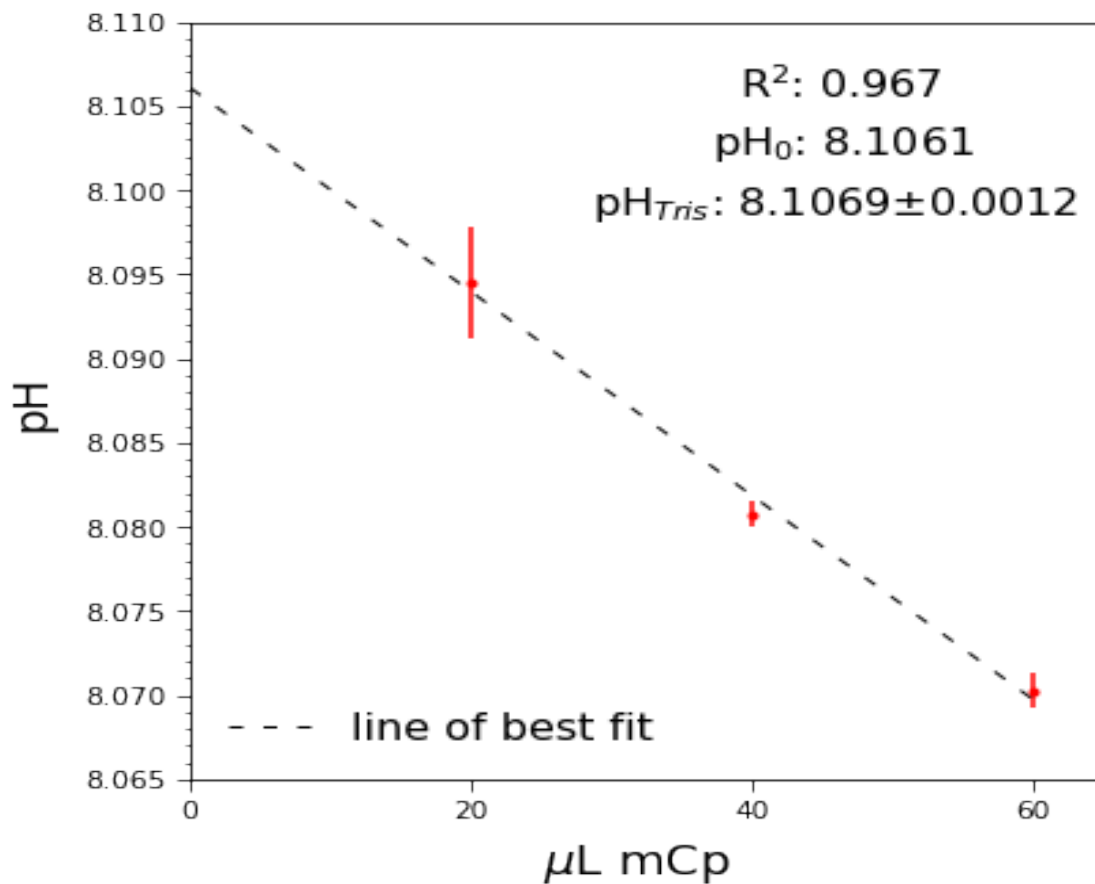


**Figure 2.8:** Effect of volume of dye added on calculated pH. Data was collected by sequential additions of dye to a Tris buffer solution. The  $y$ -axis intercept is assumed to be equal to the  $\text{pH}_0$ . Note: pH is on the Total scale.

## **Chapter 3**

# **Inter-laboratory Comparison and Validation Studies**

### Abstract

Validation of established analytical methodologies is crucial in ensuring comparability of generated results with those analysed in different laboratories and using different methods. This is especially important if generated data is to be used as a benchmark for future comparisons. Due to the aforementioned, the established TA titration methodologies were validated through participation in AQ-15, a seawater carbonate chemistry inter-laboratory validation exercise ran by WEPAL-QAUSIMEME. Additionally, a peer-based inter-laboratory validation exercise was ran in collaboration with the Ocean BioGeosciences group at the National Oceanography Centre Southampton. Results from the AQ-15 validation exercise indicated excellent agreement between assigned test material values and results obtained through the use of established TA titration apparatus and computational procedures. This was evidenced by  $z'$  scores  $< 2$ , indicating satisfactory performance and assurance of data quality for use in international carbonate system monitoring programmes. Additionally, the results of the peer-based inter-laboratory validation indicated good agreement between DCU and NOC returned TA values, with values differing by  $\sim 6 \mu\text{mol} \cdot \text{kg}^{-1}$ . Furthermore, details of the laboratory based calibration of in situ  $\text{pCO}_2$  and pH measurements made by sondes on the Dublin Bay data buoy are discussed. Data buoy recorded  $\text{pCO}_2$  agreed well with  $\text{pCO}_2$  calculated from TA and DIC, differing by  $\sim 6 \mu\text{atm}$ . Data buoy recorded pH differed to pH measured spectrophotometrically by  $\sim 0.2$  pH units, with discrepancies likely related to issues with glass cell electrode pH measurements including frequency of calibration, ionic strength of sample matrix compared to that of the buffer calibration solution, and pH scale used.



### 3.1 Inter-laboratory validation

A critical step in the validation of the aforementioned TA analysis procedures was participation in inter-laboratory validation exercises, both independently run and those performed with collaborative researchers. To achieve independent method validation, participation in AQ15 was undertaken. AQ15 is a seawater carbonate chemistry inter-laboratory validation exercise ran by WEPAL-QAUSIMEME, Wageningen, the Netherlands. For inter-laboratory peer validation, collaboration with the Ocean Biogeosciences group in the National Oceanography Centre, Southampton UK (NOCS) was carried out. The collaboration with NOCS also served the dual purpose of allowing for complementary DIC analysis alongside TA measurement. The DIC/TA input pair was then used to calculate  $p\text{CO}_2$  and pH in a validation exercise of in situ carbonate chemistry sondes in Dublin Bay, detailed in section 3.2.

#### 3.1.1 WEPAL-QAUSIMEME

The QUASIMEME programme is a Wageningen Evaluating Programmes for Analytical Laboratories (WEPAL) ran proficiency test for marine analytical chemists. WEPAL is an accredited inter-laboratory studies organisation that provides proficiency testing for a wide range of environmental analytes (ISO/CASCO, 2010), with approximately 300 laboratories participating in WEPAL-QUASIMEME worldwide. In order to ascertain proficiency and validate performance of the TA titration methodologies established in DCU, the 2022 AQ-15 Ocean acidification exercise was participation in. AQ-15 consisted of 3 low nutrient seawater sample test materials collected from the Eastern Atlantic Ocean and Baltic Sea. These test materials were filtered and homogenised prior to analysis and then assigned TA and DIC concentrations, with RSD (%) values less than 0.3. In our case, samples were only measured for TA. The data generated in DCU through the analysis of the AQ15 test materials will be referred to as reported data.

WEPAL utilise sophisticated statistical methods to calculate population character-

istics without the dependence on arbitrary outlier removal and subjective interpretations (Cofino et al., 2000; Molenaar et al., 2018). The approach involves the implementation of a Normal Distribution Approximation (NDA) model. This approach is parameterised to reproduce population characteristics as truly normal distributions. The NDA mean is centered around the highest density of all reported values and represents the consensus of all data. Reported data that lie substantially away from the NDA mean contribute less than those that occur nearer or on the mean. The Total Error is give as the standard deviation for proficiency assessment:

$$TotalError = \sqrt{U_x^2 + \left( \frac{NDAMean * PE(\%)}{100} + 0.5 * CE \right)^2} \quad (3.1)$$

where  $U_x^2$  is the uncertainty in the assigned value, PE is proportional error and CE is constant error. Values for PE and CE are set by the Scientific Advisory Board of QUASIMEME and are based on the required standard of performance to enable participating laboratories to assess assessment over time; and achievable targets based on current best practice methodology and data quality goals required for monitoring programmes. For AQ15, PE is set at 1% and CE at 2. Median and median of absolute deviations (MAD) values are also reported. A  $z'$  score for each participants reported value is calculated by:

$$z' score = \frac{Reported Value - NDAMean}{Total Error} \quad (3.2)$$

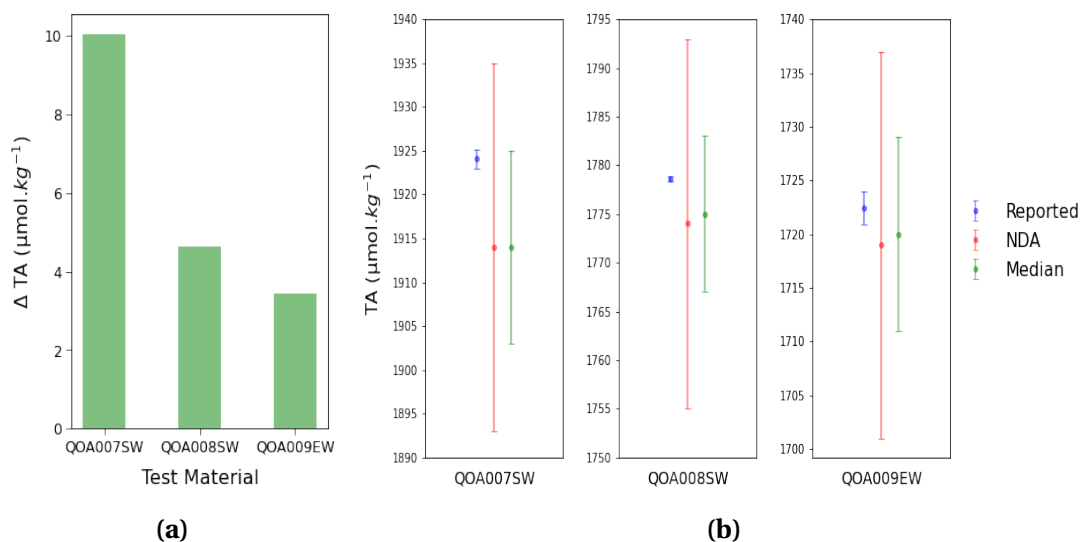
$z'$  scores can be interpreted as indicators of data quality and are categorised as follows:  $|z'| < 2$  satisfactory performance,  $|z'| < 3$  questionable performance,  $|z'| > 3$  unsatisfactory performance. For the reported data, all returned  $|z'|$  values were  $< 2$ , indicating satisfactory performance and assurance of data quality for use in international carbonate system monitoring programmes.

As can be seen from table 3.1 the TA values generated by methodologies established in DCU agree well with NDA values. Compared to the test materials, reported TA was

**Table 3.1:** WEPAL inter-laboratory proficiency test results. Mean and error values reported in  $\mu\text{mol}\cdot\text{kg}^{-1}$ .

Test material	Matrix	Source	Salinity	Reported value	NDA mean	Difference	Total Error	NDA st.dev	NDA rel. st. (%)	n	Median	MAD	Model Mean	Uncertainty
QOA007SW	Seawater	Gulf of Biscay	35.61	1924.05 $\pm$ 1.11	1914.0	10.05	21.0	16.0	0.80	26.0	1914.0	11.0	1914.30	3.90
QOA008SW	Seawater	North Sea	35.63	1778.63 $\pm$ 0.29	1774.0	4.63	19.0	12.0	0.70	27.0	1775.0	8.0	1773.70	2.80
QOA009EW	Seawater	Baltic Sea	7.62	1722.45 $\pm$ 1.51	1719.0	3.45	18.0	12.0	0.70	27.0	1720.0	9.0	1718.50	2.90

consistently higher, on average  $5.67 \pm 3.09 \mu\text{mol}\cdot\text{kg}^{-1}$ . This consistency may be suggestive of slight systematic errors arising most likely from small inaccuracies in the assigned calibrated acid concentration value. Furthermore, the good agreement between replicates ( $n=3$ ) as observed by similar standard deviation values for all test materials indicate that discrepancies likely do not arise from errors in analysis or computational procedures. The discrepancies fell well within the Total Error, *i.e.* the standard deviation of NDA, associated with each test material indicating good performance in regard to AQ15 participant results. Additionally, when considering the mean difference between reported and NDA TA values, reported values are of a sufficient quality as described by "Weather" carbonate system measurement quality goals outlined in section 0.3.

**Figure 3.1:** Graphical representations of agreement between OGRE laboratory reported TA values for WEPAL-QUASIMEME AQ15 test materials (a) plot of the difference between reported TA and NDA mean values (b) plots indicating the mean and standard deviation for reported TA, NDA TA and median TA values. Note that reported TA fell within the range of median standard deviation for each test material.

Discrepancies between reported TA and NDA values for test materials were consistently higher for more saline samples. This could potentially be a result of titrant composition, as the ionic strength of acid titrant used in TA analysis had not been adjusted to match that of seawater, see section 2.5. Given the relatively low salinity of test material QOA009EW, the non-carbonate inorganic acid-base species associated with marine seawater, such as borate see equation 2.6, may have been present in already reduced amounts such that ionic strength had a negligible effect. Furthermore, as the impact on ionic strength dependant activity coefficients during the titration was minimised by refactoring ionic strength after each titrant addition, this could indicate that simple dilution corrections are only applicable to lower salinity samples.

### 3.1.2 VINDTA comparison

Having set up and configured TA titration methods in DCU, there was a need to compare results with established TA titration procedures, such as those at the NOCS. The TA titration methods used at NOCS is an open-cell multi-step potentiometric titration using a VINDTA 3C (Mintrop, 2016). The titration methodology and TA computational procedures for VINDTA analysis differ slightly to the methods discussed in this manuscript and are described in SOP 3a in Dickson et al. (2007).

Coastal surface seawater samples were collected on 16/11/21 and 15/12/21 from the Dublin Bay Data Buoy (53°21.318'N 006°05.366'W). Samples were poisoned upon collection with saturated HgCl<sub>2</sub>. Samples for TA analysis in DCU were contained in acid washed 250 mL HDPE bottles stored in the fridge and analysed within 1 week. Samples for analysis at NOCS were contained in 500 mL greased (Apiezon L) ground glass stopper borosilicate glass vials stored under positive closure in the dark at ambient temperature. Previous research has indicated no statistically significant impact from storage in HDPE versus borosilicate bottles (Huang et al., 2012). Samples for TA analysis were filtered using 0.7 μm effective pore size GF/F glass microfiber filters directly prior to analysis to remove particulates. The samples were analysed for both TA

and DIC using the VINDTA and for TA using the established methods in DCU. This allowed for a comparison between DCU generated and NOC generated TA values ( $TA_{DCU}$  and  $TA_{NOC}$ , respectively.) Samples for TA analysis in DCU were measured within 1 day of collection, whereas the NOC samples were stored for between 8 - 16 months before analysis.

**Table 3.1:** Comparison between reported TA values of identical seawater samples analysed in NOC and DCU. TA units in  $\mu\text{mol}\cdot\text{kg}^{-1}$

Sample	Date collected	Date analysed DCU	Date analysed NOC	Salinity	$TA_{DCU}$	$TA_{NOC}$	$\Delta TA$
Buoy 001	16/11/21	17/11/21	22/07/22	33.753	$2333.01 \pm 5.63$	$2327.70 \pm 4.50$	5.31
Buoy 002	14/12/21	15/12/21	22/07/22	33.4357	$2340.01 \pm 2.64$	$2332.70 \pm 4.00$	7.31
LS 001C	15/03/21	15/03/22	22/07/22	32.721	$2316.62 \pm 1.61$	$2334.20 \pm 0.93$	-17.58

As can be seen by table 3.1,  $TA_{DCU}$  values for Buoy 001 and Buoy 002 are both higher than the  $TA_{NOC}$  reported values. A possible explanation for this could be related to the  $\text{HgCl}_2$  used to preserve the samples. It has been reported that the use of  $\text{HgCl}_2$  can decrease TA over storage periods of 1 month, with this decrease in TA increasing with higher  $\text{HgCl}_2$  concentration (Mos et al., 2021). Furthermore, Mos et al. (2021) reported that the largest  $\text{HgCl}_2$  effect is observed for estuarine samples. As the samples were collected from an estuary influenced area, this could indicate that  $\text{HgCl}_2$  played a role in the discrepancies between  $TA_{DCU}$  and  $TA_{NOC}$ .

LS001C displays a reduced TA value when comparing DCU and NOC generated results, contrary to Buoy 001 and Buoy 002. A possible explanation for this is the increased storage time, 16 months for LS 001C compared to 8 for Buoy 001 and Buoy 002. As samples were filtered upon analysis, this increased storage time may have allowed for particulate carbonates present in the stored sample to dissolve, increasing alkalinity (Bockmon and Dickson, 2014). Furthermore, as samples were stored in borosilicate glass vials, dissolution of silicate over extended time periods could have increased TA (Mos et al., 2021), although there is conflicting evidence to this (McGrath et al., 2013). If LS 001C  $\Delta TA$  is treated as an outlier due to uncertainties related to extended sam-

ple storage and omitted in comparisons of DCU and NOC generated TA results,  $\Delta$ TA for Buoy 001 and Buoy 002 are relatively small; on the order of  $\sim 6 \mu\text{mol}\cdot\text{kg}^{-1}$ . Given that this difference falls below the "Weather" data quality goals as outlined section 0.3 and is in agreement with the results obtained in section 3.1.1, this demonstrates a high degree of agreement between DCU and NOC generated TA results.

### 3.2 Dublin Bay data buoy

The inter-laboratory comparison studies also facilitated the validation of  $\text{pCO}_2$  and pH measurements recorded by the Dublin Bay data buoy. The data buoy was installed in October 2021 and is located in the northern portion of Dublin Bay ( $53^\circ 21.318' \text{N}$   $006^\circ 05.366' \text{W}$ ). The buoy houses a CONTROS HydroC  $\text{CO}_2$  sonde for continuous *in-situ* seawater  $\text{pCO}_2$  measurements and a Sea-Bird Scientific HydroCAT-EP sonde that records a suite of parameters, including temperature, pressure, salinity, pH, dissolved oxygen and fluorescence.  $\text{pCO}_2$  is measured every hour, while pH is measured every 10 minutes. The recorded  $\text{pCO}_2$  and pH measurements that most closely aligned with time of sample collection were used in the comparison study outlined below.

A challenge in the establishment and maintenance of remote sensors is accurate calibration of analytical equipment. In-laboratory carbonate system analysis presented an excellent opportunity to validate data buoy recorded  $\text{pCO}_2$  and pH. This was achieved by comparing data buoy recorded  $\text{pCO}_2$  and pH ( $\text{pCO}_{2\text{DB}}$  and  $\text{pH}_{\text{DB}}$ ) with  $\text{pCO}_2$  and pH calculated using measured TA and DIC as input parameters ( $\text{pCO}_{2\text{C}}$  and  $\text{pH}_{\text{C}}$ ). Furthermore,  $\text{pH}_{\text{C}}$  and  $\text{pH}_{\text{DB}}$  were also compared with pH measured using spectrophotometric analysis ( $\text{pH}_{\text{S}}$ ). Although  $\text{pCO}_2$  and pH data for validation was generated for samples collected on 16/11/21 and 14/12/21, only data for 16/11/21 could be used comparatively. This was due to damage sustained by the buoy during Storm Barra in December 2021 that rendered both the CONTROS and Sea-Bird sondes nonoperational, resulting in no recorded  $\text{pCO}_2$  and pH data for 14/12/21. Although it is acknowledged that only a single data point is presented in this validation study, it is important to note

**Table 3.2:** Comparison between directly measured  $p\text{CO}_2$  ( and pH as recorded by the Dublin Bay data buoy with calculated  $p\text{CO}_2$  and pH. Laboratory based spectrophotometric measurements of pH are also reported.

Replicate	Salinity	Measured					Calculated	
		DIC	TA	pH <sub>S</sub>	pH <sub>DB</sub>	pCO <sub>2DB</sub>	pH <sub>C</sub>	pCO <sub>2C</sub>
Buoy <sub>001</sub> NOC	33.753	2158.95	2327.7±4.50	7.966±0.007	8.14	468.99±0.64	7.986±0.010	477.17±11.61
Buoy <sub>001</sub> DCU			2333.01±5.63				7.998±0.012	463.85±13.82

that the produced  $p\text{CO}_{2C}$  and  $\text{pH}_C$  values are the end products of validated analytical and computational procedures, and that the high degree of agreement observed between reported variables justifies the exercise.

Both TA and DIC were measured using a VINDTA 3C system in the NOCS. TA was additionally measured in DCU using the aforementioned open-cell methods. Precision of TA and DIC was calculated as the standard deviation of the difference between replicate results of substandards ( $n=3$ ). Precision for  $\text{TA}_{\text{DCU}}$ ,  $\text{TA}_{\text{NOC}}$  and DIC were 2.63, 0.89 and  $1.22 \mu\text{mol}\cdot\text{kg}^{-1}$ , respectively.  $\text{pH}_S$  was measured as detailed in section 2.7.2.  $\text{pH}_S$  measurements were calibrated using tris buffer in artificial seawater supplied by Dr. A. Dickson, Scripps Institute of Oceanography, USA. Precision of  $\text{pH}_S$  was 0.0041 and was calculated as the difference between the measured pH of tris buffer and pH of tris buffer as calculated using the expression of DelValls and Dickson (1998).  $\text{pH}_S$  reported in table 3.2 was adjusted to in situ temperature using *CO2SYS* (Lewis and Wallace, 1998).

Both  $\text{TA}_{\text{DCU}}$  and  $\text{TA}_{\text{NOC}}$  were used alongside DIC and  $\text{pH}_S$  in subsequent carbonate chemistry calculations. Carbonate system calculations were carried out using *CO2SYS*, using the carbonate equilibrium constants of Lueker et al. (2000), total boron scale of Lee et al. (2010),  $K(\text{HSO}_4^-)$  of Dickson (1990) and  $K(\text{HF})$  of Perez and Fraga (1987).

The reported  $p\text{CO}_{2\text{DB}}$  and  $\text{pH}_{\text{DB}}$  were taken as the values recorded by each parameters respective sonde at the time of sample collection. The error on  $p\text{CO}_{2\text{DB}}$  is given as sonde recorded standard deviation of one measurement cycle. No error is reported for  $\text{pH}_{\text{DB}}$  as only singular measurements were recorded at each measurement point. Re-

ported errors for  $TA_{DCU}$ ,  $TA_{NOC}$  and  $pH_S$  are given as the standard deviation between triplicate measurements, whereas errors for  $pCO_{2C}$  and  $pH_C$  are given as the standard deviation of the values calculated from each respective TA replicate.

### 3.2.1 $pCO_2$ comparisons

Comparisons of  $pCO_{2C}$  and  $pCO_{2DB}$  show excellent agreement, within  $6 \mu atm$  and falling well within previously reported differences between calculated and directly measured  $pCO_2$  (Watson et al., 2017; Jiang et al., 2014). Differences between  $pCO_{2C}$  values and  $pCO_{2DB}$  are less than the reported error for each respective  $pCO_{2C}$ , indicating that discrepancies between measured and calculated  $pCO_2$  lie within attributable analytical error.  $pCO_{2C}$  generated using  $TA_{DCU}$  values show better agreement with  $pCO_{2DB}$ . This could be due the aforementioned issues involving sample storage on  $TA_{NOC}$  samples. As  $TA_{DCU}$  were analysed within 1 day of collection storage related artefacts were minimised, possibly explaining the closer agreement between  $pCO_{2C}$  using  $TA_{DCU}$  and  $pCO_{2DB}$ . Considering this,  $pCO_{2C}$  calculated using  $TA_{DCU}$  may be a more representative value of  $pCO_2$  for comparison with  $pCO_{2DB}$ . Given the good agreement between the previously mentioned, this would indicate that  $pCO_{2DB}$  gives an accurate representation of  $pCO_2$  values.

### 3.2.2 pH comparisons

Comparisons of sonde measured, spectrophotometrically measured and calculated pH indicate discrepancies. pH differences are greatest when comparing  $pH_{DB}$  with  $pH_C$  and  $pH_S$ .  $pH_{DB}$  was recorded by the Sea-Bird Scientific HydroCAT-EP sonde using glass cell and reference electrodes. Issues with glass cell electrode pH measurements are well documented and are related to a number of factors: frequency of calibration (Frankignoulle and Borges, 2001; Seiter and DeGrandpre, 2001), ionic strength of sample matrix compared to that of the buffer calibration solution (Millero et al., 1993; Dickson et al., 2015) and pH scale used (Clayton and Byrne, 1993; Millero, 2007; Zeebe and



Wolf-Gladrow, 2003). The aforementioned are likely causes of the  $\sim 0.15$  difference observed when comparing  $\text{pH}_{\text{DB}}$  with  $\text{pH}_{\text{C}}$  and  $\text{pH}_{\text{S}}$ . The difference between  $\text{pH}_{\text{DB}}$  and  $\text{pH}_{\text{S}}$  falls within previously reported discrepancies ( $\pm 0.2$  pH units) between glass cell electrode and spectrophotometric pH measurements (McLaughlin et al., 2017). Daily calibrations could possibly bring  $\text{pH}_{\text{DB}}$  more in line with  $\text{pH}_{\text{C}}$  and  $\text{pH}_{\text{S}}$  (McLaughlin et al., 2017), however this presents a challenging endeavour for remote sensing applications, such as the Dublin Bay data buoy.

Differences between  $\text{pH}_{\text{S}}$  and  $\text{pH}_{\text{C}}$  were  $-0.020$  and  $-0.0318$  for  $\text{pH}_{\text{C}}$  values calculated using  $\text{TA}_{\text{NOC}}$  and  $\text{TA}_{\text{DCU}}$ , respectively. Although in better agreement by an order of magnitude compared to the pH difference observed when comparing  $\text{pH}_{\text{DB}}$  with  $\text{pH}_{\text{C}}$  and  $\text{pH}_{\text{S}}$ , these values are indicative of either computational or analytical errors. The existence of discrepancies between spectrophotometric pH and pH calculated using the DIC/TA input pair is well documented and is a global ocean phenomenon (Williams et al., 2017; Carter et al., 2018). Other than analytical errors on the input parameters used to calculate pH, these discrepancies are thought to arise from uncertainties in the marine carbonate system thermodynamic constants used. When considering the difference between  $\text{pH}_{\text{S}}$  and  $\text{pH}_{\text{C}}$  due to maximum uncertainties in carbonate thermodynamic constants and accuracy of DIC and TA measurements, (Fong and Dickson, 2019) observed that differences could not solely be attributed to these uncertainties and likely arose from unaccounted for acid-base species that contribute to the TA, in other words OrgAlk. This highlights the importance of OrgAlk to carbonate system calculations that aim to track ocean acidification at the level required for "Climate" data quality observations.

## References

- Bockmon, E. E. and Dickson, A. G. (2014). A seawater filtration method suitable for total dissolved inorganic carbon and pH analyses. *Limnology and Oceanography: Methods*, 12(APR):191–195.
- Carter, B. R., Feely, R. A., Williams, N. L., Dickson, A. G., Fong, M. B., and Takeshita, Y. (2018). Updated methods for global locally interpolated estimation of alkalinity, pH, and nitrate. *Limnology and Oceanography: Methods*, 16(2):119–131.
- Clayton, T. D. and Byrne, R. H. (1993). Spectrophotometric seawater pH measurements: total hydrogen ion concentration scale calibration of m-cresol purple and at-sea results. *Deep-Sea Research Part I*, 40(10):2115–2129.
- Cofino, W. P., Van Stokkum, I. H., Wells, D. E., Ariese, F., Wegener, J. W. M., and Peerboom, R. A. (2000). A new model for the inference of population characteristics from experimental data using uncertainties. Application to interlaboratory studies. *Chemometrics and Intelligent Laboratory Systems*, 53(1-2):37–55.
- DelValls, T. A. and Dickson, A. G. (1998). The pH of buffers based on 2-amino-2-hydroxymethyl-1,3-propanediol ('tris') in synthetic sea water. *Deep-Sea Research Part I: Oceanographic Research Papers*, 45(9):1541–1554.
- Dickson, A. G. (1990). Standard potential of the reaction:  $\text{AgCl(s)} + \frac{1}{2}\text{H}_2\text{(g)} = \text{Ag(s)} + \text{HCl(aq)}$ , and the standard acidity constant of the ion  $\text{HSO}_4^-$  in synthetic sea water from 273.15 to 318.15 K. *The Journal of Chemical Thermodynamics*, 22(2):113–127.
- Dickson, A. G., Camoes, M. F., Spitzer, P., Fiscaro, P., Stoica, D., Pawlowicz, R., and Feistel, R. (2015). Metrological challenges for measurements of key climatological observables. Part 3: Seawater pH. *Metrologia*, 53(1):R26–R39.

- Dickson, A. G., Sabine, C. L., and Christian, J. R. (2007). *Guide to Best Practices for Ocean CO<sub>2</sub> Measurements*. Number 8.
- Fong, M. B. and Dickson, A. G. (2019). Insights from GO-SHIP hydrography data into the thermodynamic consistency of CO<sub>2</sub> system measurements in seawater. *Marine Chemistry*, 211(January):52–63.
- Frankignoulle, M. and Borges, A. V. (2001). Direct and indirect pCO<sub>2</sub> measurements in a wide range of pCO<sub>2</sub> and salinity values (the scheldt estuary). *Aquatic Geochemistry*, 7(4):267–273.
- Huang, W. J., Wang, Y., and Cai, W. J. (2012). Assessment of sample storage techniques for total alkalinity and dissolved inorganic carbon in seawater. *Limnology and Oceanography: Methods*, 10(SEPTEMBER):711–717.
- ISO/CASCO (2010). *ISO/IEC 17043:2010 Conformity assessment — General requirements for proficiency testing*.
- Jiang, Z. P., Hydes, D. J., Hartman, S. E., Hartman, M. C., Campbell, J. M., Johnson, B. D., Schofield, B., Turk, D., Wallace, D., Burt, W. J., Thomas, H., Cosca, C., and Feely, R. (2014). Application and assessment of a membrane-based pCO<sub>2</sub> sensor under field and laboratory conditions. *Limnology and Oceanography: Methods*, 12(APR):264–280.
- Lee, K., Kim, T. W., Byrne, R. H., Millero, F. J., Feely, R. A., and Liu, Y. M. (2010). The universal ratio of boron to chlorinity for the North Pacific and North Atlantic oceans. *Geochimica et Cosmochimica Acta*, 74(6):1801–1811.
- Lewis, E. R. and Wallace, D. W. R. (1998). Program Developed for CO<sub>2</sub> System Calculations.
- Lueker, T. J., Dickson, A. G., and Keeling, C. D. (2000). Ocean pCO<sub>2</sub> calculated from dissolved inorganic carbon, alkalinity, and equations for K<sub>1</sub> and K<sub>2</sub>: Validation based

- on laboratory measurements of CO<sub>2</sub> in gas and seawater at equilibrium. *Marine Chemistry*, 70(1-3):105–119.
- McGrath, T., Kivimäe, C., McGovern, E., Cave, R. R., and Joyce, E. (2013). Winter measurements of oceanic biogeochemical parameters in the Rockall Trough (2009-2012). *Earth System Science Data*, 5(2):375–383.
- McLaughlin, K., Nezhlin, N. P., Weisberg, S. B., Dickson, A. G., Booth, J. A., Cash, C. L., Feit, A., Gully, J. R., Johnson, S., Latker, A., Mengel, M. J., Robertson, G. L., Steele, A., and Terriquez, L. (2017). An evaluation of potentiometric pH sensors in coastal monitoring applications. *Limnology and Oceanography: Methods*, 15(8):679–689.
- Millero, F. J. (2007). The marine inorganic carbon cycle. *Chemical Reviews*, 107(2):308–341.
- Millero, F. J., Zhang, J. Z., Fiol, S., Sotolongo, S., Roy, R. N., Lee, K., and Mane, S. (1993). The use of buffers to measure the pH of seawater. *Marine Chemistry*, 44(2-4):143–152.
- Mintrop, L. (2016). *VINDTA Manual for Versions 3S and 3C*. 3.5 edition.
- Molenaar, J., Cofino, W. P., and Torfs, P. J. (2018). Efficient and robust analysis of inter-laboratory studies. *Chemometrics and Intelligent Laboratory Systems*, 175(December 2017):65–73.
- Mos, B., Holloway, C., Kelaher, B. P., Santos, I. R., and Dworjanyn, S. A. (2021). Alkalinity of diverse water samples can be altered by mercury preservation and borosilicate vial storage. *Scientific Reports*, 11(1):1–11.
- Perez, F. F. and Fraga, F. (1987). Association constant of fluoride and hydrogen ions in seawater. *Marine Chemistry*, 21(2):161–168.
- Seiter, J. C. and DeGrandpre, M. D. (2001). Redundant chemical sensors for calibration-impossible applications. *Talanta*, 54(1):99–106.

Watson, S. A., Fabricius, K. E., and Munday, P. L. (2017). Quantifying pCO<sub>2</sub> in biological ocean acidification experiments: A comparison of four methods. *PLoS ONE*, 12(9):1–16.

Williams, N. L., Juranek, L. W., Feely, R. A., Johnson, K. S., Sarmiento, J. L., Talley, L. D., Dickson, A. G., Gray, A. R., Wanninkhof, R., Russell, J. L., Riser, S. C., and Takeshita, Y. (2017). Calculating surface ocean pCO<sub>2</sub> from biogeochemical Argo floats equipped with pH: An uncertainty analysis. *Global Biogeochemical Cycles*, 31(3):591–604.

Zeebe, R. E. and Wolf-Gladrow, D. A. (2003). *CO<sub>2</sub> in Seawater: Equilibrium, Kinetics, Isotopes*. Number 2.

## **Chapter 4**

# ***OrgAlkCalc*: Estimation of Organic Alkalinity Quantities and Acid-base Properties With Proof of Concept in Dublin Bay**

## Abstract

The presence and influence of organic species is generally omitted in total alkalinity (TA) analysis. This has direct implications to calculated carbonate system parameters and to key descriptors of ocean acidification, especially in coastal waters where organic alkalinity (OrgAlk) can contribute significantly to TA. As titratable charge groups of OrgAlk can act as unknown seawater acid-base systems, the inclusion of the total concentration and apparent dissociation constants of OrgAlk in carbonate calculations involving TA is required to minimise uncertainty in computed speciation. Here we present *OrgAlkCalc*, an open-source Python based programme that can be used in conjunction with simply modified Global Ocean Acidification Observing Network (GOA-ON) TA titration apparatus to measure TA and OrgAlk, as well as return estimations of associated acid-base properties. The modified titration apparatus and *OrgAlkCalc* were tested using samples collected from the transitional waters of Dublin Bay, Ireland over a 8 month period (n=100). TA values ranged from 2257 - 4692  $\mu\text{mol} \cdot \text{kg}^{-1}$  and indicated that freshwater inputs pose a significant source of carbonate alkalinity to Dublin Bay. OrgAlk values ranged from 46 - 234  $\mu\text{mol} \cdot \text{kg}^{-1}$  and were generally observed to be higher in more saline waters, with elevated levels in the Autumn/Winter period. The dissociation constants of two distinct OrgAlk charge groups were identified, with pK values in agreement with previously reported values for humic substances. The majority of OrgAlk charge group concentrations were associated with carboxyl-like charge groups.

## 4.1 Introduction

Since the industrial revolution, carbon dioxide ( $\text{CO}_2$ ) exchange between the atmosphere and oceans has drastically changed due to anthropogenic carbon emission. Prior to the industrial revolution, atmospheric  $\text{CO}_2$  levels are estimated to be around 270 ppm (Wigley, 1983). More recent atmospheric  $\text{CO}_2$  measurements are substantially higher, at around 419 ppm (Dlugokencky et al., 2021). Up to one third of all anthropogenically produced  $\text{CO}_2$  has been absorbed by the oceans (Gruber et al., 2019; Sabine et al., 2004), keeping atmospheric levels lower by approximately 80 ppm (Friedlingstein et al., 2020). Seawater carbonate chemistry has undergone dramatic changes due to oceanic  $\text{CO}_2$  uptake (Fabricius et al., 2020; Orr et al., 2005; Riebesell and Gattuso, 2015), with average surface ocean pH decreasing by approximately 0.1 pH units (Caldeira and Wickett, 2003; Jiang et al., 2019; Orr et al., 2005). This lowering of seawater pH is collectively referred to as ocean acidification, a phenomena that seriously threatens the stability of ocean ecosystems, fish stocks and food security (Leis, 2018; McNeil and Sasse, 2016).

Ocean acidification can be tracked by measuring changes in seawater pH and the saturation state of seawater with respect to aragonite, a measure of carbonate ion concentration. pH is one of the four main carbonate system parameters along with dissolved inorganic carbon (DIC), fugacity of  $\text{CO}_2$  ( $f\text{CO}_2$ ) and total alkalinity (TA) (Dickson et al., 2007). By directly measuring two of these four parameters, utilising equilibrium constants specific to the nature of the aquatic system of study, as well as supplying data on temperature, salinity, pressure and specific inorganic seawater constituents, it is possible to calculate the remaining two parameters and obtain accurate information of carbonate chemistry (Zeebe, 2012).

TA, along with DIC, are popularly analysed input parameters in carbonate system calculations. TA is a conservative parameter with respect to temperature and salinity (Wolf-Gladrow et al., 2007) and does not change upon  $\text{CO}_2$  invasion or evasion, mak-



ing it is easier to sample for and store compared to other carbonate system parameters. TA measurements can also be made with a small degree of uncertainty, within  $1\text{--}2\ \mu\text{mol}\cdot\text{kg}^{-1}$ , and it is a preferred tracer variable in numerical models of the oceanic carbon cycle. TA is defined as the excess of proton acceptors over proton donors and can be represented by the following (Dickson et al., 2007):

$$\begin{aligned}
 [TA] = & [\text{HCO}_3^-] + 2[\text{CO}_3^{2-}] + [\text{B}(\text{OH})_4^-] + [\text{OH}^-] + [\text{HPO}_4^{2-}] \\
 & + 2[\text{PO}_4^{3-}] + [\text{SiO}(\text{OH})_3^-] + [\text{NH}_3] + [\text{HS}^-] \\
 & - [\text{H}^+] - [\text{HSO}_4^-] - [\text{HF}] - [\text{H}_3\text{PO}_4] + [\textit{minor bases} - \textit{minor acids}] \quad (4.1)
 \end{aligned}$$

Typically TA is attributed solely to the inorganic components of seawater such as bicarbonate ( $\text{HCO}_3^-$ ), carbonate ( $\text{CO}_3^{2-}$ ) and borate (Dyrssen and Sillén, 1967), with other inorganic seawater constituents making small contributions. Organic molecules that are present in seawater can also contribute to TA (Cai and Wang, 1998; Goldman and Brewer, 1980), with this contribution termed organic alkalinity (OrgAlk). The presence and influence of these organic species are typically omitted in the analysis of TA in the open ocean as they were once thought to be present in such small amounts that they can be safely neglected (Dickson et al., 2007). The consensus on this is changing (Fong and Dickson, 2019), with growing awareness that OrgAlk can constitute a significant portion of TA in coastal waters (Cai et al., 1998; Muller and Bleie, 2008; Patsavas et al., 2015; Song et al., 2020; Yang et al., 2015; Hernández-Ayon et al., 2007; Kerr et al., 2021), impact TA analytical procedures (Sharp and Byrne, 2020) and potentially impact carbonate system reference materials (Sharp and Byrne, 2021).

OrgAlk is thought to be a part of the dissolved organic matter (DOM) fraction that possesses charged functional groups that can react during TA titrations, thus altering the overall TA signal (Kim and Lee, 2009; Kuliński et al., 2014; Paxéus and Wedborg, 1985). The molecules that are typically associated with OrgAlk include humic sub-

stances, carboxylic acids, amines and phenols (Cai et al., 1998; Rigobello-Masini and Masini, 2001; Muller and Bleie, 2008; Paxéus and Wedborg, 1985; Emerson and Hedges, 2008). OrgAlk has also been associated with bacterial and planktonic cells (Kim et al., 2006), phytoplankton excretions (Kim and Lee, 2009; Hernández-Ayon et al., 2007) and terrigenous organic matter (Tishchenko et al., 2006).

As the contribution of organic acids to TA is not explicitly accounted for in the conventional TA equation (equation 4.1), their presence can lead to misrepresentations of carbonate alkalinity. OrgAlk presents a two-fold issue to carbonate chemistry investigations. For TA analysis to have a low degree of uncertainty, the concentrations and thermodynamic equilibrium constants of all acid-base species needs to be known so they can be accounted for. As OrgAlk presents an uncharacterised acid-base species, if OrgAlk constitutes a significant fraction of TA then there will be an inherent uncertainty in computed speciations (Riebesell et al., 2010). Furthermore, OrgAlk can present a potential analytical interference in TA computation arising from errors in estimation of the equivalence point in convention TA titrations (Sharp and Byrne, 2020). Any discrepancies in TA analysis induced by OrgAlk can potentially propagate errors in calculated carbonate system parameters (Abril et al., 2015; Hunt et al., 2011; Koeve and Oschlies, 2012) and lead to misinterpretation of key carbonate chemistry descriptors and critical indicators of acidification such as calcite and aragonite saturation states.

OrgAlk has typically been quantified by comparing directly measured TA values ( $TA_M$ ) and TA values calculated ( $TA_C$ ) using two other carbonate chemistry parameters and software programs that contain accurate carbonate system thermodynamic constants, such the multi-platform CO2SYS software program (Lewis and Wallace, 1998).  $TA_M$  is non-discriminatory and incorporates all proton acceptors formed from weak acids, regardless of inorganic or organic nature. Contributions from organic proton acceptors are not included in  $TA_C$  and it is assumed that  $TA_C$  accounts only for the inorganic protolytes in equation 4.1. OrgAlk values are calculated as the difference between  $TA_M$  and  $TA_C$  such that:

$$\text{OrgAlk} = \text{TA}_M - \text{TA}_C \quad (4.2)$$

This method of calculating OrgAlk has been implemented in multiple studies of the carbonate system conducted across a range of marine environments (Delaigue et al., 2020; Hammer et al., 2017; Hernández-Ayon et al., 2007; Kim and Lee, 2009; Kuliński et al., 2014; Patsavas et al., 2015). It is important to note that OrgAlk values calculated in this manner are inclusive of any residual errors associated with  $\text{TA}_C$  attributed to either errors in the input parameters or the thermodynamic models that relate them (Fong and Dickson, 2019). Furthermore, errors in  $\text{TA}_C$  may be more pronounced in low salinity coastal waters where carbonate system thermodynamic constants have not been as rigorously evaluated (Woosley, 2021). These factors may be responsible for larger misrepresentations of calculated OrgAlk in coastal compared to pelagic waters, highlighting the importance of more direct OrgAlk measurement methods.

Methods to directly measure OrgAlk have been developed and employed in a number of studies (Cai et al., 1998; Hunt et al., 2011; Muller and Bleie, 2008; Yang et al., 2015; Song et al., 2020). These methods offer advantages over OrgAlk calculated per equation 4.2 as they are free from the aforementioned residual errors in  $\text{TA}_C$  and carbonate system thermodynamic models while also allowing for the estimation of OrgAlk acid-base characteristics. Direct OrgAlk methods have been recommended for implementation on hydrographic research cruises in order to characterise OrgAlk in spatially heterogeneous oceanic waters (Sharp and Byrne, 2020). The ability to quantify the organic fraction of alkalinity and provide estimations of the pK values associated with its apparent titratable functional groups would allow investigators to incorporate OrgAlk into carbonate system calculations, potentially minimising OrgAlk associated

error propagation (Millero et al., 2002). This has previously been undertaken by considering OrgAlk as an aggregate of multiple distinct charge group species, each considered as a monobasic acid-base system with its own pK and total concentration (Cai et al., 1998; Muller and Bleie, 2008; Song et al., 2020).

The main objectives of this study were to utilise simple, cost-effective apparatus to perform TA analysis with the ability to quantify OrgAlk and provide estimates of its associated acid-base properties. To achieve these goals we adapted GOA-ON TA titration apparatus and methods to incorporate an OrgAlk quantification step and developed *OrgAlkCalc*, an accessible Python based computational procedure that allows users to process TA and OrgAlk titration files while simultaneously estimating the concentration and apparent pK values of OrgAlk present. The aforementioned titration apparatus, methods and computational procedures were tested using coastal seawater samples collected from Dublin Bay, Ireland.

## 4.2 Materials and methods

### 4.2.1 Study Location and Sampling Procedure

Seawater samples were collected during 6 sampling events from July 2021 to March 2022 from Dublin Bay and its associated transitional water bodies. Dublin Bay is a macrotidal system (Dyer, 1973) and has long been recognised as highly anthropogenically influenced (Adeney, 1908; Evans et al., 2003; Grey et al., 2021). The main freshwater inputs to the Bay arise from the River Liffey, whose catchment areas are characterised by an upland south eastern area underlain by granites and a flat, low lying limestone area over the remainder of the catchment basin (Irish Environmental Protection Agency, 2021). Dublin Bay is recognised as an area of cyclic biological activity, with discharges of hypernutrient river water and associated phytoplankton blooms recorded (O'Higgins and Wilson, 2005). These features make Dublin Bay an ideal study location to test *OrgAlkCalc* as it experiences biogeochemical processes similar to other

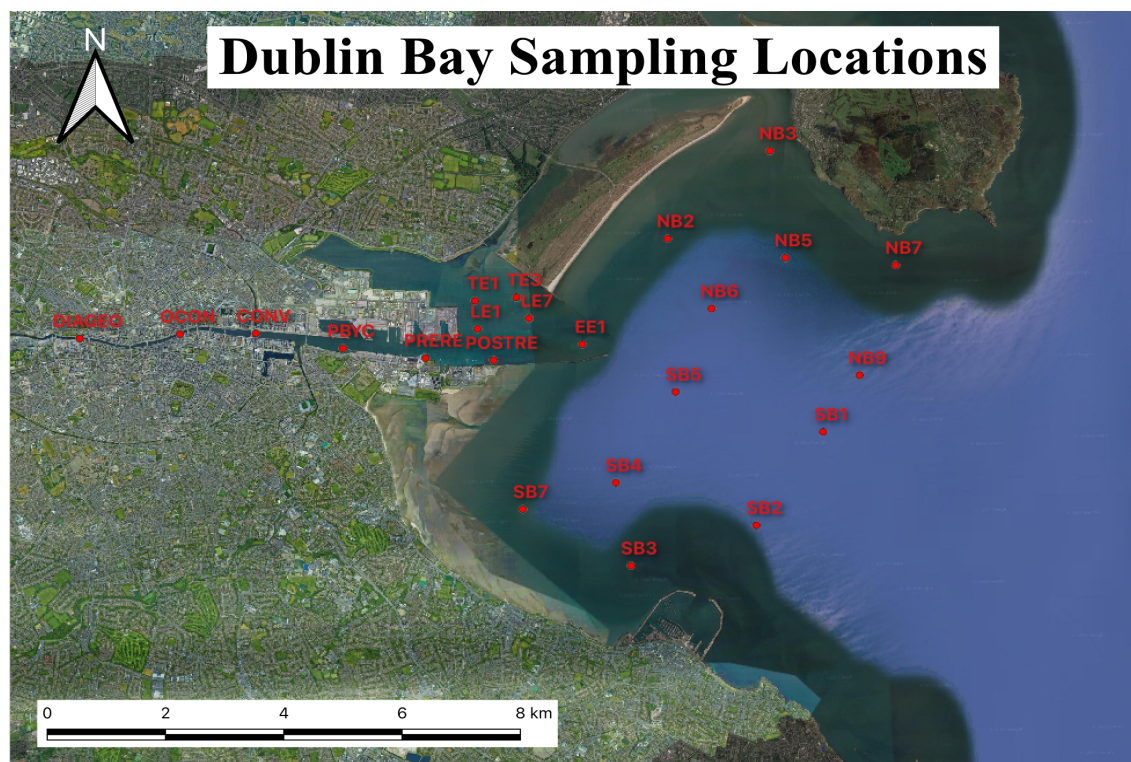


**Figure 4.1:** Map illustrating locations of sample acquisition in Dublin Bay and its associated transitional waters.

studies of OrgAlk (Cai et al., 1998; Hernández-Ayon et al., 2007; Yang et al., 2015). Surface seawater samples for TA and OrgAlk were collected in acid washed high density polyethylene (HDPE) bottles that were stored on ice and in the dark until filtration in the laboratory. Samples were analysed within two weeks of collection. In-situ temperature, salinity, and pH were collected using a calibrated Hanna HI98194 multiparameter probe. Samples for TA and OrgAlk analysis were vacuum filtered on the same day as collection using GF/F grade glass microfiber filters. 250 mL of filtrate was transferred to acid washed 250 mL HDPE bottles, poisoned with 50  $\mu$ L saturated mercuric chloride and refrigerated until analysis.

## 4.2.2 Apparatus and reagents

### Titration Apparatus

The titration apparatus followed a modified GOA-AN 'in a box' kit GOA-ON (2022) The electrode used to monitor titration progression was a Metrohm® Aquatrode plus, a

combined pH electrode for pH titrations in ion-deficient aqueous media. This electrode was chosen as to accommodate the analysis of low ionic strength estuarine samples. The reference electrolyte used was 3 M KCl. The bridge electrolyte used was 0.7 M NaCl. This was intended to match the ionic strength of the seawater samples analysed (Mintrop, 2016). Although the bridge electrolyte can be adjusted to match the ionic strength of the sample, it was decided to use 0.7 M NaCl for all samples as after an exchange of electrolyte, the electrode requires significant time until the system is stable again (Metrohm, 2021). The electrode was used in conjunction with a PHAMP-1 Sensorex battery-powered pH/ORP pre-amplifier. HCl and NaOH were dispensed from separate NIST-Traceable calibrated Gilmont GS-1200-A micrometer burette-style dispensers, with a manufacturer specified uncertainty of  $\pm 0.5\%$  of reading or  $\pm 1$  scale division. The temperature of each titrant was recorded using 4-wire platinum resistance thermometers (PRT) fixed to each respective burette and insulated with polyethylene foam. Accurate titrant temperature data was essential as the density of the titrant solutions were determined as a function of temperature to convert volume dispensed to mass units. Titrant temperature was observed to vary slightly over the duration of OrgAlk analysis, on average  $\leq 0.5$  °C, reinforcing the importance of recording temperature at each titration point. Sample temperature was recorded throughout the titration using a 4-wire corrosion resistant PRT immersed in the sample solution. PRTs were calibrated using an icepoint calibration prior to use. All titrations were carried out at  $25 \pm 0.1$  °C using a circulating water bath and jacketed 50 mL titration vessel. The titration vessel was placed on top of a magnetic stirrer to facilitate adequate mixing. A separate water bath was used to bring samples to 25 °C prior to analysis. The electrode and each PRT were connected to a Keithley model 2701 digital multimeter with a model 2700 switch system installed. The electrode electromotive force (emf) readout and respective temperatures of each titrant and sample were recorded using Keithley Kickstart instrument control software on a desktop computer.

## Reagents

0.1 M HCl was made using HCl concentrate (Honeywell Fluka) diluted to 1L with DI water and standardised using certified reference materials (CRM) from Prof. A. G. Dickson at the Scripps Institution of Oceanography. 0.1 M NaOH was made using NaOH concentrate (Reagecon) diluted to 1L with DI water sparged with ultrapure N<sub>2</sub> to be CO<sub>2</sub> free, and standardised against NIST traceable, dried potassium hydrogen phthalate Standard Reference Material (Certipur) (Muller and Bleie, 2008). The resulting NaOH solution was subsequently stored in screw cap HDPE bottles securely wrapped with parafilm in an appropriately greased (Dow Corning High Vacuum grease) vacuum chamber to minimise ambient CO<sub>2</sub> dissolution. The carbonate content of the NaOH solution is discussed in detail in section 4.3.1. As sample ionic strength varied across the study area, matching titrant and sample ionic strength would only be possible through the use of multiple individually standardised titrant solutions. Given the apparatus used in this investigation this was not a feasible option. Furthermore, for the TA titration, it is likely that changes in ionic strength resulting from titrant addition is more important for closed-cell titrations where all acid-base reactions are relevant in the evaluation of the whole titration curve; compared to an open-cell approach such as employed in this study where strictly it is only K(HSO<sub>4</sub>) and K(HF) that are involved (A. Dickson, personal communication). In addition to any implications for activity coefficients and subsequently the various pK values used, changes in solution composition resulting from titrant addition can also impact the degree to which the pH electrode exhibits Nernstian behaviour. This impact is acknowledged, although it is believed to be small (Okamura et al., 2014). For the NaOH titration, uncertainties associated with slight changes in ionic strength were minimised through the inclusion of functions in *OrgAlkCalc* that refactor sample ionic strength accounting for titrant addition, allowing for recalculation of the relevant ionic strength dependant pK values at each titration point.

### Titration Procedure and Data Handling

TA was analysed in an open-cell, potentiometric titration procedure as outlined in SOP 3b of Dickson et al. (2007). OrgAlk was analysed using methods adapted from Cai et al. (1998), Ko et al. (2016) and Song et al. (2020). The titration procedure was divided into three distinct stages: the TA, NaOH and OrgAlk titrations. During the TA titration a known mass of sample was acidified with HCl to a pH of  $\sim 3.5$ , allowed to degas for 10 minutes and then titrated with 0.02 mL increments of HCl to a final pH of  $\sim 3$ ; this resulted in approximately 20 titration data points. For the NaOH titration, increments of NaOH were added to the now acidified seawater under an  $N_2$  atmosphere such that the pH increased by  $\sim 0.1$  upon each NaOH addition. The NaOH titration ceased when the sample had been returned to its original pH, with approximately 50 titration data points generated per sample. The OrgAlk titration then proceeded identically to the TA titration procedure, with the exception of the  $CO_2$  degassing stage. The alkalinity value returned from the OrgAlk titration is attributed to organic proton acceptors as well as introduced carbonate alkalinity present in the NaOH titrant as sample carbonate alkalinity was consumed during the TA titration.

#### 4.2.3 OrgAlkCalc

All TA, NaOH and OrgAlk titration files were processed using *OrgAlkCalc* to calculate final TA values as well as estimate the quantity and associated acid-base properties of titratable organics for each sample. *OrgAlkCalc* is a Python based, open-source programme that allows users to process TA and OrgAlk titration files generated through the use of adapted GOA-ON apparatus with minimal programming experience. TA is calculated using a simple Gran approach (Gran, 1952) coupled with a non-linear least squares curve fitting (NLSF) procedure (Dickson et al., 2003). To estimate OrgAlk concentrations and associated pK values, *OrgAlkCalc* uses an iterative NLSF procedure along with a simple model derived from charge balance equation 4.3 (Song et al., 2020; Ko et al., 2016; Cai et al., 1998). The charge balance equation can be described by the



following:

$$\begin{aligned}
 & V_0 \sum \frac{X_{iT}}{1 + \frac{[H^+]}{K_i}} + V_0 \frac{B_T}{1 + \frac{[H^+]}{K_B}} + V_0 \frac{P_T}{1 + \frac{[H^+]}{K_P}} + V_0 \frac{Si_T}{1 + \frac{[H^+]}{K_{Si}}} \\
 & + V_b \frac{CTNa}{1 + \frac{[H^+]}{K_{C_1}} + \frac{K_{C_2}}{[H^+]}} + 2 \cdot V_b \frac{CTNa}{1 + \frac{[H^+]^2}{K_{C_1} \cdot K_{C_2}} + \frac{[H^+]}{K_{C_2}}} + (V_0 + V_a)(H_0) \quad (4.3) \\
 & - (V_0 + V_a + V_b)([H^+] - [OH^-]) - V_b \cdot C_{NaOH} = 0
 \end{aligned}$$

where  $V_0$  is the initial mass of sample,  $V_a$  is the total volume of acid added during the TA titration and  $V_b$  is the volume of base added at each titration point.  $K_i$ ,  $K_B$ ,  $K_P$  (as  $H_2PO_4^-$ ),  $K_{Si}$ ,  $K_{C_1}$  and  $K_{C_2}$  refer to the dissociation constants of charge group  $i$  of organic acids, boric acid, phosphoric acid, silicic acid and carbonic acid, respectively.  $X_{iT}$ ,  $B_T$ ,  $P_T$  and  $Si_T$  are the total concentrations of charge group  $i$  of organic acids, borate, phosphate and silicate, respectively.  $CTNa$  refers to the total concentration of  $CO_3^{2-}$  in the NaOH titrant.  $[H^+]$  and  $[OH^-]$  are the concentration of protons and hydroxide ions, while  $H_0$  is the initial proton concentration of the NaOH titration.  $C_{NaOH}$  is the concentration of the NaOH titrant.

The curve fitting technique proceeded in four distinct stages: (1) NaOH titration data in the range  $pH \leq 5$  was used to constrain  $H_0$ ,  $X_1$  and  $K_1$ . This approach was taken as in this low pH range the contribution of charge groups with high pK values can be omitted (Cai et al., 1998). (2)  $H_0$  was then fixed and a non-linear curve fitting technique is performed iteratively for curve data in the range  $pH \leq pH_{max} \cdot 0.75$ , where  $pH_{max}$  is the maximum pH of the NaOH titration, in order to constrain  $X_1$  and  $K_1$ . The initial estimates of  $H_0$  and  $X_i$  are taken as the concentration of  $H^+$  at the start of the NaOH titration and the OrgAlk concentration returned from the Orgalk titration, respectively. Initial estimates of  $K_i$  are provided by the user in the master titration file. (3) Values of  $X_1$  and  $K_1$  are then fixed and values of  $X_2$  and  $K_2$  are constrained using all data. (4) Finally,  $X_2$  and  $K_2$  are fixed and values of  $X_3$  and  $K_3$  are constrained using all data. Model returned values for  $K_3$  were retained only if the inclusion of an additional  $K$  term reduced the residuals of the fit. After each step, the model outputs were used

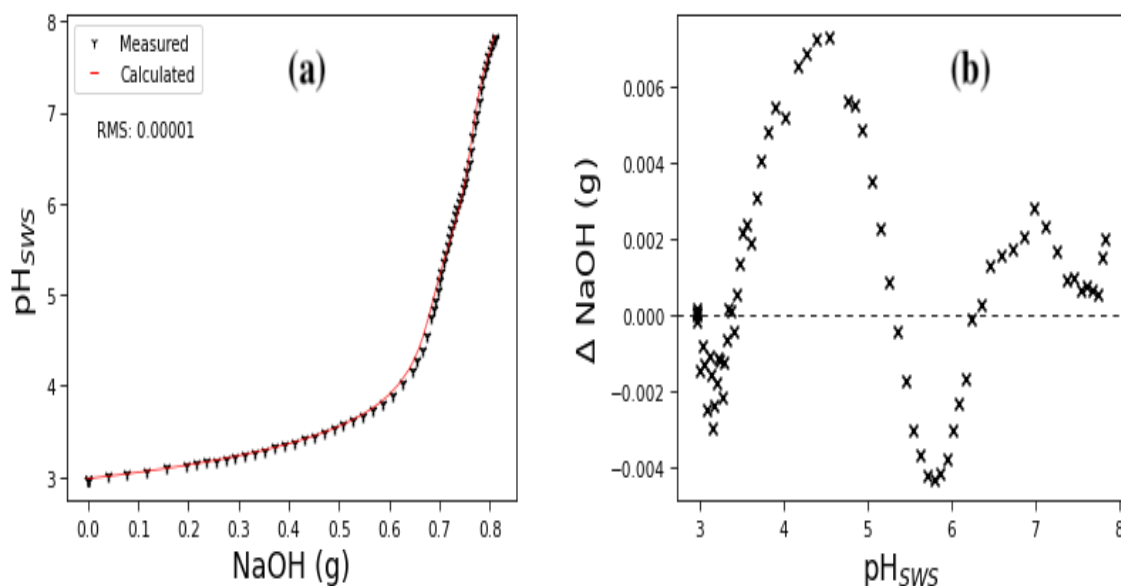


**Figure 4.2:** (a) Plot of  $\text{pH}_{\text{SWS}}$  as a function of mass of NaOH added during the NaOH titration. The black markers indicate  $V_{b_M}$  added while the red line indicates  $V_{b_C}$ . The goodness of fit is reflected by the root mean square residual value. (b) Plot of the residuals as a function of  $\text{pH}_{\text{SWS}}$ , where  $\Delta \text{NaOH} = V_{b_M} - V_{b_C}$ .

in a rearranged equation 4.3 to solve for  $V_b$ . The model calculated  $V_b$  ( $V_{b_C}$ ) value is compared to the experimentally derived  $V_b$  ( $V_{b_M}$ ) value in order to produce a root mean square (RMS) residual value, see figure 4.2. Some structure was seen in the residuals due to the degrees of freedom in the nonlinear curve fitting, with this slight overfitting as expected. It is plausible that this effect could be reduced by applying additional constraints on the fitting, for example L1 regularisation. As the residuals are small and we do not aim to estimate outside the range of available data, such techniques were deemed to be unnecessary for this work. However, it does indicate that there may be potential to improve this nonlinear curve fitting using machine learning techniques. For each curve fitting procedure, the initial conditions are set to iterate curve fitting until the difference between each consecutive repetitions returned RMS ( $\Delta \text{RMS}$ ) is less than  $1 \times 10^{-10}$ , with this value referred to as the convergence factor. In the instance that  $\Delta \text{RMS}$  is greater than the convergence factor after 100 repetitions, the convergence factor increases by a factor of 10. This process repeats until  $\Delta \text{RMS} < \text{convergence factor}$ . The final convergence factor value is recorded and serves as an initial indication

of the validity of model returned results.

Each titration resulted in the generation of an individual titration data file. Each file was amended to include volume of titrant dispensed data. Metadata integral to sample processing such as mass of sample, salinity, titrant mass and concentration data; and total concentrations of optionally included nutrient species such as phosphate and silicate were stored within a master titration file. Users specify their choice of carbonate system constants (Lueker et al., 2000; Cai et al., 1998; Dickson and Millero, 1987; Millero, 2010; Prieto and Millero, 2002) in the master titration file. Users should acknowledge the potential for added uncertainty on model results arising from disparities between pH scale inherent to the choice of constants, although the degree of added uncertainty is likely small as the difference between  $\text{pH}_T$  and  $\text{pH}_{\text{SWS}}$  are approximately 0.01 (Marion et al., 2011). The master titration file also included user supplied values for the initial estimates of *OrgAlk* dissociation constants used in the NLSF procedure, as well as an user supplied optional value for the total concentration of *CTNa*. *CTNa* values are in units of  $\mu\text{mol} \cdot \text{kg}^{-1} \cdot \text{g}^{-1}$  in order to allow for titration specific *CTNa* calculation based on mass of NaOH titrant added. Processed data was then automatically exported to a master results file for further analysis. This allows for the convenient batch processing of multiple samples. Once processed, sample information was automatically exported to a master results file for post-processing.

## 4.3 Results and Discussion

### 4.3.1 *OrgAlkCalc* Performance

To test the performance of *OrgAlkCalc* 103 individual titration files were processed for both concentration of TA and *OrgAlk* as well as apparent associated pK values. Of the 103 titrations, 3 were omitted in further data processing due to data corruption. The remaining 100 data files, when fit to the model, returned RMS values in line with previously reported literature values of 0.001 - 0.01 (Song et al., 2020; Ko et al., 2016).

Post-processing was performed using specific criteria in order to produce final charge group concentration and apparent pK outputs. As the NaOH titration data used in the curve fitting procedure was constrained to a certain pH range, model outputs with pK values outside of this range were regarded as having a high degree of uncertainty. Of the pK values returned that were outside the aforementioned pH range, all were higher than the maximum pH of the NaOH titration. Additionally, the charge group concentrations associated with these pK values were consistently unrealistically high. Although high-pK organics can potentially have important influences on carbonate system behaviour if their concentrations are sufficiently high, given the inherent uncertainty with returned pK values outside the range of input data and unrealistically high associated charge group concentrations they were omitted from further discussion. Potential procedures to address high-pK organics include full range titration to higher pH values, such as outlined in (Song et al., 2020).

### **NaOH $\text{CO}_3^{2-}$ content**

An important factor to consider in the OrgAlk computational procedures is the  $\text{CO}_3^{2-}$  content of the NaOH titrant (*CTNa*). The presence of  $\text{CO}_3^{2-}$  in the NaOH titrant has been attributed to dissolved  $\text{CO}_2$  (Song et al., 2020) as well as reagent impurities (Yang et al., 2015). Although methods to account for *CTNa* in subsequent curve fitting procedures were undertaken in this study, the inclusion of procedures to largely eliminate *CTNa*, such as carbonate precipitation facilitated by sufficient calcium addition, could minimise the attendant uncertainties inherent to accounting for *CTNa* algorithmically. The  $\text{CO}_3^{2-}$  content of the NaOH titrant was measured over the analysis period by performing the previously detailed titration procedure on a 0.7 M NaCl solution that had been purged of  $\text{CO}_2$  using ultrapure  $\text{N}_2$ . As the 0.7 M NaCl solution was theoretically free of organics and had the majority of its carbonate alkalinity removed through the initial TA titration, the alkalinity value returned from the OrgAlk titration corresponded to carbonate introduced through the addition of the NaOH titrant. Over

the analysis period mean  $CTNa$  values varied from 25 - 61  $\mu\text{mol} \cdot \text{kg}^{-1} \cdot \text{g}^{-1}$ .

To account for  $CTNa$  effects on computed charge group concentrations and apparent pK values, *OrgAlkCalc* allows the user the option to include  $CTNa$  terms in equation 4.3. This function enables users to run *OrgAlk* characterisations with or without the inclusion of  $CTNa$  terms. Along with inclusion in equation 4.3,  $CTNa$  is also subtracted from the initial estimates of  $X_{iT}$  in the NLSF procedure. Care is required if

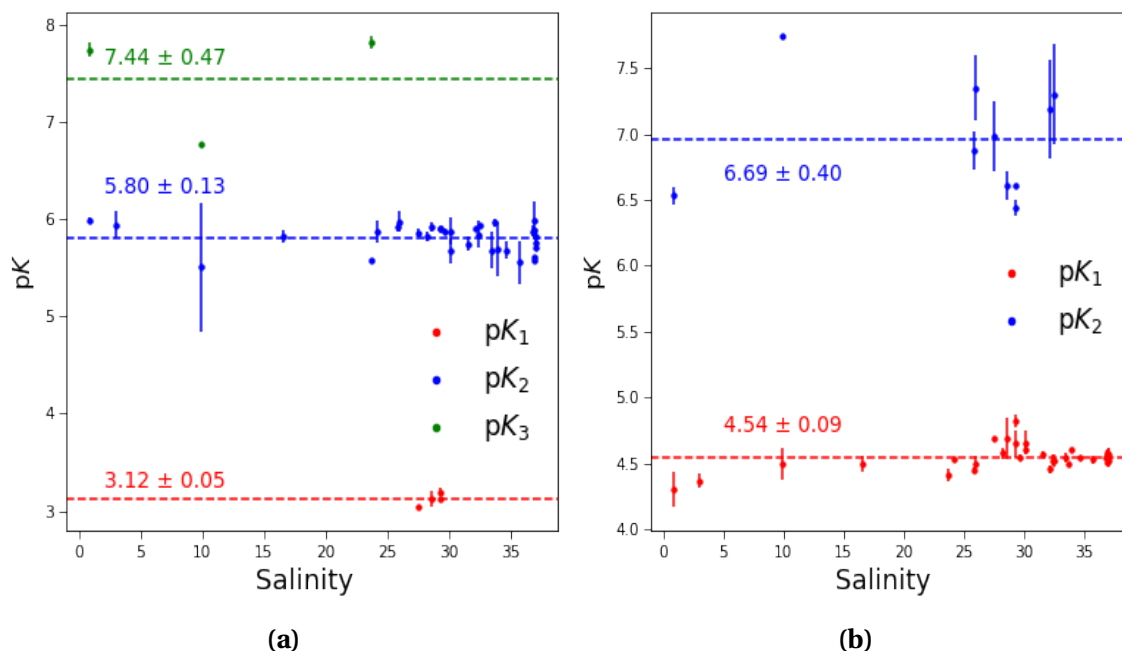


**Figure 4.3:** (a) Observed pK values when  $CTNa$  was unaccounted for in *OrgAlkCalc* curve fitting procedures. Note the similarity in magnitude between  $pK_2$  and the dissociation constant of  $\text{CO}_2$  to bicarbonate in seawater,  $pK \approx 5.8$  (b) Observed pK values when  $CTNa$  was accounted for. Occurrence of pK values centered around  $pK \approx 5.8$  was greatly diminished and resulting  $pK_1$  and  $pK_2$  values associated with the apparent dissociation constants of titratable organics were in better agreement with previously reported literature values. Error bars indicate standard deviation of replicate measurements ( $n=3$ ).

$CTNa$  is omitted in the curve fitting procedure, as substantial differences in returned charge group concentrations and associated pK values were observed when  $CTNa$  was unaccounted for. Failure to incorporate  $CTNa$  resulted in the observation of a charge group with a pK value centered around  $5.80 \pm 0.13$  across the salinity gradient, see  $pK_2$  in 4.3a. This pK value is similar in magnitude to the pK assigned to the dissociation of  $\text{CO}_2$  to bicarbonate in seawater ( $pK_{1C}$ ), approximately 5.8. When  $CTNa$  was explic-

itly included in the model, the occurrence of apparent organic charge group pK signal similar  $pK_{1C}$  was largely removed, see 4.3b. The close agreement between  $pK_3$  and  $pK_2$  in figures 4.3a and 4.3b respectively suggest that failure to account for *CTNa* can lead to issues in the delineation of apparent organic charge group pK values similar in magnitude to that of  $pK_{1C}$ . When accounting for *CTNa* returned organic charge group pK were in closer agreement to previously reported pK values for titratable organics associated with *OrgAlk*, see table 4.2. From the aforementioned it appears that NaOH  $CO_3^{2-}$  content can have significant implications on organic charge group pK values obtained through the titration procedures detailed in this study in conjunction with *OrgAlkCalc*. Not accounting for *CTNa* was observed to result in the inability to delineate between the apparent pK values of titratable organics and the dissociation of  $CO_2$  to  $HCO_3^-$  in seawater. Evidently, it is essential to remove as much  $CO_2$  from the system in order to minimise *CTNa* associated uncertainties on returned pK values.

### 4.3.2 Alkalinity distributions

#### TA

TA values ranged from 2264.84 - 4675.52  $\mu\text{mol}\cdot\text{kg}^{-1}$ , with the highest concentrations observed in less saline waters. TA displayed relatively conservative mixing, indicating that predominately the mixing of high TA freshwater with lower TA marine water governed distribution within the bay, see figure 4.4a. Certain recorded salinity values (NB9, SB7, SB5, NB3, SB1, SB3 and SB4 of the 06/08/2021 sampling event), were unusually high when compared to the average Irish Sea salinity of 35. Although salinity values greater than 36 have been previously recorded in Dublin Bay (DPC, 2022), the high salinity values could possibly be due to instrument related data artefacts. The elevated TA value observed at salinity  $\sim 16$  is attributed to sample acquired at the confluence point of the Royal Canal with the River Liffey on 10/03/22. Although the lining of the canal is composed of impervious clay, lime is recorded as being extensively used in the construction of lock chambers along the canal (Clarke, 1992) posing a possible

source of the observed elevated TA. The freshwater systems that discharge into Dublin Bay are significant sources of TA, with values well over the average oceanic water TA range of 2000 - 2500  $\mu\text{mol}\cdot\text{kg}^{-1}$ . As the catchment area of the Liffey is a mixture of urbanised and agricultural lands, land cover type could play a role in elevated TA export (Raymond and Cole, 2003). Furthermore, the bedrock morphology of the river system catchment area likely plays a large role in dictating TA export. The Royal Canal flows across predominately carbonate bedrock, possibly explaining the relatively high TA values. In a study of four contrasting coastal systems in Ireland, McGrath et al. (2019) reported consistently higher TA levels in systems that had a primarily carbonate bedrock morphology. The data presented in this study appears to agree with this finding.

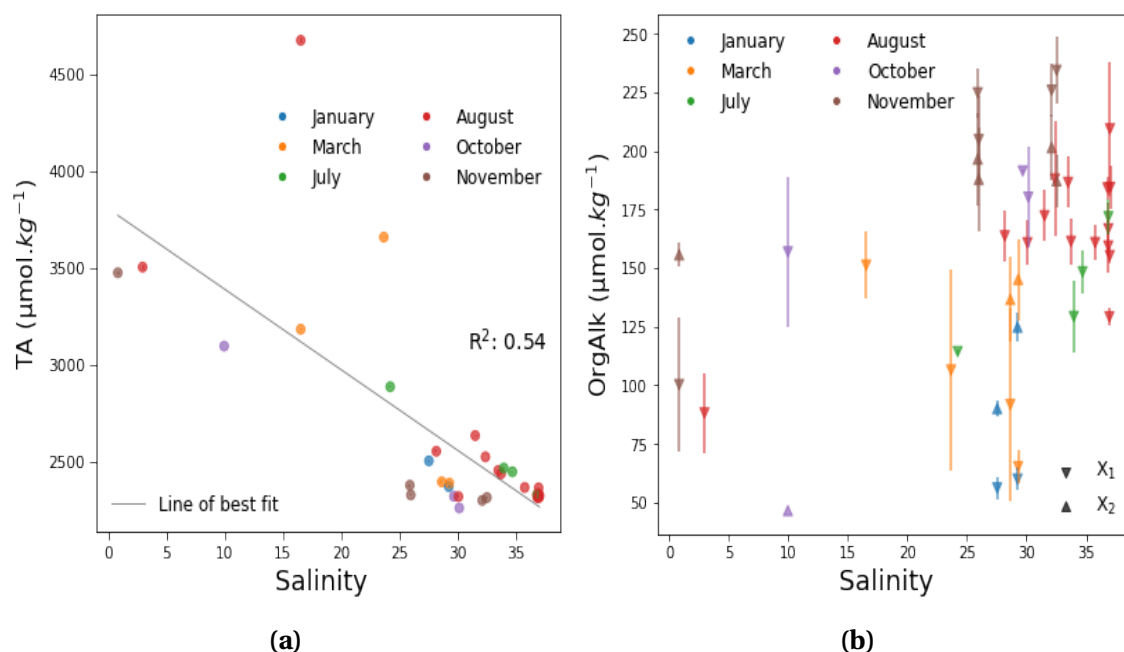


**Figure 4.4:** (a) TA distributions within Dublin Bay and its associated transitional waters classified by month. Elevated TA concentrations were observed in less saline waters indicating that freshwater inputs to Dublin Bay constitute a considerable source of TA (b) Concentrations of OrgAlk charge groups  $X_1$  and  $X_2$  as a function of salinity, classified by month. Note the elevated OrgAlk values in Winter and Spring sampling events. Error bars indicate standard deviation between replicate measurements ( $n=3$ ). TA uncertainties can be seen in table 4.1.

## OrgAlk

Observed OrgAlk values ranged from approximately 56 to 234  $\mu\text{mol}\cdot\text{kg}^{-1}$  for  $X_1$  and approximately 46 to 201  $\mu\text{mol}\cdot\text{kg}^{-1}$  for  $X_2$ . The highest OrgAlk values were observed in more marine influenced areas. OrgAlk distributions within the bay did not display conservative mixing, indicating that mechanisms other than mixing played a role in OrgAlk concentration distributions along the salinity gradient. OrgAlk charge group concentrations were highest in the Autumn/Winter period and lowest in the Spring/-Summer period. The median annual, Summer and Winter flow rates for the River Liffey are 6.1, 2.2 and 27.4  $\text{m}^3\cdot\text{s}^{-1}$ , respectively (DHI, 2018). This considerable disparity in seasonal flow rates could be a factor in elevated Autumn/Winter OrgAlk values; higher discharge rates may allow for enhanced transference of terrestrially derived organics. Further variations in OrgAlk concentrations can possibly be explained by biologically driven OrgAlk production, with several studies associating elevated OrgAlk concentrations with microbial activity (Ko et al., 2016; Kim and Lee, 2009; Muller and Bleie, 2008; Hernández-Ayon et al., 2007).

### 4.3.3 OrgAlk charge group characteristics

The pK values observed in this study are in line with those reported in previous investigations, as can be seen from table 4.2. The values presented in table 4.2 reflect the heterogeneous nature of organic acid pK values observed in natural samples. Two distinct pK values were observed for Dublin Bay transitional waters:  $\text{pK}_1$  at  $4.54\pm 0.09$  and  $\text{pK}_2$  at  $6.69\pm 0.40$ , as seen in figure 4.3b. Compilations of pK values of acidic functional groups (Smith and Martell, 1983; Izatt and Christensen, 1976) summarised as frequency histograms by Perdue et al. (1984) indicate that the frequency of occurrence of carboxyl group pK displays approximately normal distribution with a mean value of  $\sim 4.5$ , whereas phenolic groups display a mean around  $\sim 10$ .  $\text{pK}_1$  falls within this broad range of pK values associated with carboxyl functional groups, with  $\text{pK}_2$  possibly more phenolic in nature. The observed values for  $\text{pK}_1$  and  $\text{pK}_2$  agree with the range of pK val-



ues associated with humic substances, specifically carboxyl and phenolic groups that represent a significant portion of DOM in natural waters (Hertkorn et al., 2006; Ritchie and Perdue, 2003; Tipping et al., 2011). The consistent distribution of  $pK_1$  values observed across the salinity gradient until a salinity of  $\sim 24$  can possibly be explained by a lack of modification in the nature and the proportion of different functional groups present on DOM. Recent  $^{13}\text{C}$  and  $^{15}\text{N}$  spectroscopic analysis of DOM collected from the Siene estuary, France, indicated that DOM underwent minimal modification across the estuarine system (Venel et al., 2021). On average,  $pK_1$  constituted the bulk of OrgAlk charge groups, accounting for  $80\% \pm 7\%$  of OrgAlk concentrations. The prevalence of  $pK_1$  could be indicative of a single charge group associated with OrgAlk in the transitional waters of Dublin Bay. This may indicate that ubiquitous, recalcitrant DOM accounts for a large portion of OrgAlk. From table 4.1,  $pK_2$  was observed to more frequently in the Autumn/Winter period, suggesting a possible seasonal control on OrgAlk acid-base properties.

The nature of OrgAlk as characterised by estimation of its pK values may further be explained by associations with humic substances. In a study of riverine fulvic acids, Paxéus and Wedborg (1985) identified the presence 6 charge groups: (I) 2.66, (II) 4.21, (III) 5.35, (IV) 6.65, (V) 8.11 and (VI) 9.54. Using the classification of Yang et al. (2015), is possible that  $pK_1$  is combination of groups II and III whereas  $pK_2$  is a combination of groups IV and V. The concept that OrgAlk can largely be defined by a single, bulk pK value for large-scale regional data sets has been previously reported. Kuliński et al. (2014) and Ulfsbo et al. (2015) utilised empirical characterisations of OrgAlk in conjunction with DOM concentrations to calculate a bulk pK value. Although beneficial in application to regional data sets, this approach requires the over-determination of the carbonate system and likely suffers from inaccuracies for OrgAlk concentration  $\leq 8 \mu\text{mol} \cdot \text{kg}^{-1}$  (Yang et al., 2015).

For the NaOH titration, as the model used to estimate the acid-base properties of OrgAlk had no ionic strength dependencies of pKs, estimated pK values inherently

have an associated uncertainty. Previous investigation on pK variation of humic acids across the ionic strength commonly encountered in estuarine environments ( $I = 0.01 - 1.0 \text{ M}$ ) indicated a maximum uncertainty of 0.75 (Masini et al., 1998). Uncertainties in returned charge group concentrations and associated acid-base properties likely arise also from the use of conventional carbonate system and ancillary acid-base species thermodynamic equilibrium constants in waters of heterogeneous ionic strength. Additionally, although the GOA-ON apparatus outlined in this study are described as being capable of producing "Weather" quality TA measurements (Newton et al., 2014), there is still an innate uncertainty associated with the use of titrant dispensation systems of limited accuracy and indeterminate precision. The degree of uncertainty associated with the aforementioned can be diminished through rigorous burette calibration and accurate titrant density information. Acknowledging the inherent uncertainty on model generated pK values, OrgAlk pK estimations coupled with OrgAlk concentrations allow investigators to incorporate OrgAlk into carbonate system calculations, minimising OrgAlk associated error propagation (Millero et al., 2002; Song et al., 2020). Failing to account for OrgAlk when using TA and DIC as the input pair in carbonate system calculations can cause large misrepresentations of calculated  $p\text{CO}_2$  (Yang et al., 2015). For rigorous carbonate system calculations in coastal waters, it is critical to consider OrgAlk contributions.

#### 4.4 Conclusion

This study has indicated that existing and widely available GOA-ON TA titration apparatus can be simply modified to be used in conjunction with *OrgAlkCalc* in order to investigate the quantity and acid-base properties of OrgAlk. The findings presented in this study reinforce the current understanding of OrgAlk acid-base properties; typically carboxyl and phenolic groups represent a significant portion of charge groups present on DOM associated with OrgAlk in transitional waters. While estimates of the total concentrations and apparent acid-base properties of titratable organics can be

obtained, given the complexity of alkalinity titrations in transitional waters a degree of uncertainty remains associated with returned parameters. The outlined methodology and software allows GOA-ON carbonate system investigators the ability to include complementary OrgAlk analysis in conjunction with existing TA titration procedures to facilitate systematic descriptions of OrgAlk in coastal waters with respect to salinity, seasonal and trophic state of a system. Given the heterogeneity in concentration and equilibrium behaviour of OrgAlk components and difficulty in their rigorous characterisation, the inclusion of OrgAlk terms in carbonate system calculations remains a challenging endeavour. Furthermore, the suitability of TA as an appropriate input parameter in carbonate system calculations in coastal waters remains questionable, unless methods to include OrgAlk influences are incorporated.

## References

- Abril, G., Bouillon, S., Darchambeau, F., Teodoru, C. R., Marwick, T. R., Tamooch, F., Ochieng Omengo, F., Geeraert, N., Deirmendjian, L., Polsenaeere, P., and Borges, A. V. (2015). Technical note: Large overestimation of pCO<sub>2</sub> calculated from pH and alkalinity in acidic, organic-rich freshwaters. *Biogeosciences*, 12(1):67–78.
- Adeney, W. (1908). Effect of the new drainage on Dublin Harbour. In *Handbook to the Dublin District British Association*, page 387.
- Cai, W.-j. and Wang, Y. (1998). The chemistry, fluxes, and sources of carbon dioxide in the estuarine waters of the Satilla and Altamaha Rivers, Georgia. 43(4):657–668.
- Cai, W. J., Wang, Y., and Hodson, R. E. (1998). Acid-base properties of dissolved organic matter in the estuarine waters of Georgia, USA. *Geochimica et Cosmochimica Acta*, 62(3):473–483.
- Caldeira, K. and Wickett, M. E. (2003). Anthropogenic carbon and ocean pH. *Nature*, 425(September):2003.
- Clarke, P. (1992). *The Royal Canal: The complete story*. Elo Publications, Dublin.
- De Souza Sierra, M. M., Arend, K., Fernandes, A. N., Giovanela, M., and Szpoganicz, B. (2001). Application of potentiometry to characterize acid and basic sites in humic substances: Testing the BEST7 program with a weak-acid mixture. *Analytica Chimica Acta*, 445(1):89–98.
- Delaigue, L., Thomas, H., and Mucci, A. (2020). Spatial variations in CO<sub>2</sub> fluxes in the Saguenay Fjord (Quebec, Canada) and results of a water mixing model. *Biogeosciences*, 17(2):547–566.
- DHI (2018). Ringsend WwTP - EIAR modelling services Water Quality Modelling. (May).

- Dickson, A. G., Afghan, J. D., and Anderson, G. C. (2003). Reference materials for oceanic CO<sub>2</sub> analysis: A method for the certification of total alkalinity. *Marine Chemistry*, 80(2-3):185–197.
- Dickson, A. G. and Millero, F. J. (1987). A comparison of the equilibrium constants for the dissociation of carbonic acid in seawater media. *Deep Sea Research Part A, Oceanographic Research Papers*, 34(10):1733–1743.
- Dickson, A. G., Sabine, C. L., and Christian, J. R. (2007). *Guide to Best Practices for Ocean CO<sub>2</sub> Measurements*. Number 8.
- Dlugokencky, E., Mund, J., Crotwell, A., Crotwell, M., and Thoning, K. (2021). Atmospheric Carbon Dioxide Dry Air Mole Fractions from the NOAA GML Carbon Cycle Cooperative Global Air Sampling Network, 1968-2020, Version: 2021-07-30.
- DPC (2022). Dublin Port Company: Maintenance Dredging Programme 2022 – 2029 Application for Foreshore Licence Coastal Processes Risk Assessment. (February 2021).
- Dyer, K. (1973). *Estuaries: a physical introduction*. John Wiley & Sons, first edition.
- Dyrssen, D. and Sillén, L. G. (1967). Alkalinity and total carbonate in sea water. A plea for p-T-independent data - Dyrssen - 2010 - Tellus - Wiley Online Library. *Tellus*.
- Emerson, S. and Hedges, J. I. (2008). *Chemical Oceanography and the Marine Carbon Cycle*. Cambridge University Press.
- Evans, G. L., Williams, P. J. B., and Mitchelson-Jacob, E. G. (2003). Physical and anthropogenic effects on observed long-term nutrient changes in the Irish Sea. *Estuarine, Coastal and Shelf Science*, 57(5-6):1159–1168.
- Fabricius, K. E., Neill, C., Van Ooijen, E., Smith, J. N., and Tilbrook, B. (2020). Progressive seawater acidification on the Great Barrier Reef continental shelf. *Scientific Reports*, 10(1):1–15.

- Fong, M. B. and Dickson, A. G. (2019). Insights from GO-SHIP hydrography data into the thermodynamic consistency of CO<sub>2</sub> system measurements in seawater. *Marine Chemistry*, 211(January):52–63.
- Friedlingstein, P., O’Sullivan, M., Jones, M. W., Andrew, R. M., Hauck, J., Olsen, A., Peters, G. P., Peters, W., Pongratz, J., Sitch, S., Le Quéré, C., Canadell, J. G., Ciais, P., Jackson, R. B., Alin, S., Aragão, L. E., Arneeth, A., Arora, V., Bates, N. R., Becker, M., Benoit-Cattin, A., Bittig, H. C., Bopp, L., Bultan, S., Chandra, N., Chevallier, F., Chini, L. P., Evans, W., Florentie, L., Forster, P. M., Gasser, T., Gehlen, M., Gilfillan, D., Gkritzalis, T., Gregor, L., Gruber, N., Harris, I., Hartung, K., Haverd, V., Houghton, R. A., Ilyina, T., Jain, A. K., Joetzjer, E., Kadono, K., Kato, E., Kitidis, V., Korsbakken, J. I., Landschützer, P., Lefèvre, N., Lenton, A., Lienert, S., Liu, Z., Lombardozzi, D., Marland, G., Metzl, N., Munro, D. R., Nabel, J. E., Nakaoka, S. I., Niwa, Y., O’Brien, K., Ono, T., Palmer, P. I., Pierrot, D., Poulter, B., Resplandy, L., Robertson, E., Rödenbeck, C., Schwinger, J., Séférian, R., Skjelvan, I., Smith, A. J., Sutton, A. J., Tanhua, T., Tans, P. P., Tian, H., Tilbrook, B., Van Der Werf, G., Vuichard, N., Walker, A. P., Wanninkhof, R., Watson, A. J., Willis, D., Wiltshire, A. J., Yuan, W., Yue, X., and Zaehle, S. (2020). Global Carbon Budget 2020. *Earth System Science Data*, 12(4):3269–3340.
- GOA-ON (2022). Global Ocean Acidification Observing Network, 'in a Box' TA titration kits.
- Goldman, J. C. and Brewer, P. G. (1980). Effect of nitrogen source and growth rate on phytoplankton-mediated changes in alkalinity. *Limnology and Oceanography*, 25(2):352–357.
- Gran, G. (1952). Determination of the equivalence point in potentiometric acid-base titrations. *Dansk tidsskrift for farmaci*, 35:236–242.
- Grey, A., Cunningham, A., Lee, A., Monteys, X., Coveney, S., McCaul, M. V., Murphy, B. T., McCloughlin, T., Hidaka, B., and Kelleher, B. P. (2021). Geochemical mapping of

- a blue carbon zone: Investigation of the influence of riverine input on tidal affected zones in Bull Island. *Regional Studies in Marine Science*, 45:101834.
- Gruber, N., Clement, D., Carter, B. R., Feely, R. A., van Heuven, S., Hoppema, M., Ishii, M., Key, R. M., Kozyr, A., Lauvset, S. K., Monaco, C. L., Mathis, J. T., Murata, A., Olsen, A., Perez, F. F., Sabine, C. L., Tanhua, T., and Wanninkhof, R. (2019). The oceanic sink for anthropogenic CO<sub>2</sub> from 1994 to 2007. *Science*, 363(6432):1193–1199.
- Hammer, K., Schneider, B., Kuliński, K., and Schulz-Bull, D. E. (2017). Acid-base properties of Baltic Sea dissolved organic matter. *Journal of Marine Systems*, 173:114–121.
- Hernández-Ayon, M. J., Zirino, A., Dickson, A. G., Camiro-Vargas, T., and Valenzuela-Espinoza, E. (2007). Estimating the contribution of organic bases from microalgae to the titration alkalinity in coastal seawaters. *Limnology and Oceanography: Methods*, 5(7):225–232.
- Hertkorn, N., Benner, R., Frommberger, M., Schmitt-Kopplin, P., Witt, M., Kaiser, K., Kettrup, A., and Hedges, J. I. (2006). Characterization of a major refractory component of marine dissolved organic matter. *Geochimica et Cosmochimica Acta*, 70(12):2990–3010.
- Hunt, C. W., Salisbury, J. E., and Vandemark, D. (2011). Contribution of non-carbonate anions to total alkalinity and overestimation of pCO<sub>2</sub> in New England and New Brunswick rivers. *Biogeosciences*, 8(10):3069–3076.
- Irish Environmental Protection Agency (2021). 3rd Cycle Liffey and Dublin Bay Catchment Report (HA 09). (1).
- Izatt, R. M. and Christensen, J. J. (1976). *Heats of Proton Ionization, pK, and Related Thermodynamic Quantities*. CRC Press, 3rd editio edition.
- Jiang, L. Q., Carter, B. R., Feely, R. A., Lauvset, S. K., and Olsen, A. (2019). Surface ocean pH and buffer capacity: past, present and future. *Scientific Reports*, 9(1):1–11.

- Kerr, D. E., Brown, P. J., Grey, A., and Kelleher, B. P. (2021). The influence of organic alkalinity on the carbonate system in coastal waters. *Marine Chemistry*, 237:104050.
- Kim, H. C. and Lee, K. (2009). Significant contribution of dissolved organic matter to seawater alkalinity. *Geophysical Research Letters*, 36(20):1–5.
- Kim, H. C., Lee, K., and Choi, W. (2006). Contribution of phytoplankton and bacterial cells to the measured alkalinity of seawater. *Limnology and Oceanography*, 51(1 D):331–338.
- Ko, Y. H., Lee, K., Eom, K. H., and Han, I. S. (2016). Organic alkalinity produced by phytoplankton and its effect on the computation of ocean carbon parameters. *Limnology and Oceanography*, 61(4):1462–1471.
- Koeve, W. and Oschlies, A. (2012). Potential impact of DOM accumulation on  $f_{CO_2}$  and carbonate ion computations in ocean acidification experiments. *Biogeosciences*, 9(10):3787–3798.
- Kuliński, K., Schneider, B., Hammer, K., Machulik, U., and Schulz-Bull, D. (2014). The influence of dissolved organic matter on the acid-base system of the Baltic Sea. *Journal of Marine Systems*, 132:106–115.
- Leis, J. M. (2018). Paradigm lost: Ocean acidification will overturn the concept of larval-fish biophysical dispersal. *Frontiers in Marine Science*, 5(FEB):1–9.
- Lewis, E. R. and Wallace, D. W. R. (1998). Program Developed for CO<sub>2</sub> System Calculations.
- Lueker, T. J., Dickson, A. G., and Keeling, C. D. (2000). Ocean pCO<sub>2</sub> calculated from dissolved inorganic carbon, alkalinity, and equations for K<sub>1</sub> and K<sub>2</sub>: Validation based on laboratory measurements of CO<sub>2</sub> in gas and seawater at equilibrium. *Marine Chemistry*, 70(1-3):105–119.



- Marion, G. M., Millero, F. J., Camões, M. F., Spitzer, P., Feistel, R., and Chen, C. T. (2011). PH of seawater. *Marine Chemistry*, 126(1-4):89–96.
- Masini, J. C., Abate, G., Lima, E. C., Hahn, L. C., Nakamura, M. S., Lichtig, J., and Nagatomy, H. R. (1998). Comparison of methodologies for determination of carboxylic and phenolic groups in humic acids. *Analytica Chimica Acta*, 364(1-3):223–233.
- McGrath, T., McGovern, E., Gregory, C., and Cave, R. R. (2019). Local drivers of the seasonal carbonate cycle across four contrasting coastal systems. *Regional Studies in Marine Science*, 30:100733.
- McNeil, B. I. and Sasse, T. P. (2016). Future ocean hypercapnia driven by anthropogenic amplification of the natural CO<sub>2</sub> cycle. *Nature*, 529(7586):383–386.
- Metrohm (2021). Ion-selective electrodes (ISE) Manual.
- Millero, F. J. (2010). Carbonate constants for estuarine waters. *Marine and Freshwater Research*, 61:139–142.
- Millero, F. J., Pierrot, D., Lee, K., Wanninkhof, R., Feely, R., Sabine, C. L., Key, R. M., and Takahashi, T. (2002). Dissociation constants for carbonic acid determined from field measurements. *Deep-Sea Research Part I: Oceanographic Research Papers*, 49(10):1705–1723.
- Mintrop, L. (2016). *VINDTA Manual for Versions 3S and 3C*. 3.5 edition.
- Muller, F. L. and Bleie, B. (2008). Estimating the organic acid contribution to coastal seawater alkalinity by potentiometric titrations in a closed cell. *Analytica Chimica Acta*, 619(2):183–191.
- Newton, J., Feely, R. A., Jewett, E., Williamson, P., and Mathis, J. (2014). *Global Ocean Acidification Observing Network: requirements and governance Plan*. Number October.

- O'Higgins, T. G. and Wilson, J. G. (2005). Impact of the river Liffey discharge on nutrient and chlorophyll concentrations in the Liffey estuary and Dublin Bay (Irish Sea). *Estuarine, Coastal and Shelf Science*, 64(2-3):323–334.
- Okamura, K., Kimoto, H., Hatta, M., Noguchi, T., Nakaoka, A., Suzue, T., and Kimoto, T. (2014). Potentiometric open-cell titration for seawater alkalinity considering temperature dependence of titrant density and Nernst response of pH electrode. *Geochemical Journal*, 48(2):153–163.
- Orr, J. C., Fabry, V. J., Aumont, O., Bopp, L., Doney, S. C., Feely, R. A., Gnanadesikan, A., Gruber, N., Ishida, A., Joos, F., Key, R. M., Lindsay, K., Maier-Reimer, E., Matear, R., Monfray, P., Mouchet, A., Najjar, R. G., Plattner, G. K., Rodgers, K. B., Sabine, C. L., Sarmiento, J. L., Schlitzer, R., Slater, R. D., Totterdell, I. J., Weirig, M. F., Yamanaka, Y., and Yool, A. (2005). Anthropogenic ocean acidification over the twenty-first century and its impact on calcifying organisms. *Nature*, 437(7059):681–686.
- Patsavas, M. C., Byrne, R. H., Wanninkhof, R., Feely, R. A., and Cai, W. J. (2015). Internal consistency of marine carbonate system measurements and assessments of aragonite saturation state: Insights from two U.S. coastal cruises. *Marine Chemistry*, 176:9–20.
- Paxéus, N. and Wedborg, M. (1985). Acid-base properties of aquatic fulvic acid. *Analytica Chimica Acta*, 169(C):87–98.
- Perdue, E. M., Reuter, J. H., and Parrish, R. S. (1984). A statistical model of proton binding by humus. *Geochimica et Cosmochimica Acta*, 48(6):1257–1263.
- Prieto, F. J. M. and Millero, F. J. (2002). The values of  $pK_1 + pK_2$  for the dissociation of carbonic acid in seawater. *Geochimica et Cosmochimica Acta*, 66(14):2529–2540.
- Raymond, P. A. and Cole, J. J. (2003). Increase in the export of alkalinity from North America's largest river. *Science*, 301(5629):88–91.

- Riebesell, U., Fabry, V. J., and Hansson, L. (2010). *Guide to best practices for ocean acidification research and data reporting*.
- Riebesell, U. and Gattuso, J. P. (2015). Lessons learned from ocean acidification research. *Nature Climate Change*, 5(1):12–14.
- Rigobello-Masini, M. and Masini, J. C. (2001). Application of modified Gran functions and derivative methods to potentiometric acid titration studies of the distribution of inorganic carbon species in cultivation medium of marine microalgae. *Analytica Chimica Acta*, 448(1-2):239–250.
- Ritchie, J. D. and Perdue, E. (2003). Proton-binding study of standard and reference fulvic acids, humic acids, and natural organic matter. *Geochimica et Cosmochimica Acta*, 67(1):85–96.
- Sabine, C. L., Feely, R. A., Gruber, N., Key, R. M., Lee, K., Bullister, J. L., Wanninkhof, R., Wong, C., Wallace, D., Tilbrook, B., Millero, F. J., Peng, T.-H., Kozyer, A., Ono, T., and Rios, A. F. (2004). The Oceanic Sink for Anthropogenic CO<sub>2</sub>. *Science*, 305(July):5–12.
- Sharp, J. D. and Byrne, R. H. (2020). Interpreting measurements of total alkalinity in marine and estuarine waters in the presence of proton-binding organic matter. *Deep-Sea Research Part I*.
- Sharp, J. D. and Byrne, R. H. (2021). Technical note: Excess alkalinity in carbonate system reference materials. *Marine Chemistry*, 233:103965.
- Smith, R. M. and Martell, A. E. (1983). Critical Stability Constants Volume 6: Second Supplement. *Biochemical Education*, 11(2):77.
- Song, S., Wang, Z. A., Gonnee, M. E., Kroeger, K. D., Chu, S. N., Li, D., and Liang, H. (2020). An important biogeochemical link between organic and inorganic carbon cycling: Effects of organic alkalinity on carbonate chemistry in coastal waters influenced by intertidal salt marshes. *Geochimica et Cosmochimica Acta*, 275:123–139.

- Tipping, E., Lofts, S., and Sonke, J. E. (2011). Humic Ion-Binding Model VII: A revised parameterisation of cation-binding by humic substances. *Environmental Chemistry*, 8(3):225–235.
- Tishchenko, P. Y., Wallmann, K., Vasilevskaya, N. A., Volkova, T. I., Zvalinskii, V. I., Khodorenko, N. D., and Shkirnikova, E. M. (2006). The contribution of organic matter to the alkaline reserve of natural waters. *Oceanology*, 46(2):192–199.
- Ulfso, A., Kuliński, K., Anderson, L. G., and Turner, D. R. (2015). Modelling organic alkalinity in the Baltic Sea using a Humic-Pitzer approach. *Marine Chemistry*, 168:18–26.
- Venel, F., Nagashima, H., Rankin, A. G., Anquetil, C., Klimavicius, V., Gutmann, T., Buntkowsky, G., Derenne, S., Lafon, O., Huguet, A., and Pourpoint, F. (2021). Characterization of Functional Groups in Estuarine Dissolved Organic Matter by DNP-enhanced  $^{15}\text{N}$  and  $^{13}\text{C}$  Solid-State NMR. *ChemPhysChem*, 22(18):1907–1913.
- Wigley, T. M. (1983). The pre-industrial carbon dioxide level. *Climatic Change*, 5(4):315–320.
- Wolf-Gladrow, D. A., Zeebe, R. E., Klaas, C., Körtzinger, A., and Dickson, A. G. (2007). Total alkalinity: The explicit conservative expression and its application to biogeochemical processes. *Marine Chemistry*, 106(1-2 SPEC. ISS.):287–300.
- Woosley, R. J. (2021). Evaluation of the temperature dependence of dissociation constants for the marine carbon system using pH and certified reference materials. *Marine Chemistry*, 229:103914.
- Yang, B., Byrne, R. H., and Lindemuth, M. (2015). Contributions of organic alkalinity to total alkalinity in coastal waters: A spectrophotometric approach. *Marine Chemistry*, 176:199–207.
- Zeebe, R. E. (2012). History of Seawater Carbonate Chemistry, Atmospheric  $\text{CO}_2$ , and Ocean Acidification. *Annual Review of Earth and Planetary Sciences*, 40(1):141–165.

**Table 4.1:** Compiled TA and total concentrations of OrgAlk charge groups with associated associated apparent pK value returned by *OrgAlkCalc* for Dublin Bay transitional water samples. Error on give parameters is taken as the standard deviation of replicate measurements (n=3)

Sampling Date	Site	Salinity	Temperature (°C)	pH	TA ( $\mu\text{mol}\cdot\text{kg}^{-1}$ )	X <sub>1</sub> ( $\mu\text{mol}\cdot\text{kg}^{-1}$ )	pK <sub>1</sub>	X <sub>2</sub> ( $\mu\text{mol}\cdot\text{kg}^{-1}$ )	pK <sub>2</sub>	RMS
20/07/2021	Conv	23.67	15.10	7.85	3659.96±7.27	106.35±42.66	4.4±0.045			$(7.45\pm 4.32)\times 10^{-4}$
	PBYC	24.22	15.07	7.85	2888.32±6.62	114.24±0.89	4.53±0.013			$(5.13\pm 1.03)\times 10^{-4}$
	E7	33.97	15.33	7.86	2469.11±10.49	129.21±15.09	4.6±0.008			$(6.52\pm 1.12)\times 10^{-4}$
	LE5	34.71	15.22	7.85	2449.63±4.21	148.29±9.08	4.54±0.005			$(7.44\pm 1.06)\times 10^{-4}$
	NB6	36.88	16.48	7.97	2333.97±18.24	171.8±7.36	4.58±0.017			$(10.06\pm 0.81)\times 10^{-4}$
06/08/2021	Diageo	2.96	17.02	7.85	3505.57±12.45	88.02±16.86	4.36±0.053			$(3.27\pm 1.84)\times 10^{-4}$
	O'Connell	16.54	17.00	7.90	3185.03±4.21	151.15±14.32	4.49±0.059			$(10.98\pm 3.06)\times 10^{-4}$
	Post Ringsend	28.17	19.23	7.50	2555.57±7.84	163.62±10.88	4.57±0.042			$(9.17\pm 2.03)\times 10^{-4}$
	NB3	30.07	14.31	8.21	2321.64±4.54	160.69±9.59	4.6±0.028			$(9.85\pm 0.62)\times 10^{-4}$
	PBYC	31.51	17.54	7.87	2636.53±3.92	172.21±10.83	4.56±0.023			$(13.26\pm 0.56)\times 10^{-4}$
	Conv	32.39	17.47	7.86	2526.71±1.76	187.91±24.57	4.52±0.043			$(10.35\pm 1.25)\times 10^{-4}$
	Pre Ringsend	33.49	18.58	7.91	2456.23±5.07	186.45±10.84	4.54±0.038			$(11.09\pm 1.06)\times 10^{-4}$
	EE1	33.74	17.93	7.87	2439.66±2.92	161.3±9.84	4.49±0.019			$(8.5\pm 1.5)\times 10^{-4}$
	TE1	35.76	17.23	7.94	2368.68±2.49	160.76±7.7	4.52±0.031			$(8.72\pm 0.57)\times 10^{-4}$
	NB9	36.79	16.63	7.98	2329.54±1.2	184.11±4.59	4.53±0.007			$(12.44\pm 0.48)\times 10^{-4}$
	SB7	36.86	16.86	7.98	2318.05±1.45	159.3±11.23	4.5±0.017			$(10.02\pm 1.14)\times 10^{-4}$
	SB5	36.87	16.84	7.97	2319.02±2.56	166.67±10.97	4.55±0.039			$(11.18\pm 1.01)\times 10^{-4}$
	NB3	36.96	15.02	7.86	2366.51±3.69	129.08±3.55	4.55±0.012			$(8.12\pm 0.26)\times 10^{-4}$
	SB1	36.99	16.36	7.97	2317.06±3.69	155.21±3.44	4.52±0.004			$(9.47\pm 0.82)\times 10^{-4}$
	SB3	37.00	16.39	7.97	2332.31±21.89	209.29±28.7	4.56±0.049			$(11.21\pm 1.47)\times 10^{-4}$
SB4	37.03	16.42	7.96	2324.91±5.25	184.32±9.15	4.54±0.075			$(11.01\pm 2.91)\times 10^{-4}$	
05/10/2021	Diageo	9.96	13.04	7.91	3098.02±3.28	156.79±32.28	4.49±0.118	46.37*	7.74*	$(5.88\pm 0.86)\times 10^{-4}$
	TE3	29.68	14.49	8.19	2323.34±2.65	191.32±0.71	4.54±0.017			$(7.62\pm 1.13)\times 10^{-4}$
	SB2	30.15	14.98	8.19	2262.84±3.76	180.17±21.48	4.65±0.092			$(8.26\pm 1.06)\times 10^{-4}$
04/11/2021	Diageo	0.83	7.26	8.41	3476.48±9.9	100.15±28.57	4.29±0.136	155.55±5.137	6.53±0.07	$(2.73\pm 2.28)\times 10^{-4}$
	LE1	25.90	13.10	8.67	2380.23±7.59	224.74±10.68	4.44±0.023	196.43±19.846	6.87±0.143	$(9.21\pm 0.76)\times 10^{-4}$
	NB3	25.99	13.62	8.57	2330.19±3.62	204.78±18.69	4.5±0.056	187.72±22.099	7.34±0.245	$(12\pm 1.92)\times 10^{-4}$
	NB7	32.11	13.69	8.41	2301.92±17.19	225.84±11.08	4.45±0.029	201.31±13.825	7.18±0.374	$(11.24\pm 1.63)\times 10^{-4}$
27/01/2022	SB3	32.52	13.58	8.23	2316.63±1.65	234.3±14.11	4.52±0.051	187.17±11.239	7.3±0.384	$(13.87\pm 0.45)\times 10^{-4}$
	LE1	27.54	10.46	7.93	2506±2.31	56.02±4.71	4.68±0.011	89.92±3.471	6.98±0.263	$(0.11\pm 0.03)\times 10^{-4}$
	NB7	29.24	9.63	8.05	2373.13±3.27	59.8±4.78	4.81±0.048	124.71±6.326	6.6±0.018	$(0.11\pm 0.01)\times 10^{-4}$
10/03/2022	Conv	16.54	17.20	7.80	4675.52±12.56					
	NB2	28.64	11.96	7.97	2397.82±14.85	91.66±41.06	4.68±0.154	136.5±17.898	6.6±0.104	$(1.25\pm 1.52)\times 10^{-4}$
	NB5	29.29	12.81	7.97	2391.04±1.41	65.11±6.89	4.64±0.105	145.07±17.34	6.44±0.062	$(0.16\pm 0.01)\times 10^{-4}$

\* No reported uncertainty as n=1

**Table 4.2:** Literature reported OrgAlk pKa values.

Study	Sample matrix	Sample source	OrgAlk ( $\mu\text{mol.kg}^{-1}$ )	pK values	Source
This study	Coastal seawater	Dublin Bay, Ireland	46 - 234	4.54 $\pm$ 0.09, 6.96 $\pm$ 0.40	Humic substances
Cai et al. (1998)	Coastal seawater	Georgia estuaries, USA	80 - 105	4.46, 6.64, 8.94	Organic acids
Ko et al. (2016)	Phytoplankton culture	N/A	15 - 40	4.9 $\pm$ 0.1, 6.9 $\pm$ 0.1	Phytoplankton DOM
	Coastal seawater	Southern Korean Coast	1 - 15	4.4 $\pm$ 0.2, 6.1 $\pm$ 0.2	Phytoplankton DOM
Song et al. (2020)	Coastal seawater, groundwater	Southeastern Massachusetts, USA	20 - 80	4.1 - 5.5, 7.4 - 8.4	DOM carboxyl and phenolic functional groups
Muller and Bleie (2008)	Fjord water culture	Sotra Island, Norway	2 - 22	4.0 $\pm$ 0.2, 9.1 $\pm$ 0.2	Phytoplankton DOM
Yang et al. (2015)	Coastal seawater	Coastal Gulf of Mexico	0 - 40	5.31 - 5.45, 7.05 - 7.32	Fulvic acids
De Souza Sierra et al. (2001) <sup>a</sup>	Mangrove Sediments	Santa Catarina Island, Brazil	N/A	5.69 $\pm$ 0.15, 9.62 $\pm$ 0.24	Fulvic Acids
				5.90 $\pm$ 0.09, 9.41 $\pm$ 0.11	Humic Acids
Kuliński et al. (2014) <sup>b</sup>	Coastal seawater	Baltic Sea	22 - 58	7.53	Dissolved organic material

<sup>a</sup>Mean reported pK values. <sup>b</sup>Bulk pK value

## **Chapter 5**

# **Organic Alkalinity Dynamics in Irish Coastal Waters**

## Abstract

Total alkalinity (TA) is a popularly measured carbonate system parameter and is widely used in calculations of key carbonate system descriptors such as the calcium carbonate saturation state, an important indicator of ocean acidification. Organic alkalinity (OrgAlk) is recognised as a considerable contributor to TA in coastal waters, with this having implications on the use of TA to calculate key carbonate chemistry descriptors. As titratable charge groups of OrgAlk can act as unknown acid-base species, the inclusion of the total concentration and apparent dissociation constants of OrgAlk in carbonate calculations involving TA is required to minimise uncertainty in computed speciation. Here we present an investigation of the prevalence and properties of OrgAlk, as well as the impact of OrgAlk on carbonate chemistry calculations in a transitional waterbody. Water samples were collected during low and high tide over a 5 week period in Rogerstown Estuary, Dublin Ireland. TA and OrgAlk were measured using modified Global Ocean Acidification Observing Network (GOA-ON) titration apparatus in conjunction with *OrgAlkCalc*, an open-source Python based computational programme. pH was measured on the total scale spectrophotometrically using meta-cresol purple (mCp) as the indicator dye. Dissolved inorganic carbon (DIC), the partial pressure of CO<sub>2</sub> (pCO<sub>2</sub>), in situ pH on the total scale (pH<sub>T</sub>) and the saturation state of aragonite ( $\Delta\Omega_A$ ) were calculated using pH and both OrgAlk adjusted TA and non-OrgAlk adjusted TA as the input parameters. Optical analysis of DOM was conducted to complement OrgAlk characterisations and to further elucidate OrgAlk sources and dynamics. OrgAlk charge groups concentrations ranged from 35 - 198  $\mu\text{mol}\cdot\text{kg}^{-1}$ , with the highest concentrations observed in more marine waters. Two apparent charge groups were associated with OrgAlk, with pK values of  $4.38\pm 0.27$  and  $6.95\pm 0.43$ . Differences between calculated carbonate system parameters when using OrgAlk adjusted TA and non-OrgAlk adjusted TA ranged from 88–254  $\mu\text{mol}\cdot\text{kg}^{-1}$  DIC, -98–67  $\mu\text{atm}$  pCO<sub>2</sub>, -0.02–0.12 pH<sub>T</sub> and 0.02–0.64  $\Delta\Omega_A$ . Variability in the differences in calculated carbonate systems was largely a factor of OrgAlk charge group concentration and pK. This work highlights the importance of considering OrgAlk if using TA as an input parameter in carbonate system investigations of coastal waters.



## 5.1 Introduction

Carbonate system calculations involving TA requires accurate information on the total concentrations and dissociation constants of all seawater acid-base species if calculated parameters are to be free of inherent uncertainty. TA measurements made without information of the acid-base properties of organic contributors may not be fully interpretable (Riebesell et al., 2010), and can lead to uncertainties in calculated carbonate system speciation. As the prevalence and impact of OrgAlk in the coastal ocean becomes more recognised (Fong and Dickson, 2019; Kerr et al., 2021), methods to identify the potential sources and dynamics of OrgAlk are of growing importance. Failure to account for OrgAlk when using TA in carbonate chemistry calculations is recognised as a potential source of uncertainty in calculated carbonate system parameters (Hu, 2020; Koeve and Oschlies, 2012; Kuliński et al., 2014; Yang et al., 2015; Hunt et al., 2011). By performing complementary OrgAlk titrations alongside conventional open-cell TA titrations, estimations of OrgAlk charge group concentrations and associated acid-base properties can be obtained. This then allows for the minimisation of uncertainty propagation to calculated carbonate system parameters and key descriptors of carbonate chemistry through the incorporation of OrgAlk species in calculations involving TA. This approach of directly incorporating OrgAlk as a distinct and significant component of TA is contemporary in the field of coastal carbonate system investigations (Song et al., 2020; Sharp and Byrne, 2020) and has been incorporated into state of the art carbonate chemistry calculation software, such as *PyCO2SYS* (Humphreys et al., 2020).

Direct assessments of OrgAlk provides information vital to the minimisation of errors on calculated parameters by returning estimates of the concentrations and acid-base properties of charge groups associated with OrgAlk. The apparent pK values of these charge groups give an indication of the general molecular classes to which they belong, such as carboxyl or phenolic. As the aforementioned functional groups are

near ubiquitous in coastal seawater dissolved organic matter (DOM) (Cortés-Francisco and Caixach, 2015; Catalá et al., 2020), additional descriptive analysis of coastal DOM in conjunction with OrgAlk analysis may allow for greater insights into OrgAlk and for the characterisation of its potential genesis and dynamics. Furthermore, numerous investigations have observed a clear association between OrgAlk and DOM in the coastal ocean (Song et al., 2020; Kuliński et al., 2014; Lukawska-Matuszewska et al., 2018; Sharp and Byrne, 2020), reinforcing the linkage between the two and the potential benefits of complementary DOM characterisation.

Descriptive analysis of coastal DOM involves the measurement of chromophoric dissolved organic matter (CDOM) and fluorescent dissolved organic matter (FDOM), two intrinsically linked parameters. CDOM refers to the fraction of DOM that interacts with solar radiation, whereas FDOM refers to the fraction of CDOM that exhibits fluorescence upon excitation at specific wavelengths (Nelson and Siegel, 2013). Each can be measured with relative ease and provides insights into the optical properties of DOM. The optical properties of DOM are routinely used as indicators of DOM source and inherent molecular composition across a wide range of environments (Coble, 2007; Fellman et al., 2010; Stedmon and Nelson, 2015). Interpretation of the absorbance and fluorescence spectra of filtered coastal seawater samples typically involves the utilisation of indices that link the optical properties of DOM to specific identifiers of DOM source or molecular signature (Gabor et al., 2014; Lee et al., 2018).

In this study, we aimed to assess the impacts of OrgAlk on carbonate chemistry calculations, as well as utilise optical analysis of DOM to provide a greater understanding of the potential sources and dynamics of the DOM associated with OrgAlk in transitional waters. This was achieved through the use of modified Global Ocean Acidification Observing Network (GOA-ON) TA titration apparatus coupled with *OrgAlkCalc*, an open source Python based computational programme, to provide data on TA concentrations as well as estimations of the quantity and acid-base properties of charge groups associated with OrgAlk. The aforementioned was conducted alongside spec-

trophotometric pH analysis in order to calculate dissolved inorganic carbon (DIC), the partial pressure of CO<sub>2</sub> pCO<sub>2</sub> and key carbonate chemistry descriptors. The impact of OrgAlk on calculated carbonate system parameters was assessed by using both OrgAlk adjusted and non-OrgAlk adjusted TA as an input parameter alongside pH in carbonate chemistry calculations. Complementary optical analysis was conducted through the analysis of UV-Vis and fluorescence spectra of OrgAlk samples.

## 5.2 Materials and methods

### 5.2.1 Study location

Rogerstown Estuary is an enclosed transitional waterbody covering an area of 3.5 km<sup>2</sup>, with a catchment area of approximately 45 km<sup>2</sup>. The catchment area can largely be classified as rural and agricultural in nature, being termed as the "market garden" of Dublin City. The estuary is classed as a Special Area of Conservation (SAC), with much of it listed as a nature reserve. The estuary was previously known for substantial anthropogenic inputs in the form of fertiliser runoff (Fahy et al., 1975), with the Irish Environmental Protection Agency Trophic Status Assessment Scheme (TSAS) classifying the estuary as intermediate in regard to eutrophication susceptibility (O'Boyle et al., 2013).

The estuary is divided into distinct western and eastern sections by the Dublin-Belfast railway line, constructed in the 1840's. Each section undergoes complete inundation during high tide, with the western section continuing to drain a mixture of riverine and tidally introduced marine waters for 3.5 hours after low tide (Fahy et al., 1975). The most notable fluvial inputs enter the estuary via the western section, namely the Ballyboghil and Ballough Rivers. The eastern section also receives smaller freshwater inputs from a number of unnamed drainage channel as well as from the Palmerstown River and Horestown Stream. The catchment areas of the aforementioned freshwater sources are characterised by intense agricultural activity (Central and Regional Fish-

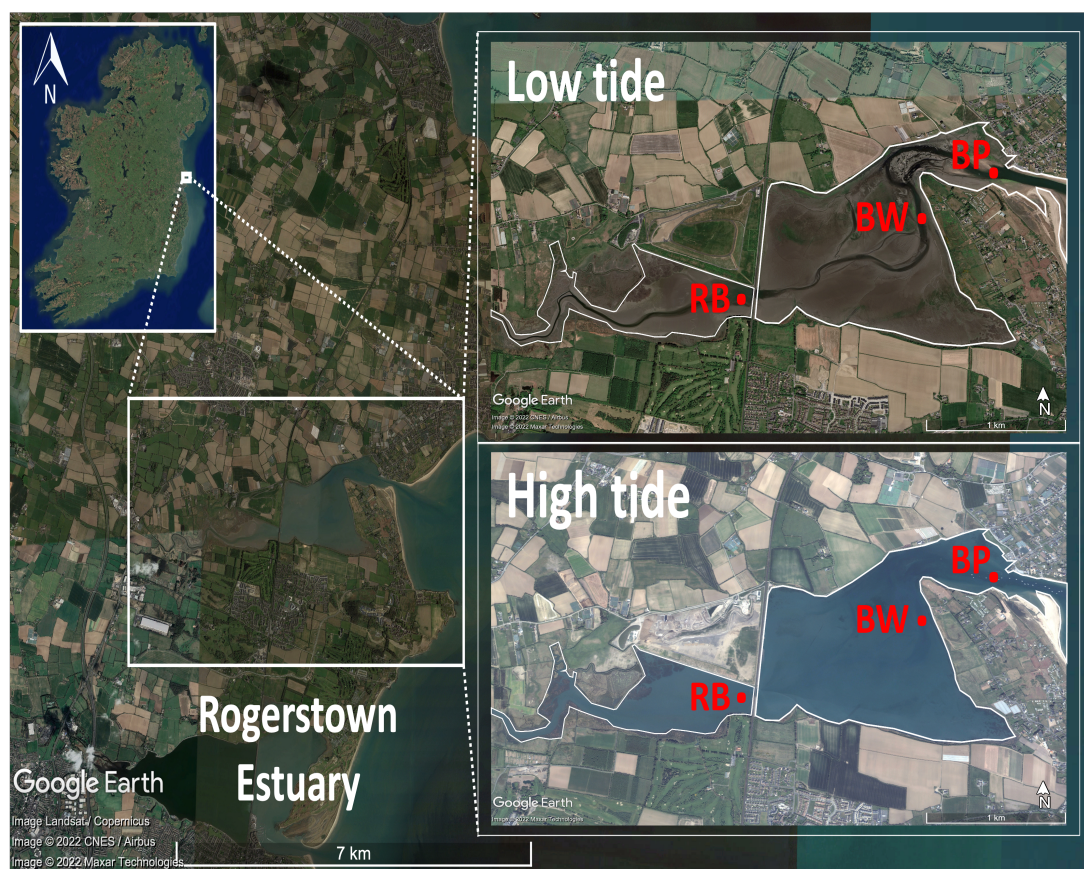


**Figure 5.1:** The location of the study area in North County Dublin, Ireland. Water samples were collected from 3 locations within Rogerstown Estuary over a 5 week period: Burrow pier (BP), bird watching area (BW) and rail bridge (RB). Samples were collected from each location during consecutive high and low tides.

eries Board, 2008). Furthermore, the majority of catchment areas of Rogerstown Estuary is limestone in nature (Fay et al., 2007), suggesting relatively high fluvial TA concentrations.

Surface transitional water samples were collected once a week over a 5 week period from 12/04/22 to 10/05/22. For each sampling event, samples were collected during both high tide (HT) and low tide (LT). This was performed in order to identify possible trends between terrestrially influenced LT and more marine influenced HT conditions. For a subset of 3 of the 5 sampling events, samples for fluorescence and UV-Vis optical analysis of DOM were collected. In-situ salinity, temperature, pH and dissolved oxygen (DO) data for each sample was collected using a calibrated Hanna HI98194 multiparameter probe.

### 5.2.2 Carbonate system analysis

Samples for TA and OrgAlk analysis were collected in acid-washed 250 mL HDPE bottles and stored on ice until being vacuum filtered using furnaceed GF/F glass fibre filters. TA and OrgAlk samples were then poisoned with a saturated mercuric chloride solution before being refrigerated until analysis. TA analysis was carried out using an open-cell, potentiometric titration procedure as outlined in SOP 3b of Dickson et al. (2007) using modified GOA-ON TA titration apparatus, detailed in 2.2. The 0.1 M HCl titrant used was standardised using CRMs provided by Dr. A. Dickson, Scripps Institute of Oceanography, USA. OrgAlk was measured using the apparatus and methodology detailed in section 2.3. The 0.1 M NaOH titrant used was standardised using NIST traceable, oven dried potassium hydrogen phthalate Standard Reference Material (Certipur). All titrations were carried out at  $25\text{ }^{\circ}\text{C} \pm 0.01$  and within 1 week of sample collection. Generated TA and OrgAlk titration data was processed using *OrgAlkCalc*, as outlined in section 2.4.

Samples for pH analysis were collected in clean 50 mL borosilicate glass serum bottles. Samples were collected using a short length of flexible Tygon tubing as per the methodology detailed by Sabine (2020) and closed using a rubber septa and crimp, negating ambient CO<sub>2</sub> exchange. Samples for pH analysis were stored in lightproof insulated bags as to minimise temperature changes. Once back in the laboratory, samples were allowed to come to 25 °C in a water bath. Filtration was conducted prior to analysis as outlined in section 2.7.2.

pH analysis was performed using a Shimadzu UV 2600 scanning UV-Vis spectrophotometer with a TCC-100 thermoelectrically temperature controlled cell holder installed, with 3 mM mCp as the indicator dye. Spectrophotometric pH analysis preceded as detailed in section 2.7.2, with TRIS buffer provided by Dr. A. Dickson, Scripps Institute of Oceanography, USA, used during each analysis event to validate the methodology. Multiple sequential dye additions were performed in order to determine dye addition associated sample pH perturbation effects. As can be seen from table 5.1b,

there was no statistically significant difference (confidence interval 95%) between the experimentally derived pH values of TRIS buffer ( $\text{pH}_{\text{mCp}}$ ) using the previously detailed apparatus and methodology and pH values of TRIS calculated using the equation of DelValls and Dickson (1998) ( $\text{pH}_{\text{TRIS}}$ ). The asterisked value in table 5.1a was omitted from statistical analysis. The significantly higher difference observed can be directly related to the TRIS buffer used on 19/04/2022. In this instance, the TRIS buffer used had been previously opened on 12/04/2022. It is believed that as the TRIS buffer used was not opened directly on the day of analysis, this may have played a role in the marked increase in observed  $\text{pH}_{\text{mCp}} - \text{pH}_{\text{TRIS}}$  difference. In all other instances, freshly opened bottles of TRIS were used.

**Table 5.1:** (a) Comparisons of  $\text{pH}_T$  values of TRIS buffer found using mCp ( $\text{pH}_{\text{mCp}}$ ) indicator dye and calculated using the formula of DelValls and Dickson (1998) ( $\text{pH}_{\text{TRIS}}$ ). (b) Two-sample equal variance t-test to compare mean  $\text{pH}_{\text{mCp}}$  and  $\text{pH}_{\text{TRIS}}$  values.

(a)								(b)			
Date	TRIS ID	T(K)	$\text{pH}_{\text{mCp}}$	$\text{pH}_{\text{TRIS}}$	Difference	Mean	St.dev		$\text{pH}_{\text{mCp}}$	$\text{pH}_{\text{TRIS}}$	
12/04/2022	T38 - 0164	298.06	8.0901	8.0963	0.0062	0.0050	0.0008	Mean	8.073	8.078	
19/04/2022	T38 - 0164	297.89	8.0176	8.1016	0.0839*			Variance	0.00023	0.00022	
26/04/2022	T38 - 0165	299.13	8.0581	8.0630	0.0049			Observations	3	3	
04/05/2022	T38 - 0151	298.62	8.0740	8.0788	0.0048			Pooled Variance	0.00023		
10/05/2022	bottle ID	298.17	8.0889	8.0929	0.0039			Hypothesized Mean Difference	0		
*Data omitted in calculation of mean and standard deviation.								df	4		
								t Stat	-0.37		
								P(T<=t) one-tail	0.36		
								t Critical one-tail	2.13		
								P(T<=t) two-tail	0.72		
								t Critical two-tail	2.77		

Carbonate chemistry calculations were performed using *PyCO2SYS* (Humphreys et al., 2020) with processed TA and  $\text{pH}_T$  values as the input pair used to calculate DIC,  $\text{pCO}_2$ , *in-situ*  $\text{pH}_T$  and the saturation state with respect to aragonite ( $\Omega_A$ ). It is important to note that in lower ionic strength coastal waters  $\text{Ca}^{2+}$  concentrations may deviate from the value calculated by *PyCO2SYS*, in which  $\text{Ca}^{2+}$  concentration is assumed to scale proportionally with salinity and be zero in freshwater (Lewis and Wallace, 1998;

Zeebe and Wolf-Gladrow, 2003). Elevated  $\text{Ca}^{2+}$  concentrations have been observed in coastal systems where the bedrock morphology of the associated riverine catchment area is carbonate-rich (McGrath et al., 2019), with this impacting calculated  $\Omega_A$  (see equation 12). As no  $\text{Ca}^{2+}$  data was available for Rogerstown waters, reported  $\Omega_A$  data comes with the caveat that it does not explicitly account for the potential impact of elevated  $\text{Ca}^{2+}$  concentrations. However, as a main objective of this research was to investigate the implications of using non-OrgAlk adjusted TA as an input parameter in carbonate chemistry calculations, the omission of potential  $\text{Ca}^{2+}$  related impacts on  $\Omega_A$  still allows for the computation of discrepancies in  $\Omega_A$  when calculated with and without OrgAlk considerations. In all calculations, the following carbonate system and ancillary thermodynamic equilibrium constants were used:  $K_{C1}$  and  $K_{C2}$  of Lueker et al. (2000),  $K_F$  of Perez and Fraga (1987),  $K_S$  of Dickson (1990) and  $B_T$  of Lee et al. (2010).

A recent feature added to *PyCO2SYS* enables the incorporation of additional alkalinity components, as per the model of Sharp and Byrne (2020). This allows for the inclusion of the respective concentrations and associated pK values of OrgAlk charge groups into carbonate chemistry calculations where TA is a primary input parameter. TA is conventionally defined as the excess of proton acceptors over proton donors, where proton acceptors are bases formed from weak acids with dissociation constants ( $K_a$ )  $\leq 10^{-4.5}$  and proton donors acids with  $K_a \geq 10^{-4.5}$  at zero ionic strength and at 25°C (Dickson, 1981). Contributions of an OrgAlk charge group ( $X_i$ ) to TA can therefore be calculated by designating the species as either a proton acceptor or proton donor using this definition. If the total concentration of charge group  $X_i$  ( $T_{X_i}$ ) can be described by:

$$T_{X_i} = [HX_i] + [X_i^-] \quad (5.1)$$

and its dissociation constant ( $K_{X_i}$ ) by:

$$K_{X_i} = [X_i^-][H^+]/[HX_i] \quad (5.2)$$

then the sign and magnitude of its alkalinity contribution ( $A_{X_i}$ ) is dependant on  $K_{X_i}$  (Wolf-Gladrow et al., 2007) and can be found by:

$$A_{X_i} = \begin{cases} -[HX_i] & \text{if } -\log(K_a) \leq 4.5 \\ +[X_i^-] & \text{if } -\log(K_a) > 4.5 \end{cases} \quad (5.3)$$

Inclusion of the  $[HX_i]$  and  $[X_i^-]$  terms resulted in a value for OrgAlk adjusted TA that was subsequently used in carbonate system calculations. Reported OrgAlk concentrations are taken as the sum of the individual charge group concentration at in situ conditions as calculated through *PyCO2SYS*, with respect to associated pK values and subsequent status as either proton donor or acceptors as per equation 5.3. The concentrations of OrgAlk charge groups and associated pK values observed in this study can be found in table 5.4.

In order to assess the impact of OrgAlk, the differences between carbonate system parameters and key descriptors of carbonate chemistry calculated using OrgAlk adjusted TA and non-OrgAlk adjusted TA were calculated. Using the aforementioned, the differences in DIC ( $\Delta$ DIC),  $p\text{CO}_2$  ( $\Delta p\text{CO}_2$ ), *in-situ*  $\text{pH}_T$  ( $\Delta \text{pH}_T$ ), and saturation state of seawater with respect to aragonite ( $\Delta\Omega_A$ ) were calculated. It should be noted that  $\text{pH}_T$  was a directly calculated input parameter, and the values of  $\Delta \text{pH}_T$  discussed relate to in situ  $\text{pH}_T$  calculated using  $\text{pH}_T$  measured at 25 °C and either OrgAlk adjusted TA or non-OrgAlk adjusted TA.

Uncertainties in calculated carbonate system parameters were found using the methods detailed in Orr et al. (2018) and the related version of *CO2SYS*. Uncertainties in TA were taken as the standard deviation of repeat measurements (n=3). The uncertainty in pH measurement was taken as 0.005 pH units, the mean uncertainty based on multiple (n=4) TRIS buffer validation exercises, see table 5.1a. As well as estimating for uncertainties inherent to input parameters in carbonate chemistry calculations, literature reported uncertainties on the thermodynamic equilibrium constants used were



also accounted for (Orr et al., 2018). Uncertainties in salinity and temperature were assigned as per manufacturer specifications, being 0.02% and 0.15 °C, respectively.

It is important to note that estimated charge group acid-base properties of OrgAlk are challenging to characterise using the rigorous definition of proton donors and acceptors of Dickson (1981). In waters where TA is mainly composed of carbonate alkalinity, with some contributions from other inorganic acid-base species, the choice of  $K_a = 4.5$  as a cut off between proton acceptors and donors is robust as it separates the relevant proton acceptors and donors by more than three orders of magnitude based on their  $K_a$  at zero ionic strength and at 25°C (Wolf-Gladrow et al., 2007). Given the highly heterogeneous nature of organic molecules in regard to their chemical composition (Repeta, 2015; Carlson and Hansell, 2015) and acid-base properties (Tipping and Hurley, 1992; Perdue et al., 1984; Altmann and Buffle, 1988) the charge group concentrations and apparent pK values of OrgAlk are likely heterogeneous. Furthermore, investigations of OrgAlk have identified charge groups with  $pK \approx 4.5$ , with these charge groups associated with carboxyl functional groups (Cai and Wang, 1998; Song et al., 2020; Ko et al., 2016). Additionally, compilations of literature reported pK values of acidic functional groups (Smith and Martell, 1983; Izatt and Christensen, 1976) summarised as frequency histograms by Perdue et al. (1984) indicate that the frequency of occurrence of carboxyl group pK displays approximately normal distribution with a mean value of  $\sim 4.5$ . This has direct implications on OrgAlk associated with carboxyl groups, as even if the acid-base properties of these charge groups are estimated, the unambiguous characterisation of their role as proton acceptors or donors remains challenging given inherent uncertainties in estimated pK values.

### 5.2.3 DOM analysis

Samples for DOM analysis were collected in furnaceed 100 mL amber glass vials with Teflon lined screw cap lids. Once acquired, DOM samples were stored on ice and in the dark until being filtered using a peristaltic pump and an inline filter holder with

0.45  $\mu\text{m}$  nylon membrane filters. All filtration apparatus was thoroughly rinsed with methanol, UP water and finally the sample solution itself prior to filtration. Once filtered, samples were stored in a freezer at  $-25\text{ }^{\circ}\text{C}$ . A more detailed account of DOM glassware pretreatment and the filtration procedure can be found in section 2.8.

Absorption spectra were recorded using a dual-beam Shimadzu UV 2600 scanning UV-Vis spectrophotometer with a 1 cm pathlength quartz cuvette. Spectra were recorded across the range 240 - 600 nm with an interval of 0.5 nm and scan speed set to slow. UP water was used as the blank. Absorption values ( $A$ ) were converted to Napierian absorption coefficients ( $a$ ) using:

$$a = 2.303 \cdot A \cdot l^{-1} \quad (5.4)$$

where  $l$  is the pathlength in meters.  $a$  values were then log transformed and linear regression performed on the wavelength intervals 275 - 295 nm and 350 - 400 nm to calculate the spectral slope of each,  $S_{275-295}$  and  $S_{350-400}$  respectively. These wavelength intervals were chosen as previously reported spectral slope variation for riverine, transitional and marine waters was greatest in these regions (Helms et al., 2008). Additionally, slope ratio ( $S_R$ ), an indicator of molecular weight (MW) and exposure to photochemical degradation (Helms et al., 2008; Guéguen and Cuss, 2011) was calculated as  $S_R = S_{275-295} : S_{350-400}$ . Further literature reported absorbance indices were also calculated:  $a_{350}$ , an indicator of DOM lignin phenol content (Benner and Kaiser, 2011; Hernes and Benner, 2003);  $a_{325}$ , an indicator of the presence of aromatic substances (Catalá et al., 2015; Nelson et al., 2004), and  $a_{254}$ , commonly used as a measure of relative concentration of CDOM (Li et al., 2021) that has also been related to DOC concentration (Catalá et al., 2018).

Fluorescence spectra were recorded using a LS-55 Perkin-Elmer Fluorescence Spectrometer and a 1 cm pathlength quartz fluorescence cuvette. Three dimensional excitation–emission fluorescence spectra were constructed using excitation wavelengths ( $\lambda_{Ex}$ ) 200 - 450 nm with 5 nm intervals. Emission wavelengths ( $\lambda_{Em}$ ) were scanned

**Table 5.2:** Optical indices used in this study to provide insights into DOM characteristics; (a) absorbance based indices and (b) fluorescence based indices.

(a)			(b)		
Index	Purpose	Reference	Index	Purpose	Reference
$S_R$	Indicative of DOM molecular weight and exposure to photochemical degradation	Helms et al. (2008), Guéguen and Cuss (2011)	BIX	Indicative of recent autochthonous contribution to DOM pool	Huguet et al. (2009), Parlanti et al. (2000)
$a_{350}$	Indicator of lignin phenol content of DOM	Benner and Kaiser (2011), Hernes and Benner (2003)	Peak B	Related to tyrosine-like, protein-like fluorescence	
$a_{254}$	Relative CDOM concentration	Li et al. (2021), ?, Catalá et al. (2018)	Peak T	Related to tryptophan-like, protein-like fluorescence	
$a_{325}$	Related to CDOM aromaticity	Catalá et al. (2015), Nelson et al. (2004)	Peak A	Related to humic-like fluorescence	Coble (1996)
			Peak M	Related to marine humic-like fluorescence	
			Peak C	Related to humic-like fluorescence	

across the range 300 to 600 nm with 0.5 nm intervals. UP water was used as the blank and was subtracted from sample spectra. Inner-filter effects were minimised using the approach of Ohno (2002). EEMs were normalized to the integral of the Raman peak between 390 nm and 410 nm for  $\lambda_{Ex}$  of 350 nm using a Milli-Q water blank (Lawaetz and Stedmon, 2009). A more detailed discussion of fluorescence spectra processing can be found in section 2.8. Ramen and Rayleigh peaks were removed using *eemR* (Massicotte, 2017), with removed Ramen and Rayleigh scatter replaced with 0. Once processed, the DOM fluorescence peaks of Coble (1996) were identified and labelled. The literature reported fluorescence index, biological index (BIX) (Huguet et al., 2009; Parlanti et al., 2000), that gives an indication of recent autochthonous DOM production was also calculated.

## 5.3 Results and Discussion

### 5.3.1 OrgAlk dynamics

Two distinct charge groups associated with OrgAlk,  $X_1$  and  $X_2$  were identified in the transitional waters of Rogerstown Estuary over the study period. Charge group concentrations ranged from 33 - 118  $\mu\text{mol}\cdot\text{kg}^{-1}$  for  $X_1$  and from 93 - 198  $\mu\text{mol}\cdot\text{kg}^{-1}$  for

$X_2$ . OrgAlk charge group concentrations were overall higher in the more marine influenced waters of the estuary, with the largest concentrations associated with  $X_2$ . Distinctions in the variability of charge group concentration was observed with respect to tidal state. Concentrations of  $X_1$  did not appear to vary considerably across the salinity gradient during low tide compared to observed variability in  $X_1$  concentrations at high tide. This is evidenced by the standard deviation values for  $X_1$  concentrations during low and high tides, 25.94 and 16.77  $\mu\text{mol}\cdot\text{kg}^{-1}$ , respectively. Concentrations of  $X_2$  were observed to generally decrease with increasing salinity for both low and high tide, possibly suggesting a terrestrial origin of DOM associated with charge group  $X_2$ . The

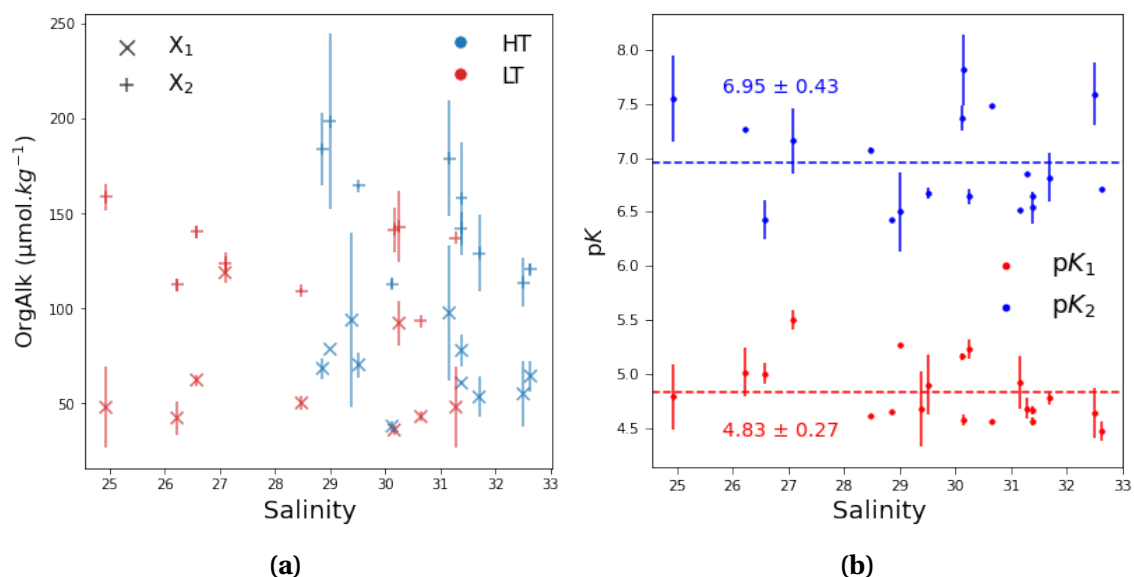


**Figure 5.2:** (a) Observed concentrations of OrgAlk charge groups  $X_1$  and  $X_1$  identified in Rogerstown Estuary across the study period as a function of salinity and tidal state. Note: HT - high tide, LT - low tide (b) Apparent pK values associated with identified charge groups  $X_1$  ( $pK_1$ ) and  $X_2$  ( $pK_2$ ).

$pK$  values associated with  $X_1$  ( $pK_1$ ) and  $X_2$  ( $pK_2$ ) were  $4.84 \pm 0.28$  and  $6.95 \pm 0.43$  ( $n=19$  for both), respectively. Variation in both  $pK_1$  and  $pK_2$  was observed across the salinity gradient.

The observed charge group  $pK$  values closely agree with those observed in Dublin Bay ( $pK_1 4.54 \pm 0.09$ ,  $pK_2 6.69 \pm 0.40$ ), suggesting that the acid-base properties of OrgAlk associated DOM does not significantly vary between these two transitional waterbodies. The apparent  $pK$  values of these organic acid groups were used to give estimate

classification of charge group type. Similarly to Dublin Bay,  $pK_1$  and  $pK_2$  fall within the broad range of  $pK$  values associated with carboxyl functional groups. The observed values for  $pK_1$  and  $pK_2$  are in agreement with  $pK$  values typically associated with humic substances, specifically carboxyl groups that represent a significant portion of DOM in marine waters (Hertkorn et al., 2006; Ritchie and Perdue, 2003; Tipping et al., 2011). Previous studies of DOM acid-base properties have identified charge groups with similar  $pK$  values (Yang et al., 2015; De Souza Sierra et al., 2001; Watanabe et al., 2021), detailed in table 5.3. Similarly to the observed OrgAlk charge group  $pK$  in Dublin Bay, the  $pK$  values of this study can be classified using literature reported charge groups  $pK$  values. Using the riverine fulvic acid charge group classification of Paxéus and Wedborg (1985),  $pK_1$  can be related to a combination of the charge groups II and III and  $pK_2$  to a combination of IV and V, in line with previous investigations (Yang et al., 2015).

**Table 5.3:** Observed OrgAlk charge group  $pK$  values compared to previously reported and literature values

Study	Sample matrix	Sample source	OrgAlk ( $\mu\text{mol} \cdot \text{kg}^{-1}$ )	Reported $pK$	OrgAlk source
This study	Transitional water	Rogerstown Estuary, Ireland	35 - 198	4.48±0.28, 6.95±0.43	Humic substances
Dublin Bay study	Coastal seawater	Dublin Bay, Ireland	46 - 234	4.54±0.09, 6.69±0.40	Humic substances
Song et al. (2020)	Coastal seawater, groundwater	Southeastern Massachusetts, USA	20 - 80	4.1 - 5.5, 7.4 - 8.4	DOM carboxyl and phenolic functional groups
Yang et al. (2015)	Coastal seawater	Coastal Gulf of Mexico	0 - 40	5.31 - 5.45, 7.05 - 7.32	Fulvic acids
De Souza Sierra et al. (2001)*	Mangrove Sediments	Santa Catarina Island, Brazil	N/A	5.69±0.15, 9.62±0.24	Fulvic Acids
				5.90±0.09, 9.41±0.11	Humic Acids
Watanabe et al. (2021)*	Stream and surface waters	Central Scotland	N/A	3.56±0.08, 5.98±0.15	Humic acids

\*Mean reported  $pK$  values.

### 5.3.2 Effects of OrgAlk on carbonate system calculations

The omission of OrgAlk in carbonate system calculations had readily observable effects on returned parameters and key carbonate chemistry descriptors. In the calculation of the impacts of OrgAlk omission,  $\Delta\text{DIC}$ ,  $\Delta p\text{CO}_2$ ,  $\Delta p\text{H}_T$ , and  $\Delta\Omega_A$  were expressed

as a function of relative OrgAlk abundance (OrgAlk:TA) in order to minimise effect of environmental variability in both OrgAlk and TA. The aforementioned values were calculated by subtracting carbonate parameters calculated using OrgAlk adjusted TA as an input parameter from carbonate parameters calculated using non-OrgAlk adjusted TA. Error bars in figure 5.3 relate to the estimations of uncertainty in calculated carbonate system parameters arising from uncertainties in input parameters and thermodynamic equilibrium constants used, as found using the uncertainty propagation software detailed in Orr et al. (2018). Although this is not specific to uncertainties relating to error associated with estimations of OrgAlk charge group concentrations and apparent acid-base properties, they fully encompass the possible uncertainty arising from the aforementioned. Consequently, error bars in figure 5.3 likely overestimate true uncertainties arising solely from OrgAlk.

When using non-Orgalk adjusted TA, calculated DIC was consistently overestimated, with  $\Delta$ DIC ranging from 88 to 254  $\mu\text{mol}\cdot\text{kg}^{-1}$ . A strong correlation between OrgAlk:TA and  $\Delta$ DIC observed ( $r^2=0.81$ ), with 0.01 increase in OrgAlk:TA corresponding to a  $\sim 11$   $\mu\text{mol}\cdot\text{kg}^{-1}$  overestimation in calculated DIC. This evaluation of  $\Delta$ DIC is in line with previously literature reported values of  $\Delta$ DIC corresponding to an OrgAlk:TA value of 0.01 given by Yang et al. (2015), who reported a 18.9  $\mu\text{mol}\cdot\text{kg}^{-1}$  overestimation of DIC for an OrgAlk:TA value of 0.008.

The distribution of both  $\Delta$ pCO<sub>2</sub> and  $\Delta$ pH<sub>T</sub> showed similarities, with both over and underestimations observed across the range of OrgAlk:TA. Overestimation in pCO<sub>2</sub> increased with increasing OrgAlk:TA, with overestimations ranging from 2 - 67  $\mu\text{atm}$ . Although a general trend of pCO<sub>2</sub> overestimation was observed, pCO<sub>2</sub> was also underestimated at lower OrgAlk:TA values. Similarly, a sign change in  $\Delta$ pH<sub>T</sub> was observed with increasing OrgAlk:TA. It was found that for both  $\Delta$ pCO<sub>2</sub> and  $\Delta$ pH<sub>T</sub> the sign of the difference in each respective parameter was related to the magnitude of pK value associated with charge group concentrations, see appendix figures A2 and A1. For pCO<sub>2</sub>, the largest overestimation largely coincided with the presence of lower pK<sub>2</sub> values ( $\sim 6.6$ ),

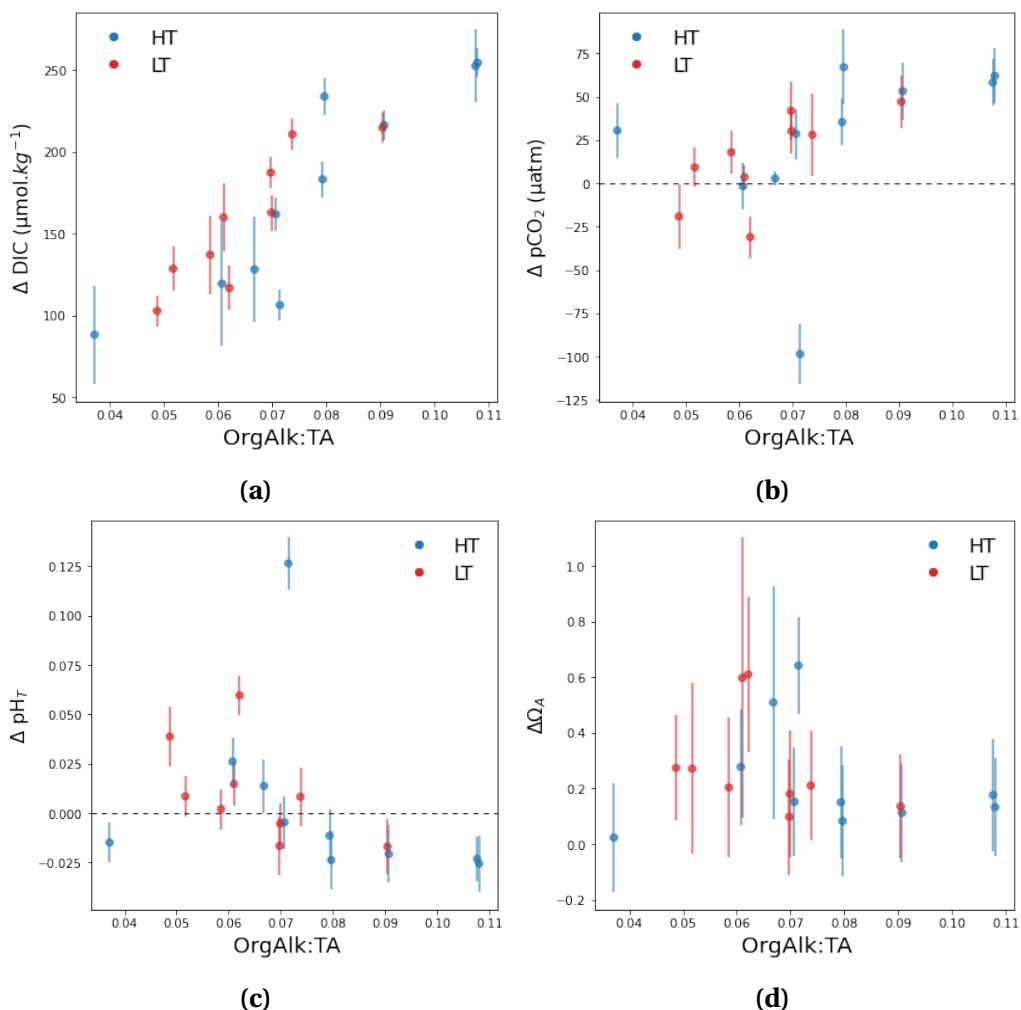


**Figure 5.3:** OrgAlk effects on calculated carbonate chemistry parameters (a) DIC, (b)  $\text{pCO}_2$ , (c) *in situ*  $\text{pH}_T$  and (d)  $\Omega_A$  expressed as a function of OrgAlk:TA.

whereas underestimations related to the occurrence charge groups with higher  $\text{pK}_2$  values. Similarly, changes in the sign of  $\Delta \text{pH}_T$  was related to  $\text{pK}$ : overestimations of pH largely coincided with higher values of  $\text{pK}_2$ , whereas underestimations coincided with lower values of  $\text{pK}_2$ . Organic acids with elevated  $\text{pK}$  values close to the pH of seawater will exhibit greater buffering than low  $\text{pK}$  organics, therefore using non-OrgAlk adjusted to convert pH measurements made at laboratory conditions to *in situ* conditions ignores the impact of potentially significant acid-base species. A potential remedy to this is to alternatively use DIC to convert pH to *in situ* conditions, as once adequate removal of volatile organics is achieved, DIC measurements are largely free from organic acid induced uncertainty.

Values of calculated  $\Delta\Omega_A$  ranged from 0.02 to 0.64. As aforementioned, uncertainties presented for  $\Delta\Omega_A$  measurements are inclusive of input measurement and thermodynamic equilibrium constant uncertainty and likely over estimate true  $\Delta\Omega_A$  uncertainty, however they constrain the upper limits of uncertainty associated with this parameter. No clear trend with increasing OrgAlk:TA was observed, however elevated  $\Delta\Omega_A$  observed at OrgAlk:TA $\approx$ 0.07 coincided with the occurrence of pK<sub>2</sub> values of  $\sim$ 7.5. When accounting for overestimations,  $\Omega_A$  ranged from 1.66 to 6.42, with a mean and median value of 2.90 and 2.37 respectively, indicating overall saturation across the study area over the study period. It is likely that errors in  $\Omega_A$  due to OrgAlk are of more significance in waters where  $\Omega_A \approx 1$ , as uncertainties could lead to misclassification of saturation state and thus actual susceptibility of a waterbody.

### 5.3.3 Carbonate chemistry distributions

Carbonate chemistry distributions within Rogerstown Estuary over the study period suggested that both abiotic processes such as tidal mixing and riverine discharge as well as biological action played a role in carbonate system dynamics. TA values ranged from 2319 - 4410  $\mu\text{mol} \cdot \text{kg}^{-1}$ , with TA values observed in less saline waters well above the range typical of marine waters (Millero, 2001). The largest TA concentrations were observed at low tide, with larger variations in TA across the salinity gradient during low tide. High tide TA concentrations were generally consistent at higher salinities, suggesting a more uniform marine TA pool. Distributions of TA across the salinity gradient indicate that the freshwater inputs to Rogerstown Estuary represent a significant source of alkalinity to the marine waters of the study area. The highest reported TA concentrations are in line with those previously reported for other east coast Irish rivers with similar bedrock geological characteristics (McGrath et al., 2016, 2019) and with concentrations reported for the River Liffey.

DIC values ranged from 1807 - 4245  $\mu\text{mol} \cdot \text{kg}^{-1}$ , and like TA, in less saline waters were above the range typical of marine waters. This may possibly be due to carbon-



**Table 5.4:** Carbonate system parameter values in Rogerstown Estuary over the study period. OrgAlk adjusted TA and  $\text{pH}_T$  were used as the input parameters, with *PyCO2SYS* (Humphreys et al., 2020) used to perform carbonate chemistry calculations. Uncertainties in calculated parameters were found using the methodology of Orr et al. (2018).

Date	Sample station	Salinity	Temperature (°C)	TA ( $\mu\text{mol} \cdot \text{kg}^{-1}$ )	DIC ( $\mu\text{mol} \cdot \text{kg}^{-1}$ )	$\text{pH}_T$ (in situ)	$\text{pCO}_2$ ( $\mu\text{atm}$ )	$\Omega_A$
12/04/2022	BPHT	31.38	8.01	2411.29±2.70	2019.00±6.20	8.114±0.01	323.65±10.72	1.93±0.12
	BWHT	31.15	8.16	2381.43±1.80	1950.32±5.81	8.124±0.01	305.52±10.07	1.91±0.11
	RBHT	28.86	8.19	2931.65±4.93	2518.95±7.63	8.10±0.01	425.15±14.18	2.23±0.13
	BPLT	30.24	8.64	2423.61±0.99	2021.91±6.02	8.139±0.01	307.86±10.04	2.05±0.12
	BWLT	26.57	8.69	2721.21±16.19	2348.11±6.49	8.176±0.01	336.40±11.13	2.37±0.14
	RBLT	9.94	8.62	4410.18±51.89	4245.30±50.66	8.215±0.011	682.38±24.67	2.82±0.16
19/04/2022	BPHT	32.63	9.86	2349.14±1.01	2037.40±6.70	7.995±0.009	436.91±13.62	1.66±0.1
	RBHT	32.5	10.81	2460.18±23.82	1807.12±22.09	8.586±0.009	86.85±2.88	5.16±0.28
	BPLT	30.64	7.48	2585.16±0.62	2291.40±6.58	8.087±0.01	392.77±13.37	2.0±0.12
	BWLT	27.09	8.02	3033.40±1.60	2647.95±6.49	8.076±0.01	479.08±16.13	2.12±0.13
	RBLT	20.19	8.56	3559.01±4.40	3379.88±8.32	8.138±0.01	564.08±19.04	2.63±0.15
26/04/2022	BPHT	31.7	9.78	2401.63±0.73	2030.59±6.89	8.137±0.009	310.02±9.73	2.21±0.13
	BWHT	31.38	10.01	2392.75±3.78	1990.12±7.34	8.162±0.009	286.39±8.94	2.29±0.13
	BPLT	31.28	14.86	2468.70±0.72	2053.29±7.42	8.136±0.007	322.04±8.86	2.69±0.15
	BWLT	30.16	16.16	2671.38±2.17	2228.91±9.35	8.163±0.006	330.77±9.0	3.18±0.17
	RBLT	24.93	15.32	3280.32±6.26	2561.42±14.39	8.511±0.007	162.77±4.68	6.42±0.34
04/05/2022	BPHT	29.39	15.19	2330.66±21.96	2041.15±20.80	8.081±0.007	371.56±10.72	2.31±0.13
	BWHT	29.28	13.21	2348.18±0.86	2100.08±7.58	8.181±0.007	297.07±8.53	2.72±0.15
	RBHT	28.99	13.17	2401.17±16.12	1931.73±14.75	8.151±0.007	294.77±8.67	2.33±0.13
	BWLT	24.85	12.58	2904.13±1.83	2718.03±7.36	8.076±0.008	514.6±15.02	2.46±0.14
	RBLT	22.48	13.83	3115.70±34.48	2747.28±11.40	8.408±0.008	234.93±6.81	4.99±0.27
10/05/2022	BPHT	30.12	11.43	2319.56±28.88	1969.77±26.26	8.153±0.008	294.59±9.6	2.28±0.13
	BPLT	28.47	15.31	2555.45±16.93	2150.84±16.66	8.184±0.007	305.96±8.66	2.99±0.17
	BWLT	26.22	15.92	2833.46±0.69	2383.38±9.24	8.254±0.007	291.19±7.98	3.74±0.20
	RBLT	22.73	16.37	3115.70±8.22	2724.60±33.00	8.364±0.007	262.07±7.79	5.02±0.28

ate mineral enriched surface waters arising from geochemical weathering of the river basin catchment area. The DIC concentrations encountered in the more marine waters are similar to those previously reported for the Irish Sea (McGrath et al., 2016). Similar to TA distributions, terrestrially derived DIC appears to be the largest contributor in less saline waters. In more marine influence waters, elevated DIC concentrations coincided with reduced DO concentrations, with this observed above the 1:1 mixing line in figure 5.4b. Furthermore, data points below this line coincided with relatively higher DO concentrations.  $\text{O}_2$  saturation values can be observed in the appendix ta-

ble ?? Respiration is known contributor to DIC (Looman et al., 2019; Shen et al., 2019), therefore this would suggest that the occurrence of microbial respiration (Robinson, 2019; Noriega and Araujo, 2014) may be a biological control on DIC distributions.

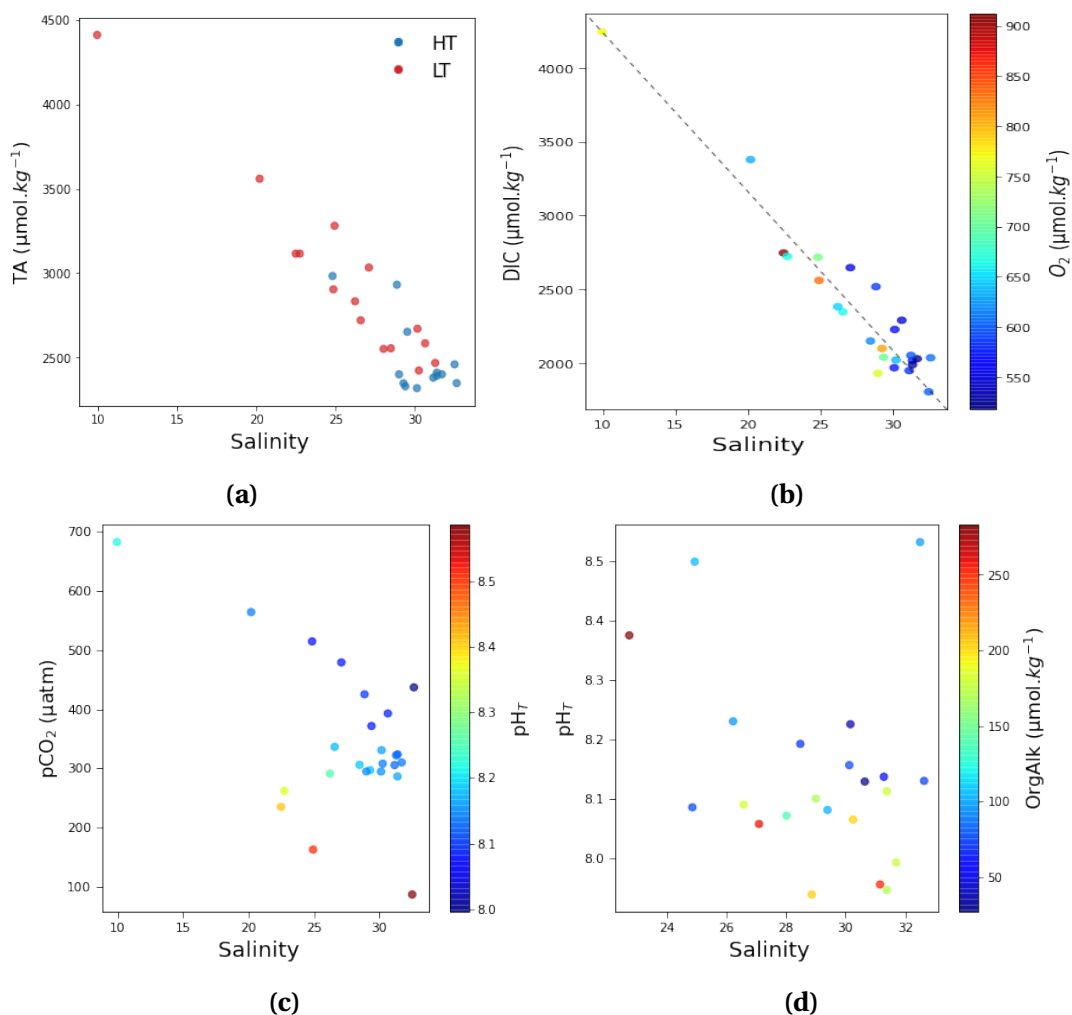


**Figure 5.4:** Observed distributions of (a) TA, (b) DIC, (c)  $\text{pCO}_2$  and (d)  $\text{pH}_T$  with respect to salinity and either additionally measured parameters or tidal state.

$\text{pCO}_2$  ranged from 86 to 682  $\mu\text{atm}$  over the study period. As river waters tend to be supersaturated in respect to  $\text{CO}_2$  (Raymond et al., 2000), the highest  $\text{pCO}_2$  concentrations were observed in less saline waters, with decreasing  $\text{pCO}_2$  along the salinity gradient generally observed. Marked undersaturation in  $\text{pCO}_2$  was observed to coincide with the highest observed  $\text{pH}_T$  values and elevated DO concentrations (appendix figure A3). This could suggest a possible biological control on  $\text{pCO}_2$  in this instance, as primary production will decrease  $\text{pCO}_2$  (Sarma et al., 2021; Delille et al., 2009) and

subsequently increase pH. As decreases in  $p\text{CO}_2$  saturation was observed concurrently with decreases in pH and elevated DO concentrations, this suggests that primary production played a role on carbonate system dynamics within the estuary. Further investigation involving complementary photosynthetic pigment analysis may elucidate further the magnitude of primary production effects on  $p\text{CO}_2$  dynamics. It is noted that although the observed decrease in  $p\text{CO}_2$  can possibly be linked to uptake during photoautotroph activity, pH changes through other processes will also impact  $p\text{CO}_2$  concentrations.

$\text{pH}_T$  ranged from 7.99 - 8.58 with a large variation observed across the salinity range, with the vast majority of values  $\leq 8.3$ . This pH range was expected based on the work of O'Boyle et al. (2013), who measured pH values within Rogerstown Estuary and reported the 5<sup>th</sup> and 95<sup>th</sup> percentile of observed pH as 7.90 and 8.40, respectively. It is important to note that the aforementioned pH measurements were made using a combination electrode and were likely reported on the  $\text{pH}_{\text{NBS}}$  scale. This renders direct comparisons a challenge, however the reported values of O'Boyle et al. (2013) serve as a good indication of the mean pH range within Rogerstown Estuary. In more saline waters lower OrgAlk concentration was observed to coincide with decreased  $\text{pH}_T$ . This may reflect the acid nature of OrgAlk charge groups, specifically  $X_1$ .

### 5.3.4 Optical properties of DOM

Observed results from fluorescence and UV-VIS spectroscopic analysis of estuarine DOM indicated distinct differences in CDOM characteristics across the estuary. All DOM optical analysis results can be seen in appendix table A2.  $a_{254}$  was observed to decrease conservatively across the salinity gradient, indicating that less saline waters were a source of CDOM to the estuary. The occurrence of humic-like fluorophores, peaks A, M and C, decreased conservatively towards the marine end member, indicating mixing of fluvial humic-like FDOM with marine water is likely the largest factor determining humic-like FDOM distributions. The largest observed  $a_{325}$  values co-

incided with the largest humic-like fluorophores signal, indicating the aromatic nature of FDOM in less saline humic influenced waters. It is noted that forcings other than mixing, such as biological controls, can also affect distributions of humic-like fluorophores (Coble, 1996). The highest humic-like fluorescence intensities were associated with peak A, further indicating a potentially terrestrial source of humic-like FDOM. The observed higher humic-like fluorophore signal corresponded with lower  $S_R$  values, suggesting that freshwater sources to the estuary contain more humic-like FDOM of a relatively higher MW compared to the that of the marine end member. The shift from relatively higher MW FDOM to lower MW FDOM with increasing salinity has been previously attributed to the process of photochemical degradation across the freshwater-marine continuum (Helms et al., 2008) as well as microbial transformation (Chen et al., 2021). Furthermore,  $S_R$  values for terrestrially derived FDOM are generally  $< 1$  whereas marine FDOM and photochemically degraded terrestrial DOM are typically  $> 1.5$  (Stedmon and Nelson, 2015). As can be seen in figure 5.5a,  $S_R$  values  $> 1.5$  are observed only in the more marine regions of the salinity gradient.  $S_R$  values  $\approx 1.5$  are observed at lower salinities, suggesting photochemical degradation and microbial transformation of terrestrially derived humic materials may have already occurred by this point along the freshwater-marine continuum.

Further indications of a terrestrial origin of humic-like FDOM is given by observed  $a_{350}$  values.  $a_{350}$  has been found to positively correlate with lignin phenol content of DOM (Hernes and Benner, 2003; Benner and Kaiser, 2011). As lignin is almost exclusively found in terrestrial vascular plants (Hedges and Mann, 1979), it is an unambiguous biomarker of terrigenous organic matter (Fichot et al., 2016).  $a_{350}$  was higher in lower salinity waters, suggesting that riverine inputs constitute the largest source of lignin phenols to the estuary, see figure 5.5c. In lower salinity waters humic-like fluorophore signal is considerably higher than protein-like fluorophore signal. This may suggest that the FDOM in the lower salinity waters of this study are predominately a mixture of relatively high MW terrestrially derived humics with some contribution

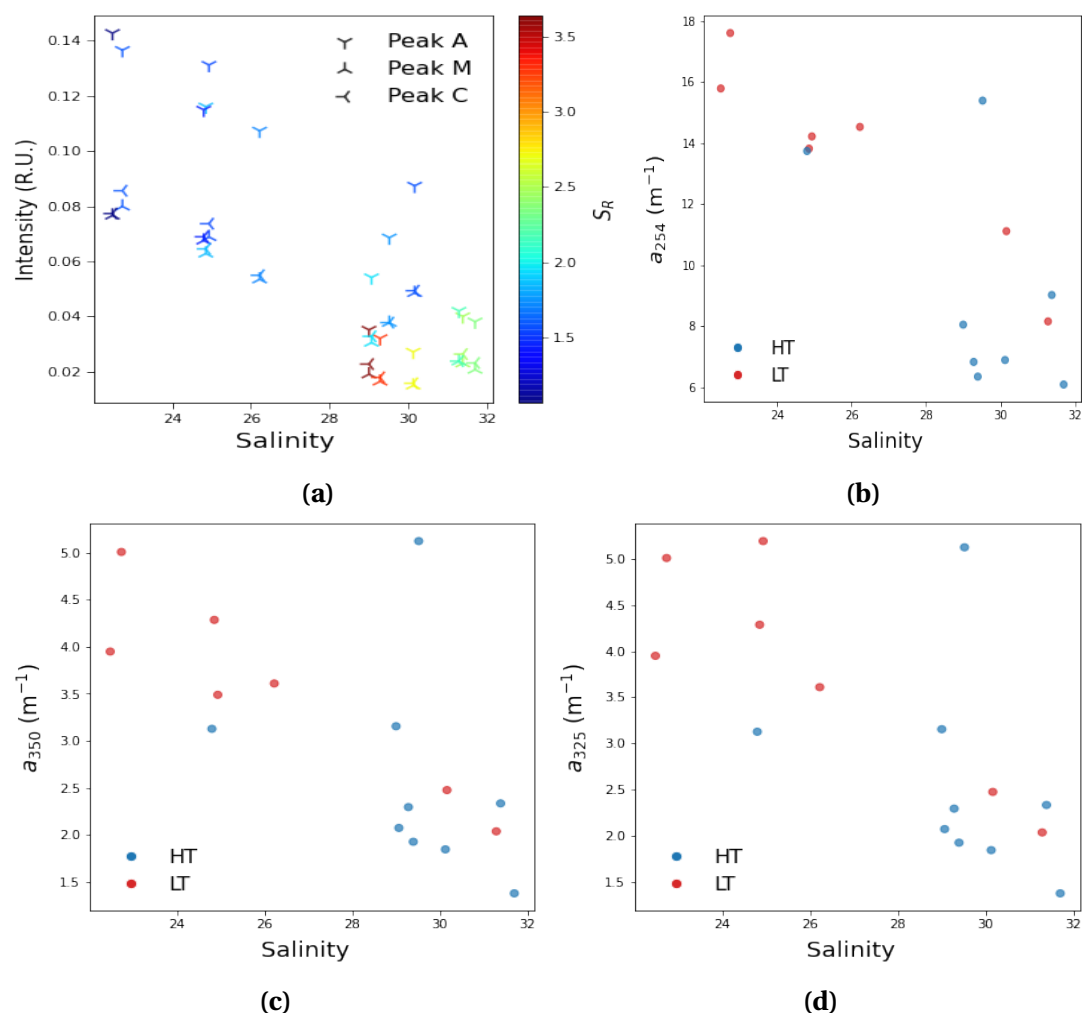


**Figure 5.5:** (a) Observed distributions of humic-like fluorescence peaks across the salinity gradient with corresponding  $S_R$  values, (b)  $a_{254}$  absorption coefficient values, indicative of relative CDOM concentration, (c)  $a_{350}$  absorption coefficient values, indicative of DOM lignin phenol content and (d)  $a_{325}$  absorption coefficient values, indicative of CDOM aromaticity across the salinity gradient.

from possibly marine protein-like FDOM, likely introduced by tidal inundation.

The signal from both protein-like fluorophores, peaks B and T, displayed a generally decreasing trend up to  $S \approx 29$ . When  $S > 29$ , protein-like fluorophore signal increased significantly, see appendix figure A4. Of the two protein-like fluorophores peak T signal was greater, with this peak associated with the production of biolabile DOM (Orta-Ponce et al., 2021). This marked increase in protein-like fluorophores signal corresponded with higher BIX values, suggesting that the elevated protein-like FDOM observed in more saline waters can possibly be attributed to enhanced biological activ-

ity. It is recognised that protein-like fluorescence can arise from sources unrelated to microbial activity, such as plant derived polyphenols and phenol containing hydrocarbons (Rosario-Ortiz and Korak, 2017). Marine microbes are known to produce DOM by extracellular excretion (Biddanda and Benner, 1997; Jiao et al., 2010), therefore indicators of enhanced biological activity could give evidence of DOM production and subsequent increase in protein-like fluorophores signal. This suggests that the protein-like fluorophore signal observed beyond  $S > 29$  can potentially be attributed to DOM associated with microbial respiration.

Linking OrgAlk with information derived from absorbance and fluorescence spectrophotometric analysis allowed for further insights into the DOM associated with OrgAlk charge groups. Concentrations of charge group  $X_2$  were observed to generally increase with increasing  $a_{350}$ , see appendix figure A5. As the pK associated with  $X_2$ ,  $pK_2$ , had a mean value of  $6.95 \pm 0.43$ ,  $X_2$  is thought to arise from phenolic-like functional groups present on DOM. The association between  $X_2$  and  $a_{350}$  gives further evidence of the phenolic nature of this charge group. As general charge group type can be inferred from returned OrgAlk pK values, further characterisation through optical analysis allowed for more robust characterisation of DOM associated with OrgAlk. Across the salinity gradient, aromatic, high MW humic-like FDOM dominated in less saline waters, whereas in more marine waters observations suggest a microbially derived potentially protein-like FDOM source. This was evidenced by prevalence of higher humic-like fluorophore signal in less saline waters, along with elevated  $a_{325}$  and  $a_{350}$  compared to the occurrence of important indicators of biological activity such as elevated BIX and peak T signal in more marine waters.

## 5.4 Conclusion

This study has indicated that negating to incorporate the organic fraction of TA when using TA as an input parameter in carbonate chemistry calculations has direct ramifications to computed carbonate system parameters. Using non-OrgAlk adjusted TA can

lead to the introduction of uncertainties in calculated carbonate system parameters in transitional waters, and misrepresentations of true carbonate system status. OrgAlk was found to be a significant fraction of TA in the transitional waters of Rogerstown Estuary, with OrgAlk charge groups associated with carboxyl and phenolic functional groups present on DOM. Complementary optical analysis of DOM was shown to be a useful tool in further elucidating the potential origins of OrgAlk. Given the complex fate of DOM in the coastal ocean and the role it plays in OrgAlk, simple optical analysis of DOM complementary to OrgAlk measurement can allow for further refinement in the current understanding of OrgAlk pathways. As many modern TA titration methods produce TA values that are indiscriminate of inorganic and organic alkalinity fractions, this leaves open the possibility for the propagation of errors to calculated carbonate system parameters if TA is assumed to be exclusively inorganic in nature. Given that in transitional waters the concentration of OrgAlk associated charge groups can be elevated, it is important to consider the incorporation of OrgAlk into carbonate chemistry calculations if TA is to be used in carbonate chemistry calculations. As TA remains a popularly measured input parameter in studies of the carbonate system across a wide range of pelagic and coastal environments, the issue of OrgAlk remains a challenge to be addressed.

## References

- Altmann, R. S. and Buffle, J. (1988). The use of differential equilibrium functions for interpretation of metal binding in complex ligand systems: Its relation to site occupation and site affinity distributions. *Geochimica et Cosmochimica Acta*, 52(6):1505–1519.
- Benner, R. and Kaiser, K. (2011). Biological and photochemical transformations of amino acids and lignin phenols in riverine dissolved organic matter. *Biogeochemistry*, 102(1):209–222.
- Biddanda, B. and Benner, R. (1997). Carbon, nitrogen, and carbohydrate fluxes during the production of particulate and dissolved organic matter by marine phytoplankton. *Limnology and Oceanography*, 42(3):506–518.
- Cai, W.-j. and Wang, Y. (1998). The chemistry, fluxes, and sources of carbon dioxide in the estuarine waters of the Satilla and Altamaha Rivers, Georgia. 43(4):657–668.
- Carlson, C. A. and Hansell, D. A. (2015). *DOM Sources, Sinks, Reactivity, and Budgets*.
- Catalá, T. S., Martínez-Pérez, A. M., Nieto-Cid, M., Álvarez, M., Otero, J., Emelianov, M., Reche, I., Arístegui, J., and Álvarez-Salgado, X. A. (2018). Dissolved Organic Matter (DOM) in the open Mediterranean Sea. I. Basin-wide distribution and drivers of chromophoric DOM. *Progress in Oceanography*, 165(November 2017):35–51.
- Catalá, T. S., Reche, I., Álvarez, M., Khatiwala, S., Guallart, E. F., Benítez-Barrios, V., Fuentes-Lema, A., Romera-Castillo, C., Nieto-Cid, M., Pelejero, C., Fraile-Nuez, E., Ortega-Retuerta, E., Marrasé, C., and Álvarez-Salgado, X. A. (2015). Water mass age and aging driving chromophoric dissolved organic matter in the dark global ocean T. *Global biogeochemical cycles*, (29):917–934.
- Catalá, T. S., Rossel, P. E., Álvarez-Gómez, F., Tebben, J., Figueroa, F. L., and Dittmar, T. (2020). Antioxidant Activity and Phenolic Content of Marine Dissolved Organic



- Matter and Their Relation to Molecular Composition. *Frontiers in Marine Science*, 7(November).
- Central and Regional Fisheries Board (2008). Rogerstown Estuary: Sampling Fish for the Water Framework Directive - Transitional waters 2008. The Central and Regional Fisheries Board. Technical report.
- Chen, Q., Chen, F., Gonsior, M., Li, Y., Wang, Y., He, C., Cai, R., Xu, J., Wang, Y., Xu, D., Sun, J., Zhang, T., Shi, Q., Jiao, N., and Zheng, Q. (2021). Correspondence between DOM molecules and microbial community in a subtropical coastal estuary on a spatiotemporal scale. *Environment International*, 154:106558.
- Coble, P. G. (1996). Characterization of marine and terrestrial DOM in seawater using excitation-emission matrix spectroscopy. *Marine Chemistry*, 51(4):325–346.
- Coble, P. G. (2007). Marine optical biogeochemistry: The chemistry of ocean color. *Chemical Reviews*, 107(2):402–418.
- Cortés-Francisco, N. and Caixach, J. (2015). Fragmentation studies for the structural characterization of marine dissolved organic matter. *Analytical and Bioanalytical Chemistry*, 407(9):2455–2462.
- De Souza Sierra, M. M., Arend, K., Fernandes, A. N., Giovanela, M., and Szpoganicz, B. (2001). Application of potentiometry to characterize acid and basic sites in humic substances: Testing the BEST7 program with a weak-acid mixture. *Analytica Chimica Acta*, 445(1):89–98.
- Delille, B., Borges, A. V., and Delille, D. (2009). Influence of giant kelp beds (*Macrocystis pyrifera*) on diel cycles of pCO<sub>2</sub> and DIC in the Sub-Antarctic coastal area. *Estuarine, Coastal and Shelf Science*, 81(1):114–122.
- DelValls, T. A. and Dickson, A. G. (1998). The pH of buffers based on 2-amino-2-hydroxymethyl-1,3-propanediol ('tris') in synthetic sea water. *Deep-Sea Research Part I: Oceanographic Research Papers*, 45(9):1541–1554.

- Dickson, A. G. (1981). An exact definition of total alkalinity and a procedure for the estimation of alkalinity and total inorganic carbon from titration data. *Deep Sea Research Part A, Oceanographic Research Papers*, 28(6):609–623.
- Dickson, A. G. (1990). Standard potential of the reaction:  $\text{AgCl(s)} + \frac{1}{2}\text{H}_2(\text{g}) = \text{Ag(s)} + \text{HCl(aq)}$ , and the standard acidity constant of the ion  $\text{HSO}_4^-$  in synthetic sea water from 273.15 to 318.15 K. *The Journal of Chemical Thermodynamics*, 22(2):113–127.
- Dickson, A. G., Sabine, C. L., and Christian, J. R. (2007). *Guide to Best Practices for Ocean CO<sub>2</sub> Measurements*. Number 8.
- Fahy, E., Goodwillie, R., Rochford, J., and Kelly, D. (1975). Eutrophication of a partially enclosed estuarine mudflat. *Marine Pollution Bulletin*, 6(2):29–31.
- Fay, D., Kramer, G., Zhang, C., McGrath, D., and Grennan, E. (2007). Soil Geochemical Atlas of Ireland. *Environmental Protection*, page 128.
- Fellman, J. B., Hood, E., and Spencer, R. G. (2010). Fluorescence spectroscopy opens new windows into dissolved organic matter dynamics in freshwater ecosystems: A review. *Limnology and Oceanography*, 55(6):2452–2462.
- Fichot, C. G., Benner, R., Kaiser, K., Shen, Y., Amon, R. M., Ogawa, H., and Lu, C. J. (2016). Predicting dissolved lignin phenol concentrations in the coastal ocean from chromophoric dissolved organic matter (CDOM) absorption coefficients. *Frontiers in Marine Science*, 3(FEB):1–15.
- Fong, M. B. and Dickson, A. G. (2019). Insights from GO-SHIP hydrography data into the thermodynamic consistency of CO<sub>2</sub> system measurements in seawater. *Marine Chemistry*, 211(January):52–63.
- Gabor, R. S., Baker, A., McKnight, D. M., and Miller, M. P. (2014). *Fluorescence Indices and Their Interpretation*.

- Guéguen, C. and Cuss, C. W. (2011). Characterization of aquatic dissolved organic matter by asymmetrical flow field-flow fractionation coupled to UV-Visible diode array and excitation emission matrix fluorescence. *Journal of Chromatography A*, 1218(27):4188–4198.
- Hedges, J. I. and Mann, D. C. (1979). The characterization of plant tissues by their lignin oxidation products. *Geochimica et Cosmochimica Acta*, 43(11):1803–1807.
- Helms, J. R., Stubbins, A., Ritchie, J. D., and Minor, E. C. (2008). Absorption spectral slopes and slope ratios as indicators of molecular weight, source, and photo-bleaching of chromophoric dissolved organic matter. *Limnology and Oceanography*, 53(3):955–969.
- Hernes, P. J. and Benner, R. (2003). Photochemical and microbial degradation of dissolved lignin phenols: Implications for the fate of terrigenous dissolved organic matter in marine environments. *Journal of Geophysical Research: Oceans*, 108(9).
- Hertkorn, N., Benner, R., Frommberger, M., Schmitt-Kopplin, P., Witt, M., Kaiser, K., Kettrup, A., and Hedges, J. I. (2006). Characterization of a major refractory component of marine dissolved organic matter. *Geochimica et Cosmochimica Acta*, 70(12):2990–3010.
- Hu, X. (2020). Effect of Organic Alkalinity on Seawater Buffer Capacity: A Numerical Exploration. *Aquatic Geochemistry*, (0123456789).
- Huguet, A., Vacher, L., Relexans, S., Saubusse, S., Froidefond, J. M., and Parlanti, E. (2009). Properties of fluorescent dissolved organic matter in the Gironde Estuary. *Organic Geochemistry*, 40(6):706–719.
- Humphreys, M. P., Gregor, L., Pierrot, D., van Heuven, S., Lewis, E. R., and Wallace, D. W. (2020). PyCO2SYS: marine carbonate system calculations in Python.
- Hunt, C. W., Salisbury, J. E., and Vandemark, D. (2011). Contribution of non-carbonate

- anions to total alkalinity and overestimation of  $p\text{CO}_2$  in New England and New Brunswick rivers. *Biogeosciences*, 8(10):3069–3076.
- Izatt, R. M. and Christensen, J. J. (1976). *Heats of Proton Ionization,  $pK$ , and Related Thermodynamic Quantities*. CRC Press, 3rd editio edition.
- Jiao, N., Herndl, G. J., Hansell, D. A., Benner, R., Kattner, G., Wilhelm, S. W., Kirchman, D. L., Weinbauer, M. G., Luo, T., Chen, F., and Azam, F. (2010). Microbial production of recalcitrant dissolved organic matter: Long-term carbon storage in the global ocean. *Nature Reviews Microbiology*, 8(8):593–599.
- Kerr, D. E., Brown, P. J., Grey, A., and Kelleher, B. P. (2021). The influence of organic alkalinity on the carbonate system in coastal waters. *Marine Chemistry*, 237:104050.
- Ko, Y. H., Lee, K., Eom, K. H., and Han, I. S. (2016). Organic alkalinity produced by phytoplankton and its effect on the computation of ocean carbon parameters. *Limnology and Oceanography*, 61(4):1462–1471.
- Koeve, W. and Oschlies, A. (2012). Potential impact of DOM accumulation on  $f\text{CO}_2$  and carbonate ion computations in ocean acidification experiments. *Biogeosciences*, 9(10):3787–3798.
- Kuliński, K., Schneider, B., Hammer, K., Machulik, U., and Schulz-Bull, D. (2014). The influence of dissolved organic matter on the acid-base system of the Baltic Sea. *Journal of Marine Systems*, 132:106–115.
- Lawaetz, A. J. and Stedmon, C. A. (2009). Fluorescence intensity calibration using the Raman scatter peak of water. *Applied Spectroscopy*, 63(8):936–940.
- Lee, K., Kim, T. W., Byrne, R. H., Millero, F. J., Feely, R. A., and Liu, Y. M. (2010). The universal ratio of boron to chlorinity for the North Pacific and North Atlantic oceans. *Geochimica et Cosmochimica Acta*, 74(6):1801–1811.

- Lee, M. H., Osburn, C. L., Shin, K. H., and Hur, J. (2018). New insight into the applicability of spectroscopic indices for dissolved organic matter (DOM) source discrimination in aquatic systems affected by biogeochemical processes. *Water Research*, 147:164–176.
- Lewis, E. R. and Wallace, D. W. R. (1998). Program Developed for CO<sub>2</sub> System Calculations.
- Li, D., Pan, B., Han, X., Li, J., Zhu, Q., and Li, M. (2021). Assessing the potential to use CDOM as an indicator of water quality for the sediment-laden Yellow river, China. *Environmental Pollution*, 289(April):117970.
- Looman, A., Santos, I. R., Tait, D. R., Webb, J., Holloway, C., and Maher, D. T. (2019). Dissolved carbon, greenhouse gases, and  $\delta^{13}\text{C}$  dynamics in four estuaries across a land use gradient. *Aquatic Sciences*, 81(1):0.
- Lueker, T. J., Dickson, A. G., and Keeling, C. D. (2000). Ocean pCO<sub>2</sub> calculated from dissolved inorganic carbon, alkalinity, and equations for K<sub>1</sub> and K<sub>2</sub>: Validation based on laboratory measurements of CO<sub>2</sub> in gas and seawater at equilibrium. *Marine Chemistry*, 70(1-3):105–119.
- Lukawska-Matuszewska, K., Grzybowski, W., Szewczun, A., and Tarasiewicz, P. (2018). Constituents of organic alkalinity in pore water of marine sediments. *Marine Chemistry*, 200:22–32.
- Massicotte, P. (2017). eemR: Tools for Pre-Processing Emission-Excitation-Matrix (EEM) Fluorescence Data.
- McGrath, T., McGovern, E., Cave, R. R., and Kivimäe, C. (2016). The Inorganic Carbon Chemistry in Coastal and Shelf Waters Around Ireland. *Estuaries and Coasts*, 39(1):27–39.
- McGrath, T., McGovern, E., Gregory, C., and Cave, R. R. (2019). Local drivers of the

seasonal carbonate cycle across four contrasting coastal systems. *Regional Studies in Marine Science*, 30:100733.

Millero, F. J. (2001). *Chemical Oceanography*. Taylor and Francis, fourth edition.

Nelson, N. B., Carlson, C. A., and Steinberg, D. K. (2004). Production of chromophoric dissolved organic matter by Sargasso Sea microbes. *Marine Chemistry*, 89(1-4):273–287.

Nelson, N. B. and Siegel, D. A. (2013). The global distribution and dynamics of chromophoric dissolved organic matter. *Annual Review of Marine Science*, 5:447–476.

Noriega, C. and Araujo, M. (2014). Carbon dioxide emissions from estuaries of northern and northeastern Brazil. *Scientific Reports*, 4(Table 1):1–9.

O’Boyle, S., McDermott, G., Noklegaard, T., and Wilkes, R. (2013). A Simple Index of Trophic Status in Estuaries and Coastal Bays Based on Measurements of pH and Dissolved Oxygen. *Estuaries and Coasts*, 36(1):158–173.

Ohno, T. (2002). Fluorescence inner-filtering correction for determining the humification index of dissolved organic matter. *Environmental Science and Technology*, 36(4):742–746.

Orr, J. C., Epitalon, J. M., Dickson, A. G., and Gattuso, J. P. (2018). Routine uncertainty propagation for the marine carbon dioxide system. *Marine Chemistry*, 207(October):84–107.

Orta-Ponce, C. P., Rodríguez-Ramos, T., Nieto-Cid, M., Teira, E., Guerrero-Feijóo, E., Bode, A., and Varela, M. M. (2021). Empirical leucine-to-carbon conversion factors in north-eastern Atlantic waters (50–2000 m) shaped by bacterial community composition and optical signature of DOM. *Scientific Reports*, 11(1):1–13.

Parlanti, E., Wörz, K., Geoffroy, L., and Lamotte, M. (2000). Dissolved organic matter

fluorescence spectroscopy as a tool to estimate biological activity in a coastal zone submitted to anthropogenic inputs. *Organic Geochemistry*, 31(12):1765–1781.

Paxéus, N. and Wedborg, M. (1985). Acid-base properties of aquatic fulvic acid. *Analytica Chimica Acta*, 169(C):87–98.

Perdue, E. M., Reuter, J. H., and Parrish, R. S. (1984). A statistical model of proton binding by humus. *Geochimica et Cosmochimica Acta*, 48(6):1257–1263.

Perez, F. F. and Fraga, F. (1987). Association constant of fluoride and hydrogen ions in seawater. *Marine Chemistry*, 21(2):161–168.

Raymond, P. A., Bauer, J. E., and Cole, J. J. (2000). Atmospheric CO<sub>2</sub> evasion, dissolved inorganic carbon production, and net heterotrophy in the York River estuary. *Limnology and Oceanography*, 45(8):1707–1717.

Repeta, D. J. (2015). *Chemical Characterization and Cycling of Dissolved Organic Matter*.

Riebesell, U., Fabry, V. J., and Hansson, L. (2010). *Guide to best practices for ocean acidification research and data reporting*.

Ritchie, J. D. and Perdue, E. (2003). Proton-binding study of standard and reference fulvic acids, humic acids, and natural organic matter. *Geochimica et Cosmochimica Acta*, 67(1):85–96.

Robinson, C. (2019). Microbial respiration, the engine of ocean deoxygenation. *Frontiers in Marine Science*, 5(JAN):1–13.

Rosario-Ortiz, F. L. and Korak, J. A. (2017). Oversimplification of dissolved organic matter fluorescence analysis: Potential pitfalls of current methods. *Environmental Science and Technology*, 51(2):759–761.

Sabine, C. (2020). GOA-ON in a Box: Collecting Discrete Samples for Analysis.

- Sarma, V. V., Prasad, M. H., and Dalabehera, H. B. (2021). Influence of phytoplankton pigment composition and primary production on pCO<sub>2</sub> levels in the Indian Ocean. *Journal of Earth System Science*, 130(2).
- Sharp, J. D. and Byrne, R. H. (2020). Interpreting measurements of total alkalinity in marine and estuarine waters in the presence of proton-binding organic matter. *Deep-Sea Research Part I*.
- Shen, C., Testa, J. M., Li, M., Cai, W. J., Waldbusser, G. G., Ni, W., Kemp, W. M., Cornwell, J., Chen, B., Brodeur, J., and Su, J. (2019). Controls on Carbonate System Dynamics in a Coastal Plain Estuary: A Modeling Study. *Journal of Geophysical Research: Biogeosciences*, 124(1):61–78.
- Smith, R. M. and Martell, A. E. (1983). Critical Stability Constants Volume 6: Second Supplement. *Biochemical Education*, 11(2):77.
- Song, S., Wang, Z. A., Gonnee, M. E., Kroeger, K. D., Chu, S. N., Li, D., and Liang, H. (2020). An important biogeochemical link between organic and inorganic carbon cycling: Effects of organic alkalinity on carbonate chemistry in coastal waters influenced by intertidal salt marshes. *Geochimica et Cosmochimica Acta*, 275:123–139.
- Stedmon, C. A. and Nelson, N. B. (2015). *The Optical Properties of DOM in the Ocean*. Elsevier Inc., second edi edition.
- Tipping, E. and Hurley, M. A. (1992). A unifying model of cation binding by humic substances. *Geochimica et Cosmochimica Acta*, 56(10):3627–3641.
- Tipping, E., Lofts, S., and Sonke, J. E. (2011). Humic Ion-Binding Model VII: A revised parameterisation of cation-binding by humic substances. *Environmental Chemistry*, 8(3):225–235.
- Watanabe, A., Katoh, M., McMaster, M., and Anderson, H. A. (2021). Characterisation of Dissolved Organic Matter Fractions Released from Scottish Peatlands. *Analytical Sciences*, 37(12):1719–1725.



- Wolf-Gladrow, D. A., Zeebe, R. E., Klaas, C., Körtzinger, A., and Dickson, A. G. (2007). Total alkalinity: The explicit conservative expression and its application to biogeochemical processes. *Marine Chemistry*, 106(1-2 SPEC. ISS.):287–300.
- Yang, B., Byrne, R. H., and Lindemuth, M. (2015). Contributions of organic alkalinity to total alkalinity in coastal waters: A spectrophotometric approach. *Marine Chemistry*, 176:199–207.
- Zeebe, R. E. and Wolf-Gladrow, D. A. (2003). *CO<sub>2</sub> in Seawater: Equilibrium, Kinetics, Isotopes*. Number 2.

# **Conclusion and Future Work**

## Implications of OrgAlk

The work presented in this thesis has further added to the growing consensus that the fraction of TA contained with the term [*minor bases – minor acids*] of equation 2.6 is non-negligible, and can have a significant contribution to TA in the coastal ocean. This identifies a crucial area of study in carbonate chemistry research. As observed through the data presented in this thesis, OrgAlk can pose a non-negligible fraction of TA, with the implications of its omission when using TA as an input parameter in carbonate system calculations evidenced. Given the anthropogenically driven changes in ecosystem wide carbon cycling, measurements of the carbonate system free from large uncertainties are crucial to our understanding of global and localised carbon system dynamics. As TA remains a popularly measured parameter in coastal ocean carbonate system studies due to its relative ease of sampling and storage compared to pH and DIC, measures to incorporate OrgAlk are of growing importance if uncertainties in calculated parameters and key descriptors of carbonate chemistry are to be minimised. Evidently, methods to estimate the concentration and acid-base properties of OrgAlk associated charge groups are of benefit to coastal ocean carbonate system researchers.

## OrgAlk Analytical Approaches

The driving motivation of the research presented in this thesis was to investigate the identified limitation of TA measurements with respect to OrgAlk in the coastal ocean and to establish bespoke apparatus and methodologies to address this issue. This was achieved by first assessing the existing literature and identifying the current state of analytical techniques available to coastal carbonate ocean system researchers to characterise OrgAlk. Initially, TA measurement procedures were established and subsequently validated through participation in the WEPAL/QUASIMEME ran interlaboratory comparison study for marine carbonate analytical chemists, AQ15. The widely available and cost-effective GOA-ON TA apparatus was then modified to incorporate

specific OrgAlk titration procedures. Open-source and accessible software, *OrgAlkCalc* was developed in order to allow for estimations of the concentration and associated acid-base properties of OrgAlk charge groups. This was undertaken with the goal of allowing for the inclusion of OrgAlk as distinct acid-base species in TA calculations to aid in the mitigation of uncertainties associated with OrgAlk omission. The modifications made to GOA-ON TA apparatus and described OrgAlk titration procedures coupled with *OrgAlkCalc* are beneficial to the scientific community as they provide cost-effective and open-access utilities to coastal ocean carbonate system researchers across 16 countries.

## OrgAlk Characteristics

The results presented in this thesis build on the growing consensus that titratable organics present in coastal waters can constitute a significant portion of TA. The estimations of the concentrations and acid-base properties of OrgAlk in Irish coastal waters presented agree with the existing view that OrgAlk is largely derived from carboxyl and phenol groups present on humic substances. This was evidenced by the apparent pK values observed in Dublin Bay ( $pK_1:4.54\pm0.09$ ,  $pK_2:6.69\pm0.40$ ) and Rogerstown Estuary ( $pK_1:4.83\pm0.27$ ,  $pK_2:6.93\pm0.43$ ).  $pK_1$  for both study sites were observed to agree exceptionally well with established literature reported pK values for carboxyl functional groups, whereas  $pK_2$  for both study agreed with literature reported phenolic functional group pK values (Paxéus and Wedborg, 1985; Ko et al., 2016; Cai et al., 1998; Song et al., 2020). The occurrence of similar charge groups across the two coastal water systems studied in this thesis as well as reported in similar studies may suggest that of the heterogeneous array of DOM present in transitional waters, specific charge groups may constitute the bulk of OrgAlk. The occurrence of OrgAlk charge groups associated with carboxyl functional displaying pK value around 4.5 presents a complex challenge in the characterisation of OrgAlk components as proton donors or acceptors given the conventional definition of alkalinity (Dickson, 1981).

## Irish Coastal Carbonate Chemistry

The establishment of TA, OrgAlk and spectrophotometric pH analysis procedures that have been proven to produce data of a "Weather" quality standard has facilitated the investigation of coastal ocean carbonate system dynamics. The carbonate chemistry data presented in this research builds on existing data and serves as additional resources for future comparison, particularly with respect to OrgAlk. Of the transitional waterbodies studied in this thesis, both the Liffey and Rogerstown Estuaries had relatively high TA concentrations in their fluviially influenced waters, with this likely related to the bedrock morphology of each respective river basin catchment area as outlined by previous studies of Irish coastal carbonate chemistry (McGrath et al., 2016, 2019). Additionally, where  $\Omega_a$  was measured, on no occasion was  $\Omega_a \leq 1$ , indicating no instances of undersaturation. Although the carbonate data presented represents only a brief temporal range in systems that could possibly undergo seasonal variation in carbonate chemistry, it suggests that specific coastal systems in Ireland may be able to buffer against detrimental changes in pH arising from ocean acidification. Future studies of Irish coastal carbonate dynamics are required in order to elucidate further the processes that govern carbonate chemistry in biogeochemically active and terrestrially influenced transitional waters.

## Future Work and Concluding Remarks

The research carried out in the the production of this thesis has led to the establishment of analytical methods for carbonate system measurement, with a special focus on OrgAlk. Further refinement of the OrgAlk titration apparatus through incorporation of titration specific instrumentation, such as software controlled titrant dispensing units would be of great interest. Properly operated, this would allow for minimisation of one of the largest sources of potential uncertainty in TA titrations, titrant dispensation. Additionally, *OrgAlkCalc* will be further developed to improve the model outputs and

updated accordingly with the latest relevant thermodynamic equilibrium constants. One area that is of significant interest is further research into the relationship between the optical properties of DOM and OrgAlk. The data presented in chapter 5 suggested that optical properties of DOM could shed further light on OrgAlk source and dynamics. Further work would entail the optical analysis of DOM on larger scales as to performed detailed statistical analysis, such as Parallel Factor analysis (PARAFAC), that can be used to decompose fluorescence EEMs into their underlying chemical components. This may allow elucidation of the molecular characteristics of OrgAlk. Additionally, of great interest is investigation of microorganism related parameters, such as chlorophyll in order to assess the possible biological controls on OrgAlk.

In the Anthropocene, the field of marine carbonate chemistry is of cogent significance. In order to address the critical issues of potentially drastic changes in seawater carbonate chemistry, it is necessary to further strengthen our understanding of how this complex and multifaceted system works. One aspect of potential uncertainty in the accurate measurement of coastal carbonate chemistry is the organic fraction of total alkalinity. This thesis has presented further evidence of the significance of OrgAlk and provided to the scientific community a potential utility for its characterisation.

## References

- Cai, W. J., Wang, Y., and Hodson, R. E. (1998). Acid-base properties of dissolved organic matter in the estuarine waters of Georgia, USA. *Geochimica et Cosmochimica Acta*, 62(3):473–483.
- Dickson, A. G. (1981). An exact definition of total alkalinity and a procedure for the estimation of alkalinity and total inorganic carbon from titration data. *Deep Sea Research Part A, Oceanographic Research Papers*, 28(6):609–623.
- Ko, Y. H., Lee, K., Eom, K. H., and Han, I. S. (2016). Organic alkalinity produced by phytoplankton and its effect on the computation of ocean carbon parameters. *Limnology and Oceanography*, 61(4):1462–1471.
- McGrath, T., McGovern, E., Cave, R. R., and Kivimäe, C. (2016). The Inorganic Carbon Chemistry in Coastal and Shelf Waters Around Ireland. *Estuaries and Coasts*, 39(1):27–39.
- McGrath, T., McGovern, E., Gregory, C., and Cave, R. R. (2019). Local drivers of the seasonal carbonate cycle across four contrasting coastal systems. *Regional Studies in Marine Science*, 30:100733.
- Paxéus, N. and Wedborg, M. (1985). Acid-base properties of aquatic fulvic acid. *Analytica Chimica Acta*, 169(C):87–98.
- Song, S., Wang, Z. A., Gonnee, M. E., Kroeger, K. D., Chu, S. N., Li, D., and Liang, H. (2020). An important biogeochemical link between organic and inorganic carbon cycling: Effects of organic alkalinity on carbonate chemistry in coastal waters influenced by intertidal salt marshes. *Geochimica et Cosmochimica Acta*, 275:123–139.

# Appendix



## Appendix

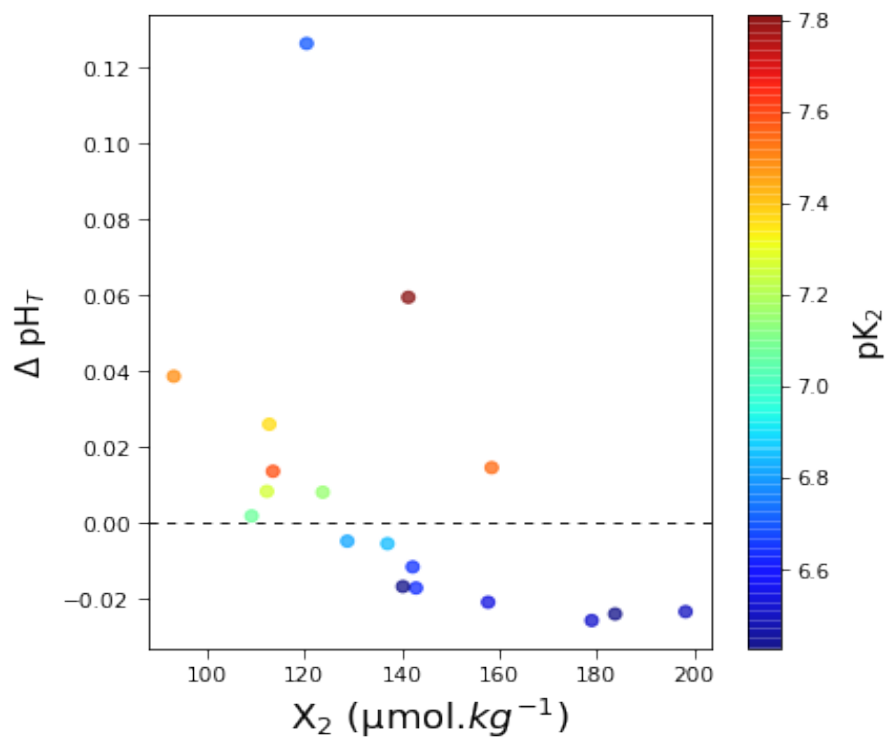


**Figure A1:**  $\Delta \text{pH}_T$  as a function of  $X_2$  concentration with respect to associated  $\text{pK}_2$  values.  $\text{pH}_T$  overestimations largely coincided with the occurrence of high  $\text{pK}$  charge groups, whereas  $\text{pH}_T$  underestimations coincided with lower  $\text{pK}$  charge groups.

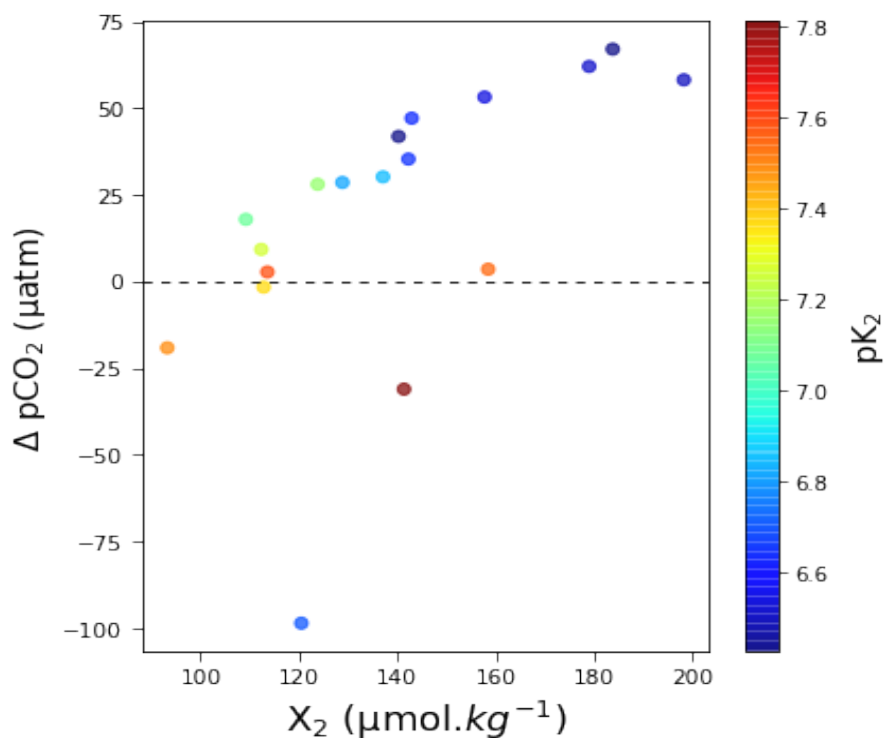


**Figure A2:**  $\Delta p\text{CO}_2$  as a function of  $X_2$  concentration with respect to associated  $pK_2$  values. The largest  $p\text{CO}_2$  overestimations largely coincided with the occurrence of lower  $pK$  charge groups, whereas lower  $p\text{CO}_2$  overestimations coincided with higher  $pK$  charge groups.

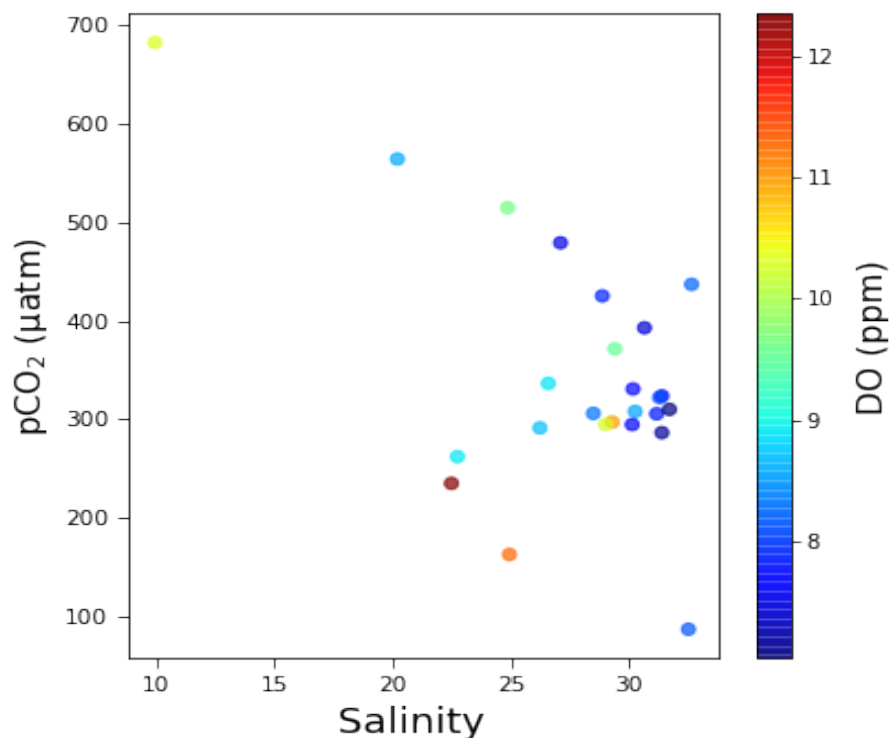


**Figure A3:** pCO<sub>2</sub> distributions with respect to salinity and DO concentrations. The marked undersaturation in pCO<sub>2</sub> coincided with elevated DO concentrations, suggesting a possible biological forcing.

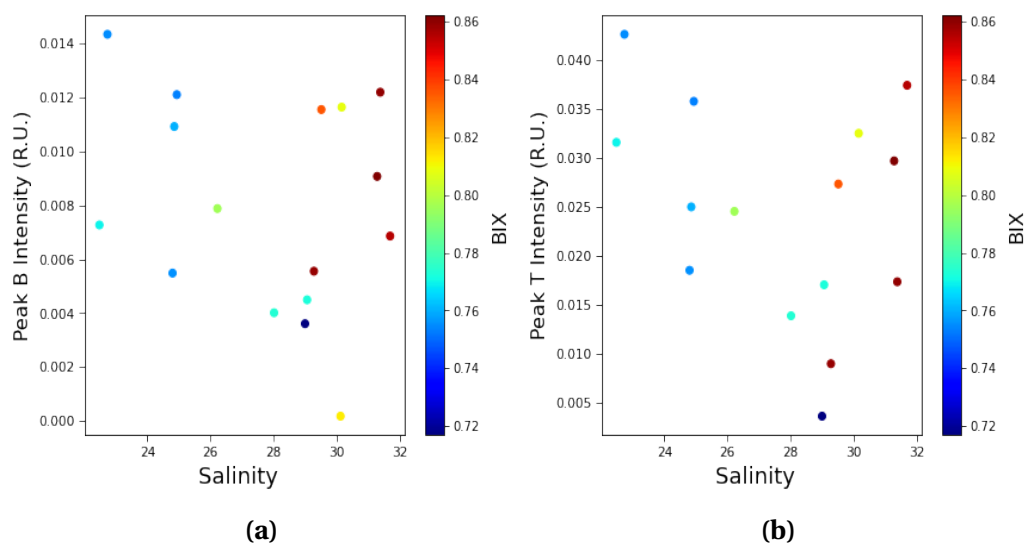


**Figure A4:** Observed intensity of (a) peak B (tyrosine-like) and (b) peak T (tryptophan-like) fluorescence as a function of salinity with corresponding BIX values, indicating a potentially recently produced autochthonous source of protein-like FDOM.

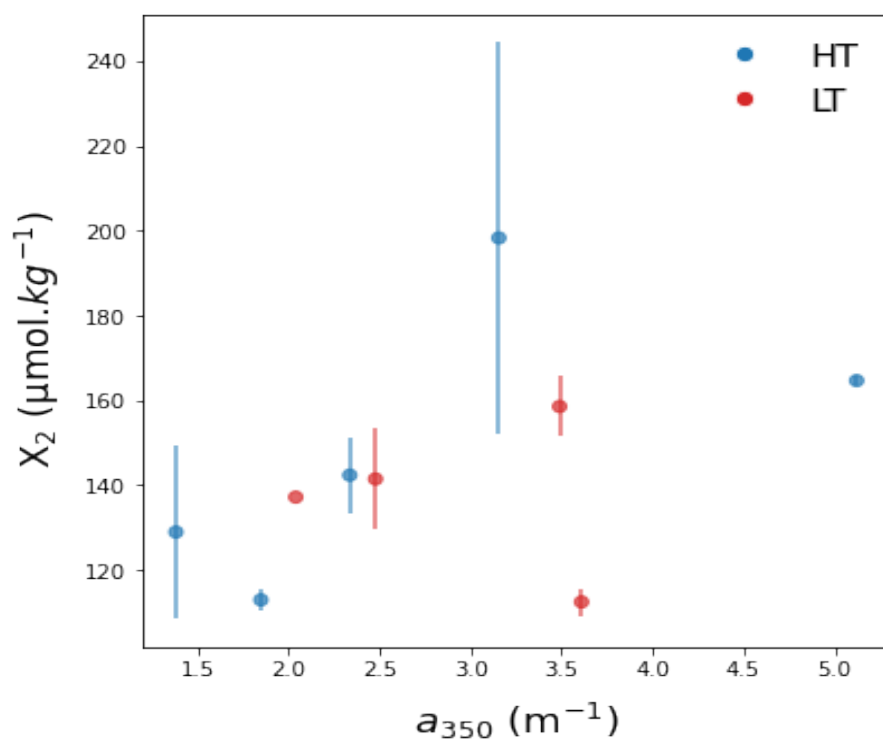


**Figure A5:** Concentrations of charge group  $X_2$  that had an apparent pK of  $6.95\pm 0.43$ , suggestive of phenolic nature, as a function of  $a_{350}$ , an indicator of lignin phenol content. As can be observed, increases in  $a_{350}$  generally coincided with increases in concentration of phenolic-like charge groups.

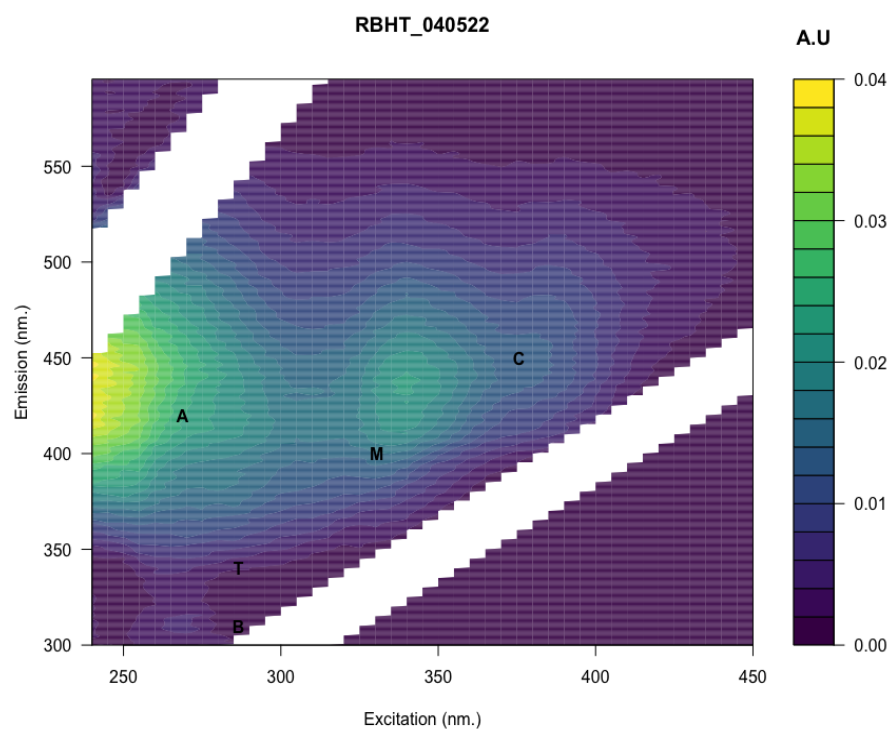


**Figure A6:** Example graph illustrating the graphical representation of an excitation/emission matrix. The letters represent the approximate peak locations as outlined by Coble (1993). The diagonal white lines relates to removal of first and second order Rayleigh scattering. A.U. stands for arbitrary units.

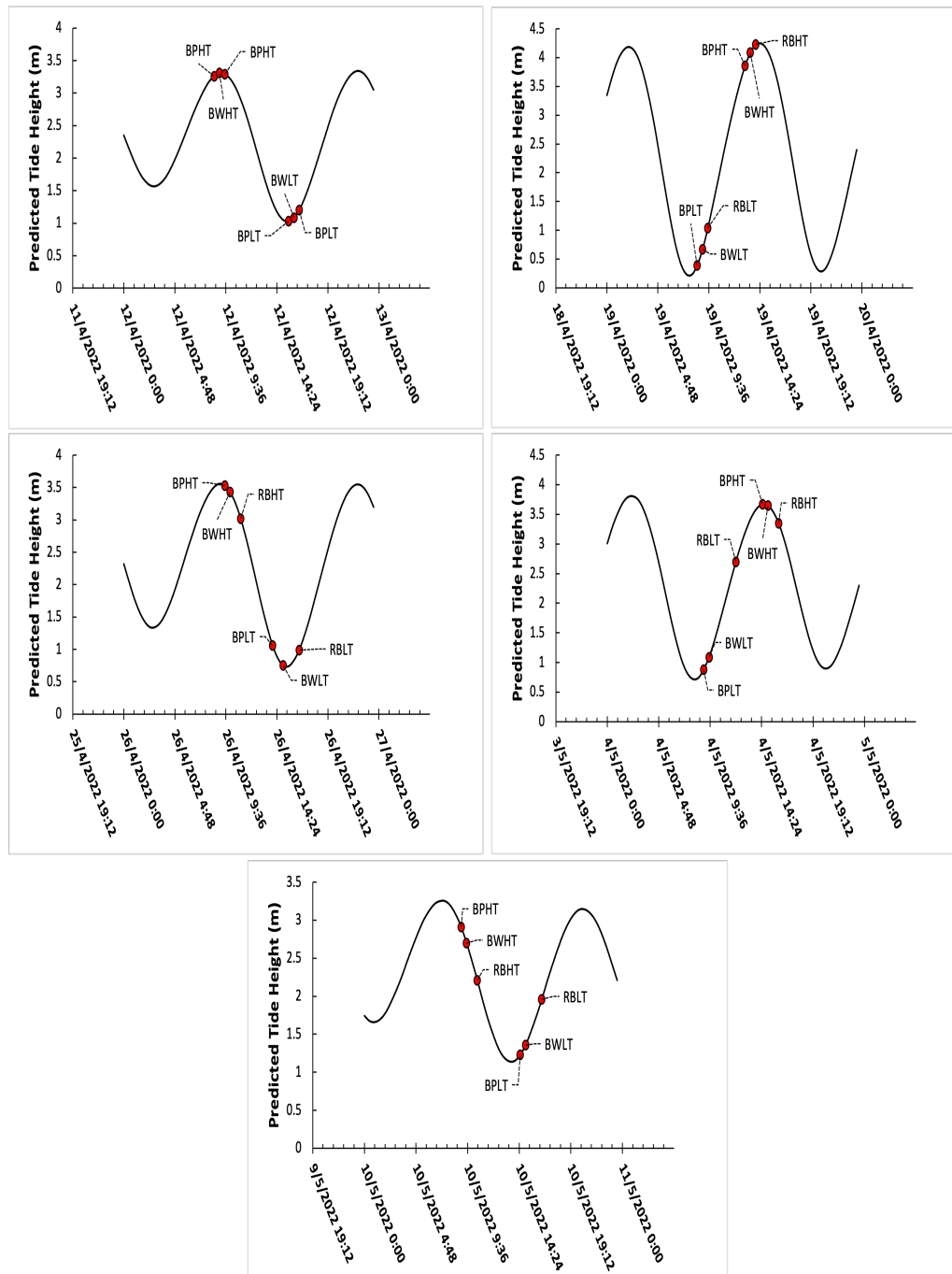


**Figure A7:** Predicted tidal height plots indicating tidal state when respective Rogerstown Estuary samples were collected. Tidal heights are taken from the nearest available tidal prediction points, Malahide, Dublin, Ireland. Position of samples on tidal curves are indicative rather than absolute as small variations are possible.

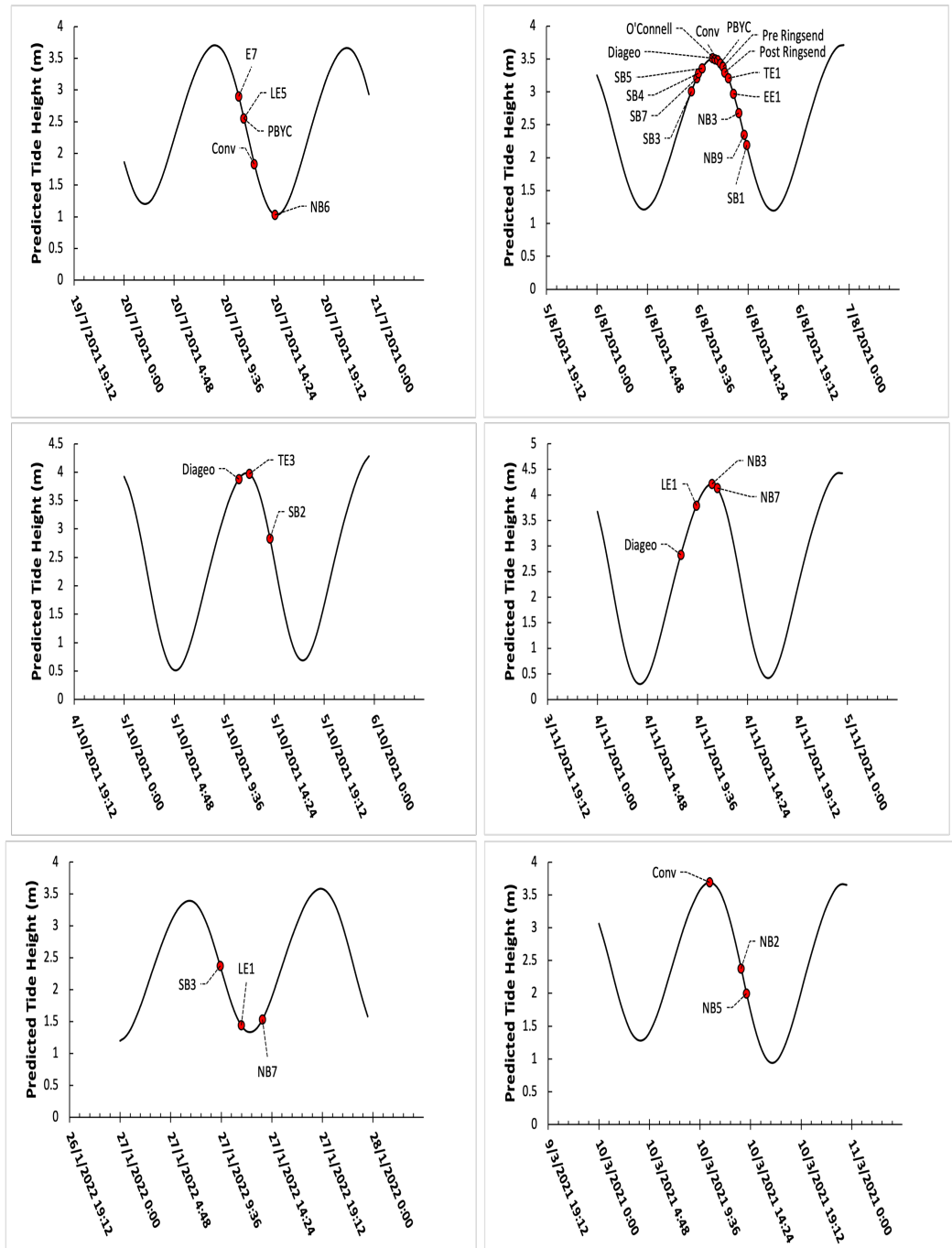


**Figure A8:** Predicted tidal height plots indicating tidal state when respective Dublin Bay samples were collected. Tidal heights are taken from the nearest available tidal prediction points, North Wall, Dublin Bay, Dublin, Ireland. Position of samples on tidal curves are indicative rather than absolute as small variations are possible.

**Table A1:** Data used in *pyCO2SYS* in carbonate system calculations. Note: units of TA,  $\text{PO}_3^{3-}$ ,  $\text{NH}_3$ ,  $X_1$  and  $X_2$  are  $\mu\text{mol}\cdot\text{kg}^{-1}$ . For  $\text{PO}_3^{3-}$  and  $\text{NH}_3$ , data collection commenced on 26/04/22 with maximum alkalinity contributions for the aforementioned relatively small; 0.01 - 7.34  $\mu\text{mol}\cdot\text{kg}^{-1}$ .

Date	Sample station	TA	pH <sub>T</sub> (@25°C)	Salinity	Temperature out (°C)	Temperature in (°C)	$\text{PO}_3^{3-}$	$\text{NH}_3$	$X_1$	$K_{X1}$	$X_2$	$K_{X2}$
12/04/2022	BPHT	2411.29	7.836	31.38	8.01	25			77.81	4.561	157.71	6.54
	BWHT	2381.43	7.844	31.15	8.16	25			97.53	4.921	178.97	6.517
	RBHT	2931.65	7.822	28.86	8.19	25			68.3	4.659	183.76	6.429
	BPLT	2423.61	7.874	30.24	8.64	25			92.18	5.233	142.91	6.64
	BWLT	2732.66	7.909	26.57	8.69	25			62.23	5.007	140.24	6.426
19/04/2022	BPHT	2349.14	7.892	32.63	9.86	25			64.29	4.476	120.48	6.707
	RBHT	2460.18	8.373	32.5	10.81	25			54.93	4.643	113.58	7.587
	BPLT	2585.16	7.859	30.64	7.48	25			42.98	4.56	93.24	7.487
	BWLT	3033.4	7.827	27.09	8.02	25			118.69	5.506	123.8	7.156
26/04/2022	BPHT	2401.63	7.901	31.69	9.78	25	1.82	1.23	53.32	4.781	128.83	6.82
	BWHT	2392.75	7.922	31.38	10.01	25	3.91	2.52	60.64	4.673	142.24	6.649
	RBHT	2653.07	N/A	29.51	10.47	25	5.85	4.11	70.26	4.904	164.55	6.669
	BPLT	2468.7	7.976	31.28	14.86	25	4.49	2.12	47.99	4.685	137.07	6.849
	BWLT	2671.38	8.086	30.16	16.16	25	5.2	3.14	35.92	4.578	141.35	7.812
	RBLT	3280.32	8.372	24.93	15.32	25	6.03	6.25	47.87	4.792	158.44	7.546
04/05/2022	BPHT	2330.66	7.919	29.39	15.19	25	3.87	2.52	93.76	4.678		
	RBHT	2401.17	7.948	28.99	13.17	25	3.91	2.16	78.45	5.266	198.21	6.502
10/05/2022	BPHT	2319.56	7.971	30.12	11.43	25	3.75	1.69	37.95	5.164	112.82	7.367
	BPLT	2555.45	8.037	28.47	15.31	25	0.22	3.26	50.16	4.619	109.2	7.076
	BWLT	2833.46	8.121	26.22	15.92	25			42.27	5.021	112.34	7.262



**Table A2:** Observed optical properties of DOM in Rogerstown Estuary over the study period. Note: n/a values relate to sample loss due to bottle breakage.

Date	Sample station	Salinity	BIX	Peak B (R·U·)	Peak T (R·U·)	Peak A (R·U·)	Peak M (R·U·)	Peak C (R·U·)	$S_R$	$a_{254}$ (m <sup>-1</sup> )	$a_{325}$ (m <sup>-1</sup> )	$a_{350}$ (m <sup>-1</sup> )
26/04/2022	BPHT	31.69	0.85	0.006	0.037	0.038	0.02	0.023	2.35	6.09	1.82	1.37
	BWHT	31.38	0.85	0.012	0.017	0.04	0.023	0.026	2.47	9.02	3.02	2.33
	RBHT	29.51	0.83	0.011	0.027	0.068	0.037	0.037	1.75	15.39	6.34	5.12
	BPLT	31.28	0.86	0.009	0.029	0.042	0.023	0.023	2.17	8.15	2.83	2.03
	BWLT	30.16	0.8	0.011	0.032	0.087	0.048	0.049	1.57	11.11	3.64	2.47
	RBLT	24.93	0.75	0.012	0.035	0.131	0.068	0.073	1.55	14.21	5.18	3.48
04/05/2022	BPHT	29.39	n/a	n/a	n/a	n/a	n/a	n/a	3.69	6.34	2.29	1.92
	BWHT	29.28	0.85	0.005	0.008	0.032	0.016	0.017	3.28	6.83	2.73	2.29
	RBHT	28.99	0.71	0.003	0.003	0.035	0.019	0.022	3.64	8.05	3.65	3.15
	BPLT	28.01	0.77	0.004	0.013	0.06	0.03	0.029	n/a	n/a	n/a	n/a
	BWLT	24.85	0.76	0.01	0.024	0.116	0.062	0.064	1.85	13.82	5.46	4.28
	RBLT	22.48	0.76	0.007	0.031	0.142	0.076	0.077	1.06	15.79	5.41	3.94
10/05/2022	BPHT	30.12	0.81	0	0	0.027	0.014	0.015	2.71	6.89	2.36	1.84
	BWHT	29.06	0.77	0.004	0.017	0.054	0.03	0.032	1.95	10.21	2.86	2.07
	RBHT	24.79	0.75	0.005	0.018	0.114	0.067	0.068	1.45	13.74	4.54	3.12
	BWLT	26.22	0.79	0.007	0.024	0.107	0.053	0.054	1.71	14.53	5.05	3.6
	RBLT	22.73	0.75	0.014	0.042	0.136	0.079	0.085	1.59	17.6	6.75	5

**Table A3:** D.O. concentrations observed in Rogerstown Estuary during the duration of the study.

Date	Sample station	Salinity	Temperature (°C)	D.O. (%)	D.O. (mg.L <sup>-1</sup> )	O <sub>2</sub> (μmol·kg <sup>-1</sup> )
12/04/2022	BPHT	31.38	8.01	90.3	7.72	235.5912655
	BWHT	31.16	8.16	91.1	7.80	238.0776881
	RBHT	28.86	8.19	89.9	7.87	240.6387403
	BPLT	30.25	8.64	99.6	8.55	261.4190601
	BWLT	26.58	8.69	99.9	8.89	272.6503074
	RBLT	9.94	8.62	98.1	10.30	319.575821
19/04/2022	BPHT	32.64	9.86	98.5	8.23	250.9829073
	BWHT	32.50	10.71	102.0	8.45	257.7556
	RBHT	32.50	10.81	96.9	8.16	249.197617
	BPLT	30.64	7.48	84.3	7.41	224.9710559
	BWLT	27.09	8.02	82.8	7.50	229.6315853
	RBLT	20.20	8.56	89.2	8.57	263.8018072
26/04/2022	BPHT	31.70	9.78	83.0	7.03	214.5384033
	BWHT	31.38	10.01	84.2	7.14	217.9564098
	RBHT	29.52	10.47	98.4	8.44	258.0244267
	BPLT	31.28	14.86	102.0	8.11	247.8060581
	BWLT	30.16	16.16	98.0	7.73	236.4589827
	RBLT	24.93	15.32	135.9	11.29	347.4254699
04/05/2022	BPHT	29.39	15.19	119.0	9.53	291.6294081
	BWHT	29.28	13.21	133.0	10.97	335.9168191
	RBHT	29.00	13.17	124.2	10.26	313.9258797
	BPLT	28.02	11.82	111.8	9.51	291.7709901
	BWLT	24.85	12.58	111.5	9.63	295.555037
	RBLT	22.48	13.83	142.7	12.35	379.8001284
10/05/2022	BPHT	30.12	11.43	92.3	7.68	234.7203847
	BWHT	29.06	11.59	95.6	8.02	245.3156641
	RBHT	24.80	12.71	93.4	7.98	244.9295874
	BPLT	28.48	15.31	103.8	8.29	253.7957629
	BWLT	26.22	15.92	108.1	8.70	266.9065216
	RBLT	22.73	16.37	108.6	8.91	274.0932799